

Bård M. Pedersen

Alkali-reactive and inert fillers in concrete

Rheology of fresh mixtures and expansive reactions

Trondheim, June 2004

Doctoral thesis for the degree of doktor ingeniør

Norwegian University of Science and Technology
Faculty of Engineering Science and Technology
Department of Structural Engineering



Acknowledgements

This work has been carried out within the “Doctors of Engineering” program initiated by the Scancem Group (presently a part of the Heidelberg Cement Group). I am grateful to my employer NorBetong AS for the financial support, and in particular to Ernst Mørtzell who has supported and encouraged me and given valuable advice during the entire study.

I would like to express my gratitude to my main supervisor Professor Magne Maage for his commitment, advice and support throughout the study. I am also grateful to supervisor Sverre Smeplass for his support and valuable advice and discussions during the whole process. Furthermore, thanks to my colleagues at the Department of Structural Engineering, especially to Erik Sellevold for fruitful discussions and comments to the manuscript, and to Jon Wallevik for long discussions and valuable advice concerning the rheological measurements. I would also like to thank Ove Loraas and Bjørn Ingebrigtsen at the concrete laboratory for all the assistance and help with my experimental work. The experimental work done by Dan Granerud and Arne Christian Johansen is also highly appreciated.

A great part of my experimental work has been carried out at SINTEF Cement and Concrete. Special thanks to Per Arne Dahl, who has been very helpful in organizing much of this work and has given valuable advice. I also wish to express my gratitude to Harald Justnes, Tor Arne Hammer, Jan Lindgård, and Marit Haugen for valuable contributions. Also thanks to Knut Lervik and Tone Østnor and the rest of the staff at the laboratory at SINTEF Cement and Concrete for all the assistance and help.

I am grateful to Viggo Jensen and Børge Wigum, who both have contributed a lot to the alkali-silica part of the thesis. Both have been very supportive and enthusiastic during the whole project, and have given me valuable advice in the process of preparing the final manuscript. Viggo has also performed much of the micro-structural analyses. Also thanks to Stig Brox who has read parts of the manuscript and has given me useful input on how to write proper English. I would also like to thank the members of FARIN for introducing me to the world of mineralogy and petrography. Maarten Broekmans has tried to make me understand some of the fundamental aspects of silica structure and silica dissolution. Also thanks to associates at NorBetong, NorStone, Norcem and Scancem Chemicals who have contributed to this work.

Finally, I am grateful to family and friends for being patient and supportive during these years. Especially, I wish to thank my wife Runa and my sons Erlend and Børge for being patient with me.

Bergen, February 2004

Bård M. Pedersen

Abstract

Due to the rather limited obtainable resources of natural aggregates suitable for concrete purposes, the technology of crushed aggregates becomes more important. The production of crushed aggregates generates large amounts of fines or fillers, presently to some extent considered to be leftovers. From an environmental point of view, as well as from an economic point of view, it is important to be able to utilize these fines. Because of the large surface area of the filler fraction of the aggregate, the addition of filler may modify the rheological properties of fresh concrete to a great extent. Recently, the need for good fillers has increased due to the development of self-compacting concrete. To attain the much higher flowability of self-compacting concrete compared to ordinary vibrated concrete, the volume of the fluent phase, i.e. the matrix phase, has to be increased. At the same time, the self-compacting concrete has to be stable. The addition of filler may then be beneficial from a technical point of view. In addition, the use of fillers may be more cost efficient than other possible solutions.

There are examples in the literature that fillers may modify the properties of the hardened state as well as the properties of the fresh state of concrete. Fillers have been reported to accelerate the cement hydration in some cases. Examples of increased compressive strength also exist. This is believed to be due to a general filler effect, i.e. that the cement hydration products may grow faster and become more evenly distributed in the presence of small mineral particles. In addition to the general filler effect, there might be chemical effects, in some cases pozzolanic reactions.

The present study has focused on fillers classified as alkali-reactive. The alkali-silica reaction in concrete is known to result in cracking and overall expansion of structural elements. There are some examples in the literature indicating that the finest particles of alkali-reactive aggregates should not be considered dangerous in concrete. Some researchers have reported that filler particles below a critical limit, which has been reported to be in the order of 50 μm for some rocks, may give pozzolanic reactions, and consequently be beneficial. However, there have been reported cases where particles smaller than 20-30 μm gave very fast and deleterious reactions. In the present study, alkali-reactive fillers from two Norwegian cataclastic rocks have been investigated. The study has included fillers of Icelandic glassy rhyolite and crushed bottle glass. Non-reactive reference fillers were included in the study, as well as silica fume and fly ash known to mitigate alkali-silica reactions.

The direct pozzolanic reactivity of the fillers has been quantified by mixing calcium hydroxide, filler and artificial pore water. The loss of calcium hydroxide over time measured by TGA is then a direct measure of the pozzolanic reactivity. When testing the 0-20 μm fractions of the different fillers at 20°C, the materials could be divided into two distinct classes with respect to pozzolanity:

- The pozzolanic reactivity of fly ash, glass and rhyolite filler was distinct
- The pozzolanic reactivity of mylonite, cataclasite and quartz fillers was insignificant at the age of 28 days

All the materials being highly pozzolanic have a distinct amorphous silica phase, while the silica phase of the non-pozzolanic materials is well crystalline quartz. The known deformation and sub-grain development due to cataclasis of the tested reactive Norwegian rocks does not seem to increase the pozzolanic reactivity much.

The mylonite filler has also been tested at curing temperatures of 38°C and 80°C. The pozzolanic reactivity was very low also at 38°C. However, at a temperature of 80°C, corresponding to the temperature used by the accelerated mortar bar test, the pozzolanic reactivity was significant. Non-reactive granite/gneiss filler of glaciofluvial origin was also pozzolanic at 80°C. It may then be suggested that all fillers of rocks containing silica will be more or less pozzolanic at such high temperatures as 80°C.

Based on testing by the concrete prism method, the fillers could be divided into two distinct classes with respect to their effect on alkali-silica reactions in concrete:

- Fly ash, silica fume, glass filler and rhyolite filler significantly reduced the expansions compared to the reference concrete
- Mylonite and cataclasite filler had no effect or gave increased expansions compared to the reference concrete

These results are based on experiments by the concrete prism test, which is believed to provide a realistic picture of the real behaviour in field conditions. Micro structural analyses, using optical microscopy and electron probe micro analyser, have given additional information regarding the performance of glass filler, mylonite filler and rhyolite filler compared to the reference concrete, and confirmed the expansion results of the concrete prism test.

The effect of the tested fillers with respect to alkali-silica reactions matched their pozzolanic reactivity. Fillers being highly pozzolanic reduced the expansions due to ASR, while non-pozzolanic alkali-reactive fillers gave in most cases increased expansion compared to the reference mix. Consequently, such alkali-reactive fillers should be treated as potentially deleterious in concrete.

The accelerated mortar bar test has been widely used around the world to test the effect of different additives, such as silica fume, fly ash and slag. Other additional materials, such as crushed bottle glass, have also been tested using this method. Some studies have indicated a rather strong correlation between the results obtained by concrete prism testing and results obtained by accelerated mortar bar testing. In

the present study, extensive testing of fillers by the accelerated mortar bar test was carried out to give a preliminary screening of the materials. Testing of rhyolite filler, glass filler, fly ash and silica fume reduced the expansions significantly compared to the reference mortar when tested by the accelerated mortar bar test. This is in accordance with the results obtained for the same fillers by the concrete prism test. However, the accelerated mortar bar test also predicted the Norwegian reactive rock fillers to inhibit expansions due to alkali-silica reactions. This contradicts the predicted effect of these fillers by the concrete prism test. Testing of non-reactive limestone filler gave no effect at all on mortar bar expansion. This indicates that the effect of the Norwegian reactive rock fillers by this method is due to chemical, and not physical effects. Due to the high temperature used by the accelerated mortar bar test (80°C), the quartz in these rock fillers are believed to react pozzolanic. Methods such as the accelerated mortar bar test, or other methods using very high temperatures, should consequently not be used to evaluate the effect of rock fillers containing silica, unless their pozzolanic reactivity are evident also at lower temperatures.

The pozzolanic materials (fly ash, silica fume, rhyolite and glass filler) gave a significant increase in compressive strength. This is believed to be due to their pozzolanic reactivity. No significant effect on the compressive strength of any of the Norwegian rock fillers (mylonite, cataclasite and granite/gneiss filler) was noticed at normal filler addition levels.

The present study has given valuable information concerning the practical implications of using alkali-reactive fillers. The similarity between the alkali-silica reaction and the pozzolanic reaction has been highlighted. However, some of the more fundamental issues concerning the paradox of the alkali-silica reaction and the pozzolanic reaction are still far from being fully understood, and it is clear that more basic research is needed in this area.

Testing of the effects of fillers on the rheological properties of fresh concrete was done by matrix testing within the present study. The matrix refers to the fluent phase of the particle-matrix model. It consists of the cement paste and all powders of particle size < 0.125 mm, including the aggregate filler. Some of the limitations of the particle-matrix model with respect to self-compacting concrete have been treated in the present study. The characterisation of the matrix phase by simple flow viscometers are believed to be insensitive to the small, but significant, changes in yield stress. A more fundamental characterisation of the matrix phase has been introduced. By using the Physica rheometer with parallel plate configuration, the fundamental measures yield stress and plastic viscosity could be obtained.

The effect of fillers on the flow resistance ratio of the matrix has been tested. As expected, addition of filler increased the flow resistance ratio. The effect of the different fillers varied much, to a large extent due to the variations in particle size distribution. The granite/gneiss filler, which is coarse compared to the crushed rock fillers, gave the lowest flow resistance ratio. Fly ash, which has a particle size

distribution similar to cement, gave the highest flow resistance ratio. Replacement of cement by filler reduced the flow resistance ratio for most of the fillers. The exception was fly ash and glass filler, which gave the opposite effect. In addition to the particle size grading of the fillers, the mineralogy seems to have some influence. In this respect, limestone filler gave rather low flow resistance ratios in relation to its fine particle size distribution.

A laboratory program using the Physica rheometer to give a more fundamental characterisation of the effects of filler on the matrix has been carried out. The plastic viscosity obtained from testing by the Physica rheometer is more or less an equivalent measure to the empirical flow resistance ratio obtained by the FlowCyl testing. Consequently, the effect of the fillers with respect to plastic viscosity was basically equal to their effect on flow resistance ratio. The replacement of cement by filler has been shown to alter the rheological properties significantly. Generally, fillers gave lower yield stress and plastic viscosity than equal volumes of cement. An increase in plastic viscosity was generally followed by an increase in yield stress. However, it has been shown that the ratio between yield stress and plastic viscosity is highly dependent on the type and dosage of plasticizer. The new co-polymers generally reduced the yield stress to a much higher extent than lignosulphonate or naphthalene. Further, the co-polymer seems to level out the large differences due to different fillers, which may be apparent when using other types of plasticizers. Also the cement type has been shown to influence the ratio between yield stress and plastic viscosity largely.

A study of the relationship between the rheological properties of the matrix phase and self-compacting concrete has indicated that the yield stress of the matrix phase has a crucial influence on the empirical slump-flow measure. No straightforward correlation between the rheological properties of self-compacting concrete and the corresponding matrix phase was found. Studies on rheological properties of the matrix phase should be considered useful to gain fundamental knowledge regarding the effects of different constituents. Matrix testing may to some extent be useful to predict the effects in self-compacting concrete, but the limitations should be kept in mind when using matrix results to predict the behaviour of a given constituent in concrete. The study has confirmed the basic principles of the particle-matrix model for self-compacting concrete. However, further work is needed to go deeper into the very complex relationship between the concrete rheology and the matrix rheology.

Table of contents

Acknowledgements.....	I
Abstract.....	II
Table of contents	VI
Notations and definitions.....	XII
1 INTRODUCTION	1
1.1 Background	1
1.2 Objectives	3
1.3 Organisation of the thesis.....	4
2 ALKALI-SILICA REACTION – THEORETICAL BACKGROUND	5
2.1 Introduction.....	5
2.2 Different alkali-aggregate reactions	5
2.3 History of AAR.....	5
2.4 Effects of ASR	6
2.4.1 General effects	6
2.4.2 ASR in relation to other damaging mechanisms	6
2.4.3 Structural effects	7
2.5 Mechanisms of reaction.....	9
2.5.1 General	9
2.5.2 Dissolution of silica.....	9
2.5.3 Formation and swelling of alkali-silica gel	12
2.5.4 The effect of calcium hydroxide (CH) on the ASR.....	14
2.5.5 Observations for slowly reacting aggregates.....	16
2.6 Alkali reactive minerals and rocks	17
2.6.1 General	17
2.6.2 Norwegian reactive rocks.....	17
2.6.3 Effect of the particle size.....	19
2.6.3.1 Literature review on the effect of the particle size.....	19
2.6.3.2 Fracture mechanical approach to the effect of the particle size	23
2.6.3.3 Concluding remarks on the effect of the particle size	25

2.7	Relevance of alkalis.....	26
2.7.1	Effect of alkalis	26
2.7.2	Alkalis in the cement.....	27
2.7.3	Other sources of alkalis	28
2.8	Relevance of the moisture condition.....	29
2.8.1	Introduction	29
2.8.2	Description of the moisture condition	29
2.8.3	Effect of the moisture condition on the ASR	32
2.8.3.1	Laboratory results	32
2.8.3.2	Field results of the moisture condition.....	35
2.8.3.3	Concluding remarks regarding the moisture condition	36
2.9	ASR inhibiting additives.....	37
2.9.1	Introduction.....	37
2.9.2	Silica fume, fly ash and slag.....	37
2.9.3	Other inhibiting additives and admixtures	40
2.10	ASR test methodology.....	40
2.10.1	Petrographic examination.....	40
2.10.2	Mortar and concrete prism methods	41
2.11	General effects of fillers in concrete	42
2.11.1	Effects on mechanical and durability properties	42
2.11.2	Pozzolanic reaction versus ASR.....	43
3	PROPERTIES OF FRESH CONCRETE – THEORETICAL BACKGROUND	46
3.1	Introduction.....	46
3.2	Description of the rheological properties of fresh concrete.....	46
3.3	Rheology – basic theory	47
3.3.1	General	47
3.3.2	Basic concepts of viscometry	48
3.3.3	Yield stress and rate of shear.....	51
3.3.4	Shearing concepts.....	53
3.3.5	Time dependent phenomena.....	53
3.4	Particle interaction and viscosity.....	56
3.4.1	Introduction	56
3.4.2	Surface forces.....	56
3.5	Effects of plasticizers	58
3.6	The Particle-Matrix (PM) model.....	59
3.6.1	Introduction	59
3.6.2	Description of the model.....	59

3.6.3	Characterisation of the matrix phase	61
3.6.4	Mixing and testing of the matrix	62
3.7	Effects of fillers on the rheological properties of concrete	63
3.7.1	General	63
3.7.2	Literature review on the effects of fillers on the rheological properties.....	66
3.7.2.1	Filler modified cement paste (matrix).....	66
3.7.2.2	Filler modified mortar and concrete.....	68
3.7.2.3	Effects of mineral parameters	70
3.7.3	Concluding comments to the effects of fillers.....	71
4	HYPOTHESES	72
5	EXPERIMENTAL INVESTIGATIONS	73
5.1	Introduction.....	73
5.2	Test methods and calculations	73
5.2.1	Pozzolanic reactivity by thermo gravimetric analysis (TGA)	73
5.2.1.1	Relevance of the TGA method	73
5.2.1.2	Methodology of TGA	74
5.2.1.3	Precision of the TGA method	75
5.2.2	Concrete prism test (CPT).....	76
5.2.2.1	Relevance of the CPT	76
5.2.2.2	Repeatability of the CPT method.....	78
5.2.3	Accelerated mortar bar test (AMBT)	80
5.2.3.1	General.....	80
5.2.3.2	Modified conditions of the AMBT	81
5.2.3.3	Repeatability of the AMBT	81
5.2.4	Electron probe microanalyzer (EPMA).....	83
5.2.5	Optical microscopy	83
5.2.6	Test methods for matrix rheology	83
5.2.6.1	General.....	83
5.2.6.2	Matrix characterisation by the FlowCyl viscometer	84
5.2.6.3	Matrix characterisation by the Physica rheometer	86
5.2.7	Test methods for rheological properties of concrete	89
5.2.7.1	General.....	89
5.2.7.2	Slump-flow method	90
5.2.7.3	Testing of rheological properties by the BML viscometer	90
5.2.8	Chemical and mineralogical characterisation.....	91
5.2.9	Particle size distribution	91
5.2.10	Capillary suction and porosity.....	92
5.2.11	Other methods	93

5.3	Materials	93
5.3.1	Cements.....	93
5.3.2	Silica fume	95
5.3.3	Coarse and fine aggregates.....	95
5.3.4	Fillers	97
5.3.4.1	Description of the filler materials	97
5.3.4.2	Mineralogical and chemical composition of the fillers.....	98
5.3.4.3	Particle size distribution of the fillers	100
5.3.5	Plasticizers	101
5.4	Experimental programme	102
5.4.1	General.....	102
5.4.2	Pozzolanic reactivity.....	102
5.4.3	Alkali-silica reactions by the concrete prism test (CPT).....	103
5.4.4	Alkali-silica reactions by the accelerated mortar bar test (AMBT).....	105
5.4.5	Modified conditions of the AMBT.....	106
5.4.6	Parameter study of matrix rheology by the FlowCyl viscometer.....	107
5.4.7	Parameter study of matrix rheology by the Physica rheometer.....	108
5.4.8	Relationship between the rheological properties of matrix and self-ompacting concrete (SCC)	109
6	EFFECTS OF ALKALI-REACTIVE FILLERS IN CONCRETE - RESULTS AND DISCUSSION	111
6.1	Introduction	111
6.2	Pozzolanic reactivity of fillers in concrete	112
6.2.1	General.....	112
6.2.2	Pozzolanic reactivity at 20°C	112
6.2.3	Temperature effect on pozzolanic reactivity	113
6.2.4	Concluding discussion on pozzolanic reactivity	114
6.3	Alkali-silica reactivity	115
6.3.1	Introduction.....	115
6.3.2	Expansions due to ASR depending on the type of filler.....	117
6.3.2.1	Expansions by the concrete prism test (CPT)	117
6.3.2.2	Expansions by the accelerated mortar bar test (AMBT).....	119
6.3.2.3	Discussion of the observed differences between the AMBT and the CPT results.....	121
6.3.3	Expansions due to ASR depending on the particle size and the amount of filler.....	122
6.3.3.1	Expansions by the concrete prism test (CPT)	122
6.3.3.2	Expansions by the accelerated mortar bar test (AMBT).....	124
6.3.4	Expansions due to ASR depending on the alkali content and the temperature.....	126
6.3.4.1	Effect of NaOH addition on the expansion of concrete prisms.....	126
6.3.4.2	Effect of alkalinity on the expansion of mortar bars	127
6.3.4.3	Effect of temperature on the expansion of mortar bars.....	131
6.3.5	A limited study of the expansion in an early phase.....	132

6.4	Micro structure depending on the type of filler	134
6.4.1	General	134
6.4.2	Observations of textural changes and reaction products by optical microscopy	135
6.4.2.1	Specimens from concrete prism testing	135
6.4.2.2	Specimens from accelerated mortar bar besting	136
6.4.3	Observations and chemical analyses by the electron probe micro analyser (EPMA).....	136
6.5	Compressive strength and capillary suction depending on the type of filler ...	140
6.5.1	General	140
6.5.2	Influence of fillers on the compressive strength.....	140
6.5.3	Influence of fillers on the capillary suction.....	143
6.5.4	Concluding remarks on the compressive strength and the capillary suction ..	144
6.6	Summary and concluding discussion	145
7	EFFECTS OF FILLERS ON THE RHEOLOGICAL PROPERTIES OF FRESH CONCRETE - RESULTS AND DISCUSSION.....	148
7.1	Introduction.....	148
7.2	Influence of fillers on the rheological properties of the matrix.....	149
7.2.1	Introduction	149
7.2.2	Influence of fillers on the flow resistance ratio λ_Q	150
7.2.2.1	General.....	150
7.2.2.2	Effects of addition of fillers	150
7.2.2.3	Replacement of cement by filler	151
7.2.3	Influence of fillers on the plastic viscosity and the yield stress	155
7.2.3.1	General.....	155
7.2.3.2	Influence of different filler types	155
7.2.3.3	Replacement of cement by filler	159
7.2.4	Influence of different types and amounts of plasticizers on the rheological properties of the matrix	160
7.2.5	Combined effects of fillers and plasticizers on the rheological properties of the matrix	161
7.2.6	Combined effects of cements and plasticizers the on rheological properties of the matrix	163
7.3	Correlation between the rheological properties of SCC and the corresponding matrix phase.....	164
7.3.1	Introduction	164
7.3.2	Rheological properties of SCC.....	167
7.3.3	Influence of the constituent materials on the rheological properties of concrete.....	170
7.3.4	Relationship between the rheological properties of concrete and matrix	173
7.3.5	Concluding discussion regarding the relationship between concrete and matrix rheology	176
7.4	Summary and concluding discussion	17

8	CONCLUSIONS OF THE EXPERIMENTAL WORK.....	180
8.1	Effects of fillers on the pozzolanic reactivity and alkali-silica reactivity	180
8.2	Effects of fillers on the compressive strength	181
8.3	Effectss of fillers, plasticizers and cements on the rheological properties of the matrix.....	181
8.4	Correlation between the rheological properties of matrix and concrete.....	182
9	REFERENCES	183

APPENDICES

A1	Particle size distributions of fine and coarse aggregates
A2	Particle size distributions of filler
A3	Mix design of concretes tested by the CPT
A4	Mix design of mortars tested by the AMBT
A5	Mix design of self-compacting concretes
B1	Results of pozzolanic reactivity
B2	Concrete results – alkali-silica reactions, compressive strength and capillary suction
B3	Mortar results
B4	Electron probe microanalyzer, chemical data and photos
C1	Results of the matrix testing by the FlowCyl viscometer
C2	Results of the matrix testing by the Physica rheometer
C3	Self-compacting concrete – test results
D	Optical microscopy report with photos – concrete specimens
E	Optical microscopy report with photos – mortar specimens

Notations and definitions

Cement-chemical notations used in the thesis:

A	Al_2O_3
C	CaO
F	Fe_2O_3
H	H_2O
S	SiO_2
C_3S	$3\text{CaO}\cdot\text{SiO}_2$
C_2S	$2\text{CaO}\cdot\text{SiO}_2$
C_4AF	$4\text{CaO}\cdot\text{Al}_2\text{O}_3\cdot\text{Fe}_2\text{O}_3$
C_3A	$3\text{CaO}\cdot\text{Al}_2\text{O}_3$
CH	$\text{Ca}(\text{OH})_2$
CSH	calcium silicate hydrate products of the general formula $(\text{CaO})_x\cdot\text{SiO}_2\cdot(\text{H}_2\text{O})_y$

Other notations and definitions:

A	area
AAR	alkali-aggregate reaction
AMBT	accelerated mortar bar test
ASR	alkali-silica reaction
B	brittleness number
CPT	(Canadian) concrete prism test
D	length or diameter of a particle (m)
D_c	critical particle size
D_{10}	size of which 10 % of the particles are smaller
D_{50}	median particle size (50 % smaller particles)
D_{90}	size of which 90 % of the particles are smaller
DCS	degree of capillary saturation
DS	degree of saturation
E	modulus of elasticity
EPMA	electron probe microanalyzer
F	force
filler	aggregate particles or other mineral particles below 0.125 mm in diameter
G	shear modulus
HSOPC	high strength ordinary Portland cement
K	capillary number
m	resistivity number
matrix	the fluid phase of the PM model, cement, water, admixtures, filler, all powders of diameter < 0.125 mm
Na_2O -eqv.	weight % of Na_2O + 0.658 weight % of K_2O
OPC	ordinary Portland cement

PM model	particle-matrix model
powder	cement, filler, fly ash, silica fume and other powdered additions
PS	polished section
R	radius
RH	relative humidity
ROPC	rapid ordinary Portland cement
s/c ratio	silica fume/cement ratio (by weight)
SCC	self-compacting concrete
SEM	scanning electron microscope
SF	slump-flow measure
SROPC	sulphate resistant ordinary Portland cement
TGA	thermo gravimetric analysis
TS	thin section
v	velocity
V	volume
w/b ratio	water/binder ratio (by weight), binder includes cement and silica fume
w/c ratio	water/cement ratio (by weight)
w/p ratio	water/powder ratio (by weight)
WDS	wavelength dispersive X-ray spectrometer
XRD	X-ray diffraction
XRF	X-ray fluorescence
ε	strain
ε_{∞}	strain capacity of the matrix
γ	shear strain
$\dot{\gamma}$	shear rate
γ_c	fracture energy
η_{app}	apparent viscosity
$\eta(\dot{\gamma})$	viscosity function
λ_Q	flow resistance ratio obtained by the FlowCyl viscometer
μ	plastic viscosity
σ_0	tensile strength
τ	shear stress
τ_0	yield stress

1 Introduction

1.1 Background

The availability of good natural sources of concrete aggregates is limited in Norway, as well as in many other countries. The total natural sand and gravel resources are estimated to be about 12 000 million m³ in Norway. With the present rate of exploitation, these resources should theoretically last for about 450 years (Danielsen 2003). However, the volumes being available are much smaller than this due to the following reasons listed by Danielsen (2003):

- Restrictions on exploitation due to other area needs and local/national regulations
- Low suitability due to geological and technical reasons
- Unsuitable location in relation to the markets
- Protection of ground water
- Low profitability

Some of the Norwegian glaciofluvial deposits best suited for concrete purposes, located in the county of Rogaland, have an expected lifetime of less than 30 years with the present rate of exploitation. Even though many other resources have expected lifetimes up to 100 years, the importance to further develop the technology of production and utilization of crushed aggregates becomes evident. The production of crushed aggregates of good shape and grading generally generates large amounts of fines. These fines are presently to some extent classified as leftovers.

A major challenge for the aggregate producers is to achieve a balance between the produced fractions and the sold fractions. Some fractions may be dumped in the market at very low prizes, but normally there is still a need to deposit leftovers from the aggregate production. As an example, the aggregate producer NorStone, which has an annual production volume in the order of five million tonnes, deposits approximately 25 000 tonnes of fines from the washing process. Currently, the need to deposit other fractions is limited for NorStone, but this may change much over time. Going back some years, the situation was totally different, as large volumes of the 0-2 mm fraction had to be deposited. Utilization of all or some of the excess materials will give a positive contribution to the environment as well as increase the profitability.

The filler¹ fraction of the aggregate plays an important role in controlling many properties of concrete due to its great surface area. Properties of fresh concrete, i.e.

¹ The definition of filler in this work is particles with a diameter < 0.125 mm. The corresponding limit in NS-EN 12620 – “Aggregate for Concrete”, is 0.063 mm.

properties controlling mobility, stability and compactibility, can be greatly modified by different filler materials. Some fillers may also have a large influence on both durability and mechanical properties.

Recently, the development of self-compacting concrete (SCC) has created an increased need for good fillers. The main differences between ordinary concrete and self-compacting concrete of equal grade are the increased need for matrix, i.e. the fluid phase of the concrete, and the need to stabilise the matrix phase. In that respect, the addition of filler is the most economic and in most cases the best technical solution. This opens for the utilization of sand or gravel with high amounts of filler, as well as the development of industrial fillers. The finest parts of the sand, currently often removed by washing, might then be the most valuable part of the production volume.

Due to the fact that an important field of the utilization of crushed aggregates is for road surface applications (e.g. asphalt), many production plants are based on rocks with very good mechanical performance. In many cases this category of rock may be mylonite, and mylonites incorporating silica are classified as potentially alkali-reactive. An important matter when making use of alkali-reactive sources in cement-based materials is to know what effect these fines have on the long-term properties of concrete. Both positive and negative effects of alkali-reactive fines have been reported in the literature, as will be reviewed in Chapter 2.

Alkali-silica reactions of Norwegian aggregates are very slow, and it will typically take more than 15-20 years before serious damage occurs. This leads to the need for highly accelerated methods. Among the numerous existing methods the South-African accelerated mortar bar test (Oberholster & Davis 1986) and the Canadian concrete prism test (Can3-A23.2-14A) are recommended for Norwegian aggregates (Jensen 1993). The concrete prism test takes at least one year. When using pozzolanic materials, a longer testing time is often preferred. The accelerated mortar bar test, which requires only 14 days of exposure, has been used extensively around the world to test the effect of different mineral additives, even though the method was not designed for this purpose. In this investigation, both of these methods have been applied. An important issue of the work, in addition to clarify the reaction mechanisms for different types of fillers, has been to analyse to what extent these methods are useful in predicting the effects of different mineral fillers.

The studies of fresh concrete have been based on the Particle-Matrix (PM) model, which is described in Chapter 3. The effect of filler materials, cements and plasticizers, can then be verified by testing the matrix phase, which is the cement paste including the filler. During this project, the limitations of the PM model with respect to self-compacting concrete became evident. Studies of more sophisticated methods to describe the matrix phase were then incorporated in the studies, including a study of the relationship between the rheology of SCC and that of the corresponding matrix phase.

The study of the performance of alkali-reactive fillers in concrete has been carried out using Norwegian mylonite and Norwegian cataclasite, in addition to non-reactive fillers of different sources. Rhyolite from Iceland was included to get a wider range of materials. Additionally, crushed bottle glass, fly ash and silica fume have been included. There are several other possible alkali-reactive materials, which could possibly have given totally different performance than the chosen materials. The investigation of the performance of the present materials may be a contribution to a better understanding of the complex aspects of the influence of the particle size on alkali-silica reactions in concrete. The development of a full theoretical understanding on this very complex field is, however, out of scope of this work.

1.2 Objectives

The main objective of this study has been to develop knowledge to obtain a higher level of resource utilization in the production of crushed aggregates. The most central part of this has been to clarify the possibilities and limitations of using crushed rock fines in concrete. There has been a special focus on fillers from rocks classified as alkali-reactive, with special attention to mylonite filler from Tau.

The present work has focused on the utilization of fillers from two points of view:

1. Durability effects of fillers classified as alkali-reactive
2. Effects of fillers on the rheological properties of fresh concrete

The objectives of this study were as follows:

1. Examine the effects of using alkali-reactive and inert fillers in cement-based systems with respect to expansions due to alkali-silica reaction
2. Examine the effect of fillers of different origins on the mechanical properties.
3. Study the possibilities and limitations of using the accelerated mortar bar test to predict the long-term effects related to alkali-silica reaction
4. Examine the effects of different fillers on the flow resistance ratio of filler modified cement paste tested by the FlowCyl viscometer
5. Develop testing methodology for a more fundamental characterisation of the matrix phase than attained by the FlowCyl, and verify the relevance towards self-compacting concrete
6. Examine the effects of different fillers in combination with different plasticizers on the fundamental rheological properties of filler modified cement paste

1.3 Organisation of the thesis

A literature study reported in Chapter 2 gives the theoretical background for alkali-aggregate reactions in concrete. A literature review on the effects of filler materials on alkali-aggregate reactions is included. The theoretical background of fresh concrete properties is reported in Chapter 3, including a short review on effects of fillers related to fresh concrete properties. A variety of test methods are briefly discussed in the theory chapters. Chapter 4 presents the hypotheses which have been investigated within this study. A comprehensive description of the test methods used in the present study is given in Chapter 5. This chapter also gives an outline of the experimental work, as well as relevant information regarding the materials used in the present study. All results are presented in Chapters 6 and 7 together with discussions of the most important findings. The major conclusions are summarized in Chapter 8.

2 Alkali-silica reaction – theoretical background

2.1 Introduction

The alkali-silica reaction (ASR), or more general, the alkali-aggregate reaction (AAR), is a chemical-physical reaction between certain reactive aggregates and alkali-hydroxides in the concrete. The reaction forms a gel that in the presence of water might swell, which when restrained creates internal forces leading to degrading of the concrete. This chapter gives an overview of some important aspects regarding the alkali-silica reaction. Special attention is given to the effect of different particle sizes, and in particular the effect of fillers from alkali-reactive sources. A note is also included regarding effects of fillers on properties of hardened concrete other than those directly related to ASR.

2.2 Different alkali-aggregate reactions

Alkali-aggregate reactions (AAR) are generally classified into two groups, where the first group of alkali-silica reactions can be divided into two subgroups:

- 1 a): The fast alkali-silica reaction (ASR) was identified first, and it is generally the most rapid type of alkali-aggregate reaction. It occurs with silica of heterogeneous and porous structure, some of them are also hydrous. This “classical” type of ASR includes rocks as chert, opal and chalcedony; see Section 2.6.1 for details.
- 1 b): All of the observed Norwegian alkali-reactive rocks are considered to be of the so-called slow/late expanding alkali-silicate/silica reaction (SLEASS) (Jensen 1993). The alkali reactive rocks classified to this group are generally crystalline quartz-bearing rocks, and in many of these rocks strained quartz is believed to be the reactive component. The reaction of SLEASS can be distinguished from the “classical” ASR by a delayed onset of expansion in concrete prism testing, and generally it will take a very long time (up to 15-20 years) before serious damage occurs on concrete structures. Further information of Norwegian reactive rocks is given in Section 2.6.2.
- 2: A second type of AAR is the so-called alkali-carbonate reaction, which has been reported in association with dolomitic limestone. This type of reaction will not be treated here.

2.3 History of AAR

The alkali-aggregate reaction was first explicitly described in the literature by Stanton in 1940. At that time, he was able to demonstrate that severe cracking in a number of concrete structures in California, going back to the 1920s and 1930s, was basically a consequence of the characteristics of the cements and the aggregates

(Poole 1992). The high-alkali cements in combination with opaline aggregates were responsible for the observed deleterious reactions.

Since then, a great number of articles on this topic have been published, and eleven international conferences on AAR have been arranged. According to Diamond (1997), there were published approximately 1300 papers on AAR up to 1991, and surely several hundreds after 1991. Even though it is evident that there has been a tremendous development of knowledge of AAR up to now, and that many of the problems associated with utilization of potentially alkali-reactive aggregates have been solved, some of the more fundamental aspects of the reactions are still not fully understood.

The scientific fundament for the Norwegian knowledge of ASR was established in two research projects from 1988 to 1992, which are summarised in a Doctor Technicae thesis by Jensen (1993). However, the first publication regarding alkali-silica reaction was written as early as 1962 by Musæus, who performed a study on possibly alkali reactivity on phyllite (Jensen 1993). Kjennerud published in 1978 results from an investigation of a swimming pool as well as turbine foundations in a hydropower plant (Jensen 1993). He concluded that alkali-aggregate reactions were responsible for the damages in both cases. According to Jensen (1993), ASR was not enough confirmed to become accepted as a degrading mechanism for Norwegian aggregates until 1988. A review of the early Norwegian history of ASR is given in the doctoral thesis of Jensen (1993), while the recent Norwegian history of ASR is summed up in the thesis by Broekmans (2002).

National guidelines regarding ASR were published by the Norwegian concrete association in 1996, providing criteria for the use of potentially alkali-reactive aggregates (Norwegian concrete association 1996). New guidelines are to be published in 2004.

2.4 Effects of ASR

2.4.1 General effects

The most common observation on structures affected by ASR is development of cracks in the concrete surface. A surface not subjected to directional stress will develop an irregular crack-pattern, which is often referred to as map cracking. Other typical characteristics include expansion, gel exudations and misalignments of structural elements and “pop-outs” (Poole, 1992).

2.4.2 ASR in relation to other damaging mechanisms

The development of ASR often goes together with other damaging mechanisms, as reinforcement corrosion and frost damages, and the primary mechanism of damage may be difficult to decide. The cracks generated by ASR will open up the internal structure of the concrete and might then lead to an increased mobility of detrimental ions such as chlorides, then causing an increased risk of corrosion of reinforcement.

On the other hand, freezing and thawing may lead to increased crack intensity and crack widths. Further, this may lead to an increased mobility of internal and possibly external alkali and hydroxide ions towards the reactive aggregates, consequently giving a higher risk of ASR.

In steam cured concrete, delayed ettringite formation (DEF) together with alkali-silica gel have been observed as described by Shayan & Ivanusec (1995). Their results favoured the conclusion that in most cases where alkali-silica gel is found together with ettringite, the alkali-silica reaction is the primary cause of damage. In the systems they examined, they found no DEF in the cases where no ASR was detected. The term delayed ettringite formation, or secondary ettringite, is according to the common terminology related to internal sulphate attack. In particular, this term is related to ettringite formation in heat-cured concrete, where primary ettringite is thermally decomposed and forms again at later ages. However, according to Collepardi (2003), the term DEF should include ettringite formed at later ages, no matter the reason why the ettringite is formed. Ettringite is commonly found together with alkali-silica gel in concrete. Jensen (1993) reported that in thin-sections of concrete with deleterious ASR, ettringite-like crystals were found in 87 % of the samples. However, Jensen (1993) also found ettringite-like crystals in 66 % of the samples without ASR.

Collepardi (2003) discussed a holistic approach to the phenomenon of DEF, and listed three essential elements for the formation of DEF:

- Micro-cracking
- Exposure to water
- Late sulphate release

Micro cracking may be caused by alkali-aggregate reactions, but there are also a number of other mechanisms that may cause micro cracks, e.g. freezing/thawing cycles, plastic shrinkage, dynamic loads etc. The excess to water is also essential for the formation of deleterious ASR, and will be further discussed in Section 2.8. Due to the absorption of water by the alkali-silica gel, concrete with ASR may maintain high moisture content, and thereby be more vulnerable to the formation of ettringite. The mechanisms of delayed ettringite formation are not yet fully understood. Whatever the mechanisms of ettringite formation are, it may cause additional cracking and expansion of the concrete.

2.4.3 Structural effects

The consequences of ASR on structural members may be difficult to estimate. Generally, ASR may cause substantial reduction in engineering properties. Swamy & Al-Asali (1988) reported that at an expansion of 0.1 %, the reduction in flexural strength was nearly 50 %, and about 20 % for the dynamic modulus of elasticity. At an expansion of 0.6 %, the reduction in compressive strength was 40 %, whereas the

loss in flexural strength was as high as 75 %. They stated, however, that the losses in engineering properties do not occur at the same rate or in proportion to expansion. It is therefore doubtful if given values of expansion limits can be specified for all types of structures, and critical limits need to be defined according to the actual type of structure.

Jones & Clark (1997) also reported a reduction in compressive strength, the degree of reduction increasing with increasing expansion. Further, they reported the loss in E-modulus to be generally caused by micro cracks, with substantial reduction in the E-modulus even at low expansions. The direct tensile strength of concrete is also reported to be significantly reduced by ASR.

The actual situation in a structure is much more complicated than what has been described above, due to the restraint effect by the reinforcement. Jones & Clark (1997) reported that the E-modulus was significantly higher on cores removed from the direction of restraint than those removed in the perpendicular direction. A similar effect on compressive strength, though smaller, has also been found. The prestress developed by the ASR expansion is also reported to increase the shear strength and stiffness of beams.

The expansion caused by ASR may cause significant problems. The Elgseter Bridge in Trondheim, which was built in 1950, is an example of a Norwegian structure with severe damages caused by ASR. The structure is a 220 m long continuous beam bridge supported by eight rows of columns. Each row consists of four columns with a diameter of 800 mm. Jensen (2000 and 2003) has described the problems related to severe alkali-silica reactions. The inspection of the bridge in 1991 revealed that the expansion joint, originally 20 cm, was only 1 cm at that time. The reason for the reduced expansion joint is most likely due to overall expansion of the bridge, possibly in combination with landslide of abutments. In the columns, several vertical cracks with a maximum crack-width of 2 mm were found. The cracks can be followed from the ground level to the underside of the beams. Monitoring of moisture and crack developments was established in 1995, and a pilot project searching for possibilities to reduce the humidity is in progress (Jensen 2003). According to Wigum & Thorenfeldt (2003), there is a need to strengthen the columns. They have reported a set of laboratory experiments with wrapping of columns with carbon fibre reinforced polymer sheets. The results indicate that the wrapping is capable of hindering the volume expansion caused by the ASR.

Further discussions of structural effects and repair and maintenance of affected structures is out of scope of this work. However, this is believed to be a very important field that needs further research.

2.5 Mechanisms of reaction

2.5.1 General

There exist different views on the fundamental aspects of the reaction mechanisms. According to Chatterji & Thaulow (2000), there have been proposed two contrasting mechanisms regarding the fundamental aspects of ASR, the one by Powers and Steinour (1955a,b) and the other by Chatterji et al (1986, 1992). Despite the fact that these theories share some elements, they differ significantly in the role of the calcium ion. While Powers and Steinour (1955 a,b) claimed that in the presence of calcium, a non-swelling calcium-alkali-silica complex is formed, Chatterji et al. (1986, 1992) claimed that calcium has the opposite effect, i.e. calcium causes a gel with a high potential to swell. A third mechanism, where the expansion is claimed to be depending on the electrostatic repulsion between the electrical double layer that form around electrically charged silica particles, has recently been proposed (Prezzi et al. 1997, Rodrigues et al. 1999). However, there are other views on ASR than those described above. Some of these may share some elements from one or two of the theories described above, while other may differ completely. One such view is represented by a paper by Wang & Gillott (1992), where the alkali-silica reaction and the pozzolanic reaction are considered to be competing reactions going on at the same time, involving the same materials.

In the following, some fundamental aspects of the mechanisms of the alkali-silica reaction will be discussed. Most of the published work regarding mechanisms of ASR is based on observations for reactions of the fast or classical type. As will be further discussed in section 2.5.5, many of the fundamental aspects are anyhow comparable for the fast type and the slow/late type of reaction.

2.5.2 Dissolution of silica

According to Glasser (1992), the chemistry of the alkali-silica reaction can be described as a 3-step process. Initially, the high-pH fluid reacts with the siloxane (Si-O-Si) bonds to form OH-groups (silanol-groups) on the interface of the silica as seen in Figure 2.1. While the attack from alkali-hydroxides is slow and mainly takes place on the surface in the case of well-crystallised silica, poorly crystallised (and especially hydrous) silica permits penetration of alkalis and hydroxide into the reactive particles (Dent Glasser & Kataoka 1981).

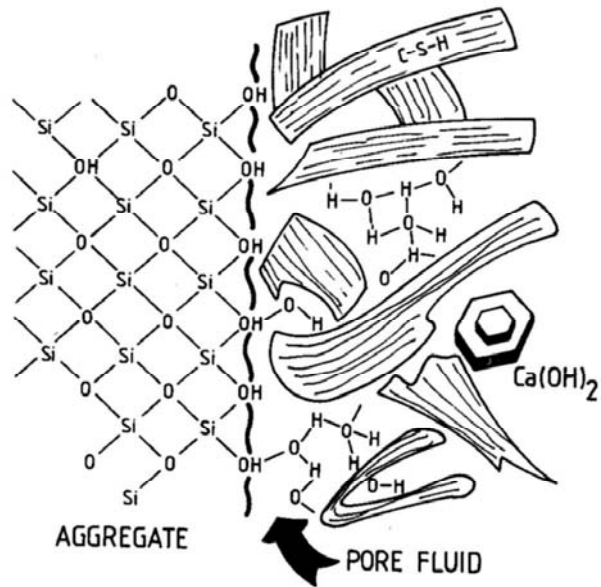
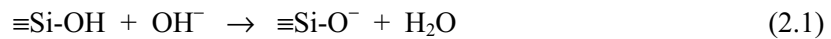
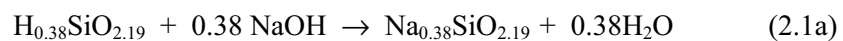


Figure 2.1 Illustration of the microstructure of the interface between the cement paste and the siliceous part of an aggregate. From Glasser (1992).

The following chemical process can be expressed by 2 steps as described by Dent Glasser & Kataoka (1981):

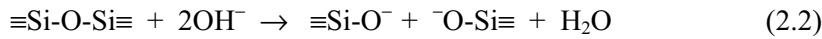


The silanol groups are acidic, and the reaction with the basic pore solution (2.1) is an acid-base reaction. The negative charges are balanced by cations, and the overall stoichiometry of the reaction can be represented as:

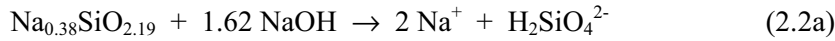


In this case, the charge is balanced by the sodium cation, but other cations may also participate. This step can be regarded as an exchange of sodium for protons, without any breakage of Si-O-Si bondings.

If more hydroxide ions are available, this will, however, promote an attack of the siloxan-bridges and a disintegration of the silica structure:



In the case of sodium-cations the overall reaction can be written as follows:



It should be noted that the dissolution of silica is not so much controlled by the alkalis, but rather by the hydroxide ions. Dissolution of silica is an essential parameter in controlling the alkali-silica reactivity, and in a recent review by Broekmans (1999), some fundamental considerations with respect to silica dissolution have been summed up. According to Broekmans (1999), a further deprotonization from the final stage in equation (2.2a) may happen at high pH like in concrete.

The dissolution of silica is highly dependent of the pH of the pore water. A higher pH gives an increase in the dissolution rate. Other important controlling factors involve the silica particle size (an increase in solubility with decreasing particle size for a convex surface), and the form of silica, i.e. polymorphs and quality of crystal lattice. The latter points will be further discussed in section 2.6. Temperature is also an important factor. Generally, the solubility of silica increases with increasing temperature (Rimstidt 1997, Dove & Rimstidt 1994). This is illustrated in Figure 2.2, which also shows the solubility of different silica structures.

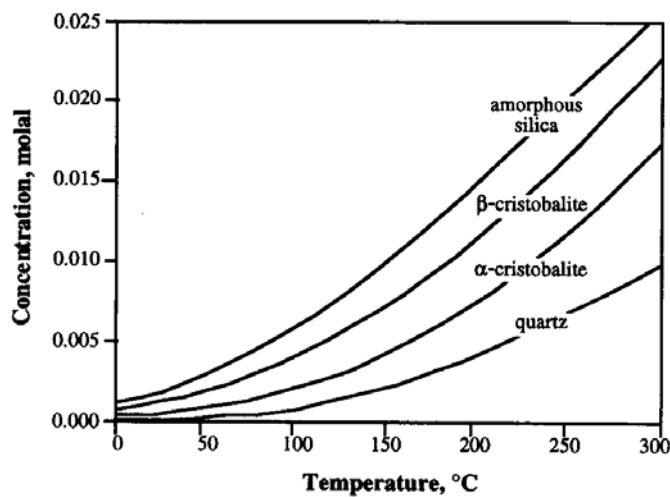


Figure 2.2 Solubilities of quartz, cristobalite and amorphous silica in water. From Dove & Rimstidt (1994).

2.5.3 Formation and swelling of alkali-silica gel

The chemical solubility reaction is followed by the formation of an alkali-silica gel. This gel is generally not a pure silica gel, but will normally include significant amounts of sodium, potassium and calcium. Many scientists have published chemical data on alkali-silica gels, some of these have been compiled by Poole (1992). The variety in chemical composition is large. As an example, the quantity of CaO varies from nearly zero to 30 %. Also the span of variation in alkalis is great, from about zero to 17.9 % and 13.9 % for Na₂O and K₂O, respectively. The viscosity of the gels varies, as their chemical composition does, but generally the gels tend to be less viscous as they gradually absorb moisture and swell. The effect of the moisture condition in concrete will be treated separately in Section 2.8

Jensen (1993) studied the reaction products of Norwegian concretes. He found three types of reaction products: 1) amorphous gel (sometimes laminated/ recrystallized), 2) cryptocrystalline reaction products and 3) lamella crystals/ fan-shaped agglomerates. A comprehensive list of chemical data for the reaction products, both including field concrete and laboratory concrete, can be found in the thesis of Jensen (1993).

There have been performed some studies of synthetic gel, and Krogh (1975) reported that both sodium-silica gels and potassium-silica gels swell, even though the deformation properties of these seem to be different and that Na₂O generally seem to give less expansion in mortar than an equal amount of K₂O. Also the gel high in sodium and silica, but low in calcium did swell. On the other hand, the gels low in sodium, both with low and high calcium amounts, did not swell at all.

Diamond et al. (1981) carried out experiments on synthetic sodium silicate gels of different chemical composition. Gels of different Na₂O: SiO₂-ratios and different calcium amounts were studied. The sorption isotherms showed a behaviour that was expected to the authors, where the gels high in sodium gave the highest water-binding capacity. The span of water content went from about 30% to 160% of ignited solids. Calcium had no special influence on the results. They also carried out tests to measure free swelling with water access through a membrane, and in a companion experiment the gels were confined by a piston loaded with just sufficient force to prevent swelling, the loading was adjusted throughout the experiment. Results from free swelling gave no correlation with chemical composition, and consequently not with the sorption isotherms. The gels showing large free swelling expansion did not necessarily develop high restrained swelling pressures. This is in accordance with Dent Glasser & Kataoka (1981), who have stated that there should not be expected to be a general correlation between the amount of free expansion and the pressure generated by a constant volume because the compressibility varies enormously. The range of free swelling was from a few percentages to almost 80 %. The range of swelling pressure was wide, from very small pressures hardly significant, to pressures of 11 MPa. The calcium bearing gels reached modest swelling pressures, but higher than many of the pure soda-silica gels. An unexpected

finding was an aging effect of the gels. Highly expansive gels gave practically no expansion when they were retested after four months of sealed storing at room temperature.

According to Diamond (2000), it is often suggested in the literature that there are at least two distinct phases of alkali-silica gels. One is rich in Ca and tends towards an alkali-rich CSH of non-swelling behaviour, while the other traditional swelling gel is composed of alkali-silicate hydrate and only minor amounts of Ca. Even though the gels rich in calcium often are considered non-swelling, Diamond (2000) points out that some authors dispute this. Thomas 1998 (in Diamond 2000) claims that some Ca is necessary to produce gel, without Ca the silica simply dissolves in alkaline solutions. Some of the aspects of the role of calcium are further discussed in Section 2.5.4. To conclude, the behaviour of alkali-silica gels seems to vary over a wide range, but the consequences of different chemical compositions seem to be unclear at the moment.

According to Diamond et al. (1981) the distress in concrete by alkali-silica reaction can be divided into two distinct stages:

1. A chemical reaction, degrading of the silica and formations of an alkali-silica gel.
2. A physical or physiochemical sorption of pore fluid by the gel, which in turn may produce swelling, then leading to overall expansion and cracking

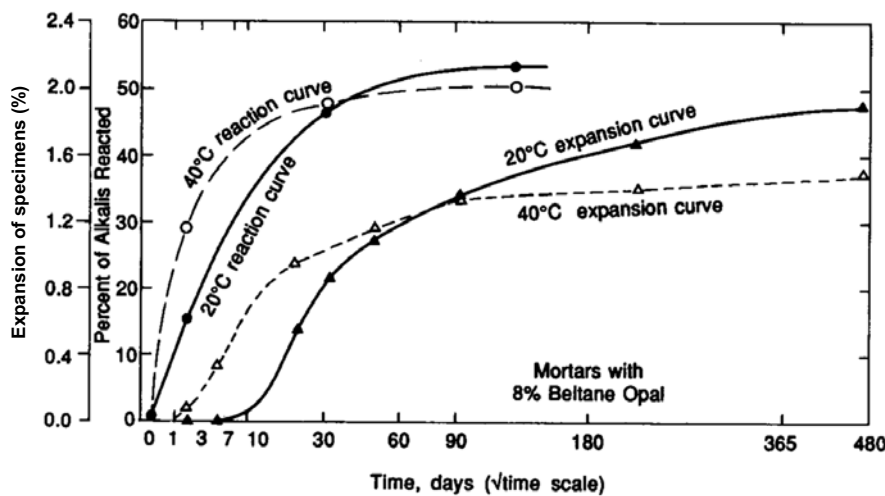


Figure 2.3 Reaction parameter curves vs. expansion curves for sealed mortar specimens at 20°C and 40°C. From Diamond et al. (1981).

The kinetics of the first step can be monitored by following the rate at which alkalis are withdrawn from the pore solution as they become incorporated into the gel. The kinetics of the second stage is followed by expansion measurements. This is illustrated in Figure 2.3 where the expansion curves are delayed compared to the reaction curves. Also note the difference in expansion with temperature, where the specimens stored at 20°C showed a slower initial reaction, but later on reached higher expansion than the specimens stored at 40°C.

The basic mechanism of the swelling process has been debated throughout the history of ASR. Hansen (described in Powers & Steinour 1955a) developed a theory that the expansion of concrete results from hydraulic pressure generated through the process of osmosis. Osmosis, as generally understood, requires a solution, an external supply of solvent and a semipermeable membrane between the solution and the solvent. He then considered the solution to be aqueous sodium silicate, the solvent to be water, and the membrane to be cement paste. Observations described by Powers & Steinour (1955a), e.g. fractures developed through the central part of the aggregate, without evidence of present fluid, hardly makes it likely that fluid pressure is the cause of the cracking. Powers & Steinour (1955a) described that when the solution is a solid (gel), the semipermeable membrane is not essential to develop osmotic pressure. The driving force of the volume increase is the difference in Gibbs free energy between the water in an aqueous solution and the water adsorbed by a solid. When equilibrium does not exist, the water will tend to move from the solution to the gel to diminish the free energy, a process which will generate pressure if the gel is confined. Powers and Steinour (1955a) wrote:

“Expansion is produced when the alkali-silica complex imbibes water. The initial, most damaging expansion probably occurs while the reaction product is still solid, though expansion may occur after the product becomes plastic or fluid, if initially formed cracks have no outlets. The force is that of swelling pressure or osmotic pressure (hydraulic), the two being fundamentally alike.”

Prezzi et al. (1997) proposed a theoretical model for the expansion of the reaction product based on the double-layer theory. The model is based on swelling caused by the repulsive forces generated by an electrical double-layer. According to Prezzi et al. (1997), the theory could explain the reduced expansion normally obtained when using pozzolanic materials, as these tend to produce gels with a high CaO/Na₂O-equivalen ratio. The theory predicts lower expansive pressures as the number of bivalent ions relative to monovalent ions is increased.

2.5.4 The effect of calcium hydroxide (CH) on the ASR

As was mentioned in Section 2.5.1, there exist different views on the role of CH. According to the hypothesis developed for opal by Powers & Steinour (1955a,b), the ratio between lime and alkalis is a major controlling factor. A high enough amount of lime at the reaction site gives a non-expansive lime-alkali-silica complex, while a small amount of lime gives a swelling alkali-silica gel. The lime must diffuse to the reaction site, through the thin lime-alkali-silica layer initially formed at the silica

particle. The thicker the reaction layer and the higher the alkali concentration, the more difficult it should be for the lime to reach the reaction site fast enough to produce a non-swelling complex. According to this hypothesis, the reaction of lime may release some of the initially reacted alkalis. Consequently, a regeneration of alkalis free to further reactions will occur.

Dent Glasser & Kataoka (1982) carried out experiments on model systems of silica gel, sodium hydroxide and calcium hydroxide. They found that if considerable amounts of calcium ions remained in solution, CSH forms. After that, the systems behave in the same way as model systems without calcium. The reaction between silica, calcium and water to form CSH is a pozzolanic reaction; see Section 2.11.2 for further discussions of the similarities between the alkali-silica reaction and the pozzolanic reaction.

The hypothesis by Chatterji et al. (1986, 1992) differs in the role of CH. According to this hypothesis, the CH accelerates the penetration of alkalis, calcium, hydroxide and water into the reactive grain. Further, it hinders the diffusion of SiO_2 out of the reactive grain. Additionally, it acts as a buffer to maintain a high hydroxide concentration. The model predicts expansion and cracking to occur if the amounts of water, alkalis, calcium and hydroxide that enters the particle are larger than the amount of alkali-silica gel being able to seep out of the particle.

The view of Chatterji et al (1986, 1992) is basically confirmed by the work of Wang & Gillott (1991). They concluded that the presence of CH worsens the ASR and increases the expansion of mortar bars containing opal. They stressed the importance of CH as a buffer to maintain a high concentration of hydroxide ions, i.e. high pH. Additionally, the calcium ions may exchange for alkali ions, then releasing alkalis being important to produce a reactive alkali-silica complex. However, the exchange of calcium ions for alkali ions in the swelling alkali-silica complex may produce a non-swelling lime-alkali-silica complex.

Struble 1987 (reported in Jensen 1993) made a set of experiments of opal, limestone and a solution being similar to the normal pore solution in concrete. No cement was added. The experiments showed that the opal simply dissolved, and in the absence of hydration products, no gel was formed. The conclusion from these experiments was that the calcium is necessary to produce an alkali-silica gel.

The role of CH seems confusing and complex, but there is clear evidence in the literature that at least some CH is essential to produce a gel of swelling nature. The similarity between the alkali-silica reaction and the pozzolanic reaction seems obvious; this will be treated further in Section 2.11.2. According to Diamond (2002), the gel may start as a labile alkali-silica sol, migrate, and pick up some calcium to become an expansive calcium-alkali-silica gel. Further, the gel may pick up more calcium and loose some alkali and end up as an alkali rich CSH, which is not expansive.

2.5.5 Observations for slowly reacting aggregates

Most of the reported work regarding mechanisms is based on experiments and observations on quickly reacting aggregates such as opal and flint, while the fundamental mechanisms for slowly reacting aggregates have been less investigated. The span of reactive components in rocks (which will be discussed separately, see Section 2.6) is very wide, and the dissolution reaction, which is the first step, is generally much faster for the classical type of alkali-silica reaction. There are anyhow reasons to believe that in some aspects the fundamental mechanisms are similar for the fast and slow reaction types. In both cases there are a breakdown of silica and a formation of gel, which in turn under certain conditions is able to swell and set up large expanding forces. According to Grattan-Bellew (1992), the main difference between the two types of reactive aggregates is the amount of soluble materials in each case. In the classical ASR as with opal, most of the material is soluble, while in the second slow type, only a minor quantity is soluble. The small amount of soluble silica may account for the late onset of the expansion relative to the faster classical reaction.

It is a well-known fact that most of the reactive aggregates of the classical type have a pessimum proportion of reactive aggregate, which gives the highest expansion. Or more precisely, there is a certain proportion of reactive aggregate to alkali-hydroxide ratio that produces the highest expansion. An increase in the amount of reactive aggregates above this pessimum value may reduce the expansion due to lack of alkali hydroxides. According to Lagerblad & Trägårdh (1992), slowly reactive Swedish aggregates do not show any pessimum behaviour, and to the author's knowledge there has not been observed any pessimum behaviour for Norwegian aggregates either. A logical explanation for this difference from the faster reacting aggregates is the much smaller amount of soluble silica as discussed by Grattan-Bellew (1992).

Jensen (1993) proposed a hypothesis on the development of alkali reactions in Norwegian slow/late aggregates based on petrographic examination and SEM/EDAX analyses of reacted concrete. He described a peripheral dense rim on reacted aggregates and the occurrence of wider interfacial cracks between individual mineral grains. He further suggested that the volume expansion caused by swelling pressure between individual crystals inside a grain in the aggregate may cause tension crack, and that these cracks subsequently can be extended to larger cracks. The expansive forces were considered to be caused by a combination of volume expansion of individual aggregates, and swelling of gel in the cement paste outside the reacted grains. Reaction products include both amorphous gel and cryptocrystalline reaction products.

The postulated reaction mechanism by Jensen, where the starting of the reaction may be in the middle of a coarse aggregate, has also been described by Lagerblad & Trägårdh (1992), who described the reactive grains to be “dissolved from the inside”. It might be difficult to understand how alkali hydroxides are able to

penetrate the dense crystalline aggregates. However, the fact is that aggregates believed to be impermeable, not always are. Data from Powers (1958) show that the coefficient of permeability of granite lies in the same region as for cement paste of w/c ratio of 0.7. This surprising fact indicates that migration of ions into the interior of the aggregate grains may easily take place.

Wigum (1996) has, based on a study of different reactive rocks by the accelerated mortar bar test, described the reaction pattern for slowly reacting aggregates. He described two main processes taking place; one process of dissolution and one process of cracking. He stated that the process of dissolution appears to produce the largest amount of gel, but the process causing cracking appears to contribute most to the expansion and also relates to the rate of expansion. There are similarities between the observations made by Wigum (1996) and those by Diamond et al. (1996) as discussed earlier, both distinguishing between the dissolution reaction taking place first, and the subsequent expansion and cracking.

2.6 Alkali reactive minerals and rocks

2.6.1 General

Even though other minerals than silica could possibly cause ASR, silica is believed to be the most important component in this respect. About 12 volume % of the entire earth's crust is made of the more or less pure oxide SiO_2 , which may exist as about 9 silica polymorphs (the exact number is according to Broekmans (1999) a matter of debate). The most common polymorph is the α -quartz. But also the high-temperature modifications tridymite and cristobalite may be present as a metastable form in young rocks (hardly of relevance concerning Norwegian rocks). Because tridymite and cristobalite are thermodynamically unstable, they are more prone to dissolution than the more stable α -quartz, and they are known to have a potential of giving deleterious ASR (Broekmans 1999).

Other silica forms that are known to behave deleteriously in concrete include chert/flint, opal and chalcedony. These are rather to be regarded as rock-names, and they are strictly speaking not silica polymorphs. Other important reactive silica forms include volcanic glass. Especially acidic volcanic glass in rhyolite, dacite and andesite as well as Icelandic basalts have proved to be alkali reactive (Jensen 1993). Artificial glasses are also reported to be deleterious in concrete.

2.6.2 Norwegian reactive rocks

In Norway, both igneous rocks, as well as sedimentary and metamorphic rocks, have been proved to be deleterious under field conditions (Jensen 1993). The group of cataclastic rocks (cataclasites and mylonites) developed by dynamic metamorphism is very important in Norway, and Jensen reported in his thesis that about 50 % of the deleterious ASR found in structures was caused by cataclastic rocks containing quartz and feldspar. The problems associated with Norwegian cataclastic rocks have

been further studied in the doctoral works by Wigum (1995a,b) and Broekmans (2002). In the present study, fillers from cataclastic rocks have been investigated.

Regarding alkali reactivity of the slow/late types as for all Norwegian reactive aggregates, microcrystalline quartz and/or quartz with lattice defects (strained quartz) are believed to be the reactive component. As discussed by both Jensen (1993) and Wigum (1995b), the use of rock lists based on traditional mineralogical classification is not adequate. A micro structural investigation is necessary to identify potentially deleterious rocks. As an example of this, the mylonite incorporated in the present study was originally classified as quartz diorite by its mineralogical composition. However, micro textural examination showed that the rock more correctly should be classified as mylonite due to its texture. Tests by the concrete prism test (see description of the method in Section 5.2.2) have confirmed the deleterious behaviour of this rock.

Jensen's micro structural investigation of reacted Norwegian aggregates showed that the grain sizes of the reactive quartz are generally small. He found two populations, the finer population with average grain sizes of 12-20 μm , and the coarser population with the average between 36-60 μm . For Norwegian conditions, the grain size of quartz is believed to be the major controlling parameter. According to the rock list for petrographic analyses, all microcrystalline quartz (grains size < 60 μm) should be classified as alkali reactive, while grain sizes in the range between 60 and 130 μm are classified as possibly alkali reactive (Norwegian Control Council for Concrete Products 2003). Quartz of grain sizes larger than 130 μm are believed to be innocuous, also including strained quartz.

The cataclasis is caused by dynamic metamorphoses and occurs mostly in thrusts and faults. The textures of the cataclastic rocks vary widely, and are generally dependent on the origin of the rock as well as the conditions during the deformation process. A general effect of the cataclasis is, however, a reduction in grain size. The matrix of the rocks can become more or less recrystallized. The grain boundaries of strained quartz can polygonize to produce small interlocking quartz crystal, so called subgrains. Wigum (1995a) have showed that the alkali reactivity of cataclastic rocks is clearly related to the total grain boundary area of quartz, a parameter he found to be strongly influenced by subgrain development.

Wigum (1995a) and Broekmans (2002) examined the crystallinity index of quartz as a quantitative measure for potential reactivity. The hypothesis was that the crystallinity index summarises irregularities and lattice defects into one index to compare different quartz types. However, there appears not any straightforward correlation between the crystallinity index and the reactivity as expressed by the accelerated mortar bar test.

2.6.3 Effect of the particle size

2.6.3.1 Literature review on the effect of the particle size

Stanton first discussed the relevance of the particle size in 1940, where he demonstrated that the amount of expansion was related to the particle size (Diamond & Thaulow 1974). Reactive aggregates in the range from about 0.17 – 0.6 mm gave greater expansion than the coarser sizes. The aggregate in this case was a siliceous magnesian limestone, containing opal and chalcedony. Vivian found in 1951 a similar pattern when studying the same aggregate (Diamond & Thaulow 1974). However, he found that aggregate sizes smaller than 50 μm gave no expansion at all, while the fraction between 50 and 70 μm caused a delayed expansion.

Results from another study of Vivian (in Hobbs & Gutteridge 1979) using Australian opaline rock as the reactive constituent (5 %) together with non-reactive aggregate are presented in Figure 2.4. The period where no expansions occurred seemed to be prolonged for the particles below 150 μm . The expansions were subsequently high for all particle sizes down to 50 μm . No expansion was observed for particles below 50 μm . The storing temperature was 20°C in this set of experiments.

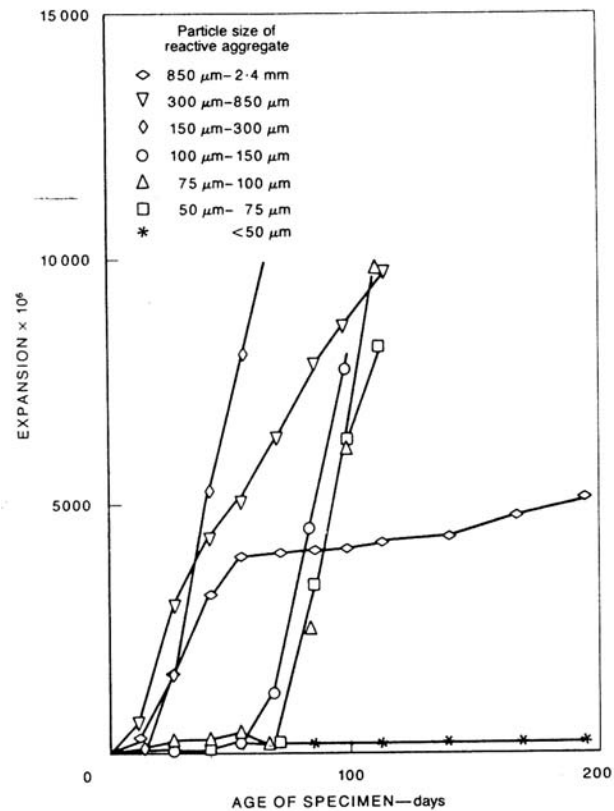


Figure 2.4. Effect of particle size on expansion of mortar bars (5 % reactive aggregate). Results from Vivian, in Hobbs & Gutteridge (1979).

Diamond & Thaulow (1974) carried out an investigation with opal of α -cristobalite type, which was crushed and sieved into fractions down to 20-30 μm . Standardised non-reactive sand was used as reference aggregate, while 5 or 10 % crushed opal of different sizes was added to the mortars. The specimens (cylinders with a diameter of 10 mm and a length of 20 mm) were stored above water at a temperature of 20°C. Results after approximately 300 days of exposure are given in Table 2.1.

Table 2.1 Effect from different ranges of particles on expansion. Data from Diamond & Thaulow (1974).

Size range (μm)	% expansion (5 % opal)	% expansion (10 % opal)
Appr. 150-125	0.65	1.61
125-90	0.52	1.74
90-74	0.77	1.49
74-53	0.57	1.77
53-44	0.89	2.08
44-30	0.54	2.81
30-20	0.13*	2.08

*Represents mean value of 3 cylinders, expansions for 2 of these were 0 or close to 0.

The results presented in Table 2.1 show that 10 % opal gave significantly higher expansions than 5 %. However, the results did not give evidence to any significant effect of the particle size, as all particle sizes were capable of producing large expansions.

Hobbs & Gutteridge (1979) examined Beltane opal of different fractions in the range from 150 μm to 4.8 mm. They made mortars with different amounts of reactive materials (from 1 to 20 %). Each fraction was tested separately in combination with non-reactive sand. The specimens (25 x 25 x 250 mm) were stored at a temperature of 20°C in water. For a given content of Beltane opal, the expansion increased with decreasing particle size. This effect was pronounced for an opaline content in the range between 4 and 6 %. However, they found that the age at which cracking occurred was independent of the particle size. Further, they found that the reaction rate is basically dependent of the volume of reactive particles and not the particle surface area. A noteworthy difference between the investigation of Hobbs & Gutteridge (1979) and that of Diamond & Thaulow (1975), is that Hobbs & Gutteridge observed intensive cracking in the specimen, while Diamond and Thaulow observed much less cracking than could be expected from the large expansions. The large differences in specimen size may be responsible for some of the observed differences in cracking intensity.

Qinghan et al. (1996) reported that use of a powder from an alkali reactive rock has proven to suppress the expansion caused by the alkali-silica reaction. They used a reactive andesite with α -cristobalite as the primary reactive component, ground to Blaine-values in the range from 290 to 1133 m^2/kg . The prisms of size 40 x 40 x 160 mm were autoclaved before they were stored at a temperature of 45°C for long term measurements. The powders were used as cement replacers in this study, while NaOH were used to adjust the alkali level in the range from 0.5 to 3.0 % Na_2O eqv. Generally, all fillers gave a reduced expansion when replacing cement. The effect on reduced expansion was greater for the finest fractions.

Icelandic rhyolite, known to be alkali reactive due to the content of volcanic glass, was earlier used as an admixture in Portland cement to produce pozzolanic cement and have proven to be an effective pozzolan according to Gudmundsson (1975). The production of pozzolanic cement is today, however, mostly based on silica fume, due to the higher pozzolanic activity of silica fume compared to rhyolite filler. In order to get a wider range of alkali reactive materials than those found in Norway, rhyolite from the same source has been investigated in the present work.

Lagerblad & Trägårdh (1992) reported that for Swedish slowly reacting aggregates the particle sizes (1-2 mm) cause greater expansions than the coarser sizes. This contradicts observations in structures, where the larger fractions were found to be as deleterious as the sand fractions. The expansion tests were performed using the Danish method (TI-B 51), where the prisms are stored in 50°C NaCl solution.

In Norway, thin section examinations of reacted concrete from structures seldom show particles sizes less than 1 mm to have reacted (Jensen 1993). Wigum et al. (1996) reported that the coarser particles seem to contribute more to the total expansion than the finer particles when tested in the accelerated mortar bar method (see Section 5.2.3). Further, for most of the samples Wigum et al. (1996) found that the finest particles, below approximately 0.30 mm, did not react. In a study by Mørtzell and Wigum (reported in Wigum 1995b), substitution of innocuous material with reactive materials showed that reactive material in the finer fraction (0.15 to 0.8 mm) gave the highest expansion. The corresponding experiment with reactive material in the larger fractions (0.8 to 4.8 mm) gave significantly lower expansion. A similar test with the same total quantity of reactive material (50%) equally distributed in all fractions gave an even smaller expansion. The described differences were observed for all ages above 28 days, while there was no significant difference at 14 days of exposure. When performing tests by the accelerated mortar bar test (described in Section 5.2.3), the filler fraction (< 0.15 mm) is removed, and no information regarding the influence from materials in the finest fraction was reported in the tests of Mørtzell and Wigum.

Nishibayashi & Yamamura (1992) reported that fine reactive aggregates gave a considerably higher expansion than the same proportion of coarse reactive aggregates. The prisms were stored at 100 % RH and 40°C.

Zhang et al. (1999) performed a study on the influence of the aggregate size. The finest fraction (0.15- 0.80 mm) had the greatest influence on the expansion, while coarser sizes caused less expansion. The reactive aggregate tested in this study was a quartz glass. The tests were performed by a method involving steam curing at 100°C followed by autoclaving at 150°C in a 10 % KOH solution)

During the years, several studies of crushed glass utilized as concrete aggregates have been published. Generally, the glass is very deleterious, causing large expansions and damages. However, fine fillers of glass have been reported to cause the opposite effect, i.e. a reduced expansion tendency. Shao et al. (2000) have shown

that glass fillers smaller than 38 μm are able to reduce the expansion relative to the control mortar containing no glass filler. This fine fraction of glass exhibits a pozzolanic behaviour that may explain this effect, and an increase in strength was also observed for this filler. The coarser fractions had less effect. The experiments were performed using the accelerated mortar bar test; see Section 5.2.3. Hudec & Ghamari (2000) reported a similar set of experiments, where glass fractions below 75 μm reduced the expansion. On the other hand, fractions larger than 75 μm gave a tendency of increased expansion of the mortar bars.

The speed of the alkali-silica reaction may increase as the particle size is reduced, simply because the specific surface area is larger for smaller particles. This has been shown by Bazant et al. (2000), who studied the effect of the particle size of waste glass. They found that for large particles, a decrease in particle size caused a larger expansion. Their intuitive explanation of this was that given smaller particle sizes, a larger volume fraction of glass undergoes ASR due to the increased surface area per volume unit of glass. This causes larger pressures. However, they found a pessimum size of approximately 1.5 mm. Below this limit, the expansions were reduced, and below 0.15 mm the expansions was the same as for specimens with no glass. This may be explained by fracture mechanics, as will be further discussed in Section 2.6.3.2.

2.6.3.2 Fracture mechanical approach to the effect of the particle size

The fracture mechanical approach to the size effect may be useful because fracture mechanical effects may count for some part of the observed differences in expansion behaviour caused by the particle size. In the following, a short note on the fracture mechanical effects caused by the particle size is given.

Bache (1984) has treated the fracture mechanical aspects of relatively stiff aggregate particles embedded in a matrix of cement paste. The system of a shrinking matrix around a stiff particle or an expanding particle in the same matrix may be treated equally. Given that the expansion caused by the particle is greater than the strain capacity of the cement paste, a composite with a large particle in a matrix will always lead to local fracture and cracking. On the other hand, if the particle is small, cracking may not be initiated even if the strain capacity of the matrix is exceeded. The reason for this is that cracking will only occur if the total deformation of the particle is greater than the cracking zone deformation needed to propagate a crack. In other words, the strain capacity of the composite is higher than the strain capacity of the matrix. According to Bache (1984), the controlling parameter for the increase in strain capacity is the inverse of the brittleness number B . The brittleness number B can be defined according to (2.3):

$$B = \frac{\sigma_0^2 D}{E \gamma_c} \quad (2.3)$$

σ_0	maximum tensile stress (N/m ²)
D	length, or diameter of a particle (m)
E	Modulus of elasticity (N/m ²)
γ_c	Fracture energy (N/m)

The brittleness number of a system will tell about the risk of crack propagation due to brittle behaviour. A higher number of B indicates a more brittle system with higher risks of crack propagation. The increase in B by increased particle diameter D will consequently lead to a higher risk of brittle behaviour. The brittleness modulus may be regarded as a measure of the ratio between the elastic energy stored prior to local fracture, and the energy needed to make a characteristic crack. Note the large effect of the tensile strength (σ_0) on the brittleness number. As the tensile strength will generally increase with increasing compressive strength, concretes of higher compressive strength have a more brittle behaviour than concretes of lower strength.

The fracture condition of an expanding particles in a matrix is illustrated in Figure 2.5. On the abscissa is the ratio of the actual particle size and the critical particle size, a ratio being proportional to the brittleness number B. On the ordinate is the critical strain of the matrix, which is the ratio between the strain caused by swelling particles and the strain capacity of the matrix.

An interpretation of Figure 2.5 is that for particles smaller than approximately 10 mm (only valid for this particular system and should not be generalized), the strain capacity of the system is equal to the strain capacity of the matrix. The strain capacity grows inversely proportional to the particle size for particles smaller than 10 mm. For this given system, the critical particle size is 10 mm.

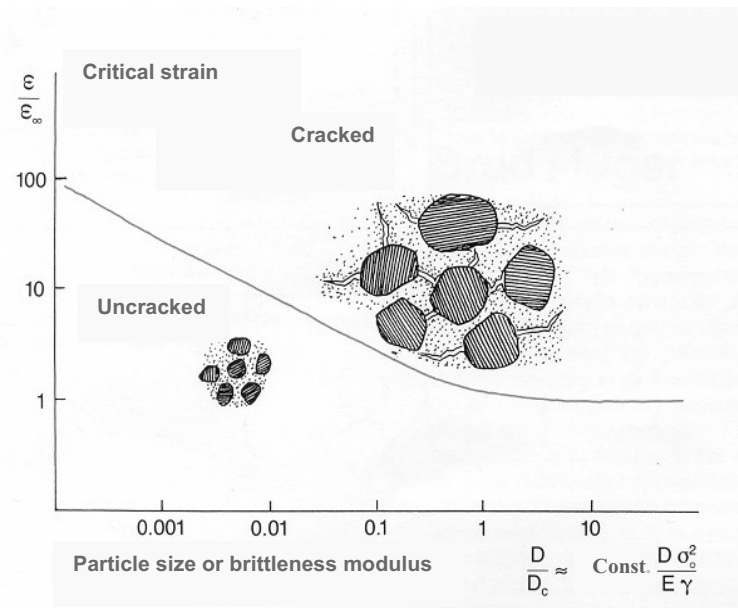


Figure 2.5 The critical strain of matrix as a function of particle size or brittleness modulus. D_c = critical particle size. Critical strain = the composite strain capacity (ϵ) divided by the strain capacity of the matrix (ϵ_∞). See Equation 2.3 for explanation of the other parameters. From Bache (1984).

Golterman (1995) used fracture mechanics to explain why cracks are not formed from aggregates under a certain limit in the cases of expanding particles, or shrinking paste. According to fracture mechanics, cracks propagate if the released energy is larger than the fracture energy needed to propagate the crack. Further, according to Golterman (1995), the released energy for a swelling particle of radius R is proportional to the R^3 , (related to volume) while the necessary fracture energy is proportional R^2 (related to area). Consequently, for a given system, there will be a critical particle size where no crack propagation will be caused by particles under this limit.

2.6.3.3 Concluding remarks on the effect of the particle size

The present situation concerning effects of the particle size seems unclear, as conflicting results have been reported. It is evident that certain materials have a “critical” limit of particle size, where particle sizes below this limit does not give harmful reactions. Some alkali-reactive materials, e.g. crushed bottle glass and Icelandic glassy rhyolite have proven to be pozzolanic when crushed down to a given particle size. However, the study of Diamond & Thaulow (1974) clearly

showed that very small particles (20-30 μm) may give deleterious reactions just as harmful as coarser particles. Due to the increased strain capacity in a system of very small swelling particles compared to greater particles as discussed in Section 2.6.3.2 this may be difficult to understand. It is, however, doubtful if the fracture mechanical approach is useful for the opal used in the study of Diamond & Thaulow (1974). Much of the opal may dissolve completely, as has been shown by Diamond (2000). On the other hand, much of the reactions on more solid particles may take place as topochemical reactions, which means that alkali hydroxide reacts on the surface and slowly works its way inside the particle (Diamond 2002). It is more likely that the fracture mechanical approach is useful in the situation with relatively solid aggregate particles that grow, crack and generate gel within the cracks.

2.7 Relevance of alkalis

2.7.1 Effect of alkalis

It is a general belief that the total amount of alkalis in the concrete is a major parameter concerning ASR. An essential part of any guideline concerning ASR is the description of the total allowable alkalis depending on the reactivity of the aggregate and incorporation of pozzolanic additives. A common measure of the alkali-content is the Na_2O -equivalent in kg/m^3 , calculated as follows:

$$\text{Na}_2\text{O-eqv.} = \text{weight \% of Na}_2\text{O} + 0.658 \text{ weight \% of K}_2\text{O} \quad (2.4)$$

The amount of potassium is then converted to the equivalent molar concentration of sodium.

As discussed in Section 2.5.2, the dissolution of silica is controlled to a large extent by the pH, i.e. the concentration of OH^- is more important than the concentration of alkalis. According to Mather (1999), the soluble alkalis from the cement are basically in the form of potassium sulphate. A solution of such a salt, is pH neutral, below the value of 12.4 in a saturated calcium hydroxide solution. The reason why alkalis can mobilise hydroxide ions to reach a pH substantially higher than 12.4, is that the sulphate ions reacts and precipitate out of the solution, usually to form calcium sulphotoaluminate or gypsum.

According to Glasser (1992), the term “alkali-aggregate reaction” is strictly speaking incorrect, what is more correct is hydroxide-aggregate reaction. As described above, the addition of alkali salts in any form will generate additional OH^- and then increase the pH. The amount of alkalis is thus relevant to the alkali-aggregate reaction, though their influence is basically to generate an increase in pH, which is the major controlling parameter. However, the alkalis may be of importance as they may influence the physical properties of the alkali-silica gel.

The general limit for sodium equivalent is presently 3 kg/m^3 of concrete in Norway when aggregates classified as potentially reactive are being utilized in combination with CEM 1 cement. Higher alkali loads requires addition of Norwegian Portland-fly ash cement or Portland cement in combination with silica fume. Some countries have limits that vary with the potential of reactivity for the given aggregate and/or the environment of the given concrete structure/member. According to Lindgård & Wigum (2003), there are examples internationally of general alkali limits both below and above the Norwegian 3-kg limit.

The critical limits of alkalis will generally be dependent on the reactivity of the given aggregate. Figure 2.6 gives an example of the connection between the alkali level and one-year expansion measured by the concrete prism test for a highly reactive Norwegian cataclasite. The alkali level was adjusted both by combining high and low alkali cements and by varying the amount of cement. The water cement ratios were not constant for the concretes presented. This might explain some of the scatter of the results. According to Figure 2.6, there is a critical limit close to $3 \text{ kg Na}_2\text{O}$ equivalent for the given aggregate.

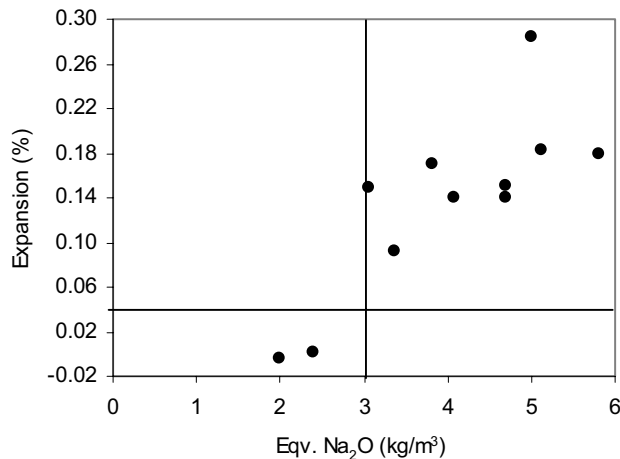


Figure 2.6 One-year expansions in the concrete prism method (see description in Section 5.2.2) as a function of Na_2O -equivalent for a Norwegian cataclasite. Expansion limit and alkali limit according to the Norwegian guidelines are marked. Data from Lindgård & Wigum (2003).

2.7.2 Alkalis in the cement

Cement is in most cases the main source of alkalis in concrete. The alkali content of the cement clinker may broadly be differentiated into two types according to Glasser (1992): alkalis normally present as condensate on the surfaces of the clinker grains,

possibly as sulphate salts, and alkalis that are locked into the crystal structure of the clinker minerals. All the clinker minerals have some potential to retain alkalis in solid solution. Much of the sodium occurs in the C_3A phase, while potassium may be more evenly distributed in all the present minerals as well as in associated glass. The two types of alkalis behave differently with respect to their release rate during hydration. While the alkalis present at the surface grains become available almost immediately, the alkalis locked into the cement grains become available more slowly during the course of hydration. According to Glasser (1992), virtually all the alkalis within the cement should be regarded as potentially available to take place in an alkali-silica reaction due to the slow nature of this. However, the CSH gel may bind some alkalis during the course of hydration, especially if there are pozzolanic materials present.

The alkali content in the cement is a function of the raw material, the fuel and the condition in the kiln during burning. A summary of chemical data for a selection of Portland cements from a number of countries throughout the world by Lawrence (1998) shows an average $Na_2O_{eqv.}$ of 0.68 %, with a minimum value of 0.03 % and a maximum value of 1.24 %.

2.7.3 Other sources of alkalis

Chemical admixtures may be a considerable source of alkalis. This is not so much the case for plasticizers due to the small amounts normally used as in the case of accelerators used for sprayed concrete. Generally, all alkalis introduced into the concrete should be regarded as potentially available and be counted in the total account of alkalis. When using fly ash as an additive, substantial amount of alkalis may be available, but the presence of fly ash tends to reduce the problem associated with harmful alkali-aggregate reactions. Fly ash and other pozzolans will be further discussed in section 2.9.2.

Leaching of alkalis from the aggregates can be an important alkali-source. A feldspar rich 0.1 mm fraction of sand (reported in Jensen 1993), stored in calcium hydroxide solution up to one year, leached more than 1 % Na_2O -equivalents by mass. The coarser fractions were much less vulnerable to leaching. According to Jensen (1993), it is speculative if such high amount of alkalis is actually available for ASR in concrete. Recent tests by Poulsen et al. (2000) have shown that a combination of inert feldspar and chert gave significantly higher expansion than a quartz aggregate with the same amount of chert, when tested according to the ASTM C 227-71 (1976) mortar bar method. The maximum expansion (at a pessimum proportion regarding amount of chert) increased about 30% for the specimens containing feldspar relative to the ones containing quartz. The authors concluded that there is no doubt that alkalis was released from the feldspar in the aggregates and contributed to the increased expansion. A recent Canadian study by Bérubé & Dorion (2000) has confirmed by measurement of water-soluble alkalis that the obtained values, even at depth in concrete, largely exceeded the soluble alkali-content expected to be released from the cement. The authors concluded that especially feldspar-rich aggregates have the potential of giving a great contribution

to the total alkali content. Further, they assumed this to be considered when designing new structures.

2.8 Relevance of the moisture condition

2.8.1 Introduction

Moisture is generally accepted to be a very important factor regarding ASR. Water is important as a transport media for the ions, but may be of even greater importance because the alkali-silica gels tend to imbibe water and swell.

2.8.2 Description of the moisture condition

The moisture condition in concrete can be described in two different ways:

1. The thermodynamic state of the pore water, typically expressed as relative humidity (RH)
2. The pore water content determined by drying and weighing. May be expressed either as the percentage of mass or volume, or as the degree of saturation.

The relative humidity is a measure of the thermodynamic state of the pore water, and not the amount of water. At a given moisture content, the RH will be a function of the pore structure, the temperature, the chemical composition of the pore water and the moisture history of the concrete.

The relationship between the RH and the water content is given as adsorption/desorption isotherms, see Figure 2.7, where the actual moisture state in a structure will be between these boundaries. Field measurements on bridges have demonstrated that the moisture state is close to a first desorption state, which is shown in Figure 2.7.

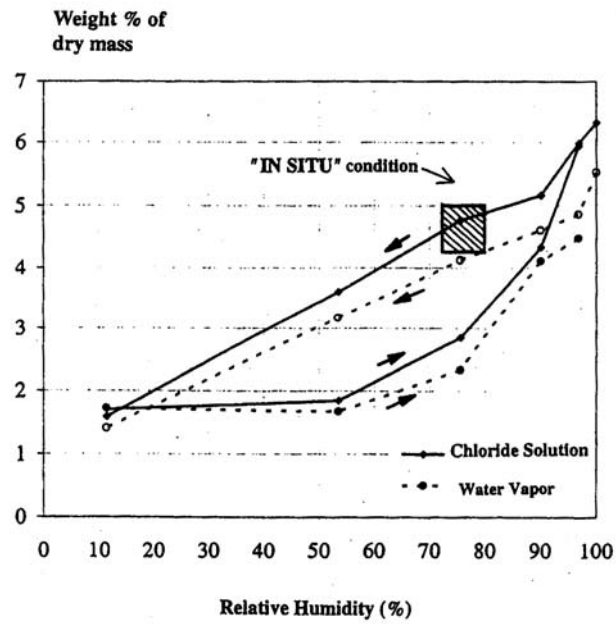


Figure 2.7 Sorption isotherms for thin discs of bridge concrete after exposure to chloride solution or water vapour pretreatment. The mean values of laboratory measurements on undisturbed field samples were in the area marked “in situ”. From Sellevold (1997).

The degree of saturation (DS) as defined in (2.5) is a direct measure of the pore filling and includes micro pores as well as macro pores.

$$DS = \frac{\text{Weight in situ} - \text{Weight after drying at } 105^{\circ}\text{C}}{\text{Weight after pressure saturation} - \text{Weight after drying at } 105^{\circ}\text{C}} \quad (2.5)$$

A more common expression for the moisture level that does not include filling of macro (air) pores, is the degree of capillary saturation (DCS) as defined in (2.6)

$$DCS = \frac{\text{Weight in situ} - \text{Weight after drying at } 105^{\circ}\text{C}}{\text{Weight after immersion in water} - \text{Weight after drying at } 105^{\circ}\text{C}} \quad (2.6)$$

The desorption isotherms for two concretes of different w/c ratios are shown in Figure 2.8 (Relling 1999). Note that the sorption isotherm is significantly higher for the low w/b-ratio concrete compared to the high w/b-ratio concrete due to the difference in pore structure. Also note that the RH is very sensitive to the moisture content for the concrete with low w/b-ratio. Based on field studies on Norwegian concrete bridges, Relling (1999) has shown that the relevant DCS-range for outdoor concrete is 70-100 %. Sellevold (1997) has reported values of DCS in the range 80-90 % measured on a coastal bridge.

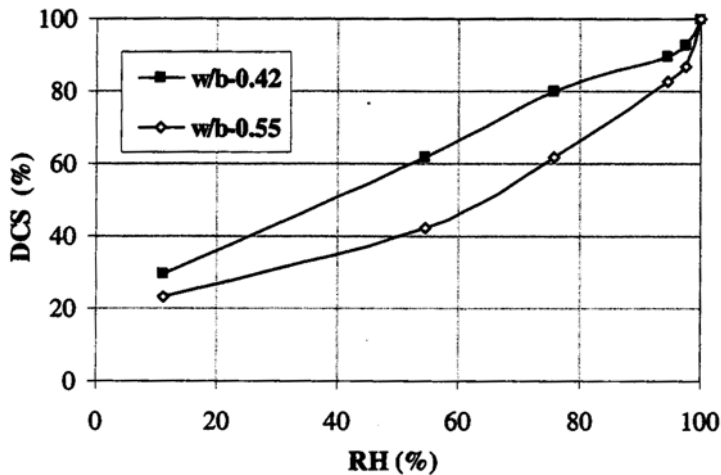


Figure 2.8 Desorption isotherms for concrete discs by the degree of capillary saturation (DCS) as a function of RH for two laboratory concretes of different w/c ratio. (5 % silica fume in concrete with w/c = 0.42). From Relling (1999).

A high alkali level will at a specific moisture level give a lower resulting RH. The maximum possible RH in a concrete rich in alkalis (or other ions) will consequently be lower. For low ion concentrations, the maximum relative humidity is a linear function of the ion concentration according to Raoult's law, given below, where n_w is moles of water and n_s moles of ions.

$$RH = \frac{n_w}{n_w + n_s} \quad (2.7)$$

Hedenblad (in Relling 1999) reported that this chemical effect on the pore water can be as much as 5 % reduction of the RH, i.e. a fully saturated concrete only exerts 95 % RH. This effect is clearly seen in Figure 2.7, where the storing in chloride solution moved the sorption isotherm curves to the left in the figure. Also carbonation and temperatures affect the sorption isotherm of concrete (both moving the curves to the right).

During this review, very few discussions of the fundamental aspects of moisture state in concrete were found in connection with ASR, and most scientists seem to use relative humidity as the only measure of moisture. DCS may be a more relevant parameter to describe the in situ moisture state than RH if the amount of water is controlling the expansion. But relative humidity gives a measure of the thermodynamic state of the pore water, and it is certainly possible to generate expansion pressures in the gel even in concretes less than saturated. We may conclude that today the relationship between the moisture state and expansion/cracking is not well known, and requires much more research before we can decide on the most relevant description of the moisture state. Also note the practical considerations: RH is apparently easy to measure, also in situ and over time. However, such measurements require much care and experience to be meaningful. DSC measures, on the other hand, are easy to perform accurately, but they are destructive and cumbersome to do, involving cutting off samples from the structure and taking them to a lab in an “undisturbed” condition.

2.8.3 Effect of the moisture condition on the ASR

2.8.3.1 Laboratory results

Vivian carried out the earliest systematic experiments on the effect of moisture condition on ASR in 1947. These results are summarized by Stark (1991) in Figure 2.9. The storage conditions included moist air, over calcium chloride (RH < 1%) and immersion in water. Some of the specimens were switched to another storage condition after 41 days. The continuous moist air condition gave the highest expansion, while the continuous water storage gave only a very small expansion. According to Stark (1991), the leaching of alkalis when prisms are stored in water significantly minimise the expansions. As could be expected, the dry condition gave a resulting shrinkage. But a dry storage followed by a moist storage gave a very rapid expansion like the curve for continuous moist curing. On the other hand, the prisms stored in dry conditions and then immersed in water gave a very small expansion in the same order as the prisms stored continually in water. This may also be a leaching effect. However, we note that the “leaching explanation” by Stark (1991) would be expected to be very size dependent since we expect moisture ingress to be much faster than the outward movement of alkalis.

These experiments demonstrate clearly the importance of moisture to produce expansion. However, the leaching effect and the lack of knowledge regarding the

internal concrete moisture state (RH or DCS) means that no quantitative information can be deduced. It is surprising that the leaching effect should be so strong.

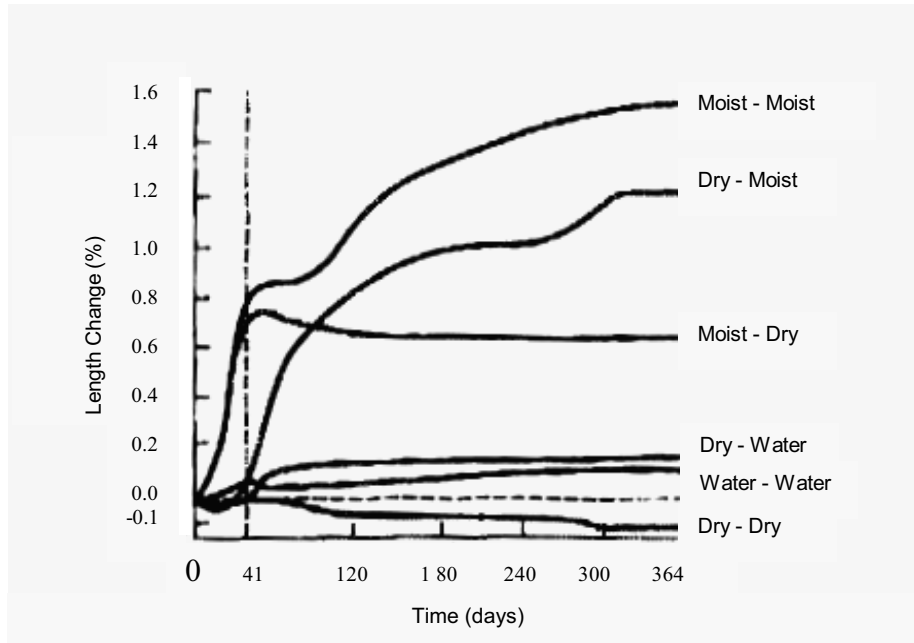


Figure 2.9. Effect of moisture availability on length change of mortar bars exhibiting ASR. From Vivian 1947, in Stark (1991).

Diamond et al. (1981) carried out experiments with sealed curing of mortars with opal aggregate at different temperatures. These experiments showed that very high expansions occurred (about 1.4% at 40°C and about 1.8 % at 20°C) even when no external water was added. Hence, the fluid being sorbed by the gel must be pore water solution, and the swelling must be a consequence of redistribution of pore water within the prism. The w/c-ratio was 0.50 in these experiments, i.e. self-desiccation did not reduce the internal RH below 90 %.

Stark (1991) conducted experiments where sets of mortar bars were tested in accordance to ASTM C227 (Storing at 38°C over water). Several sets of bars with both reactive and innocuous aggregates were made and stored until the bars with reactive aggregates reached 0.1% expansion. The bars were then stored in desiccators at different RH until length equilibrium was reached. The results are

shown in Figure 2.10, where the net expansion is the expansion of the reactive bar relative to the non-reactive bar at the same RH.

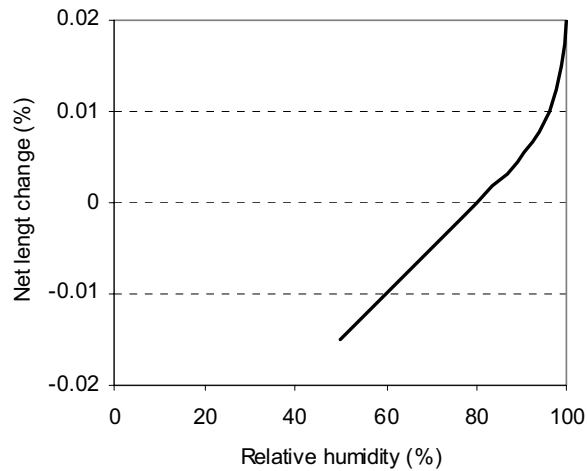


Figure 2.10 Effect of relative humidity on expansion. Net expansion is the expansion of a specimen containing reactive aggregate relative to the expansion of specimen with innocuous aggregate; see further explanation in the text. From Stark (1991).

According to Figure 2.10, 80 % RH is a threshold value. Mortar bars stored at lower RH than 80% shrank more than mortar-bars with non-reactive aggregates. This is due to the fact that reactive mortar-bars shrank from an expanded condition, and consequently that ASR gel gives a considerable high shrinkage. At 80 % RH, there were no difference between the reactive and non-reactive mixes after change to the storing in desiccators (0 % net length change). Further, these results clearly indicate that the mortar bars containing reactive aggregates continued to expand when the RH was higher than 80 %, the net expansion increasing with increasing RH up to 100 % (storing over water). The results also demonstrate that there is no pessimal RH in 80-100 % range, i.e. that the leaching explanation by Stark (1991) is not contradicted.

In an Icelandic study (Gudmundsson and Asgeirsson 1983), higher humidity gave a higher expansion for specimens stored at 38°C. The exception from this was the specimens stored at 90 % RH, which gave a somewhat higher expansion than the corresponding specimens stored at 95 % RH. Based on this study, it may be concluded that a moisture level above approximately 80 % RH is required to provide expansions due to ASR.

Results reported by Olafsson (1992) showed that the expansion of mortar bars stored at 95 % RH was slightly higher than those stored at 100 % RH at a temperature of 38°C. For RH of 90 % or lower, the tendency was that a lowering of RH gave a decrease in expansion. These experiments showed that even a RH as low as 73 % gave an expansion of 0.1 % after 24 months of storing (compared to about 0.3 % at 95 % RH). For the specimens stored at room temperature, the expansions decreased with decreasing RH. However, storing at 95 % RH was not tested at room temperature. The obtained expansions at 20°C were generally lower than those for the corresponding specimens stored at 38°C, with larger differences for the lowest levels of RH. This may indicate that a higher moisture level is needed to provide expansions due to ASR at lower temperatures.

It should be noted that the conclusion of Diamond et al. (1981) that no external supply of water is necessary to give an expansive behaviour, was drawn based on experiments with w/c ratios of 0.50. However, this may not be true for concretes or mortars of significantly lower w/c-ratios. Due to the effect of self-desiccation, the available water in concrete at w/c-ratios of 0.40 will be very low. According to the model developed by Powers in 1948 (Sellevold 1993), there will be no capillary water at w/c ratios below 0.415 at full hydration and sealed curing. In practice, there will not be full hydration, and some capillary water will be present even at low w/c ratios. Presumably, the gel water is too tightly bound to be available to an expanding gel. The relative humidity will anyhow decrease with decreasing w/c-ratio due to self-desiccation, and RH may be more relevant to consider in this respect since many measurements have been performed. According to Sellevold (1993), the relative humidity for an ordinary Portland cement concrete at w/c = 0.40 was approximately 85 % after six weeks of sealed curing. A 10 % addition of silica fume further reduced the RH to values just above 80 %. On the other hand, concrete of w/c = 0.60 gave approximately 95% RH. As we have seen, these levels are presumably enough to cause expansions. However, for concretes of w/c ratios significantly lower than 0.40, the self-desiccation may reduce the RH to levels as low as 70 %. At such low levels of RH, ASR is unlikely to happen. Thus, in such a situation, external water supply (e.g. rainwater or suction from the ground) may be a prerequisite to cause expansion and cracking due to ASR.

2.8.3.2 Field results of the moisture condition

Nilsson (1983) reported, based on field examples from concrete basement floors, that pop-outs related to alkali-silica reactions most likely occurred at RH close to 90 %. Higher RH did not cause pop-outs. His explanation for this was the lower viscosity of the gel caused by the high availability of water making the gel to “soft” to build up any pressure.

A comprehensive investigation on RH in varying climates has been carried out by Stark (1991). He showed that even in desert climates most of the concrete in highways and dams remain sufficiently damp to sustain expansive ASR (> 80% RH). And bridge decks and columns in dry climates are sufficiently damp on seasonal basis to sustain alkali reaction, and examples are given of alkali reactions

on columns in arid climate. Massive concrete members in controlled indoor environment may maintain a RH of 80-85%, and may thus be able to react according to Stark (1991). In general, he reported that the variations seemed to lie in the outer 5 cm of the concrete, while the conditions in the inner parts were to a great extent a function of the w/c ratio due to self-desiccation as discussed earlier.

In Elgseter bridge in Trondheim, Jensen (2000 and 2003) reported the RH to vary from 100 % to 87 % in the columns. Moisture profiles showed that the relative humidity was higher on the western phases compared to the eastern phases. The largest cracks also occurred on the western phases of the columns. As the west to east direction is the dominating direction of wind, the western phases of the columns will be wetted during rain, while the eastern parts will stay dryer. Jensen (2003) suggests the rainwater to be the most important source of water to cause levels of RH high enough to cause damages by ASR.

Sellevoid (1997) have reported an investigation of the moisture state of concrete from the Gimsøystraumen coastal bridge. Measurements of DCS on undisturbed field samples and continuous in situ monitoring of RH were carried out over a period of 28 months. The moisture state appears to be surprisingly stable both over time and position in the bridge. The RH was in the range from 70 to 80 %, corresponding to DCS in the range from 80 to 90 %. These measurements were done at concrete depths up to 50 mm from the surface. Sellevoid (1997) concluded that fluctuations in the moisture state generally take place in a very thin surface layer.

Relling (1999) have reported the moisture state in situ for Norwegian coastal bridges. In agreement with Sellevoid (1997), she reported the DCS to vary very little over position and time. The average values vary between approximately 80 % and 90 %. Concrete in the tidal zone was reported to be significantly wetter (> 90 %). The mean value of DCS for an inland bridge was reported to be about 80 %.

In a recent field project (Lindgård & Wigum 2003), it was found that the DCS was 90 % or higher in most cases with documented damages by ASR. It may be possible that the alkali-silica reaction will contribute to a higher moisture level due to a high hygroscopic binding capacity. According to Nielsen (1983), the sorption capacity is higher for a concrete with alkali-silica reactions than for a concrete without any signs of ASR due to the binding capacity of the gel. It is then possible that beginning ASR may be a trigger for further damaging reactions.

2.8.3.3 Concluding remarks regarding the moisture condition

Based on the reviewed literature, it may seem that at levels below approximately 80% RH, it is little danger of ASR. However, RH as low as 73 % has been reported to cause expansions due to ASR according to Olafsson (1992). The risk of deleterious reactions seems generally to increase with increasing moisture level. But there are some documented cases in there literature where a pessimum level around

90-95% RH is reported. This is by one author (Nilsson 1983) claimed to be due to the fact that the gel is of a less viscous nature when there is an excess of water, and so making it possible to escape through the pore system without building up any pressure. In some cases also leaching of alkalis can be a possible explanation, like in the reported experiments from Vivian where prisms in water gave less expansion than those stored in moist air. No tendency towards a pessimum moisture level has been recognized for Norwegian conditions to the author's knowledge. The investigations of Jensen (2003) indicated that the most severely cracked parts were the most humid parts, with RH close to 100 %. The conclusions from the recent national field project (Lindgård & Wigum 2003) also favours this conclusion that the most severely cracked parts due to ASR were the parts most heavily exposed to rain water. Examinations of some parts of structures protected against rainwater have showed no signs of ASR in potentially alkali-silica reactive concrete, presumably because the moisture content for these parts were below a threshold value needed to cause cracking and expansions due to ASR.

The review has shown that the moisture content in the concrete is a very important parameter in controlling the ASR. Further, it has revealed that there is a need for more basic research in the moisture effect area.

2.9 ASR inhibiting additives

2.9.1 Introduction

Much of the research on ASR during the last years has been on the role of different mineral additives to prevent deleterious reactions from ASR. A great part of the research on expansion inhibiting admixtures was summed up by Ramachandran (1998), including a total of 75 references. But there have been published numerous papers since that, including many papers at the ICAAR conference in Quebec in 2000. In the following, some notes regarding effects of inhibiting additives will be given.

2.9.2 Silica fume, fly ash and slag

Silica fume, fly ash and slag cements are probably the most widespread materials used to prevent ASR. Extensive research in Canada during the last years has confirmed that ternary blends containing mixtures of Portland cement, silica fume and fly ash are especially effective in reducing the expansion (Shehata & Thomas 2002). A Canadian study including slag (Bleszynski et al. 2000), made it clear that there is a synergy effect when using a combination of silica fume and slag as an additive. Ternary mixes in general caused a marked reduction in expansion equal to, or beyond, the superposition of the individual influences of the materials when used separately, see Figure 2.11.

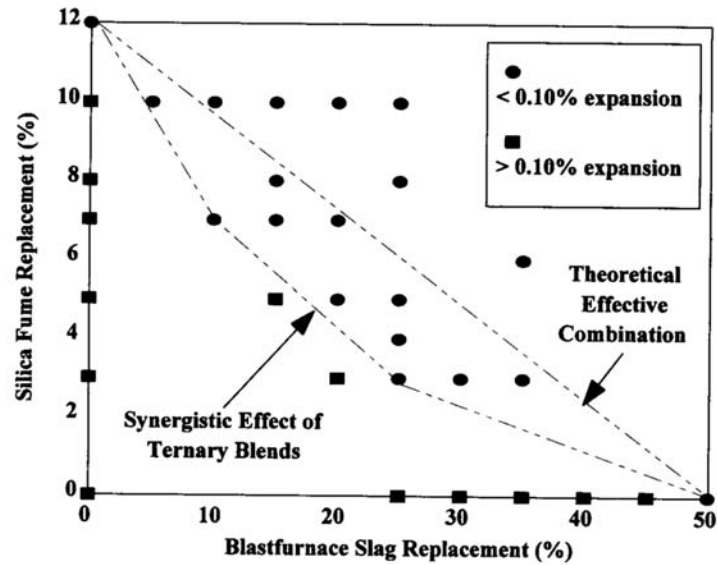


Figure 2.11 Performance of mortar ternary blend combination (Spratt limestone, accelerated mortar bar test). From Bleszynski (2000).

There has been an extensive use of silica fume in Iceland as an alkali-silica inhibiting agent. From 1979, silica fume has been interground with the clinker, and today about 7.5 % of silica fume is added to all Icelandic cement, together with a small percentage of interground rhyolite (Gudmundsson et al. 2000). The Icelandic cements with silica fume are reported to show a very good performance in laboratory testing as well as field performance with respect to ASR, and the earlier problems associated with ASR seem to be eliminated according to Gudmundsson & Olafsson (1999).

Some of the Canadian research on ternary mixes has already been mentioned, but there have also been performed extensive research on the long-term effects of addition of silica fume, slag and fly ash individually. As reported by Duchesne & Bérubé (2000 and 2001), the behaviour of different additives together with Canadian aggregates have been followed up to 9 years in laboratory experiments by a modified version of the Canadian concrete prism method (CAN/CSA-A23.2-14A). For the two reactive aggregates tested; rhyolitic tuff, and siliceous limestone (Spratt), 10 % by mass of cement of low-alkali-silica fume nearly reduced the expansion to zero after 2 years. The increase in expansion up to 9 years was evident, but slow. A 5 % addition of silica fume, on the other hand, increased the expansion for the rhyolitic tuff, while there was only a marginal reduction for the limestone. Silica fume with another chemical composition, containing 3.6 % of alkalis, was less effective in reducing the expansion. The concrete made with 50 % of slag or 50 %

fly ash by mass of cement with relatively low alkali content (Na_2O eqv. around 3 % or lower) reached expansion levels lower than obtained with a control with low alkali cement after 9 years. The 20 % fly ash concrete only reached slightly higher expansion than the low alkali control did. The tested fly ash containing 8.5 % alkalis was much less effective in reducing the expansion, especially with respect to the rhyolitic tuff, where an addition of 20 % by mass of cement had no effect at all.

According to Duchesne & Bérubé (2001), the major controlling factor regarding expansion of concrete containing mineral additives is the total alkali content in the pore solution. The alkali content should be near or below 0.6 M at one year for safe use. According to their view, mineral additives very rich in alkalis should not be used for reducing ASR.

The behaviour of the rhyolitic tuff concrete with 5 % silica fume as described by Duchesne & Bérubé (2000 and 2001) is noteworthy, as this increase in expansion for low amounts of silica fume has been noticed by other scientists as well. Kawamura et al. (1986) examined mortars with opal as the reactive aggregate, containing amount of silica fume from 5 to 20 %. The 5 % addition of silica fume made a 4-fold increase in expansion, while the 10 % addition gave a 3-fold increase. A 15 % addition gave an early reduction, but subsequently an expansion equal to that of the reference. The 20 % addition level of silica fume gave a net shrinkage at all ages. It is possible that the ability of silica fume to give an increased expansion is related to the pessimum proportion of aggregates. It seems unlikely that an increase in expansion caused by silica fume should occur in situations where the amount of reactive material is above a pessimum level, or if there is no pessimum, which is probably the case for Norwegian reactive aggregates. The reason for this is that silica fume will reduce the content of alkali hydroxides available in the pore solution due to the pozzolanic reaction. However, it has also been well known for some years that agglomerated particles of compacted silica fume, when not completely broken down during mixing, are capable of giving alkali-silica reaction that can cause significant distress in concrete as described by Rangaraju & Olek (2000). Agglomerate sizes exceeding 300 μm were reported to give significant expansion and cracking. However, Gudmundsson et al. (2000) reported that the effectiveness of silica fume is not affected by the presence of lumps up to a few hundred microns in diameter.

The mechanisms by which pozzolans provide resistance to ASR are generally concentrated on their ability to remove the alkalis by binding in the CSH gel formed by the pozzolanic reaction. The C/S ratio of the gel formed in the presence of pozzolans is, according to Ramachandran (1998), approximately 1.2, while this ratio is normally around 1.5 without any additives present. The lower ratio of C/S is suggested to give a higher capacity of binding Na_2O and K_2O in its structure, and thereby reducing the hydroxide ion concentration. Many researchers, e.g. Duchesne & Bérubé (2000 and 2001), have demonstrated the effect of reducing alkali hydroxides in the pore solution. The general effect on the permeability, where

pozzolans give a denser and less permeable structure resulting in a lower mobility of ions, has also been suggested to be important.

2.9.3 Other inhibiting additives and admixtures

Many of the additives which are effective inhibiting additives work through their pozzolanic behaviour. In addition to silica fume, fly ash and slag as already discussed, many other pozzolans have proven to be very effective, e.g. rice husk ash, volcanic ash, zeolitic materials and calcined clays (Ramachandran 1998). The role of glass powder have been debated during the later years, and many researchers claim that fine glass powder is capable of controlling the reaction due to its pozzolanic behaviour. However, there is an uncertainty when dealing with glass aggregate because of the large amount of alkalis present in the glass, which may become available in the long run.

Different chemical compounds may be very effective in controlling the ASR, and lithium-based compound have been studied a lot among other compounds. Addition of LiOH is capable of reducing the expansion (Ramachandran 1998, Thomas et al. 2000), and other compound as LiF and Li_2CO_3 have also proven to be effective (Ramachandran 1998). The mechanism by which Lithium compound works seems unclear at the moment, but according to Thomas et al. (2000), lithium may not necessarily prevent the dissolution of silica, but rather change the nature of the reaction product.

According to Ramachandran (1998), several researchers have suggested that air-entraining admixture may protect against ASR. The air bubbles in the concrete are then believed to act as a storing chamber for the reaction products, leading to a lower stress development. However, there seem to be conflicting results in the literature regarding the effect of air entraining admixtures. There is also a concern about the freeze thaw resistance, which can be affected if the alkali-silica gel fills the pores. Also the addition of lightweight aggregate has been documented to reduce the expansion caused by ASR (Boyd et al. 2000).

2.10 ASR test methodology

2.10.1 Petrographic examination

Petrographic examination of concrete aggregates is carried out for all Norwegian concrete aggregates to identify the potentially reactive aggregates. While most countries seem to use petrography as a preliminary screening method, the method may serve as a full documentation of Norwegian aggregates. As stated in the Norwegian guidelines (Norwegian Concrete Association 1996), at an indication of 20 % or more of potentially reactive rock types, the aggregate should be considered to be reactive. At an amount lower than 20 % of potentially reactive rock types, no further testing will normally be done, while at a higher level further testing is preferred.

According to Wigum et al. (2000), the current petrographic test method is qualitative in the sense that it does not attempt to quantify the amount of reactive constituents in the aggregate, but to quantify the rock types that have been proven to be ASR susceptible in practice. The potential to give harmful reactions of the aggregates classified as potentially alkali reactive varies widely, and to get a real quantification of the damaging potential there is a need for other methods than petrography. It should, however, be stated that petrography is highly important to identify the reactive aggregates.

2.10.2 Mortar and concrete prism methods

There exist a number of methods for identification and quantification of reactive aggregates. Jensen (1993) has stated that the concrete prism test (CPT) CAN-A23.3-14A and the accelerated mortar bar test (AMBT) (Oberholster & Davis 1986) are suitable for Norwegian aggregates. The concrete prism method is due to its moderate acceleration (38°C storing over water, 5 kg/m³ Na₂O-equivalent) generally believed to give results rather close to the true field condition. Testing is normally performed up to 1 year, while prolonged testing may be preferred while testing effect of mineral additives, e.g. silica fume and fly ash.

The accelerated mortar bar test originally developed by Oberholster & Davis (1986) is a highly accelerated method where the mortar bars are stored in 1 N NaOH solution at 80°C. The results are obtained after 2 weeks of storing. This method was originally designed to be used for testing of aggregates only, but has been used extensively around the world for testing mineral additives (Bérubé et al 1995). Good correlation has been achieved between results based on the AMBT and the CPT when testing pozzolans as slag, silica fume and fly ash (Bleszynski et al. 2000). There are, however, uncertainties with respect to the alkali levels, as the supply of alkali hydroxide may be considered to be nearly unlimited in the accelerated mortar bar method. Pozzolanic reactivity, as well as cement hydration kinetics, are very temperature dependent, and a temperature of 80°C will increase the pozzolanic reactivity significantly relative to lower temperatures. This may be particularly important for very slowly reactive pozzolans, which are practically inert at 20°C, but may have a significant reaction rate at 80°C. Thus, the 80°C condition may be irrelevant for assessing field performance in such cases.

The fillers examined in the present work have been tested using both the accelerated mortar bar test and the concrete prism test. Comprehensive descriptions of these two test methods are given in Chapter 5; see Section 5.2.2 and Section 5.2.3.

It should be noted that there are generally no test methods, with a possible exception for the concrete prism test, which are able to predict the field behaviour of all aggregates. An example of this is porous chert/flint, which is not classified as deleterious when tested by the AMBT even though chert is known to cause ASR (Jensen et al. 1998). Different national practices on mix design, prism sizes and storing of the specimens also make it difficult to compare test results. All test results of potentially reactive aggregates should be treated with care, and petrographic

examinations by a geologist who is familiar with the given aggregate are always preferred as additional information.

2.11 General effects of fillers in concrete

2.11.1 Effects on mechanical and durability properties

It is well known that addition of certain fillers may give a positive effect on the workability of fresh concrete, especially when dealing with lean concrete mixes. The rheological properties of fillers will be treated separately in Chapter 3, but in the following, some aspects of fillers related to hydration, mechanical properties and durability will be discussed.

Kjellsen & Lagerblad (1995) reported that replacement of cement by different pure mineral fillers increased the rate of cement hydration. While quartz, orthoclase and albite gave only a slight increase in hydration rate during the first hours, the wollastonite and calcite filler gave a higher increase in hydration rate. The general increase in hydration rate is attributed to the filler effect, assuming that nucleation and growth of cement reaction products on minerals fillers are the main reasons for this effect. Kjellsen & Lagerblad (1995) hypothesised that the mineralogy of calcite and wollastonite provides beneficial substrates for precipitation of CH at lower ion concentrations than other minerals, thus leading to an increase in hydration rate. They reported that the compressive strength was reduced linearly when fillers replaced cement, and no particular effect of mineralogy was observed. The positive effect of calcite on strength, which has been reported by some investigators, could not be demonstrated in this work. There was also a general reduction in flexural strength caused by the cement replacement. An exception from this was, however, the fibrous mineral wollastonite, which was reported to have the ability to enhance the flexural and tensile strength.

Kronlöf (1994 and 1997) have reported that quartz fillers, believed to be chemically inert, gave an increase in compressive strength by roughly 4 MPa in concrete. She described this strength increase to be due to improved interaction of paste and aggregate. Some physical factors that can explain this improvement are given below, as listed by Kronlöf:

1. Fine materials interfere with the formation and orientation of large crystals at the paste-aggregate interface
2. Large amounts of small particles may alter the rheology, reducing the internal bleeding at interfaces.
3. The wall effect does not weaken the contact between paste and fine filler; thus the function of a small aggregate particle approaches that of the unreacted cement particle core.

4. The component (paste and aggregate) are homogeneously mixed, lowering the peak stress

Sellevoid et al. (1982) reported that silica fume, as well as an inert filler (calcite) of an equal size as silica fume (approximately 0.1 μm), accelerates the cement hydration. Also the pore size distribution of the capillary pores became finer with addition of the inert filler, but to a lesser extent than with silica fume. They believed the filler effect to promote a more homogeneous spatial distribution of hydration products and thereby a reduction in sizes of continuous pores.

2.11.2 Pozzolanic reaction versus ASR

Industrial pozzolans, like silica fume and fly ash, are very common in modern concrete technology. The positive effects of pozzolanic materials on ASR have been discussed in Section 2.9.2. The term pozzolan has two distinct meanings according to Massazza (1998); the first indicates the pyroclastic rocks, often glassy and zeolitised, that occur in the neighbourhood of Pozzouli or around Rome. The second meaning, which is the basis for this discussion, includes all inorganic materials which harden in water when mixed with calcium hydroxide. The value of pozzolanic materials as binders has been known for some millenniums, and was described as early as 30-20 BC in Vitruvius “De Architectura libri decem” (“Ten books on architecture”). He wrote:

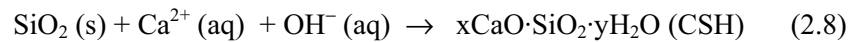
“There is also a type of powder that brings about marvellous things naturally. It occurs in the region of Baiiae and in the countryside that belongs to the towns around Mount Vesuvius. Mixed with lime and rubble, it lends strength to all the other sorts of construction, but in addition, when moles (employing this powder) are built into the sea, they solidify underwater.” (Rowland & Howe 1999).

The range in chemical composition varies widely among the pozzolanic materials, but generally, the amount of silica (and aluminium) is higher than other constituents. When reacting with calcium hydroxide (and water), aluminate- and silicate hydrates basically of the same type as those produced in the hydration of Portland cement are being formed. The C/S ratio of the CSH product is variable and depends on the type of pozzolan, temperature of curing and lime/pozzolan ratio. Ratios between 0.75 and 1.75 have been reported (Massazza 1998), while ratios of CSH produced by hydration of Portland cement are normally in the range from 1.2 – 2.3 (Odler 1998).

The pozzolanic reactions are highly relevant for concrete properties due to the great effect on both mechanical and durability properties. As discussed above, there might also be a filler effect, and when dealing with pozzolanic powders, the net effect is generally the sum of the filler effect and the pozzolanic effect. Pozzolanic reactions are also highly relevant related to alkali-silica reactions, and we have a basic paradox:

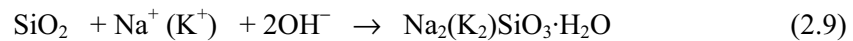
1. The reactive component in the alkali-silica reaction, disordered or amorphous silica, is generally the same component that reacts with calcium hydroxide in the pozzolanic reaction.
2. Pozzolanic materials have shown to be very effective in reducing cracking and expansion due to ASR.

The similarity between the pozzolanic reaction and the alkali-silica reaction has been pointed out by some scientists (Urhan 1986, Wang & Gillot 1992, Xu et al. 1995). The pozzolanic reaction may be expressed as follows (Urhan 1986):



The pozzolanic reaction produces CSH of composition close to the CSH produced by the hydration of Portland cement. The increased amount of CSH, which is the binder in concrete, is only desirable.

The alkali-silica reaction may be expressed as:



The resulting alkali-silica gel may be expansive on water uptake and cause cracks. The alkali-silica reaction is thus highly undesirable.

In the pozzolanic reaction (2.8), some alkali ions may become incorporated into the CSH gel, and in the alkali-silica reaction (2.9) calcium ions can substitute for alkali ions, thus leading to a formation of a material of similar composition to CSH. The Ca^{2+} ions are by several scientists believed to play a very important role in controlling the properties of the reaction products as have been treated in Section 2.5.4. Glasser & Kataoka (1982) found that the introduction of CH in a system of alkali-silica gel leads to the precipitation of a CSH gel of similar type as the reactions products of Portland cement. The precipitation of CSH goes on until the level of calcium becomes very low.

A recent publication by Hou et al. (2003) has highlighted this further. They have described the reaction sequence of ASR according to the following: After the initial hydration forming CSH and CH, the OH^- in the pore solution attacks the silica in the aggregate. The dissolved silica reacts with CH to produce additional CSH, more or less equal to the initial CSH. This is a pozzolanic reaction. After the amount of available CH has become low locally, the dissolved silica reacts directly with existing CSH. A more silica-rich and polymerised CSH is then formed. After the

CSH reaches maximum silica content, the silica content of the pore solution increases further until it begins to gel. According to their view, the alkali-silica gel may react further with CSH and CH to produce a more Ca-rich and Si-poor gel. The formation of alkali-silica gel may happen locally even though CH is available globally within the concrete, probably due to transport barriers around reactive aggregate particles.

Since CSH is formed in the pozzolanic reaction so long there is CH available near the dissolving silica according to Hou et al. (2003), it seems reasonable to believe that the pozzolanic reaction is generally favoured compared to the alkali-silica reaction. In a normal concrete there will be plenty of CH available during the whole lifetime. It is thus difficult to understand how the alkali-silica reaction can be favoured, but the hypothesis of Hou et al. (2003) that transport barriers may form locally may explain this. The conclusions of Hou et al. (2003) are much in line with the hypothesis of Powers & Steinour (1955b) regarding safe and unsafe reactions with reactive silica. Powers & Steinour (1955b) wrote that the initial reaction produces a layer of lime-alkali-silica complex of non-swelling nature. This thin layer separates the unreacted silica from lime and alkali. Lime and alkalis may then diffuse through the layer to react with silica. According to the view of Powers & Steinour (1955b), the ratio between lime and alkalis controls whether non-swelling or swelling gel is produced. Given that the amount of lime is high enough relative to alkalis, non-swelling gel will be produced. They described this non-swelling gel to be of similar, but not identical, composition as the CSH produced by the hydration of cement.

.

3 Properties of fresh concrete – theoretical background

3.1 Introduction

The properties of fresh concrete and its ability to flow and fill the mould completely, while still being homogenous, are of major importance for the quality of any given structure. Properties in the fresh state are also of high importance regarding the labour intensity needed to place the given concrete. The development of new technology like self-compacting concrete (SCC), which is compacted by its own weight, is a striking example of the possibilities of concrete. Filler technology is of large relevance regarding the properties of fresh concrete. The development of concretes of higher flowability, even up to self-compacting concrete, has made the knowledge of the influence of fillers of even greater relevance.

This chapter gives an overview of some important factors concerning properties of fresh concrete. Some basic theory regarding measurement of rheological properties and dispersion mechanisms of small particles is given. A short review of the effect of filler materials on properties of fresh concrete is included.

3.2 Description of the rheological properties of fresh concrete

Concrete is a suspension of particles ranging in size from a tenth of a micron up to tens of millimetres. The wide range of particles from colloidal size and up to stone size makes the system very complex. The large particles tend to settle quickly due to gravity, and a sufficient resistance towards segregation is a major challenge in mix design of highly flowable concretes. On the other side of the scale are the smaller particles of colloidal sizes. Much of the challenge in designing flowable systems, also being stable over time, is the balance between the attractive and repulsive forces of the smaller particles. This will be further discussed in Section 3.4.2.

The terminology of fresh concrete includes terms like workability, consistency, plasticity, compactibility, stability and pumpability. A problem with terms like these is that they are rather to be regarded as qualitative than quantitative measures, and different persons put different meanings in these terms. Tattersall & Banfill (1983) clearly distinguished between qualitative parameters, like those mentioned, and quantitative empirical like slump and Ve-be, and quantitative fundamental, like viscosity and yield stress.

There exist a variety of methods to quantify the properties of fresh concrete. The most widely used methods, like the slump test, measure only one parameter. In the slump test the concrete will flow only if the yield stress is exceeded, and the flow will stop if the stress generated by the weight of the concrete is below the yield

stress. The link between this test and the fundamental parameter yield stress is then obvious.

However, the fact that only one parameter is not sufficient to fully describe the performance of fresh concrete has been discussed by several researchers, e.g. Tattersall & Banfill (1983), Wallevik (1990) and Ferraris (1999). It is a well known fact that two concretes of equal slump might have totally different consistency and show totally different behaviour in the casting operation (Wallevik 1990). Despite this fact, the popular slump test method gives valuable information in some respect, and it has certainly proven to be useful in describing the consistency of normal concrete. As pointed out by Mørtzell (1996) it is a fact that methods like slump and flow table are simple and widely used methods, and their importance is an obvious consequence of their popularity. Comprehensive description of test methods for concrete is out of scope of this work, but descriptions of a variety of test methods and discussions of their suitability are given in a state-of-the-art report by Ferraris (1999).

Different approaches might be useful in describing the properties of fresh concrete. It seems obvious that the large span in properties from roller compacted concrete to self compacting concrete makes it necessary to use totally different approaches to describe and characterise fresh concrete. While very stiff concrete might be treated with theories normally used in soil mechanics, e.g. the Mohr-Coloumb theory (Alexandridis & Gardner 1980), concrete of high consistency might be treated as a fluid. Despite many restrictions, this approach of treating concrete as a fluid has proven to be very useful. One requirement that should be fulfilled before a concrete is treated as a fluid is workability over a certain limit, e.g. at least 100 mm slump. Another requirement is a high degree of stability, which is a precondition to use a rheological approach. The properties of concrete (and cement paste) might then be described by fundamental parameters like viscosity. In the present study, the fundamental rheological approach is the basis of the description of filler modified cement paste and self-compacting concrete.

3.3 Rheology – basic theory

3.3.1 General

Rheology is by definition “*the study of the deformation and flow of matter*”. This very wide definition, as accepted by the American Society of Rheology in 1929, involves studies on different materials such as asphalt, paints, lubricants cement paste, concrete, plastics and rubber. The definition of rheology allows the studies of materials ranging from elastic solids (Hookean materials) to Newtonian fluids within the limits of rheology. These classical extremes are anyhow treated as being out of scope of rheology, while the concern with respect to rheology is with materials between these limits (Barnes et al. 1989).

3.3.2 Basic concepts of viscometry

Viscometry is a subtopic of rheology, and it involves the study of the relation between the stress and the rate of shear.

A force F applied on the top of the material element as shown in Figure 3.1 will give a resulting shear stress (τ) (see Figure 3.2) according to Equation 3.1:

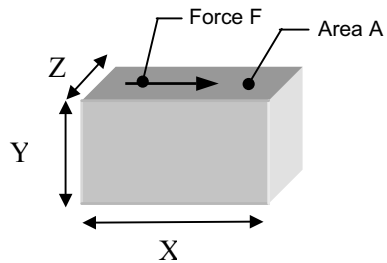


Figure 3.1 Basic material element

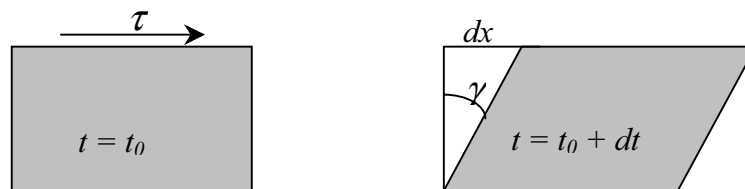


Figure 3.2. Deformation caused by shear stress

$$\tau = \frac{F}{A} = \frac{F}{XZ} \quad (3.1)$$

The stress applied on the material element will lead to a deformation dx and a deformation angle γ named shear strain as shown in Figure 3.2. For low levels of stress most materials will behave linearly elastic according to Hooke's law:

$$\gamma = \frac{\tau}{G} \quad (3.2)$$

where G is the shear modulus. The relationship between the deformation dx and the shear strain is given by Equation 3.3:

$$\gamma = \frac{dx}{Y} \quad (3.3)$$

The rate of shear is defined as shear strain per time unit as given by Equation 3.4 also relating the speed (v) of the top area (A) of the element to the rate of shear:

$$\dot{\gamma} = \frac{d\gamma}{dt} = \frac{v}{Y} \quad (3.4)$$

The relationship between shear stress and rate of shear is by definition the viscosity, expressed as the viscosity function (Irgens 1998):

$$\eta(\dot{\gamma}) = \frac{\tau}{\dot{\gamma}} \quad (3.5)$$

For a purely viscous material the shear stress is a function of the rate of shear alone:

$$\tau = \tau(\dot{\gamma}) \quad (3.6)$$

A combination of the viscosity function and the material Equation 3.6 then gives:

$$\tau = \eta\dot{\gamma} \quad (3.7)$$

A Newtonian liquid is a purely viscous liquid with a linear material Equation, i.e. a constant viscosity function ($\eta = \mu$):

$$\tau = \mu\dot{\gamma} \quad (3.8)$$

where μ = viscosity (Pas).

Most liquids will have a behaviour that differs from equation 3.8 and is then referred to as non-Newtonian liquids. Concrete might be treated as a Bingham fluid, which is an approximation proven to be very useful in describing concrete (Tattersall & Banfill 1983). A Bingham-fluid, as illustrated in Figure 3.3, is a viscoplastic material showing linearly elastic behaviour up to a certain strain with a corresponding stress, followed by a plastic behaviour corresponding to the Newtonian fluid.

The viscosity function for the Bingham material is (Wallevik 2002):

$$\eta(\dot{\gamma}) = \frac{\tau_0}{\dot{\gamma}} + \mu \quad (3.9)$$

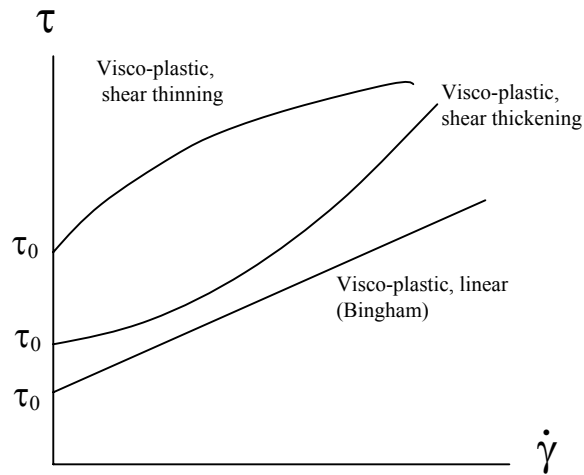


Figure 3.3. Flow curves for materials with a yield value

By combining Equation 3.5 with 3.9 the expression of the Bingham fluid is then:

$$\tau = \tau_0 + \mu\dot{\gamma} \quad (3.10)$$

The shear thinning and shear thickening materials with a yield value, as shown in Figure 3.3, can be described by the Herschel-Bulkley model:

$$\tau = \tau_0 + K\dot{\gamma}^n \quad (3.11)$$

The Bingham equation 3.10 is actually a specific case of the Herschel-Bulkley equation 3.10 with the factor $n = 1$. A factor $n > 1$ gives a shear thickening curve, while $n < 1$ gives a shear thinning curve as illustrated in Figure 3.3.

The viscosity in the Bingham-model is often referred to as plastic viscosity to distinguish from the viscosity of a Newtonian material. Another term of viscosity found in the literature is the apparent viscosity. The apparent viscosity is the

quotient of shear stress divided by the rate of shear when this quotient is dependent on the rate of shear as is the case for the Bingham model. The apparent viscosity for a Bingham material can be calculated according to Equation 3.12 (Tattersall & Banfill 1983):

$$\eta_{app} = \mu + \frac{\tau_0}{\dot{\gamma}} \quad (3.12)$$

The equation for the apparent viscosity (3.12) is equal to the viscosity function given in 3.9. The apparent viscosity may also be referred to as shear viscosity.

There are several other models than those described here that relate the shear rate to the shear stress, see Wallevik (1990) for a comprehensive list of models. Only some of these models incorporate a second factor, yield stress, in addition to viscosity.

3.3.3 Yield stress and rate of shear

It has been argued by some, e.g. Barnes & Walters (1985), that the yield stress is a consequence of the measuring technique and the measured range of shear rate. They claimed that given the rate of shear is low enough, no yield stress will be present. It is a fact, as shown by Barnes & Walters (1985), that the measured yield stress is very dependent of the rate of shear to be studied, but the yield stress is evident for a concentrated suspension such as concrete. This fact might be easily observed when using the slump test, as the concrete will stop flowing when then stress induced by the gravity is less than the yield stress of the given concrete. The existence of yield stress is less obvious in cement paste (and matrix including filler). Banfill and Kitching (1990) (reported in Banfill 1990) confirmed, by using a controlled stress rheometer, that cement pastes do possess a yield value, and cement paste only starts to flow when its yield value is exceeded. The yield stress in cement pastes or matrices is very low compared to concrete. Even though it may be difficult, it is possible to measure the yield stress if the precision of the equipment is high enough.

At a given shear rate in the concrete as a whole, the shear rate of the matrix within the concrete will be higher than the concrete shear rate as shown by Wallevik (2003). This is illustrated in Figure 3.4. Illustration B shows in detail how the shear rate of the matrix $\dot{\gamma}_m$ is larger than that of the concrete as a whole $\dot{\gamma}$.

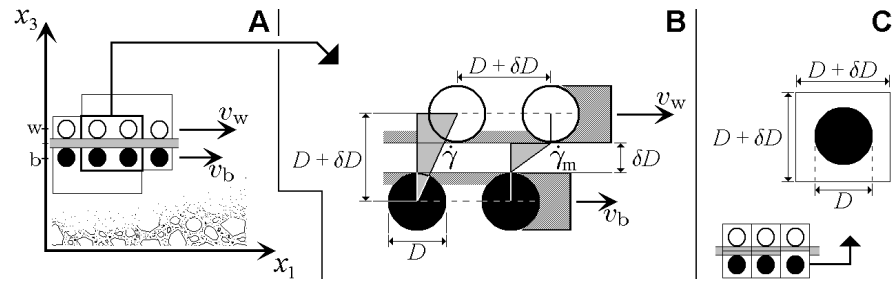


Figure 3.4. Shear rate condition of matrix inside the concrete. From Wallevik (2003).

The shear rate of the concrete as a whole can be approximated with $(v_w - v_b)/(D + \delta D)$, see Figure 3.4, Illustration B for definitions of the velocities and distances. Equally, the rate of shear of the matrix inside the concrete can be approximated with $(v_w - v_b)/\delta D$. This gives the following equation:

$$\frac{D + \delta D}{\delta D} = \frac{(v_w - v_b) / \delta D}{(v_w - v_b) / (D + \delta D)} \approx \frac{\dot{\gamma}_m}{\dot{\gamma}} \quad (3.13)$$

In Illustration C a repeating unit of a concrete sample is shown. This leads to the following relationship: $D^3/(D + \delta D)^3 \propto V_a/V_t$. V_a represents the volume fraction of the coarse aggregates (> 0.125 mm), while V_t is the total volume. Equation 3.13 can then be rewritten as follows:

$$\frac{\dot{\gamma}_m}{\dot{\gamma}} \approx \frac{D + \delta D}{\delta D} = \frac{1}{1 - D/(D + \delta D)} \propto \frac{1}{1 - (V_a/V_t)^{(1/3)}} \quad (3.14)$$

The relationship between the shear rate of the concrete as a whole and the shear rate of the corresponding matrix (or cement paste or mortar) are thus only depends on the relative volume fraction of the different phases.

3.3.4 Shearing concepts

The measurement of rheological properties of liquids necessitates the generation of a sheared flow. The ideal shearing concept would be the flow between two parallel plates, but due to the difficulty to make such an apparatus, this concept is never used in viscometry. The most widely used concept according to Wallevik (2002), is the rotating flow between two coaxial cylinders. The BML (Wallevik & Gjrv 1990) viscometer used in the present study is an example of this concept applied for concrete. There are some problems with this shear concept like the elimination of top and bottom effects, slippage and particle migration. Despite these problems, viscometers based on this concept have proven to be very useful in describing fresh concrete.

Other concepts as described by Wallevik (2002) are flow through capillaries, pipes and tubes, and rotational flow between two parallel plates. The concept of rotational parallel plates has been used in a commercial concrete viscometer developed in France, the BTRHEOM (Hu et al. 1996). The concept of rotating parallel plates has been utilized in the present study of matrix (filler modified cement paste). A further description of the equipment used in the present study is given in Chapter 5.

3.3.5 Time dependent phenomena

Many fluids, including cement-based systems such as concrete and cement paste, show time-dependent behaviour. Most cement-based systems will show a smaller or larger tendency towards tixotropic behaviour as illustrated in Figure 3.5. If a relatively high rate of shear is applied to the system, the response in terms of shear stress shows a gradual decrease towards a limit of equilibrium. The time to reach equilibrium might vary depending on the type of system and the rate of shear. A sudden decrease in rate of shear as illustrated, is followed by a sudden decrease in shear stress. The shear stress may recover or rebuild towards equilibrium. The reason for the tixotropic behaviour is a gradual breakdown of the agglomerated structure basically caused by the smaller cement grains. This process may be reversible, and the agglomerated structure may rebuild again if the shear rate is low enough.

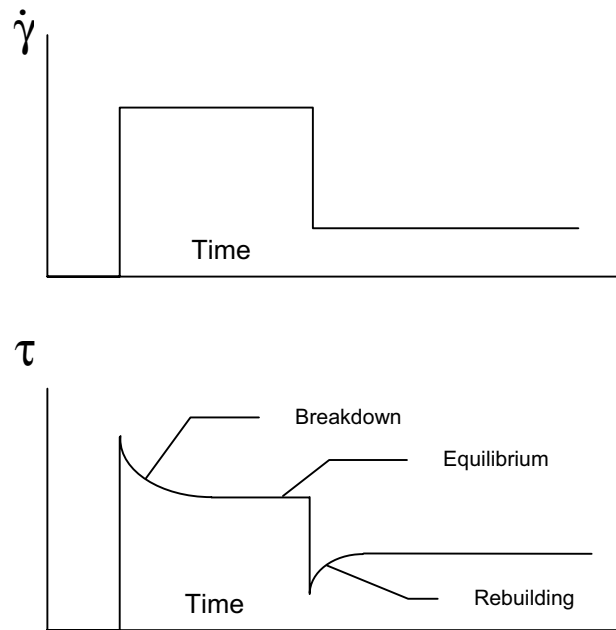


Figure 3.5. Example of response in shear stress due to stepwise changes in rate of shear for a tixotropic material.

An example of a flow curve for a tixotropic material is given in Figure 3.6. The down-curve has a lower shear stress for an equal rate of shear compared to the up-curve since the agglomerates has been broken down during the up curve. The area in the hysteresis loop is a measure of the energy needed to break down the agglomerated structure. This area might not qualify as a material parameter as it is highly dependent on the shear history of the material (Wallevik 2002), but it may be an indicator of the degree of tixotropy.

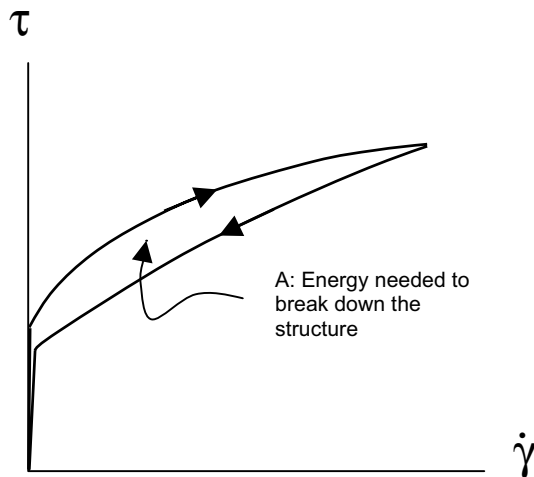


Figure 3.6. Flow curve for a material showing tixotropic behaviour.

Another class of time-dependent fluids is the rheopectic materials, which show the opposite behaviour compared to the tixotropic materials (i.e. an increase in shear stress with time at a constant rate of shear).

Most suspensions including particles of colloidal size will be tixotropic due to the tendency of coagulation. The strong time dependency of cement pastes (and matrices) makes the study of this class of materials difficult. The time dependency is also pronounced in concrete, and there is a tendency towards a stronger dependency as the w/c ratio decreases. The large volume fraction of larger particles makes it anyhow less time dependent than the corresponding cement paste, and concrete is in many senses much easier to study than cement paste due to the less time dependent behaviour. It is important to note that the rheological properties of all cement-based systems are changing continuously over time due to chemical reactions, as the hydration process starts when water is added to the system. Even though the hydration process alters the rheological properties even in a very early phase, structural changes caused by hydration are of less importance than coagulation of cement particles in the early phase from 10 to 80 minutes after water addition according to Wallevik (1990). Addition of plasticizers also tends to retard the hydration process of the cement.

3.4 Particle interaction and viscosity

3.4.1 Introduction

Interparticular forces in cement-based systems are of great interest with respect to rheology of fresh cement paste and concrete. In a suspension of cement in water, which may also include the filler fraction of the aggregate, the surface forces will be a dominant factor as the system includes particles of colloidal size. Colloids are small particles that remain suspended in a medium. Particles larger than 1 μm tend to settle due to gravity, so normally, only particles smaller than 1 μm are treated as colloids (Struble 2002). There should however not be made a distinct limit when speaking of colloidal forces, but their relative influence will decrease as the particle size increases.

The larger particles of the cement and the larger aggregates, where the surface forces are less dominant, will of course also influence the viscosity of the concrete. An increase in particle concentration is generally known to increase the shear viscosity. According to Wallevik (2003), the momentum transfer between cement particles resulting from colliding particles is directly related to the shear viscosity η of the cement paste. Likewise, the shear viscosity of a concrete is related to the momentum transfer between the particles including the larger aggregate particles.

The following section will focus on the influence on shear viscosity from the surface forces as these are dominating in the matrix systems studied in the present work.

3.4.2 Surface forces

The following discussion is based on theory basically developed for colloidal suspension. True colloidal systems involve particles in the region from about 1 μm to 1 nm, while smaller particles than 1 nm are indistinguishable from true solutions (Struble 2002). The behaviour of particles of colloidal size is controlled by surface forces causing nearby particles to attract or repel each other. In addition to the surface forces, Brownian motion (rapid, irregular motion observed in very small particles) also might play a role in preventing settling of small particles. The phenomenon discussed below, which involves interaction of coagulation and dispersion, plays a role for particles much larger than the normal limit of colloidal systems. Particles up to 20-30, or even 40 μm , are more or less dominated by surface forces according to Wallevik (2003).

Surface charges are of major importance in cementitious systems. The particles can obtain a charge either as a result of imperfections in the crystal structure near the surface or through adsorption of specific ions on the surface (Tattersall & Banfill 1983). Charges are a controlling factor as they cause particles of opposite charges to attract each other and particles of equal charges to repel each other. Particles that are not charged will attract each other and form larger agglomerates by the processes of coagulation/flocculation. Electrostatic forces may also cause coagulation and flocculation, as oppositely charged particles will attract to each other.

Charged surfaces will influence the distribution of the near-by ions in the solution, by attracting ions of opposite charges and repelling ions of the charges. In combination with blending effects caused by thermal movements of ions, this leads to the formation of an electrical double-layer, often referred to as a diffuse double layer. The complex theory of the electrical double-layer will not be treated further here, but have been described by Mørk (1999) among others. According to Justnes (2003), particles in a true system of cement particles or other mineral particles (aggregates) in suspension will have domains of both positive and negative charged sites since the ionic lattice is cut. The particles will thus have a very strong tendency to coagulate due to the electrostatic attraction between oppositely charged surfaces. Addition of a lignosulphonate plasticizer of negative charge will cause the lignosulphonate to adsorb on the positive domains of the particles, thus eliminating the coagulating effect. The effect of plasticizer will be further discussed in section 3.5.

An evidence for the existence of charged surfaces of colloidal particles is the motion of particles in response to an applied electric field. The phenomenon is known as electrophoreses. In principle, it then should be possible to determine the magnitude and sign of the charge based on the observed speed and direction of the motion. Electrophoreses technique is used to determine the so-called zeta potential, or electrokinetic potential, as described by Mørk (1999). Colloidal stability could be related to the zeta potential, but according to Tattersall & Banfill (1983), the relation is only qualitative. The z-potential of a particle may be either positive or negative, depending on the ions adsorbed on the particle surface. If the z-potential is close to zero, the particles will tend to flocculate or coagulation. A larger value of the z-potential, either being positive or negative, means better dispersion of the particles.

The DLVO-theory is often referred to in discussions of stability of colloidal systems. According to Mørk (1991), this theory considers the energy changes taking place when two particles with surface charges come near each other. The total interaction energy (V_T) is given by:

$$V_T = V_A + V_R \quad (3.15)$$

V_A is the attractive potential energy caused by van der Waal forces, while V_R is the repulsive potential energy caused by overlapping double layers. This is illustrated in Figure 3.7. Note that when the particles are approaching each other, the total potential (V_T) first passes through a weak secondary minimum, associated with flocculation of the particles. The maximum potential (V_{max}) is reached when the particles move closer. This maximum potential is an energy barrier against coagulation. If this barrier is overcome, the potential falls to the primary minimum as seen in Figure 3.7, and the particles will coagulate.

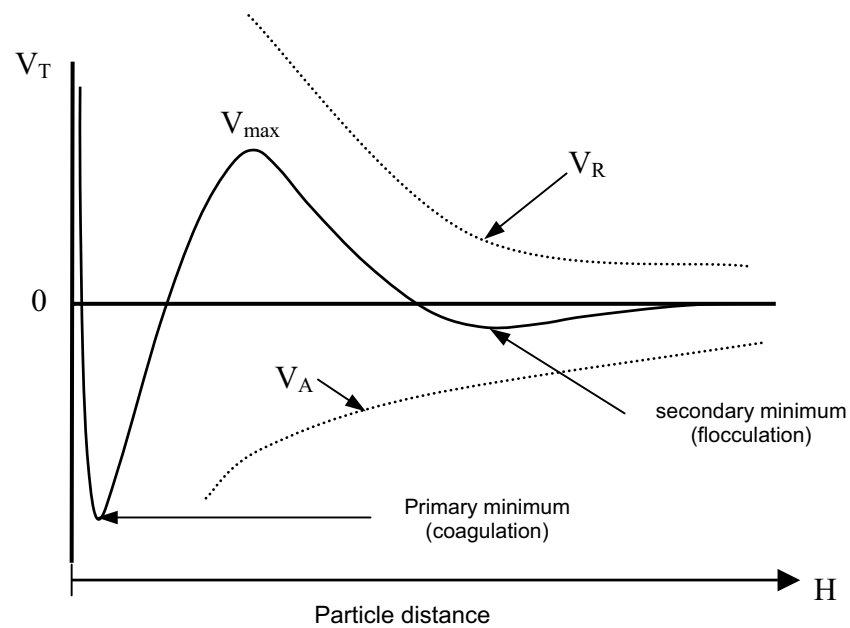


Figure 3.7 Illustration of resulting potential energy as a function of particle distance. After Mørk (1999).

The repulsive energy is a function of the electrolyte concentration, and the addition of a salt will decrease the repulsive energy and may then cause flocculation in a system with previous repulsion. The effect of the increased ion concentration is a compression of the double layer towards the solid surface. The particles then have to come closer to each other before they are electrostatically repelled (Struble 2002). This lower resulting repulsion due to increased ion concentration may cause increased shear viscosity. High-alkali cements may then give higher shear viscosities than low alkali cements due to this effect.

3.5 Effects of plasticizers

One great achievement of the new generation of plasticizers based on co-polymers is the increased efficiency. An important factor in this respect is the higher tendency of reducing the yield stress compared to the plastic viscosity (Maedler & Kusterle 1999). The new generation of synthetic polyacrylates with grafted side chains was designed to act by steric hindrance as the major dispersing mechanism (Justnes 2002). This is one of the main differences between a “traditional” superplasticizer as the Mighty 150 and the new generation. The Mighty 150, which is a naphthalene based plasticizer, as well as other products from the three first generations of plasticizers are said to rely on electrostatic repulsion as the primary mechanisms of

dispersion. According to Flatt et al. (2000) there could, however, not be distinguished clearly between these two mechanisms, and both should be taken into account in a so called “electrosteric repulsion” even though steric hindrance may dominate.

Irrespective of what mechanism that dominates, the plasticizer do adsorb on the particles (both cement and filler) in order to work in an efficient way. As any fractured mineral particle will have domains of both positive and negative charged sites, the negatively charged polymers on most plasticizers will adsorb on the positive domains. When adsorbed on the particles, the plasticizers can act by electrostatic repulsion caused by the negatively charged polymers, or by steric hindrance. The absorbed plasticizer will lead to a retardation of early hydration, which is an important mechanism of increasing the workability. According to Justnes (2002), plasticizer not adsorbed on the surface of the particles may also improve the workability by a tribology effect (reduce the friction between particles), or a surplus of polymers in the water may prevent the particles to get close enough to form agglomerates.

3.6 The Particle-Matrix (PM) model

3.6.1 Introduction

It is of large interest to be able to predict the rheological parameters based on the composition of the constituent materials, or from minimal laboratory tests. A model that will reduce the need for expensive and time-consuming trial batches of concrete is therefore beneficial. The compressible packing model developed by de Larrard is one such model (Ferraris et al. 2001). This model predicts the rheological parameters yield stress and plastic viscosity from the composition based on packing theory. Another recent model is the Nielsen model, which takes into account the amount, shape and maximum packing density of the coarse aggregates (Geiker et al. 2002b). This model links the rheological properties of the concrete with the rheological properties of the matrix phase. In this model, the matrix is defined to be the mortar and includes the fine aggregates (< 4 mm). In the present work, the particle-matrix model is the basis of the study of matrix (here filler modified cement paste). This model links the properties of the matrix to the properties of concrete. The model will be briefly described in the following section.

3.6.2 Description of the model

The particle-matrix model was developed by Ernst Mørtzell as a part of his dr.ing. project (Mørtzell 1996, Mørtzell et al. 1995). The principle of the model is illustrated in Figure 3.8.

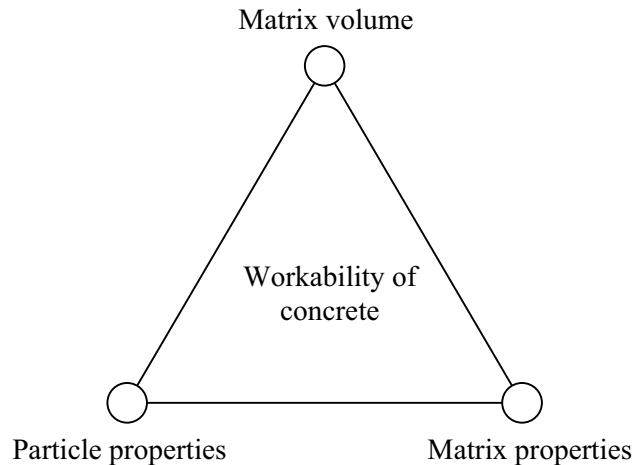


Figure 3.8 Principle of the particle matrix model, after Mørtzell (1996).

In this model concrete is considered to be a two-phase material composed of a fluent phase, i.e. the matrix, which flows in between the particle phase. The workability is then a result of the inherent properties of the fluent phase and the friction phase and their relative volume proportion.

The matrix phase is defined to consist of the water including chemical admixtures, and all particles with a diameter less than 0.125 mm. This definition of the matrix phase includes the cement, silica fume and other powdered additives as well as the fines from the aggregate. The particle phase is defined to include all particles > 0.125 mm. The characterisation of both phases is based on single parameter characterisation. The fluent phase is characterised by a parameter called the flow resistance ratio λ_Q . The flow resistance ratio is measured by the FlowCyl test described by Mørtzell et al. (1996). The FlowCyl viscometer is a cylindrical steel tube with an outlet formed as a cone ending in a narrow nozzle. The flow resistance ratio λ_Q is a representation of the difference in flow rate between the tested material and an ideal fluid. An ideal fluid (having no internal flow resistance and no external cohesion and friction) will have a λ_Q of 0.0, and a non-flowing material will have a λ_Q of 1.0. As an example, water will have a λ_Q value of 0.1 while a typical matrix of a self-compacting concrete will lie between 0.6 and 0.8. A further description of the flow resistance ratio is given in Section 5.2.6.2.

The particle phase, which is characterised by the air voids modulus (H_m) (Mørtzell et al. 1995), is based on the air voids space ratio of the fine (0.125 - 4 mm) and coarse (> 4 mm) aggregates, with the fineness modulus as correction factors. The air voids ratio depends on grading, angularity, mineralogy and surface texture. The air voids ratio is assumed to represent the sum of the relevant particle properties influencing

the concrete workability. For practical purposes, the air voids modulus approximately represents the matrix volume when the mix changes from a zero-slump concrete to a measurable slump.

The air voids modulus is defined to be:

$$H_m = v_1(H_s/(F_{m_s})^{0.5} + T_s) + v_2(H_p/(F_{m_p})^{0.5} + T_p) \quad (3.16)$$

- v_1 : volume fraction of the fine aggregate (0.125 – 4 mm)
- v_2 : volume fraction of the coarse aggregate (> 4 mm)
- H_s : air voids ratio of the fine aggregate (in volume %)
- T_s : an aggregate parameter for the fine aggregate (0.125 – 4 mm)
- T_p : an aggregate parameter for the coarse aggregate (> 4 mm)
- F_{m_s} : fineness modulus for the fine aggregate (0.125 – 4 mm)
- F_{m_p} : fineness modulus for the coarse aggregate (> 4 mm)

The workability of the concrete is also characterised by a single parameter, the slump measure. The properties of the material phases and the workability of the concrete are thus all described by single parameter empirical measures. As will be further discussed, the single parameter characterisation of the matrix phase represents a limitation of the model with respect to self-compacting concrete.

It may seem strange to include the fines from the aggregates in the particle phase, but the finest part of the aggregate is basically controlled by surface properties in the same way as the cement particles. It may be argued that the limit of 0.125 is somewhat high in this respect, but for practical reasons this limit is reasonable. The including of the filler in the fluent phase does also stabilise the matrix and then makes the experimental characterisation of this part easier. There have been reported many works on cement pastes studied using viscometers as reviewed by Banfill (1991), but a drawback of much of this research is the fact that the w/c ratios used are typically lower than those used in concrete. This is due to the problems with stability. This may fully or partly be overcome by including the finest fractions of the aggregate and any other powdered admixtures, thus increasing the viscosity and the stability of the filler modified pastes. This concept of testing filler together with different cements and plasticizers, without involving the larger aggregates, is believed to be of particular value with respect to self-compacting concrete as the filler may play a dominant role in this kind of concrete. Billberg (1999) has reported that this kind of testing is very useful in optimising combinations of cement, filler and plasticizer for self-compacting purposes. In his studies, he included aggregate particles up to 0.25 mm.

3.6.3 Characterisation of the matrix phase

Recent attempts to adapt the PM model into SCC have been reported by Smeplass and Mørtzell (2001). By keeping the aggregate composition fixed through all the experiments, the only variables were the matrix phase and the matrix/aggregate

proportion. The conclusion from this study was that the single parameter measure of the matrix, the flow resistance ratio as measured using the FlowCyl, was not able to give a satisfactory characterisation of the matrix phase. The hypothesis from this study was that the yield stress of the matrix, though being very small, is to a great extent responsible for the observed differences in concrete properties. A study by Pedersen & Mørtzell (2001) has indicated that the flow resistance ratio (λ_Q) is dominated by the plastic viscosity. The yield stress seems to have much less influence on the flow resistance ratio, at least for matrices having relatively low yield stresses.

The PM model is the basis of the present work. Originally, the idea was to characterise the effect of fillers on the concrete workability by testing filler modified cement paste (matrix) using the FlowCyl. The results discussed above have clarified some of the limits of the model. As a consequence of this, the plans became extended to include development of a more advanced characterisation of the matrix phase. This study has also included a series of self-compacting concretes to correlate the matrix results to the corresponding concretes.

3.6.4 Mixing and testing of the matrix

Tattersall and Banfill (1983) have pointed at the lack of reproducibility of the rheological properties of cement paste as a great problem. For cement pastes of a water/cement ratio of 0.45 there have been reported a 20-fold range in yield stress and a 50-fold range in plastic viscosity. Variations due to cement properties can only explain a fraction of this gap, and even when excluding differences due to mixing technique many of the variations remain due to differences in measuring equipment and measuring techniques. As pointed out by Banfill (1990), some of the problems associated with testing of cement paste are segregation during the course of the experiment and slipping due to a lubricating layer by the surface of the viscometer.

The effects of changing the mixing equipment and the mixing procedure have been demonstrated by Williams et al. (1999) and Ferraris et al. (2001). In concrete, the matrix is mixed through the ball-milling action of the coarse aggregates, and the mixing of the matrix should ideally give a simulation of this situation. Ferraris (2001) argued that a high-speed blender should be used instead of a standard paddle mixer (as Hobart) because of better correlation towards data from concrete. Williams et al. (1999) performed experiments of a high shear blender of different speeds, a Hobart mixer, and cement paste extracted from freshly mixed concrete (containing no aggregate-fines). This supposes that the extracted paste is very close to the true condition of the paste within the concrete. The results showed a great dependency of the speed of the mixer, and the extracted paste was found to be intermediate between moderately sheared mixes (1500 RPM) and high sheared mixes (2500 RPM). Thus, the mixing with very high shear rate might break down the agglomerated structure more than what is done by the aggregates in a concrete. High-speed mixing might also introduce a significant amount of air bubbles into the paste, which may alter the rheological properties significantly. It is not only the

shear rate within the mixing procedure that is of importance. The mixing time is important as well. Generally, a mixing time exceeding 5 minutes is preferred.

Ferraris & Gaidis (1992) have considered the gap between two parallel plates as a new parameter when testing cement paste, and argued that small gaps (in the order of 0.4 mm or less) would simulate the “wall effect” of the cement paste being squeezed in between the larger grains. Their experimental work indicates that this is an interesting approach, but it is uncertain to what extent the small gaps would really simulate the squeezing effect. A difference between the simulated system and the real system is that the latter has an elastic behaviour as the larger grains within the concrete might move relative to each other, while the simulation with small gap represents a stiff system.

Geiker et al. (2002a) have shown that the measuring procedure is very important, and that the rheological parameters attained from rheological measurements may be affected by different testing parameters. Their study on SCC, using the BML viscometer, showed that the time at each rotational speed is of crucial importance. If the time at each rotational speed is too short, steady state flow may not be reached within the given time. In such cases, the yield stress may be underestimated and the plastic viscosity may be overestimated. The authors suggest that a lack of steady state may explain the shear thickening behaviour of SCC reported by others, e.g. de Larrard et al. (1998).

3.7 Effects of fillers on the rheological properties of concrete

3.7.1 General

The amount of filler within the fine aggregate fraction of the aggregate may vary much due to differences in origin and processing of aggregates. Generally, the production of crushed aggregates generates large amounts of filler. Not only the amount of filler, but also the particle size distribution of the filler may vary much. It is a rather common practise among aggregate producers to process the aggregates by washing. By this, the finest particles of the filler fraction may be removed. This is generally done in order to improve the rheological properties of the concrete. Too high amounts of very small particles, especially the particles of colloidal size ($< 1 \mu\text{m}$) or slightly above this size may have a negative influence on the water demand in concrete.

In addition to the filler within the aggregate, filler may be added separately at the mixing plants. This is not a common practise in Norway at the moment. However, the development of SCC has created an increased need for fillers. The ratio between the matrix phase and particle phase is higher in SCC compared to ordinary concrete. In addition, the matrix phase needs to be more viscous. Addition of filler may be cost efficient, and in most cases the best technical solution. A good alternative to the addition of pure filler at the mixing plant is the utilization of very fine crushed sand,

e.g. 0-2 mm sand with high filler amount. By this practice, the coarser sand normally used may be combined with the fine sand to achieve the optimum filler amount for each type of concrete.

The knowledge of how fillers affect the rheological properties of concrete has become more important also for the cement manufacturers. The trend in the cement business is a decreased use of Portland clinker, and partial substitution of clinker by active or inert additions. This trend towards composite cements, such as Portland-limestone and Portland-fly ash cement, makes it very important for the cement manufacturers to understand how different filler additions influence the rheological properties, among other properties.

It is not possible to generalize the effect of filler addition in concrete. The effects on the rheological properties will vary much depending on the type and grading of the aggregate, type of cement, w/c ratio and amount of cement, and the type and dosage of plasticizer. The addition of filler may improve the workability of lean mixes much, and filler amounts in the order of 10-12 % of the fine aggregate may be beneficial. Such high amounts of filler are generally not beneficial from a rheological point of view in cement-rich concretes with low w/c ratio, as the concrete may become sticky and thereby become difficult to vibrate.

Danielsen & Wallevik (1989) have reviewed the influence of geometrical factors, i.e. particle size distribution and particle shape of aggregates. The poorer particle shape (meaning flaky and/or elongated) of a crushed aggregate compared to a natural aggregate generally gives higher air voids ratio and higher water demand. In such a case, addition of filler may reduce the water demand according to Danielsen & Wallevik (1989), even though conflicting results have been reported in the literature. Correspondingly, addition of filler may reduce the water demand/improve the rheological properties in cases of an open (convex) grading curve according to Smeplass (in Danielsen & Wallevik 1989). Filler may in these cases fill up the air voids between the coarser aggregates, and thus have a lubricating effect. Generally speaking, the relative influence of filler addition is larger in the cases of convex grading curves, and poor particle shape of the aggregate.

It is of importance to note that the z-potential of different fillers may vary much depending on the mineralogy. The z-potential has been briefly discussed in Section 3.4.2. Even though z-potential results should be treated with care, they may give some information regarding the dispersion state. Johansen et al. (1992) have measured the z-potential of different fillers, mostly mono mineral fillers. The measurements were done in pure de-ionized water, lime-water, and lime-water with lignosulphonate. The results are shown in Table 3.1.

Table 3.1 z-potentials after 30 minutes with and without admixtures. Data from Johansen et al. 1992.

	z-potentials after 30 minutes in suspension		
	H ₂ O	Ca(OH) ₂	Ca(OH) ₂ + 0.5 % P [*]
Limestone	+ 12	+26	-15
Quartz	-23	-1	-26
K-feldspar	-23	0	-19
Plagioclase feldspar	-40	0	-28
Muscovite	-39	+3	-20
Chlorite (20 % biotite)	-19	-2	-15
Amphibole (15 % biotite)	-31	+9	-11

* Lignosulphonate in % of cement weight

Note that the z-potentials were negative for all fillers except for limestone filler when measured in water. But the situation became totally different when the z-potentials were measured in lime-water. Due to adsorption of Ca ions, the values for all fillers except limestone were close to zero, meaning that we should expect these fillers to coagulate when suspended in lime-water. The adsorption of Ca ions on the limestone filler increases the z-potential, indicating that the repulsive forces will dominate and cause a stable suspension. According to Johansen et al. (1992), the suspension of filler in lime-water would simulate the true situation in cement based systems, since Ca ions will be available in such a system. The addition of lignosulphonate (right column of Table 3.1) has a crucial influence on the z-potential. All the z-potentials gets negative caused by the adsorption of lignosulphonate on the particle surfaces. The results of Johansen et al. (1992) showed that the magnitude of the negative z-potential generally increased with increasing dosage of lignosulphonate.

This kind of zeta-potential measurements reported by many scientists may be useful, for example to study if sufficient amounts of plasticizer are used. The results should, however, be treated with care. The relevance of zeta-potential is probably lower when dealing with the new generation of superplasticizers designed to have a dispersing mechanisms basically based on steric hindrance.

To sum up, the effects of fillers in concrete is believed to be dependent on the following factors:

- Particle size distribution of the aggregates
- Shape and surface properties of the aggregates
- w/c ratio and amount of cement

- type of cement
- type and dosage of plasticizer
- addition of filler, or replacement of cement

It is obvious that the effect of a certain filler may vary enormously depending of how the filler is used. In addition to the factors listed above, the effects will of course depend much of the properties of the given filler. The geometrical factors are presumably the most important. Especially the particle size distribution, and by then the specific surface area, is believed to be of major importance. According to Danielsen & Wallevik (1989), the influence of the particle shape seems to be of low significance for particles in the filler fraction, in contrast to the large influence of particle shape in the coarser fractions of the aggregate. The surface properties related to mineralogy is of importance, as have been discussed in connection with z-potentials shown in Table 3.1. The roughness of the particles may also be of some importance.

In the following sections, a literature review on the effects of fillers on the rheological properties of matrix, mortar and concrete is presented. The factors listed above should be kept in mind during the following discussion.

3.7.2 Literature review on the effects of fillers on the rheological properties

3.7.2.1 Filler modified cement paste (matrix)

Nehdi et al. (1997) studied the effect of replacing cement by limestone microfiller. The limestone microfiller had a mean particle size of 3 μm , while the mean particle size of the cement was 14 μm . A naphthalene sulphonate plasticizer was used in this set of experiment, and the w/b ratios varied from 0.3 to 0.4. The results showed that the yield stress increased as the limestone replaced cement (by volume), which was also reflected by decreased mini-slump. However, in the presence of 10 % silica fume, the yield stress decreased with increasing replacement up to 10-15 %, but decreased for higher replacement levels. It should be noted that the 10 % replacement of silica itself gave a significant increase in yield stress. The plastic viscosity decreased with increasing replacement up to 10 %, a further replacement had very little influence on the plastic viscosity. The presence of silica fume had very little influence on the plastic viscosity.

Zhang & Han (2000) studied the effect of replacing cement by ultra-fine additives, considerably finer than the cement being replaced. The average particle size was 2.9 μm and 4.5 μm for fly ash and limestone, respectively, while the average particle size of the cement was 14 μm . The w/c ratio was 0.25 in these experiments. Both the apparent viscosity and the yield stress decreased with increasing replacement up to 35 % by limestone filler and fly ash. The replacement of 10 % cement by silica fume also significantly reduced both the apparent viscosity and the yield stress.

Ferraris et al. (2001) studied the effect of replacing up to 16 % cement by fly ash of different gradings, with mean particle diameters from 3.1 to 18 μm . A naphthalene sulphonate plasticizer was used in these experiments, while the w/c ratios varied from 0.28 to 0.35. It was found that both the mean particle size of the fly ash, as well as the replacement level was important as could be expected. The 12 % replacement was optimal in reducing yield stress and plastic viscosity for the fly ash having mean particle size of 3 μm . It was also found that the mean particle size of 3 μm gave an optimum reduction in yield stress, and mean size of 5.7 μm gave a pessimum with respect to rheological properties. It should be noted that the 12 % replacement with the fly ash having 5.7 μm mean particle size was significantly increased (approximately 80 %), while the other particle sizes gave reduced yield stress. None of the different fly ashes increased the plastic viscosity, but the magnitude of reduction varied.

It seems clear that replacement of cement by microfillers of considerably finer gradings is able to reduce the plastic viscosity as well as yield stress significantly, even though some fillers may cause significant increase in yield stress. The decrease in plastic viscosity may be explained by closer packing of the particles, which are generally known to enhance the flow of particle suspensions. Nehdi et al. (1998) have discussed another factor that may be of importance in this respect. The colloidal forces depend on the average distance between the neighbouring particles, and the interposition of finer filler grains in between the cement particles may then affect the magnitude of the electrostatic attraction or repulsion. It seems like the particle size distribution of the microfiller is of crucial importance regarding the effect on rheological properties. The optimum and pessimum particles sizes, as discussed by Ferraris et al. (2001) is probably dependent on the particle size distribution of the cement which are to be replaced, since it is the total grading curve that controls the maximum packing density.

Skjølsvold & Pedersen (1997) studied the effect of adding different rock fillers to a cement paste of w/c ratio 0.5. This is in contrast to the studies presented above, where the fillers replaced cement. These rock fillers were also much coarser fillers (median particle sizes ranging from approximately 15-30 μm). A combination of lignosulphonate and melamine plasticizer was used (constant addition level relative to cement weight). The flow resistance ratio of the matrix was measured using the FlowCyl viscometer. Three different fillers (one glaciofluvial granite/gneiss filler, one crushed mylonite filler and one crushed gabbro/greenstone filler) were added at two different addition levels (20 and 40 % of cement weight). The addition of filler increased the flow resistance ratio compared to the reference mix without filler; the highest addition level gave the highest flow resistance ratio. It was found that the flow resistance ratio increased linearly with increasing surface area of the fillers. No particular influence of mineralogy and shape was found. In fact, it was very small differences in particle shape between the different fillers. It should be noted that the fillers investigated in that study were taken from the same sources as the filler studied in the doctoral study of Mørtzell (1996), which will be further discussed in

the following section. The general increase in flow resistance ratio (which is closely related to plastic viscosity) with increasing particle concentration, is well known from the literature.

3.7.2.2 Filler modified mortar and concrete

When the effects of different mineral fillers are studied in mortar or concrete, it is very important to know that the relative influence may change much depending on the ratio between the matrix and the aggregates. This has been clearly shown by Mørtzell et al. (1996), as shown in Figure 3.9. The figure shows the effect of different filler addition levels for 3 different filler types. It should be noted that the reference concrete contained no filler at all, since the filler had been removed by sieving. A normal filler level for the given aggregate composition would be approximately 70-80 kg/m³.

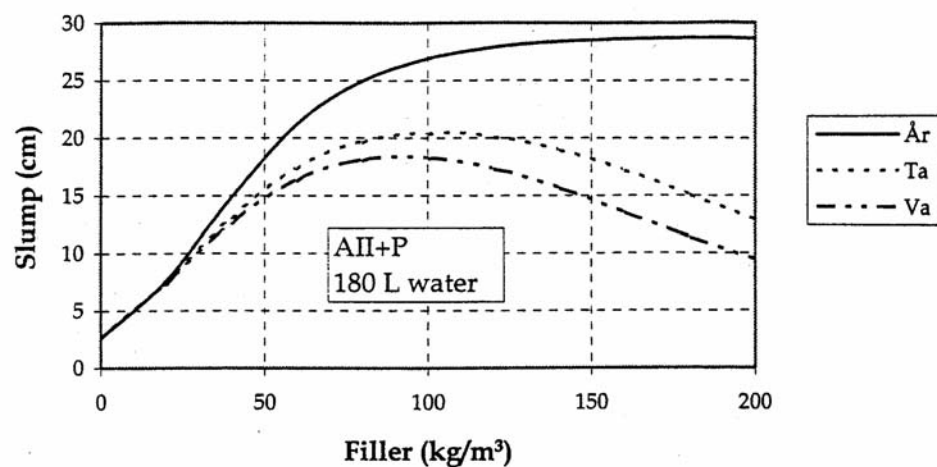


Figure 3.9 Effects of different filler types and addition levels on the slump measure. Constant w/c ratio (0.6) and amount of cement (300 kg/m³), constant amount of plasticizer relative to the cement weight (lignosulphonate + melamine). Note that the initial amounts of filler were 0%. From Mørtzell et al. (1996).

As seen in Figure 3.9, the effect of increased filler amount is equal up to about 40-50 kg/m³. The increased matrix volume dominates up to this level, and the isolated effect of increased matrix volume (meaning reduced particle concentration) is enhanced workability. The other effect of increased filler amount is an increase in the flow resistance ratio of the filler. For filler addition levels higher than 50 kg/m³, the differences in flow resistance ratios caused by the different filler become more pronounced, the relative difference increases with increasing addition level. The natural granite/gneiss glaciofluvial filler (År) gave a higher slump at high addition

level than the two other crushed fillers (mylonite labelled Ta, gabbro/greenstone labelled Va). The aggregate used in these experiments was of glaciofluvial origin, with a rather straight grading curve. The relative difference between different filler types is generally larger for aggregates of poorer grading and/or particle shape, as discussed in Section 3.7.1.

Kronlöf (1997) studied the effect of adding different inert mineral powders on the water requirement of concrete. She reported that in mixes where the particles were dispersed with a superplasticizer, the inert mineral powder lowered the water demand more the higher the initial consistency. The reduction in water demand was reported to lie in the region from 0-20 litres in the case of aggregates of good shape, and even up to 30-40 litres when angular crushed aggregates were used. The work was generally based on lean mixes with an amount of cement in the region from 140 – 285 kg/m³ (even though much higher levels of cement were also tested), and the addition level of powder was up to 7 weight % of the total aggregates. Superplasticizer was generally added in weight % of total powder (including both cement and filler). Obviously, the effect of increased matrix volume dominated over the increase in flow resistance ratio in these experiments. The higher water reduction for angular crushed aggregates compared to aggregates of good shape is in agreement with the observations by Danielsen & Wallevik (1989) as previously discussed.

Bonavetti & Irassar (1994) reported that stone dust (particles < 0.075 mm) of quartz, granite and limestone all have a negative effect in terms of increased water demand in mortar. They reported a linearly increasing water demand with an increasing addition level (the dust replaced an equal amount of sand) to a total increase in water demand of approximately 30-35 litres at 20 % addition level. They reported no use of plasticizer within this set of experiments. Similar results (in concrete) have been reported by Çelik & Marar (1996). They reported that addition of limestone dust (having particles in the range from 0 to 75 µm) decreased the slump with increasing addition level. The maximum addition level of 30 % gave a decrease from 92 to 60 mm. The amount of cement per m³ (420) as well as the w/c (0.5) were kept constant, consequently the total surface increased with the increased dust addition level. No plasticizer was used in these experiments. In these experiments, the dominating effect of adding filler obviously was an increase in the flow resistance ratio of the matrix, which dominated over the increased matrix volume.

Nehdi et al. (1998) have studied two types of limestone fillers of mean particle sizes of respectively 0.7 and 3 µm. In addition to those, ground silica and silica fume, having mean particle sizes of 13.8 and 0.26 µm respectively were used. In this set of experiments, the fillers replaced an equal part of cement by volume. The superplasticizer requirement (sulphonated naphthalene) needed to reach a constant workability in terms of slump, was decreased for all materials at all replacement levels except for the silica fume mixes. The increased plasticizer demand was most marked at the higher replacement levels (15 and 20 %) with silica fume. According to the authors, this increased demand of superplasticizer may indicate that silica

fume has a strong affinity for multi-layer adsorption of superplasticizer molecules compared to the other materials. They further reported the following in the presence of superplasticizer: The finer the microfiller, the lower the flow resistance (proportional to the yield stress) and torque viscosity of the concrete mixtures. Another positive effect of the microfillers was the inhibiting of bleeding of the fresh concrete. In these experiments reported by Nehdi et al. (1998), the matrix volume was constant since the fillers replaced cement, and the water content was constant. Consequently, the decrease in viscosity and flow yield stress must be due to reduced viscosity and yield stress of the matrix.

Ho et al. (2002) have reported a study of using quarry dust from granite as an alternative to limestone filler for SCC applications. The granite powder was slightly finer than the limestone filler, and the granite filler particles were also documented to be flakier and more elongated. Two different types of superplasticizers were used, and both types were based on polycarboxylated polyether. Tests on filler modified cement paste in a coaxial cylinder viscometer showed great differences with respect to demand of superplasticizer to reach a certain yield stress (20 Pa) as a function of the filler type. The limestone filler had the lowest demand, and the relative difference increased with increasing filler addition. At high filler replacement levels (45-55 % of cement weight), the demand for the mixes incorporating limestone filler was in the order of 25-30 % of the amount needed for the granite powder mixes. The tendencies observed in fillers modified cement paste were also confirmed in SCC mixes. The observed differences are probable to some degree a consequence of the finer grading of the granite filler and the flaky/elongated particles, but they may also be a consequence of different mineralogy.

Nehdi (2000) reported that some carbonate fillers may give a severe reduction in workability with time after an initially positive effect. He concluded that the quantity of CaO in the carbonate filler is an essential parameter, and only a few percent of CaO may cause a substantial workability reduction. The study was limited to polyacrylate dispersants. The possible reaction of calcite with C₃A may also explain some of the early workability loss according to the author.

3.7.2.3 Effects of mineral parameters

Danielsen & Wallevik (1989) have reviewed the effect of mineral parameters related to water requirement in concrete. One of the most important parameters is the amount of free mica in the finer fraction of the sand. The muscovite type of mica is generally reported to be more severe in concrete than the dark biotite in terms of increasing the water demand. There is clear evidence that weathered mica is less deleterious than the unweathered mica found in crushed aggregates. Some dark mafic minerals, like hornblende, are reported to reduce the water demand relative to other felsic minerals. They further found that carbonate rocks, like dolomite, give lower water demand, better mobility and less sensitivity to variations in shape factors than silicate rocks.

Kjellsen & Lagerblad (1995) studied the effect of natural minerals on different properties of mortars. The conclusion from experiments using mini-slump, as a measure of workability, was that the replacement of cement by calcite, wollastonite and anorthite influenced the rheological properties of the mortars positively. On the other hand, replacement by quartz, orthoclase and albite had little effect on workability. No plasticizing agents were used in these experiments.

Wallevik et al. (1995) have shown that an addition of four different types of fillers, all slightly coarser than the cement, did not alter the rheological properties of mini-concretes with $D_{\max} = 8$ mm. These four fillers were quartz, plagioclase feldspar, potassium feldspar and limestone, respectively. The water cement ratio in the set of experiments reported was 0.30, and the amount of filler was approximately 18 % by weight of cement. A naphthalene-based superplasticizer was used in all the experiments. On the other hand, a partial replacement of the quartz filler (10 % of the total filler amount) with biotite, muscovite and chlorite distinctly increased the yield stress, but did not change the plastic viscosity. An equal effect was observed for a secondary filler of amphibol containing 15 % biotite.

3.7.3 Concluding comments to the effects of fillers

There is obviously a large spectre of observed effects from filler additions, as could be expected from the large spectre of applications. The effect of different fillers can be very different depending of the basis of the mix design as have been discussed. Some of the reported experiments on fillers have been performed without any use of plasticizer. Bearing in mind the large effects of surface-active plasticizers, this makes most of this research of limited significance for modern concrete technology. There seems to be a lack of knowledge of general compatibility between fillers and plasticizers and on interactions between cement, filler and plasticizer. As the use of inert filler gains more and more importance both within filler cements and as an additive at the mixing plants, this is an obvious area where more research is needed.

4 Hypotheses

Based on literature review and pre-testing, the following hypotheses have been formulated:

Alkali-silica reactions

- Alkali-silica reactions and pozzolanic reactions are complementary reactions. All alkali-reactive materials are able to react either pozzolanic with CH to form CSH, or to produce swelling alkali-silica gel. The silica dissolution rate and the amount of CH being available locally are crucial parameters in this respect, and control whether non-swelling CSH or swelling alkali-silica gel are formed.
- Increased temperature and decreased particle sizes of the alkali-reactive rocks increases the silica dissolution rate. This promotes the pozzolanic reaction, but also the alkali-silica reaction. The use of highly accelerated methods using high temperature may alter the balance between the desirable pozzolanic reaction and the undesirable alkali-silica reaction. This is of particular importance when the inhibiting effects of additives believed to work through their pozzolanic behaviour are tested. Highly accelerated methods will not always give a reliable prediction of the long-term behaviour when pozzolanic materials are tested.

Rheological properties

- The effect of fillers on the rheological properties of fresh concrete may vary much due to differences in mineralogy and particle size distribution. The effect of a particular filler depends much on the mix design of the concrete. In particular, the type of plasticizer is important due to different dispersion mechanism and different adsorption characteristics.
- The yield stress of the matrix phase, though being small, is of large significance for the rheological properties of self-compacting concrete. The characterisation of the matrix phase by simple flow viscometers is insensitive to the small changes in yield stress. Hence, there is a need for a more fundamental characterisation of the matrix phase, involving both yield stress and plastic viscosity. By introducing the yield stress of the matrix phase as a parameter in addition to the plastic viscosity, the rheological properties of the concrete are directly correlated to the rheological properties of the matrix phase.

5 Experimental investigations

5.1 Introduction

The purpose of the experimental programme has been to test the effect of the filler materials on a variety of concrete properties. Both the effect on fresh properties and long-term effects, such as mechanical strength and properties directly related to durability, have been tested. Special attention has been given to the effects related to alkali-silica reactions.

This chapter presents test methods and calculations related to the experimental investigations. All the materials included in the experimental programme are described. Finally, an overview of the experimental programme of the present study is given.

5.2 Test methods and calculations

5.2.1 Pozzolanic reactivity by thermo gravimetric analysis (TGA)

5.2.1.1 Relevance of the TGA method

The pozzolanic reaction reduces the content of calcium hydroxide (CH) in a cement-based system. In principle, the kinetics of the pozzolanic reaction may then be observed by monitoring the CH content as a function of time. However, in the presence of Portland cement, the early pozzolanic reaction does not reduce the amount of CH. Justnes et al. (1992) have reported that silica fume reacts directly with already formed CSH, and that the direct reaction between CH and silica fume starts at later ages. Similar findings have been reported by Helmuth regarding fly ash mixes (in Biernacki et al 2001). By mixing the pozzolanic material with CH and water, leaving Portland cement out of the system, the pozzolanic reaction may be followed as the reduction of CH in this very simple system. As described by Justnes (1992), the pozzolanic reaction involves the alkalis normally present in a Portland cement system. In the absence of a natural source of alkalis, alkalis should then be added to the mix in order to accelerate the reaction speed. Artificial pore water simulating the chemistry of the actual pore water obtained when using the ordinary Portland cement, Norcem Standardsement, was therefore used as mixing water. This particular cement has a K/Na molar ratio of 2, and gives a pH of approximately 13.5. The artificial pore water was made by mixing 11.83 g of KOH and 4.22 g of NaOH per litre of water, thus giving the K/Na molar ratio of 2, and a OH^- concentration of 0.3162 moles/l, equivalent to a pH of 13.5.

Calcium hydroxide decomposes according to Equation 4.1 in a temperature range of approximately 450-550°C:



By using thermo gravimetric analysis (TGA), the pronounced weight loss due to the decomposition of CH may qualify as a measure of the pozzolanic reactivity. Similar methodology to determine the pozzolanic reactivity as used in the present study has recently been reported by Justnes & Østnor (2001) and by Biernacki et al. (2001).

5.2.1.2 Methodology of TGA

The fillers were mixed with calcium hydroxide and alkaline water in a weight proportion of 50:35:15 of filler, artificial pore water and calcium hydroxide, respectively. Some mixes had to be adjusted by adding more or less water in order to reach a compromise between workability and stability, see Section 5.4.2 for details. All mixes were left for sealed curing in small glasses at varying temperatures. A small quantity of water was added, carefully without disturbing the mix, at the top layer of the mixture in each glass at 2 days of curing. This was done to secure that the reactions not stopped due to lack of water. At the specified curing time, each sample was ground and dispersed in ethanol, followed by filtering and drying at 105°C. The thermal analyses were carried out on a NETZSCH 409 STA, with a heating rate of 10°C/min, using nitrogen as a purge gas and aluminium powder as a reference. The weight of the samples was 150 mg.

An example of the progress in consumption of calcium hydroxide in the reaction with fly ash is given in Figure 5.1. The CH decomposes in the pronounced weight drop around 500°C. At 90 days of curing, only a minor quantity of unreacted CH was left.

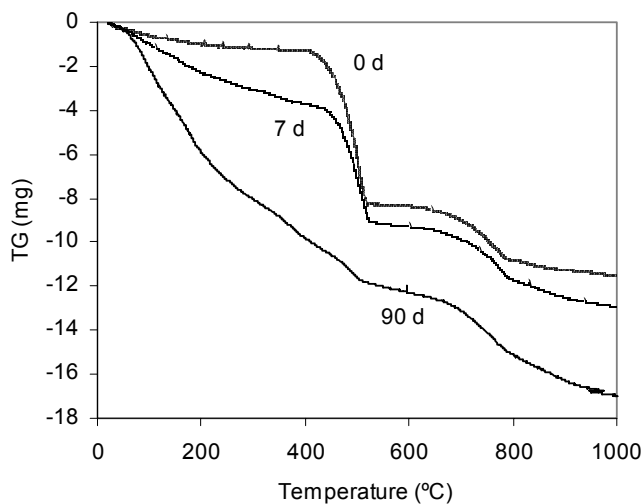


Figure 5.1. Examples of development of TG curves from 0, 7 and 90 days of curing at 20°C for equal mixes of fly ash 0-20, $\text{Ca}(\text{OH})_2$ and artificial pore water of $\text{pH}=13.5$ (see Section 5.2.1.1 for description).

5.2.1.3 Precision of the TGA method

For each mix of filler and CH, the amount of CH was determined for the starting point of the experiment, i.e. immediately after mixing. As the theoretical quantities at the starting points were known, these mixes could be used as an evaluation of the precision of the method. Together with results from the rhyolite filler at 7 days of exposure, these results are presented in Table 5.1. The calculated coefficient of variation is around 5 % according to these repeatability tests.

A TGA test on pure calcium hydroxide of the same origin as used in the pozzolanicity tests has been carried out. This test showed that 92 % of the theoretical quantity of the present water in the calcium hydroxide evaporates in the pronounced weight drop around 450-550°C. According to Table 5.1, the mean quantity of detected CH based on the initial mixes was 28.6 g. This is 83 % of the true quantity.

All the reported losses of CH in the present study is relative to the quantity measured initially by TGA. Even though the TGA measurement does not give absolute true values of the CH content, the methodology used in the present study is believed to give a reliable picture of the reduction in CH over time, since the losses are related to the amounts of CH measured initially (directly after mixing). Most of the tests were performed in series of 3-5 different curing times.

Table 5.1. Repeatability of TGA-method for determination of $\text{Ca}(\text{OH})_2$

Mixes	Quantity of $\text{Ca}(\text{OH})_2$ from TGA			Known quantity (mg)	
	Single values (mg)	Mean (mg)	Var. coeff. (%)		
Initial values, mixes with different fillers	28.2	28.3	28.6	5.0	34.5
	28.3	27.8			
	27.7	29.2			
	26.8	26.9			
	27.9	28.8			
	30.1	32.1			
	30.2	28.3			
Rhyolite, 7 days	20.6	19.5	5.2	-	
	18.6				
	20.1				
	18.8				

5.2.2 Concrete prism test (CPT)

5.2.2.1 Relevance of the CPT

The concrete prism test (CPT), CSA A23.2-14A (1994), has proven to give reliable predictions of field behaviour with respect to certain Norwegian alkali reactive aggregates, such as rhyolite, mylonite and quartzite (Jensen 1993). However, expansion results with phyllite and sandstones documented to be alkali reactive in field predicted these aggregates to be innocuous (Dahl et al. 1992, Jensen 1993). The unsuitability to predict the documented deleterious field behaviour of aggregates containing sedimentary rocks has been further described by Jensen (1996). As a result of these problems, the method has not been allowed for aggregate testing since 1993, and is presently only allowed to document the effect of mix design parameters such as pozzolans and alkali level (Norwegian Concrete Association 1996).

During the first years of Norwegian practice of the CPT at Sintef (Lindgård et al. 1993), the prisms were stored in large containers with a maximum of 24 prisms in each container. The prisms were stored vertically on a perforated rack over water. A wick of absorbent clothing were placed around the inside wall from top to bottom to ensure a sufficient moisture distribution. It is likely that this storing procedure did not give an adequate moisture situation to measure the potentially expansion caused by ASR. In particular, the expansions of concretes with sandstone aggregate were low compared to the known deleterious field behaviour.

In a study by Jensen & Fournier (2000), seven Norwegian aggregates, including two different sandstones and one phyllite, were tested according to both the Canadian

and Norwegian versions of the CPT. The Canadian version gave higher expansions for all aggregates. The differences varied from a maximum of approximately ten times (black sandstone) to about two times the Norwegian values obtained by storing in large containers. In addition to the storing conditions, some other parameters differ in the two versions of the CPT: the coarse to fine aggregate ratio is higher in the Canadian practice (60:40 versus 55:45), the prism size is smaller (7.5 cm x 7.5 cm x 30 cm versus 10 cm x 10 cm x 45 mm), and the alkali equivalent is somewhat higher according to the Canadian practice (5.25 versus 5.0 kg/m³ Na₂O equivalent). It has not been verified to what extent the different parameters have affected the results.

Some examples of results of rocks tested with the three different procedures are given in Table 5.2. Note that the reactivity within each group of aggregates might vary slightly due to different quarrying periods (one batch of Cataclasite of same origin as the one presented in Table 5.2 have given one-year expansion as low as 0.18 %, compared to 0.284 as reported here). As already discussed, there are major differences between results by the old Norwegian procedure and the Canadian procedure, but it seems like the results by the new Norwegian procedure is basically in the same order as the results obtained by using the Canadian procedure. Results obtained within the Normin 2000 project (1999) together with recent results at Norcem (Bremseth 2003) have also indicated that the Norwegian version of the CPT, with modified storing conditions, is able to predict the field performance of sandstones truly. The only difference between the new and the old version of the CPT is the storing conditions. In the new Norwegian version, the prisms are stored over water in small containers with only three prisms in each container. This is believed to give a higher and more stable moisture condition than the old version where up to 24 prisms were stored together in large containers.

Table 5.2. 1-year expansions for some aggregates tested by different procedures of the concrete prism method. Reactive coarse aggregate, non-reactive fine aggregate (< 5 mm).

Aggregate	Old Norwegian procedure	New Norwegian procedure	Canadian procedure
Mylonite	0.069 ¹	0.093 ²	0.141 ¹
Cataclasite	0.146 ¹	0.284 ³	0.276 ¹
Red sandstone	0.032 ¹	-	0.210 ¹
Black Sandstone	0.024 ¹	-	0.296 ¹
Spratt limestone	-	0.188 ²	0.170 ⁴

¹ Jensen & Fournier (2000)

² Present study

³ Meland (1999)

⁴ Fournier & Malhotra (1996)

More research is needed to evaluate the effects of the different versions of the CPT, e.g. the difference in prism sizes and the difference in mix design. However, the results presented above indicate that the moisture condition within the storing container is a critical parameter, and is probably the single most important factor.

The new Norwegian version of the CPT should be considered to be a reliable method highly suitable to predict field behaviour of aggregates, as well as assessment of mix design parameters. Some relevant details regarding the CPT version used in the present study are given in Table 5.3.

Table 5.3. Some details of the CPT version used in the present study.

Fine aggregate	45 % (< 5 mm)
Coarse aggregate	(55/3) % of each fraction: 5-10, 10-14, 14-20 mm
Water/cement ratio	0.45
Cement	400 kg
Alkalis	1.02 % Na ₂ O eqv. from cement, 0.23 % Na ₂ O eqv. from NaOH (A total of 5 kg/m ³)
Prism size	100 x 100 x 450 mm
Storage conditions	3 prisms stored vertical in each sealed container over a water reservoir. A wick of absorbent material is placed inside the wall from the top extending into the water. Stored at 38°C
Calculation of expansion	Based on total length of prisms

A low alkali plasticizer was used to adjust the workability of the separate mixes, aiming for target values of 14-18 cm slump.

5.2.2.2 Repeatability of the CPT method

The repeatability of the concrete prism method has been tested by replicate tests of two different recipes, see Table 5.4 and Table 5.5. Three separate mixes, and a total of nine prisms, were made of each recipe.

Note the large difference in expansion between the first mix in Table 5.4 and the two succeeding mixes (mean values of 0.17 % versus 0.36 %). The overall standard deviations at 52 weeks of exposure is approximately 0.01 % for both concretes, thus giving large differences in coefficient of variation due to the differences in expansion. Based on the present results, 0.01 % is believed to be an appropriate estimated value for the standard deviation of the expansion after 1 year of exposure. This value is rather high compared to the limit of expansion, which is presently 0.04 according to the Norwegian guidelines (Norwegian concrete association 1996).

Table 5.4. Replicate expansion data in % for three concrete mixes, each containing 3 prisms. Three identical batches, recipe with 5 % silica fume (by weight of cement).

Weeks	4	12	26	52
Prism number				
1	-0.002	-0.001	0.005	0.017
2	-0.005	-0.002	0.003	0.016
3	-0.003	-0.002	0.003	0.018
Mean	-0.003	-0.002	0.004	0.017
St.dev.	0.002	0.001	0.001	0.001
4	-0.012	-0.007	0.010	0.038
5	-0.014	-0.009	0.009	0.038
6	-0.014	-0.008	0.008	0.033
Mean	-0.013	-0.008	0.009	0.036
St.dev.	0.001	0.001	0.001	0.003
7	-0.010	-0.006	0.010	0.037
8	-0.010	-0.008	0.010	0.038
9	-0.011	-0.008	0.009	0.033
Mean	-0.010	-0.007	0.010	0.036
St.dev.	0.000	0.001	0.000	0.003
Overall mean	-0.009	-0.006	0.007	0.030
Overall st.dev.	0.005	0.003	0.003	0.010
Var. coeff.	-50.5	-55.6	41.0	32.8

Table 5.5. Replicate expansion data in % for three concrete mixes, each containing 3 prisms. Three identical batches, recipe with 5 % mylonite filler (by volume of total aggregate).

Weeks	4	12	26	52
Prism number				
1	0.001	0.009	0.035	0.139
2	0.000	0.008	0.033	0.128
3	0.000	0.008	0.034	0.126
Mean	0.000	0.008	0.034	0.131
St.dev.	0.001	0.000	0.001	0.007
4	-0.003	0.012	0.076	0.139
5	-0.004	0.012	0.079	0.131
6	-0.003	0.013	0.090	0.156
Mean	-0.003	0.013	0.082	0.142
St.dev.	0.000	0.000	0.007	0.013
7	-0.003	0.008	0.072	0.131
8	-0.003	0.010	0.074	0.133
9	-0.003	0.010	0.072	0.144
Mean	-0.003	0.009	0.073	0.136
St.dev.	0.000	0.001	0.002	0.007
Overall mean	-0.002	0.010	0.063	0.136
Overall st.dev.	0.002	0.002	0.022	0.009
Var. coeff.	-86.6	20.1	35.7	6.8

5.2.3 Accelerated mortar bar test (AMBT)

5.2.3.1 General

There exist different versions of the accelerated mortar bar test with small variations in mix design, in addition to large variations in prism sizes. The Norwegian practice of the AMBT method is based on the procedure described by Oberholster & Davis (1986), known as the NBRI method. The procedure of the method is given in a Sintef report (Lindgård et al. 1993). The prism size is probably the most important parameter regarding this method. Jensen & Fournier (2000) have reported the longer and thinner bars (25 x 25 x 250 mm) used by CANMET (CSA A23.2-25A 1994) to give higher expansions than the thicker and shorter ones used in Norway (40 x 40 x 160 mm). According to Jensen & Fournier (2000), this difference is basically caused by the slower diffusion of NaOH into the bars of larger cross sections. A conversion factor of 0.6 between the thinner bars and the thicker bars has been suggested.

The most common practice of the AMBT, also described in the Sintef procedure of the method, prescribes a certain grading of the tested aggregates. The tested fraction shall be between 0.15 and 4.8 mm. In the present study, crushed mylonite sand in the range between 0.125 and 4 mm was utilized as a reference. The sand was used as submitted from the producer, except that the filler (< 0.125 m) was removed by sieving. The use of a 0.125 – 4 mm fraction as well as the mix design was in accordance with the RILEM A-TC 106-2 draft (2000). A comparison between a mix design (including grading requirements) given by the Sintef-procedure and the mix design used in the present study, did not give significant differences in expansion at 14 days (0.16 % for both mix designs) for reference mixes of mylonite sand.

Some details with respect to mix design, prism size and storing conditions are given in Table 5.6.

Table 5.6. Details of the present version of the AMBT.

Water/cement ratio	0.47
Aggregate/cement ratio	2.4
Cement alkalis	1.02 % Na ₂ O equivalent
Prism size	40 x 40 x 160 mm
Storing	In 1 N NaOH solution at 80°C 3 prisms in each container
Calculation of expansion	Based on total length of prism

This method was not originally designed for testing of mineral admixtures such as silica fume, fly ash and rock fillers. Consequently, this kind of application of the method is in any case a modification of the original procedure. In the present study, the aggregate/cement ratio, as well as the water/cement ratio, was kept constant. This means that the added filler replaced an equal part of the aggregate by volume.

Due to the varying water demands of the fillers, the workability of the mortars was adjusted by using a low-alkali plasticizer.

5.2.3.2 Modified conditions of the AMBT

Testing of four series was carried out using pressure saturation with NaOH solution according to the following procedure:

The prisms were stored 28 days at ordinary conditions in 1 N NaOH solution at 80°C, thereafter dried for 3 days at 50°C, before 1 day of pressure saturation with NaOH solution at 50 atm. pressure. The ordinary storing (in 1 N NaOH solution at 80°C) proceeded after the drying and pressure saturation. The length changes were monitored during the whole process of storing, drying, pressure saturation and resumed storing at 80°C.

Some samples have also been examined using the following modified conditions of the AMBT method:

- 20°C in 1 N NaOH solution
- 38°C in 1 N NaOH solution
- 80°C in artificial pore water solution (pH = 13.5)

The artificial pore water solution was made by adding 11,2 g KOH, 4 g NaOH and 4 g Ca(OH)₂ per litre water. The amount of Ca(OH)₂ was deliberately >> than the solubility of Ca(OH)₂. The solubility of Ca(OH)₂ is reduced by increasing temperature, and by increasing pH. By having a surplus buffer of Ca(OH)₂, the actual amount of calcium ions in the solution will be self regulating, like the actual situation inside the mortar prisms.

5.2.3.3 Repeatability of the AMBT

A series of three identical mixes, each containing three prisms, were run to test the repeatability of the method (standard version with storing in 1 N NaOH solution at 80°C for 56 days). The results are given in Table 5.7.

Table 5.7. Test of repeatability, expansions in %.. Recipe with 10 % mylonite 0-125 filler (by volume of total aggregate).

Days	4	7	14	28	42	56
Bar number						
1	0.028	0.049	0.104	0.185	0.249	0.271
2	0.026	0.045	0.096	0.173	0.224	0.258
3	0.026	0.045	0.095	0.173	0.225	0.259
Mean	0.027	0.047	0.098	0.177	0.233	0.263
St.dev.	0.001	0.002	0.005	0.007	0.014	0.007
4	0.027	0.047	0.108	0.189	0.241	0.278
5	0.025	0.046	0.098	0.181	0.232	0.267
6	0.026	0.047	0.098	0.182	0.236	0.271
Mean	0.026	0.047	0.101	0.184	0.236	0.272
St.dev.	0.001	0.000	0.006	0.004	0.005	0.006
7	0.026	0.047	0.102	0.181	0.230	0.266
8	0.027	0.047	0.098	0.180	0.235	0.271
9	0.025	0.046	0.098	0.177	0.231	0.266
Mean	0.026	0.046	0.099	0.179	0.232	0.268
St.dev.	0.001	0.001	0.002	0.002	0.002	0.003
Overall mean	0.026	0.047	0.100	0.180	0.234	0.268
Overall st.dev.	0.001	0.001	0.004	0.005	0.008	0.006
Var. coeff.	4.2	2.8	4.1	2.8	3.3	2.3

Table 5.8 Estimated standard deviations.

Mean expansion (%)	Estimated st. dev. (%)
0.00	0.001
0.05	0.002
0.10	0.003
0.15	0.004
0.20	0.006
0.25	0.007
0.30	0.008

The overall tendency from the data is an increase in standard deviation with increasing expansion. Predicted standard deviations were calculated based on the linear regression line ($R^2= 0.89$) of overall standard deviation versus overall mean; see Table 5.8.

5.2.4 Electron probe microanalyzer (EPMA)

Examinations of polished concrete samples were done on a JXA-8900 electron probe microanalyzer at the Department of Materials Technology at the NTNU. An electron probe microanalyzer is basically a scanning electron microscope designed for X-ray analyses of elements from small areas. The JXA-8900 microprobe is equipped with 4 wavelength dispersive X-ray spectrometers (WDS) and an energy dispersive X-ray spectrometer (EDS). The instrument is able to analyse up to 12 elements and collect image signals from backscatter and secondary electron detectors simultaneously. Further description of the technology of EPMA may be found in standard textbooks on mineralogy, e.g. Battey & Pring (1997).

The EDS is basically suited to give qualitative data for different elements, while the WDS analyses are able to give quantitative data by spot-analyses or by scanning larger areas. In this study, each analysis was performed by scanning an area of approximately $100 \mu\text{m}^2$. Based on the analysed elements, the following oxides were stoichiometrically calculated: Na_2O , K_2O , MgO , Al_2O_3 , SiO_2 , SO_3 , CaO and FeO . The analysis total (i.e. the weight sum of all analysed oxides) was typically in the order of 70-80 % when analysing hydrated cement paste and alkali-silica gel. The large deviation from 100 % is believed to be basically due to bound water (hydrogen is not detected) and empty space. When analysing unreacted grains of cement and aggregates, the analysis total was close to 100 %.

5.2.5 Optical microscopy

The investigation was carried out by use of fluorescent impregnated thin sections (TS) and fluorescent impregnated polished section (PS) examined by polarising microscope, stereo microscope and UV - light. The dimensions of the thin sections were 30 mm x 48 mm and the polished sections 100 mm x 70 – 75 mm. The examination of concrete specimens (from CPT) has been carried out at NBTL (Norwegian Concrete and Aggregate Laboratory), while examination of mortar specimens (from AMBT) has been carried out at SINTEF Civil and Environmental Engineering, Department of Cement and Concrete. Observations of the textural changes and the reaction products caused by Alkali-silica Reaction (ASR) have been described. Description of methodology for examination in optical microscope has been described by Battey & Pring (1997).

5.2.6 Test methods for matrix rheology

5.2.6.1 General

The characterisation of the matrix phase has been performed using the FlowCyl tube viscometer and the Physica parallel plate rheometer. The mixing procedure of the matrix was equal for both methods. The cement was sieved before mixing in order to be sure to avoid large lumps, while the mixing was done as follows in a Hobart mixer:

- 1 min dry mixing of cement and filler (speed 1)
- 2 min of mixing with water and plasticizers (speed 1)
- 1 min stop, scraping of the walls within the mixing bowl
- 1 min of mixing (speed 2)
- 5 minutes stop, the bowl were covered to minimise evaporation
- 1 min of mixing (speed 2)

5.2.6.2 Matrix characterisation by the FlowCyl viscometer

The FlowCyl, which is a simple tube viscometer, measures the flow resistance ratio (λ_Q). The viscometer is a cylindrical steel tube with an outlet formed as a cone ending in a narrow nozzle. The FlowCyl is a modification of the Marsh Cone test, which was originally developed to characterise oil well cements. The FlowCyl method was developed by E. Mørtzell, and is described in detail in his doctoral thesis (1996) and in a conference paper by Mørtzell et al. (1996). See also the description of the Particle-Matrix model in Chapter three, Section 3.6. The inner diameter of the cylinder is 80 mm, while the outlet on the present version is 8 mm (versions of 6 and 10 mm also exist). The height of the cylindrical part is 300 mm, while the total length is 400 mm. A bowl placed on an electronic scale collects the matrix flowing from the cylinder, which is placed vertically on a rack.

The flow resistance ratio λ_Q is a representation of the average ratio between the flow loss in the measured liquid, and the flow of a theoretical ideal liquid (with no loss due to internal or external friction). When referring to Figure 5.2, the flow resistance ratio λ_Q is defined as the ratio between the loss-curve and the ideal-curve.

An ideal fluid will consequently have a λ_Q value of 0.0, while a non-flowing matrix will have a value of 1.0. Water will have a λ_Q value of 0.1, while values for typical matrices of SCC will lie between 0.6 and 0.8.

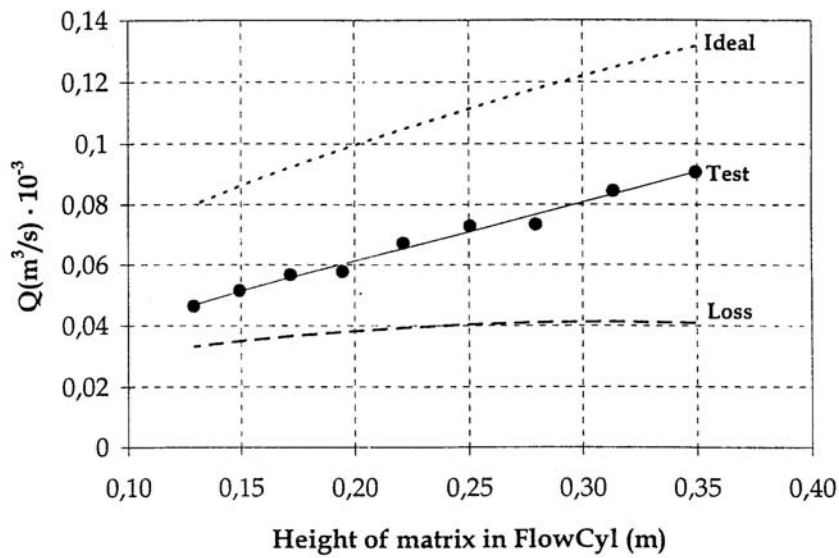


Figure 5.2 Example of FlowCyl test data. From Mørtzell et al. (1996)

The repeatability of the flow resistance ratio was tested using replicated runs in 14 experiments. According to Box et al. (1978), an estimate of the standard deviation s then can be calculated according to Equation 4.1 in the case of only two replicates of each experiment.

$$s = \sqrt{\sum d_i^2 / 2g} \quad (4.1)$$

d = difference between replicates

g = number of repeated experiments

The individual results from the 14 repeated tests are shown in Table 5.9. Based on the sum of d^2 , the standard deviation is 0.02.

Table 5.9. Data from replicate run test in FlowCyl.

Results from individual runs		Difference (d)	d ²
0.61	0.65	-0.04	0.0016
0.40	0.40	0	0
0.58	0.60	-0.02	0.0004
0.85	0.89	-0.04	0.0016
0.60	0.60	0	0
0.33	0.32	0.01	0.0001
0.41	0.44	-0.03	0.0009
0.68	0.75	-0.07	0.0049
0.36	0.35	0.01	0.0001
0.61	0.58	0.03	0.0009
0.37	0.36	0.01	0.0001
0.52	0.50	0.02	0.0004
0.82	0.80	0.02	0.0004
0.48	0.45	0.03	0.0009
$\Sigma d^2 =$			0.0123

The estimated standard deviation of 0.02 is believed to provide a measure of the total variability of the FlowCyl experiments, as each experiment includes weighing, mixing, testing and calculation. The standard deviation of 0.02 divided by the mean flow resistance ratio (0.55) gives a mean coefficient of variation of 3.6 %.

5.2.6.3 Matrix characterisation by the Physica rheometer

The rheological properties of the matrices were characterised by a Physica MCR 300 rheometer, using parallel plates with a gap of 1 mm. The lower plate is stationary, while the upper plate is rotating. The torque at the upper plate is measured continuously. The upper plate was roughened in order to minimise slippage. Wallevik (2003) have shown theoretically how the lubricating layer goes under a larger shear rate than that of the concrete as a whole, and that the relative shear rate of the lubricating layer is a function of the volume fraction of the aggregate, see description in Section 3.3.3. A typical matrix volume in the range of 350-360 liters/m³ thus results in a matrix shear rate 7-8 times larger than that in the concrete when concrete is considered to be a homogenous material. The BML viscometer operates in a shear rate range from 2 s⁻¹ – 10 s⁻¹, and the corresponding rate of shear for the matrix will then be in the range of about 20 – 80 s⁻¹. The testing was performed running a stepwise down-curve from a shear rate of 100 s⁻¹. Examples of torque-curves of four different matrices are given in Figure 5.3. Note that the time at each step was 5 seconds.

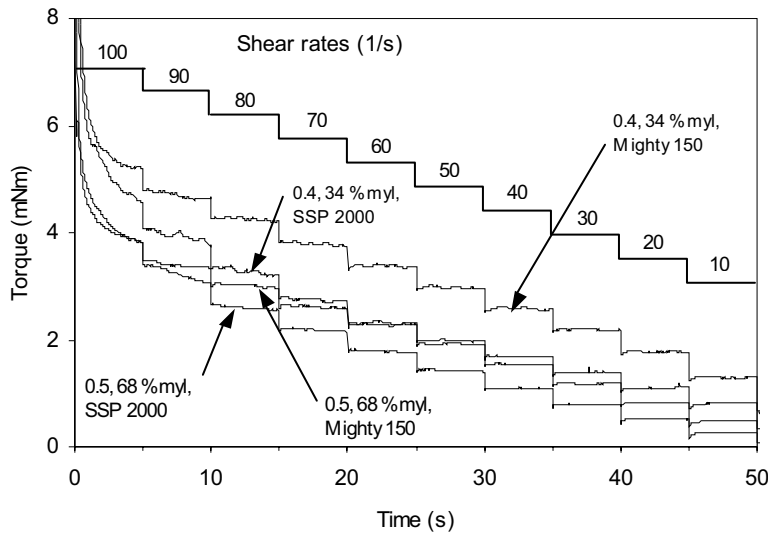


Figure 5.3 Torque versus time, 5 s measurements at each speed.

It can be seen from Figure 5.3 that the first step at the highest shear rate did not give a steady-state condition, presumably because the time was too short to brake down the flocculated or coagulated microstructure. From the third step (80 s^{-1}), a condition of steady state, or close to steady state, occurred quickly. Also note that at the lowest shear rates there were smaller or larger tendencies towards an increase in torque during the measurements, indicating rebuilding of the microstructure. This effect is more expressed at shear rates lower than 10 s^{-1} . The calculations of plastic viscosity and yield stress within the present study have been based on the range of shear rate from $80 - 20\text{ s}^{-1}$. The shear stress at each step was calculated based on the mean torque at the 2 last seconds.

It is clear that the testing procedure has a large influence on the rheological parameters to be tested. The chosen region of shear rate is important, as discussed in Section 3.3.3. Other parameters such as the time at each shear rate may be important, as shown by Geiker et al. (2002a); see Section 3.6.3. In the present study, the highest steps (shear rates of 100 and 90 s^{-1}) were used as a moderate pre-shearing of the matrix. By this procedure, a condition close to steady state was reached quickly at the succeeding steps.

Examples of shear stress- shear rate curves are presented in Figure 5.4. It can be seen that the matrices containing Mighty 150 had a behaviour relatively close to Bingham-behaviour, especially when the points at 90 and 100 are omitted. The matrices containing SSP 2000 had a more expressed shear-thickening behaviour.

Most of the tested matrices had a shear thickening behaviour, even though some had flow-curves being close to Bingham-curves. According to Cyr et al. (2000), shear thickening behaviour is very common for cement pastes containing superplasticizers, while the opposite (shear thinning) behaviour is more common in the cases with pastes containing no superplasticizers. The shear thickening behaviour is generally more expressed at higher dosages of superplasticizers. Mineral additives may also modify the intensity of the shear thickening behaviour.

Due to the shear thickening behaviour, all matrices were analysed using the Herschel-Bulkley approach (see Section 3.3.2). This approach of using the Herschel-Bulkley model has been reported in the literature by Cyr et al. (2000) for cement paste, and by de Larrard et al. (1998) to describe SCC. While the yield stress may be calculated directly by the model, the two other parameters attained when using this model is difficult to interpret physically. De Larrard et al. (1998) investigated the possibility of calculating an equivalent to the plastic viscosity of the Bingham model when using the Herschel-Bulkley model, and suggested an equation for this purpose. However, in the present study, the yield stress was calculated using the Herschel-Bulkley model, while the plastic viscosity was calculated by linear regression, i.e. according to the Bingham model.

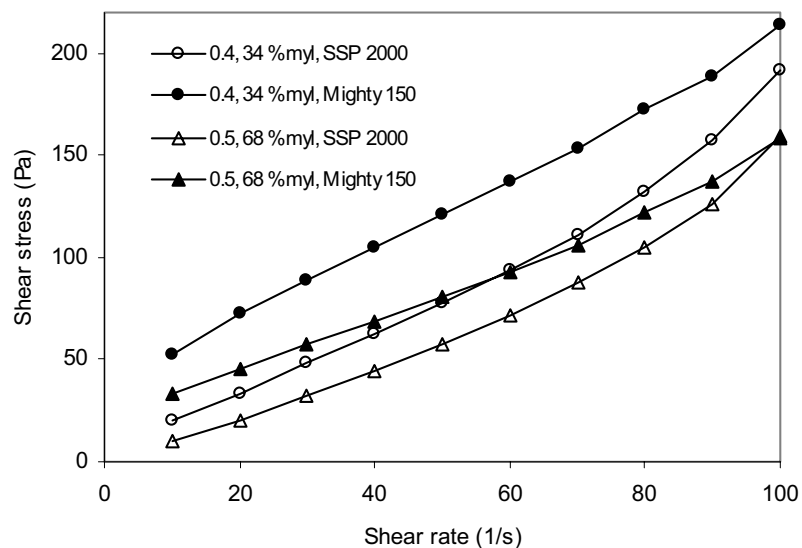


Figure 5.4 Shear stress versus shear rates.

The shear rate varies across the radius of the plate, with the maximum rate at the rim of the plate. All calculations in the present study are based on the maximum shear rates.

Repeatability testing of the Physica rheometer was carried out by repeated tests of three different mixes see; Table 5.10. The testing was done by genuine replicate testing, meaning that all tests were performed on freshly mixed matrices.

Table 5.10. Repeatability testing of matrices by the Physica rheometer.

Test nr.	Matrix 1		Matrix 2		Matrix 3	
	τ_0 (Pa)	μ (Pas)	τ_0 (Pa)	μ (Pas)	τ_0 (Pa)	μ (Pas)
1	28.1	1.27	12.2	1.44	6.5	0.75
2	28.8	1.17	10.9	1.34	5.1	0.73
3	25.7	1.18	10.5	1.35	5.3	0.71
4	32.2	1.25	11.1	1.34	5.5	0.72
Mean	28.7	1.22	11.2	1.37	5.6	0.73
St.dev.	2.7	0.05	0.7	0.05	0.6	0.02
Var. coeff. (%)	9.4	4.1	6.5	3.6	11.1	2.3

Based on the results presented in Table 5.10, the mean coefficient of variation for the yield stress is 9 % while the mean coefficient of variation for the plastic viscosity is 3.3 %. Hence, the repeatability of plastic viscosity is in the same order as the repeatability of flow resistance ratio tested by the FlowCyl (see Section 5.2.6.2).

5.2.7 Test methods for rheological properties of concrete

5.2.7.1 General

The concrete was mixed in a 60 litre Eirich mixer according to the following procedure:

- 1 minute of dry mixing of cement and aggregates
- 2 minutes of mixing, water and plasticizer was added during the first 30 seconds
- 5 minutes stop
- 2 minutes of mixing

The sand used in all the experiments was pre-wetted to a moisture level of about 4 %.

5.2.7.2 Slump-flow method

The slump-flow measure (SF) is a non-standardised method based on the ordinary slump cone. The slump flow is measured as the average diameter of the concrete after the slump cone has been lifted. The time to reach a diameter of 500 mm is also registered, and is denoted T_{500} . A description of the method is given in a national guideline for SCC (Norwegian Concrete Association 2002).

The empirical slump-flow test is a widely used method due to its simplicity, and it provides useful information regarding the mobility of the concrete. A visual, qualitative judgement of the stability of the concrete may also be done by this method.

5.2.7.3 Testing of rheological properties by the BML viscometer

The rheological tests on concrete were carried out using a Contec BML Viscometer 3. The apparatus is a coaxial cylinder viscometer, developed at the Norwegian Institute of Technology (present NTNU) in 1987 and has been described by Wallevik & Gjrv (1990). The outer cylinder is rotating at different speeds, while the inner cylinder is stationary and measures the torque. The inner cylinder is built in three parts, fixed top and bottom parts, and a middle part where the torque is measured. By this design, the top and bottom effects are eliminated, and the applied stress on the measuring unit is ideally generated from two-dimensional laminar flow. Both cylinders contain ribs to prevent slippage.

The testing was performed by running the standard procedure, which is a down curve in 7 steps. By running linear regression of the connection between torque and rotational speed, the values G and H according to the Bingham model are given. These values may be converted to τ_0 and μ by the Reiner-Riwlin equation (Wallevik 2003). All values of τ_0 and μ were directly calculated by the Freshwin-software provided by the manufacturer of the instrument, based on the torque-speed relationship from the testing.

All testing of concrete was carried out in series of 4 different matrix volumes, as the volume is known to be a parameter of major importance regarding the rheological parameters of the concrete. In addition, the relationship between the 4 points in each series gives a validation of the consistency within each series as the workability is expected to increase uniformly with increasing matrix volume. Strict repeatability testing with repeated experiments has not been carried out in the present study, but has recently been done by Wallevik (2003) at the same instrument as used in the present study. He reported repeatability testing of 3 different normal concretes of slump between 180 – 200 mm, with 4 replicates of each concrete. The results from testing at 10 and 40 minutes after water addition are given in Table 5.11.

Table 5.11. Repeatability testing of concrete by the BML-viscometer. Data from Wallevik (2003).

	Concrete 1		Concrete 2		Concrete 3		Mean
	10 min	40 min	10 min	40 min	10 min	40 min	
τ_0 (Pa)	223	351	266	387	217	300	
St.dev. (Pa)	56	24	25	64	19	13	
Var.coeff. (%)	25	7	9	17	9	4	12
μ (Pas)	17	18	8	10	7	9	
St.dev. (Pas)	2	4	2	3	1	1	
Var.coeff. (%)	9	24	25	31	16	16	20

The span in coefficient of variation is rather large, and goes from 4 to 25 % for the yield stress, with a mean value of 12 %. Correspondingly, the coefficient of variation varies from 9 to 31 % for the plastic viscosity, with a mean value of 20 %. The figures of the yield stress of the concretes tested in the present study is much lower than the results in the normal concretes reported by Wallevik (2003), while the plastic viscosities are higher than the values obtained by Wallevik (2003). Presumably, the coefficient of variation for self-compacting concrete will be slightly lower than those presented here with respect to plastic viscosity due to the higher values. Correspondingly, the coefficient of variation with respect to yield stress might be slightly higher. These assumptions are, however, of speculative nature, since no reliable results have been obtained with respect to repeatability of SCC in the BML viscometer to the author's knowledge.

5.2.8 Chemical and mineralogical characterisation

The chemical composition of the filler materials has been tested using X-ray fluorescence analysis (XRF) on a Philips PW 1480 instrument. The minerals in the crystalline filler materials have been identified by X-ray diffraction (XRD) analyses, using a Philips 1830 instrument. Semi-quantitative analyses of the minerals have been performed. Both the XRF and XRD analyses have been performed at the Department of Geology and Mineral Resources Engineering at the NTNU. The theoretical background of the XRF and XRD methods have been described by Battey & Pring (1997).

5.2.9 Particle size distribution

The particle size distribution was tested on a SediGraph 5100. This method is based on the sedimentation speed of a particle of spherical shape in a liquid, influenced only by gravity. The diameter of the spherical particle may be expressed by Stokes' law:

$$d = \sqrt{\frac{18\eta}{(\rho_s - \rho)g}}V \quad (4.2)$$

d	Stokes' diameter (m)
V	Speed of particle (m/s)
η	Viscosity of liquid (Pas)
ρ_s	Particle density (kg/m^3)
ρ	Density of liquid (kg/m^3)
g	Gravity (m/s^2)

The SediGraph apparatus measures the concentration of particles as a function of time by X-ray detection. Based on the progress of particle concentration with time, a particle size distribution may be calculated.

The given particle size distribution is expressed as equivalent spherical diameter distribution. Particle sizes differing much from spherical shape will consequently give a wrong picture of the real particle size distribution. The dispersion of particles in the testing liquid is very important, as agglomerates will be detected as larger particles. Further description of the methodology of testing may be found in the user's manual (Micromeritics 1998).

5.2.10 Capillary suction and porosity

The capillary suction test gives a quantification of the pore system of a concrete. The method used in the present study is described by Smeplass & Skjølsvold (1996). Concrete disks of 20 mm, cut from cylinders, were dried at 105°C for one week. The discs were then expressed to one-dimensional capillary suction by immersion in water. The increase in weight was monitored up to four days. By plotting the water absorption versus time, curves as illustrated in Figure 5.5 is given. The capillary number (k) and the resistance number (m) are calculated as illustrated in Figure 5.5.

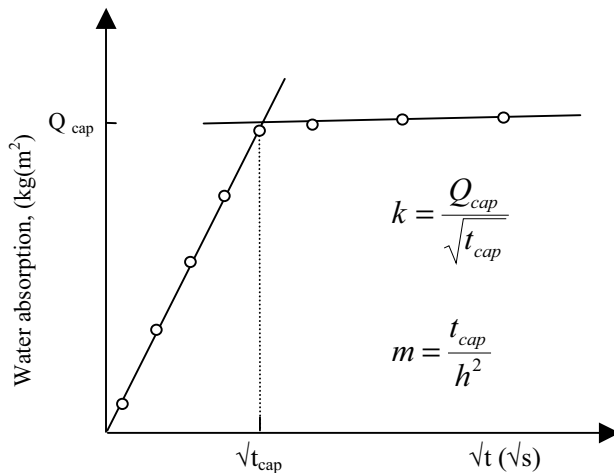


Figure 5.5. Capillary suction test, principal water absorption curve.

After ended capillary suction, the discs were submerged in water for 3 days, followed by 1 day of pressure saturation in water at 50 atm. The macro porosity (air content) and the total porosity may then be calculated in addition to the suction porosity.

5.2.11 Other methods

The air content, slump and density of fresh concrete were all measured in accordance to the Norwegian standards NS 3659, NS 3662 and NS 3660 respectively. Concrete cubes (100 mm) were used to determine the compressive strength, while cylinders of 100 x 200 mm were used for the capillary suction tests. The casting, curing and testing of the specimens were carried out in accordance to NS 3669 and NS 3668, respectively.

The precision of the compressive strength has been tested based on replicate experiments. A mean coefficient of variation of 3.7 % was found based on the present results.

5.3 Materials

5.3.1 Cements

All cements used in the present study have been delivered by Norcem and produced at the plant in Brevik. An ordinary Portland cement (Norcem Standard) has been the basis-cement, but three other cements have been utilized to some extent. Short descriptions of the cements are given below:

5 Experimental investigations

- OPC: Norcem Standardsement: General purpose ordinary Portland cement, CEM 1- 42.5 R according to NS-EN 197-1.
- HSOPC: Norcem Anleggsement: High strength low-alkali OPC, CEM 1- 52.5 N-LA according to NS 3086.
- ROPC: Norcem Industriseiment: Rapid special OPC for high early- strength, suited for winter concreting, CEM 1-42.5 RR according to NS 3086.
- SROPC: Norcem Sulfatresistent sement: Special purpose sulphate resistant, low-alkali cement, CEM 1-42.5 R-SR-LA according to NS 3086.

Chemical and physical data for the cements are given in Table 5.12.

Table 5.12. Chemical and physical data for cements.

	Cements					
	OPC ₁	OPC ₂	HSOPC ₁	HSOPC ₂	ROPC	SROPC
Chemical comp. (%)						
SiO ₂	19.89		21.30	21.01	19.35	21.81
Al ₂ O ₃	4.38		4.10	4.36	4.66	3.63
Fe ₂ O ₃	3.30		3.23	3.52	3.17	5.09
CaO	62.41		64.11	63.68	62.44	63.40
MgO	2.40		1.79	1.77	2.61	1.76
SO ₃	3.34	3.23	3.23	3.01	3.50	2.72
K ₂ O	1.07		0.47	0.55	1.14	0.47
Na ₂ O	0.32		0.19	0.17	0.38	0.14
Na ₂ O-equiv.	1.02		0.50	0.53	1.13	0.45
Loss on ignition	2.61	2.58	2.49	2.64	2.71	1.08
Bogue composition (%)						
C ₃ S	59.2		57.3	56.6	61.3	52.9
C ₂ S	12.3		17.8	17.5	9.2	22.6
C ₃ A	6.0		4.9	5.7	7.0	1.0
C ₄ AF	10.0		10.7	10.7	9.6	15.5
Le chatelier exp. (mm)	0.3	0	1.0	0.5	0.3	0
Blaine (m ² /kg)	362	362	389	375	543	357
Compr. strength (MPa)						
1 day	22.3	21.0	17.4	17.5	36.3	9.8
2 days	34.6	31.4	28.1	28.6	42.7	20.8
7 days	45.7	42.1	44	45.1	51.4	40.8
28 days	54.1	49.5	57.3	59.5	57.5	56.3

The OPC₁ batch has been used for all experiments of OPC except in two series of self-compacting concrete. The HSOPC₁ cement was used within the alkali-aggregate experiment, while the HSOPC₂ has been used within the series of rheology tests.

5.3.2 Silica fume

A non-compacted silica fume produced by Fesil has been utilized in this study. A second type of compacted silica fume (from Elkem Materials) has been used in some of the self-compacting concretes. The relevant data for the silica fumes are given in Table 5.13.

Table 5.13. Chemical and physical data for silica fumes.

	Chemical and physical data	
	Fesil	Elkem
SiO ₂ (%)	94.7	97.0
Al ₂ O ₃ (%)	0.05	0.14
Fe ₂ O ₃ (%)	0.36	0.04
MgO (%)	1.10	0.16
Cl (%)	0.03	0.03
CaO (%)	0.55	0.18
Na ₂ O eqv. (%)	0.65	0.46
SO ₃ (%)	0.54	0.35
LOI (%)	1.10	1.27
Bulk density (kg/dm ³)	0.25	0.67
BET surface (m ² /g)	22.1	19.6

5.3.3 Coarse and fine aggregates

In the following, brief descriptions of the aggregates that have been utilized in concrete, mortar or matrix are given. Gradings of the coarse and fine aggregates are given in Appendix A1.

Granite/ gneiss (Årdal):

Fine aggregate: A natural graded 0-8 mm granite/ gneiss sand of glacio-fluvial origin.

Coarse aggregate: Naturally rounded moraine aggregates, mixed with crushed overburden moraine-rock. (8-11 and 11-16 mm fractions).

The Årdal fine and coarse aggregates have practically equal mineralogy, dominated by quartz and feldspar. These aggregates are generally very well suited for concrete applications, and documented to be non-reactive with respect to ASR.

Mylonite (Dura-Splitt, Tau)

Crushed aggregate based on mylonite, formerly classified as quartz-diorite. The material has shown deleterious field performance (Jensen 1993). The following petrographic description has been given by Jensen & Fournier (2000):

“Grey-greenish, foliated and fine grained. Cataclasts or clusters with grain sizes ~0.4 mm dominate the rock and consist of altered feldspar, sericite, amphibole and carbonate minerals. Irregular bonds and linsoids of elongated re-crystallized quartz, have individual crystals on 0.01-0.05 mm. The rock was formerly classified as quartz mylonite but is more correctly classified as blastomylonite.”

The material has given the following performance in the CPT and AMBT (see Section 5.2.2 and 5.2.3, respectively, for details regarding test methods).

- 0.16 % expansion at 14 days (AMBT)
- 0.069 % expansion at 1 year (CPT, fine mylonite aggregate < 5 mm tested in combination with coarse non-reactive granite/gneiss)
- 0.093 % expansion at 1 year (CPT, coarse mylonite aggregate > 5 mm tested in combination with fine non-reactive granite/gneiss)

Cataclasite (Ottersbo)

Crushed cataclasite sand. The following petrographic description of the material has been given by Jensen & Fournier (2000):

“Greenish, homogenous and fine-grained. The major constituents are feldspar particles in a matrix of quartz, “crushed” feldspar, dark minerals and mica. Average grain size of the matrix is 0.01-0.03 mm. The feldspar crystals are max. 0.7 mm and the quartz crystals are mostly about 0.05 to 0.3 mm.”

The material has given the following performance in the AMBT and CPT:

- 0.24 % at 14 days (AMBT)
- 0.28 % at 1 year (CPT, coarse cataclasite aggregate > 5 mm tested in combination with fine non-reactive granite/gneiss)

Spratt limestone (Ontario, Canada):

Canadian reference aggregate, limestone containing 3-4 % reactive chalcedony and black chert with a conchoidal fracture. Cracking and distress due to ASR is reported to be apparent within ten years in field. (Rogers 1988)

Expansion in the CPT: 0.170 % after 1 year. (Fournier & Malhotra 1996)

5.3.4 Fillers

5.3.4.1 Description of the filler materials

The fillers were primarily chosen to give a spectre of properties with respect to alkali reactivity. In the following, a brief description of each material is given. Detailed mineralogical, chemical and physical data are tabulated in the subsequent sections. It should be noted that the definition of filler in the present work, i.e. powders with nominal particle size below 125 μm differs from the definition of filler aggregate given in the European standard EN 12620 "Aggregates for concrete". According to EN 12620, filler aggregate or fines should pass the 63 μm sieve.

The fillers have been separated into different fractions using an air classifier (ACX 200) at SINTEF Materials Technology. See Table 5.16 for details regarding the particle size distribution. The air classifier works according to the following description given by Chmelar (2003):

"The air classifier separates particle according to their particle size. The fine particles are swept up towards the classifying rotor, while the coarse material is discharged from the classifier by gravity through the coarse fraction outlet. The finer fractions presented to the classifying rotor, are selected or rejected according to the resultant of a positive air drag force opposing a negative rejecting centrifugal force, developed from the rotor speed. The selected fine fractions flows through the rotor and is discharged from the classifier through the air outlet, together with the air flow. The fine fraction is separated from the air in a downstream cyclone or filter."

Granite/gneiss:

Filler sieved from the glacio-fluvial sand from Årdal, see description in Section 5.3.3.

Limestone (Verdalskalk):

Filler from crushed limestone. The limestone is pure calcite considered non-reactive.

Mylonite (Dura-Splitt):

Filler sieved from crushed mylonite sand, delivered from Norstone's plant at Tau. For petrographic description, see mylonite in Section 5.3.3.

Cataclasite (Ottersbo)

Filler sieved from crushed cataclasite sand. For petrographic description, see cataclasite in Section 5.3.3.

Rhyolite (Hvalfjörður, Iceland)

Ground rhyolite from this source has earlier proven to be pozzolanic (Gudmundsson 1975). The material is considered highly reactive, expansion data from testing in ASTM C 227 are 0.245 % and 0.351 % at 26 and 52 weeks, respectively (Helgason

1981). However, testing of rhyolite sand of standard grading according to the Sintef-procedure in the AMBT in the present study, has given an expansion at 14 days of only 0.06 %. The expansion at 56 days was 0.59 %.

Hólmgeldsdóttir (2001) has carried out a petrographic examination of the rhyolite, a summary is given below:

“The rhyolite has a glassy texture with conchoidal fractures and flow structures. Phenocrystals are feldspars, mainly plagioclase but also microcline, and to a lesser extent pyroxene. The groundmass mineral assembly is hard to establish because of small crystal size, however, this is mainly feldspars and quartz. Opaque minerals are also existent in the more crystallised particles. The particles are altered to various extents, ranging from almost no alteration evident to almost completely alteration (rare). The alteration mineral assembly consists of zeolites, clay minerals (possibly including smectite), quartz minerals, and high temperature minerals like epidote and possibly some more.”

Quartz (Vatne)

Coarsely crystalline pure quartz, ground and sieved.

Glass (Microfiller)

A commercial Swedish filler (Microfiller) of crushed recycled glass (a mixture of white and coloured glass).

Fly ash

Danish fly ash, delivered from Norcem AS. This specific fly ash is utilized in the fly ash cement produced by Norcem, and is documented to reduce expansion caused by ASR significantly (Kjellsen et al. 2001). While the fly ash is being ground together with the Portland clinker when utilized in cement, the fly ash used in the present study was not ground.

Carbonate filler (Hydro)

Precipitated calcium carbonate filler (CaCO_3), a residual from the production of fertiliser. The particles are close to being perfect spheres due to the chemical precipitation. The filler contains small amounts of $\text{NH}_4\text{-N}$ (< 0.3 %) and $\text{NO}_3\text{-N}$ (< 0.4 %).

5.3.4.2 Mineralogical and chemical composition of the fillers

Mineralogical compositions for the rock fillers are given in Table 5.14. No crystalline quartz was detected in the rhyolite, neither by XRD nor by DTA. Cross et al. (1902) devised a set of mathematical calculations that is applicable to a whole rock analysis of a fine-grained rock, in order to determine a theoretical modal mineralogy. This is known as the CIPW norm. The calculated modal mineralogy is intended to represent the mineralogy of the rock if it had cooled and crystallized slowly. A theoretical CIPW composition of the rhyolite, based on the oxide

composition given from the XRF analysis, indicates an amount of silica in the order of 25 %.

Table 5.14. Semi-quantitative XRD-analysis of rock fillers.

Filler	Mineralogical composition (%)							
	Quartz	Plagiocl.	K-feldsp.	Mica	Epidot	Chlorite	Calcite	Amphib.
Mylonite 0-20	28	43	-	8	7	10	4	-
Mylonite 10-30	30	42	-	5	13	6	4	-
Mylonite 20-125	22	54	-	5	8	5	6	-
Cataclasite	28	37	7	-	21	7	-	-
Rhyolite *	-	30	65	2	-	3	-	-
Granite/ Gneiss	18	46	19	10	-	4	-	3
Limestone	-	-	-	-	-	-	100	-
Carbonate	-	-	-	-	-	-	100	-
Quartz	100	-	-	-	-	-	-	-

* In % of crystalline phases. Amount of silica glass uncertain, but probably in the order of 25 %.

Separation of fillers in smaller fractions may result in a varying mineralogical composition for the different fractions. No reliable conclusions can be drawn from the semi-quantitative analyses of fillers due to the uncertainty of the method, but the tendency towards varying mineralogical composition, as seen in Table 5.14, should be kept in mind. The differences observed for the mylonite filler of varying fractions are seen in the bulk chemical data given in Table 5.15, and it should be noted that a CIPW-analyses based on the bulk chemical oxide composition, gives a higher quantity of quartz within the mylonite 20-125 fraction compared to within the 0-20 fraction. This contradicts the results of mineralogical composition given in Table 5.14, where the percentage of quartz is higher for the finer (0-20) than the coarser (20-125) fraction.

Table 5.15. Oxide composition of filler materials detected by XRF.

Filler	Chemical composition detected by XRF (%)										
	Fe ₂ O ₃	TiO ₂	CaO	K ₂ O	P ₂ O ₅	SiO ₂	Al ₂ O ₃	MgO	Na ₂ O	MnO	LOI
Myl. 0-20	6.00	0.26	5.04	1.18	0.19	63.42	17.19	1.98	3.64	0.13	3.14
Myl. 10-30	5.16	0.25	5.32	0.83	0.21	66.63	15.45	1.46	3.48	0.12	2.73
Myl 20-125	3.85	0.31	5.22	0.56	0.31	70.09	14.05	0.96	3.64	0.10	2.09
Cat. 0-20	6.63	0.64	5.07	1.78	0.16	62.85	15.38	3.02	3.13	0.11	2.10
Cat. 10-40	5.78	0.58	5.40	1.78	0.15	64.26	15.80	2.14	3.41	0.09	1.59
Rhyo. 0-20	6.46	0.79	3.67	3.08	0.16	65.68	14.73	1.09	2.97	0.14	4.05
Rhyo. 0-40	6.57	0.80	3.60	2.72	0.15	65.96	14.28	1.08	2.92	0.13	3.54
Granite	6.05	0.81	2.66	4.14	0.28	63.56	15.21	2.21	3.34	0.09	1.74
Glass	0.15	0.06	10.55	0.81	0.02	70.80	2.54	1.79	11.29	0.02	1.55
Fly ash	3.11	1.64	3.59	1.19	0.84	56.38	30.31	0.94	0.38	0.03	2.80
Quartz	0.77	0.01	0.01	0.01	0.01	98.37	-	0.03	0.10	-	-0.17

5.3.4.3 Particle size distribution of the fillers

Some characteristic figures of the filler materials with respect to particle size distribution are given in Table 5.16. The grading curves are plotted in Appendix A2. The results are obtained using the SediGraph; see description in Section 5.2.9.

Table 5.16 Particle size distribution of fillers measured by the Sedigraph.

Filler	D ₁₀ μm	D ₅₀ μm	D ₉₀ μm	Blaine m ² /kg
Mylonite 0-20	2.6	8.0	16.3	
Mylonite 10-30	7.7	16.7	25.3	
Mylonite 20-125	19.2	45.7	102.5	
Mylonite 0-125	4.5	27.3	91.0	237.6
Rhyolite 0-20	2.6	8.8	18.8	
Rhyolite 10-40	5.6	23.5	38.5	
Rhyolite 0-125	2.3	24.9	71.9	
Glass 0-20	3.1	9.7	19.2	
Glass 0-125	5.8	32.3	124.7	234.0
Fly ash 0-20	3.1	8.2	18.3	
Fly ash 0-125	2.3	12.1	48.2	450.4
Cataclasite 0-20	3.0	8.4	17.6	
Cataclasite 10-40	10.9	22.4	37.7	
Cataclasite 0-125	4.1	30.6	81.7	170.5
Granite 0-20	4.0	12.5	22.0	
Granite 0-125	21.0	52.8	125	85.6
Limestone 0-30	2.3	9.7	25.0	
Limestone 0-40	1.9	12.9	37.2	
Limestone 20-125	17.5	61.6	130.7	
Limestone 0-125	2.3	18.8	77.0	350.1
Limestone Norcem 0-125*	2.0	17.2	72.0	
Carbonate 0-125	21.8	42.5	78.6	80.4
Quartz 0-125	6.3	35.9	79.8	

* Values obtained by Malvern Master Sizer.

5.3.5 Plasticizers

Five different plasticizers have been used in the present study; see short descriptions below:

- Scancem SSP-2000, Polycarboxylic co-polymer (25 % active content)
- Scancem CP-30, Polycarboxylic co-polymer (30 % active content)
- Scancem P, Sulphonated sodium-lignin (40% active content)
- Scancem Mighty 150, Sulphonated sodium-naphthalene condensate, (40 % active content.)
- Sica ViscoCrete-3, Polycarboxylic co-polymer (28 % active content)

5.4 Experimental programme

5.4.1 General

The experimental programme is divided into two main parts. Both of these main parts are divided into three different laboratory programmes.

Long-term effects:

- Pozzolanic reactivity by thermo gravimetric analysis (TGA)
- Alkali-silica reactivity by the concrete test (CPT)
- Alkali-silica reactivity by the accelerated mortar bar test (AMBT)

Mechanical strength and capillary suction tests has been carried out for all the concretes subjected to the Canadian concrete test.

Rheological properties of fresh mixtures

- Matrix parameter study by the FlowCyl viscometer
- Matrix parameter study by the Physica rheometer
- Study of the relationship between the rheological properties of matrix (measured by the FlowCyl viscometer and the Physica rheometer), and self compacting concrete (measured by the BML-viscometer and the slump-flow measure)

An outline of the experimental programme is given in the following sections.

5.4.2 Pozzolanic reactivity

The aim of this set of experiments was to test the pozzolanic reactivity of the fillers directly, by testing their ability to react with calcium hydroxide. The remaining amount of calcium hydroxide at different times was detected using the TGA, see Section 5.2.1 for background information and details of the method. The mixing proportions were as follows: 50 g filler, 15 g Ca(OH)₂ and 35 g artificial pore water. The following mixes had to be adjusted with respect to water amount: mylonite 0-30: 30 g water, mylonite 20-125: 25 g water, rhyolite 0-20: 40 g water, quartz 0-125: 25 g water. The pH of the mixing water was 13.5, see Section 5.2.1 for details of the composition of the mixing water.

An outline of the experimental plan is given in Table 5.17. See Section 5.3.4 for details of the tested fillers.

Table 5.17 Test programme for pozzolanic reactivity

Filler	Curing temperature		
	20°C	38°C	80°C
Mylonite 0-20	x*	x	x
Mylonite 10-30	x		
Mylonite 20-125	x		
Cataclasite 0-20	x		
Granite 0-20			x
Rhyolite 0-20	x		x
Fly ash 0-20	x		
Glass 0-20	x		
Quartz 0-125	x		

* Also tested at pH = 13 and 14

The remaining quantity of CH was determined at ages of 0, 1, 7, 28 and 90 days for most of the mixes, while one or more of the ages was skipped for some of the experiments. Some mixes were also tested at an age of 3 days.

5.4.3 Alkali-silica reactions by the concrete prism test (CPT)

The purpose of the experiments carried out in the Norwegian version of the concrete prism test (see Section 5.2.2 for information of the test) was to evaluate the performance of the fillers with respect to alkali-silica reactivity (ASR). Most tests were run for 2 years. In addition to the examination of expansion characteristics, testing of compressive strength after 1, 28 and 365 days and capillary suction after 365 days have been carried out for all concretes. The outline of the test programme is given in Table 5.18. All amounts are given in percentage of total aggregate volume, except the amount of silica fume given in percentage of the cement weight. The quantity of both cement and reactive mylonite gravel was kept constant for all mixes in Table 5.18, meaning that the fillers replaced an equal volume of non-reactive sand.

5 Experimental investigations

Table 5.18. Test programme for evaluation of fillers by the CPT. Non-reactive sand (0-5 mm granite), mylonite coarse aggregate (5-20 mm) and OPC in all mixes. Constant w/c ratio (0.45) and quantity of cement (400 kg/m³) for all mixes. The alkali level was adjusted by adding NaOH. Amount of filler is given in vol. % of total aggregate (5.15 and 10.3% are abridged to 5 and 10 % respectively).

Filler	Alkali load (Na ₂ O eqv., kg/m ³)		
	4	5	10
Reference	x	x	
5 % Mylonite 0-20		x	
5 % Mylonite 10-30		x	
2 % Mylonite 0-125		x	
5 % Mylonite 0-125 ¹	x	x	
10 % Mylonite 0-125	x	x	x
5 % Rhyolite 0-20		x	
5 % Rhyolite 0-125		x	
5 % Cataclasite 0-125		x	
5 % Glass 0-125		x	
5 % Fly ash 0-125		x	
5 % Silica fume ²	x		
7.5 % Silica fume ²	x	x	x

¹) The 5 kg alkali level was also tested with HSOPC and ROPC

²) Silica fume in weight % of cement

The following tests have also been run:

- Mylonite sand (0-5 mm), non-reactive coarse aggregate (5-20 mm)
- Mylonite sand (0-5 mm), non-reactive coarse aggregate (5-20 mm), filler in sand exchanged with non-reactive granite 0-125 filler
- Non-reactive sand (0-5 mm), Spratt limestone coarse aggregate (5-20 mm)
- Non-reactive sand (0-5 mm), Spratt limestone coarse aggregate (5-20), 5 % mylonite 0-125 filler

The relative volume fraction of fine aggregate (0-5 mm) was kept constant at 45 % for all mixes. The added fillers were counted as fine aggregate.

Micro structural analysis (optical microscopy on thin sections and polished sections and microprobe analysis) have been carried out on the following mixes:

- Reference (only optical microscopy)
- 5 % mylonite 0-125
- 5 % rhyolite 0-125
- 5 % glass 0-125

5.4.4 Alkali-silica reactions by the accelerated mortar bar test (AMBT)

Based on international literature, e.g. Bérubé et al. (1995), Fournier & Malhotra (1999), the method was believed to give a true prediction of the effects of supplementary materials such as fly ash, silica fume and slag. Prior to the present study, the AMBT was therefore believed to provide an adequate measure of the effects of rock fillers and other mineral fillers. The test, as described in Section 5.2.3, was therefore applied as a screening of the fillers. Additionally, the testing by the AMBT aimed towards a calibration of data based on the parallel testing by the CPT, which is believed to be the most reliable method with respect to ASR. The primary test programme carried out using the AMBT is given in Table 5.19.

Table 5.19. Primary test programme for evaluation of fillers by the AMBT method. Reactive mylonite sand was used in all mixes. Amount of filler is given in. % of total aggregate volume.

Filler	Quantity	
	10 %	20 %
Mylonite 0-20	x	x*
Mylonite 10-30		x
Mylonite 20-125		x
Mylonite 0-125	x	x
Rhyolite 0-20		x
Rhyolite 10-30		x
Rhyolite 0-125	x	x
Cataclasite 0-20	x	x*
Cataclasite 10-30		x
Glass 0-20		x
Glass 0-125	x	x
Fly ash 0-20	x	
Fly ash 0-125	x	
Granite 0-125		x
Limestone 0-20		x
Quartz		x

*Also tested with reactive cataclasite sand

Silica fume has also been tested at a level of 7.5 % of cement weight. Reference mixes of mylonite, cataclasite, granite and rhyolite (containing no filler) have also been tested.

Micro structural analyses (optical microscopy of thin sections) have been carried out for a reference mortar containing no filler, and for a mix containing 20 % 0-20 mylonite filler.

Duplicate tests of four mortar mixes were carried out using pressure saturation (see Section 5.2.3.2) of the mortar bars in NaOH solution. The aim of this set of experiments was to examine to what extent the availability of NaOH is a limiting factor. Prisms of the following four mixes were exposed to this procedure:

- Reference mix of mylonite sand
- 10 % of 0-20 mylonite filler
- 10 % 0-20 rhyolite filler
- 7.5 % silica fume

The amounts of mylonite and rhyolite fillers are given in % of total aggregate volume, while the amount of silica fume is given in percent of cement weight.

5.4.5 Modified conditions of the AMBT

In order to gain a more fundamental understanding of the observations made using the AMBT, the following mixes have been run in modified conditions of the method:

- Reference mix of mylonite sand
- 10 % 0-20 mylonite filler
- 10 % 0-20 cataclasite filler
- 7.5 % silica fume

The following modified conditions were run:

- 20°C in 1 N NaOH solution
- 38°C in 1 N NaOH solution
- 80°C in artificial pore water solution (pH = 13.5)

The amounts of mylonite and cataclasite fillers are given in % of total aggregate volume, while the amount of silica fume is given in percent of cement weight.

A limited study on the expansion in a very early phase (up to two days after moulding) has been carried out to investigate if expansions in this early phase are of significance. In this study, a reference mortar with no filler, and a mortar containing 20 % mylonite 0-20 filler were examined.

5.4.6 Parameter study of matrix rheology by the FlowCyl viscometer

The test programme was designed to test the effect of an increased filler amount at a constant w/c ratio of 0.50. In addition, the effect of replacing cement by filler was tested at a constant w/p ratio of 0.38. The basic idea of the design of the test programme is given in Table 5.20. The amount of filler given in Table 5.20 represents the amount of added mylonite filler in terms of weight % of cement. Other fillers than mylonite, differing in density, were added at an equivalent amount with respect to volume. The amount of plasticizer (SSP 2000) was 1 % of the cement weigh for the mix of w/c = 0.5 and w/p = 0.31. An equal amount of plasticizer with respect to the total powder volume was added to the other mixes.

Table 5.20. Basis programme for testing of fillers by FlowCyl viscometer. Numbers in the table represents amount of filler in volume % of cement. The w/c ratios and the w/p ratios are weight-based. Strictly speaking, the w/p ratios are valid only for mylonite filler due to the density differences.

w/p \ w/c	0.43	0.38	0.31
0.40		3 %	
0.50	17 %	34 %	68 %
0.60		64 %	

The following six fillers were tested according to the basis programme described above: Mylonite, granite, carbonate, fly ash, glass and limestone (all 0-125 gradings). Additional tests using limestone powders of 3 other gradings were also performed at a w/c ratio of 0.5 and w/p ratio of 0.38. The investigations described in this section were carried out by Johansen (2002) and have previously been reported in his MSc thesis.

5.4.7 Parameter study of matrix rheology by the Physica rheometer

The design of the test programme for matrices tested in the Physica rheometer aimed towards very stable mixes in order to avoid problems with separation. A total of 53 mixes have been tested, 15 of these have also been tested using the FlowCyl viscometer. An outline of the test programme is given in Table 5.21. The mixes of w/c = 0.5 and 67 % filler have an equal water/powder ratio on a volume basis as the mixes of w/c = 0.4 and 34% filler. This gives the possibility to directly compare the effect of exchanging cement by filler on a volume basis. The percentages of added filler, given in the table, are weight based and are strictly speaking only valid for the mylonite filler. Regarding the other fillers, equal amounts were added on a volume basis. The plasticizer dosage was based on an equal dosage per volume unit of total powder. The addition level was 0.8 % for the mixes containing 34 % of filler, and 1 % for mixes containing 67 % of filler. This gives equal dosages per volume powder.

As seen in Table 5.21, most mixes were tested in combination with two different plasticizers. This was done in order to study to what extent there are interaction effects between fillers and superplasticizers. The chosen plasticizers, SSP 2000 and Mighty 150, are both highly effective. But while the dispersing mechanism for the Mighty 150 is believed to rely basically on electrostatic repulsion, the dispersing mechanism regarding the SSP 2000 is said to rely basically on steric hindrance.

Table 5.21. Outline of test programme for matrix testing by Physica rheometer. The addition levels of filler are given in volume % of cement.

Filler	w/c = 0.4 34 % filler		w/c = 0.5 67 % filler		w/c = 0.5 34 % filler	
	SSP	Mighty	SSP	Mighty	SSP	Mighty
Mylonite 0-125	x ¹	x ¹	x ²	x ²	x ³	x
Mylonite 0-20	x					
Granite 0-125	x	x	x	x		
Granite 0-20	x					
Glass 0-125	x	x	x	x		
Granite 0-20/ 0-125	x					
Cataclasite 0-125	x		x			
Limestone 0-125	x	x	x ²	x ²	x	x
Fly ash 0-125	x	x	x			
Carbonate 0-125	x		x			
Rhyolite 0-125	x					

¹⁾ Also tested with HSOPC and ROPC

²⁾ Also tested at plasticizer dosage equivalent to dosage at w/c = 0.4 relative to cement weight

³⁾ Also tested in combinations with other plasticizers (lignosulphonate, Viscocrete-3 and CP-30. All plasticizers were tested at varying dosages

Notations and other relevant information of the materials in Table 5.21 are given in Section 5.3.

5.4.8 Relationship between the rheological properties of matrix and self-compacting concrete (SCC)

The limitations of the particle matrix (PM) model with respect to self-compacting concrete (SCC) have been discussed in Chapter 3. As a consequence of these limitations, the relationship between matrix rheology and concrete rheology has been investigated by studying the matrix from 10 series of concrete in the Physica rheometer, see Section 5.2.6 for information of the method. The concretes were tested in series of 3 or 4 matrix volumes, including a total of 38 concrete mixes in the present work. Results from four of the ten concrete series have been incorporated in this work from a national research project (Smeplass and Fredvik, 2001, Smeplass 2002). Testing of the other six concrete series was carried out as part of a MSc project. These results have previously been reported by Granerud (2002). All the matrix tests described in this section have been carried out in the present study.

The studied parameters in this work were the matrix volume and the matrix composition. The matrices were designed to cover a wide field of rheological properties in order to give large variations in the matrix volumes necessary to reach self-compacting concrete. The aggregate composition was exactly the same for all 38 concretes tested in this study. Since the matrix volume varies throughout the test programme, the volume of the aggregate varies correspondingly. This causes a

minor variation in the amount of fines from the aggregates contributing to the matrix phase. This effect has been minimised by using the average matrix volume within the series. The total effect of the relative variation in filler amount is believed to be small compared to other possible sources of error.

Table 5.22. Mix design of self-compacting concretes. Addition levels of fillers and plasticizers are given in weight % of cement.

Cement	w/b	w/p	Filler	Silica fume	Plasticizer	Matrix vol.
HSOPC	0.4	0.30	20 % limest.	5 %	1 % CP 30	325-355
HSOPC	0.4	0.30	20 % mylon.	5 %	1 % CP 30	325-370
ROPC	0.5	0.37	20 % limest.	5 %	1 % CP 30	355-400
ROPC	0.5	0.37	20 % mylon.	5 %	1 % CP 30	355-400
OPC	0.5	0.37	20 % limest.	5 %	1 % CP 30	325-370
OPC	0.5	0.37	20 % mylon.	5 %	1 % CP 30	325-370
OPC	0.6	0.32	60 % limest.	-	1.2 % SSP 2000	340-370
OPC	0.4	0.35	-	-	1 % SSP 2000	340-400
SROPC	0.4	0.36	15 % limest.	5 %	0.7 % CP 30	310-340
ROPC	0.5	0.42	-	5 %	1 % CP 30	325-370

The concrete rheology was studied using the slump flow measure and the BML viscometer, both methods have been described in Section 5.2.7. The corresponding matrices were studied using both the FlowCyl viscometer (see Section 5.2.6.2) and the Physica rheometer (see Section 5.2.6.3).

6 Effects of alkali-reactive fillers in concrete – results and discussion

6.1 Introduction

This chapter presents the most important findings from investigations on the long-term effects of using alkali-reactive fillers in concrete. Special attention has been given to investigate the effects caused by mylonite crushed rock fines from Tau, and to clarify the possibilities and limitations of using fines from this particular source. In addition to this mylonite, the study has included the following alkali-reactive fillers: Norwegian cataclasite, Icelandic rhyolite and crushed bottle glass (Swedish commercial product called “microfiller”). As non-reactive reference materials, the following materials have been tested: granite/gneiss filler of glaciofluvial origin, limestone and pure quartz filler. Most of the fillers have been separated into different fractions by air classification (see Section 5.3.4.1), giving the opportunity to test the effect of particle size distribution separately. Silica fume and fly ash, which are known to mitigate deleterious alkali-silica reactions, have been used as reference materials.

Based on the literature review, it is obvious that some materials are able to give either ASR or react pozzolanic, as has been discussed in Section 2.11.2. The particle size seems to be one important controlling parameter in this respect, as has been discussed in Section 2.6.3. It is a paradox that some materials may react pozzolanic to increase the amount of CSH, a desirable reaction giving a denser concrete of higher strength, or produce a swelling ASR gel, a harmful reaction that generates expansion and cracking of the concrete. This area is very complex, and it is out of scope of this thesis to give a covering explanation of this paradox. Nevertheless, an aim of the work presented here has been to increase the understanding of the dualism between pozzolanic behaviour and ASR, in addition to investigate the practical implications of using fillers of alkali-reactive materials.

In this chapter, results of testing of pozzolanic reactivity of the fillers, as a direct measure of the capability of reacting with calcium hydroxide (CH), are presented. Further, examinations of alkali-silica reactions, both using the concrete prism test (CPT) and the accelerated mortar bar test (AMBT), are reported. Descriptions of micro-structural analyses of four concrete samples are included. Also the effects on compressive strength and the effect on capillary suction are reported in this chapter. The studies of alkali-silica reactions in concrete and mortar were carried out by adding the fillers to reactive concrete/mortars, i.e. mixes giving expansions due to ASR. The potential of the fillers to either increase or reduce the expansions caused by ASR could then be studied. Mylonite aggregate was used as a reactive reference. Other reference materials (cataclasite, Spratt limestone and non-reactive granite/gneiss) have been used to some extent.

6.2 Pozzolanic reactivity of fillers in concrete

6.2.1 General

According to Massazza (1998), the term pozzolanic reactivity includes both the maximum amount of CH consumed in the reaction, and the rate at which the reaction occurs. In the present study, the residual amount of CH was determined by thermo gravimetric analysis (TGA), as described in Section 5.2.1. In the following sections, an overview of the results is presented. A more detailed presentation of the results is given in Appendix B1.

6.2.2 Pozzolanic reactivity at 20°C

The loss of CH was calculated based on the initial amounts of CH measured by TGA for each mix. Results of some fillers tested at a curing temperature of 20°C are shown in Figure 6.1. The results imply a wide span in capability of reacting with CH, which is a direct measure of the pozzolanic reactivity. Generally, the fillers containing crystalline silica, i.e. mylonite, cataclasite and quartz, gave low pozzolanic reactivity. The reacted quantity of CH at the age of 90 days did, however, vary from 6 % for the mylonite, to 32 % for the cataclasite filler. On the other hand, all fillers with a distinct amorphous silica phase, i.e. rhyolite, glass and fly ash, have all shown to be clearly pozzolanic.

It should be noted that there are great differences in the initial quantity of silica in the different materials presented in Figure 6.1. The content of silica varies from approximately 25 % for rhyolite, to close to 100 % for quartz, see Section 5.3.4 for detailed descriptions of the materials. This difference in the silica amount is of course of great relevance for the pozzolanic reactivity, together with the crystallinity of silica. A noteworthy point from Figure 6.1 is that cataclasite gave a slightly higher pozzolanic reactivity than mylonite, even though the amount of quartz is equal for these fillers. This may indicate a slightly higher reactivity of the quartz in the cataclasite relative to the quartz in the mylonite. When submitted as coarse aggregates in concrete, the cataclasite rock is known to be much more deleterious than the mylonite rock is, see Section 5.3.3 and 5.3.4 for details about the reactivity.

The lower pozzolanic reactivity of the pure quartz filler (see Figure 6.1) relative to the cataclasite filler, even though the amount of quartz is nearly four fold that of the cataclasite, was presumably mostly caused by the greater particle size of the pure quartz powder. But there might also be a small difference in solubility between the coarse crystalline quartz and the quartz in the cataclasite, the direct solubility has not been quantified within the present study.

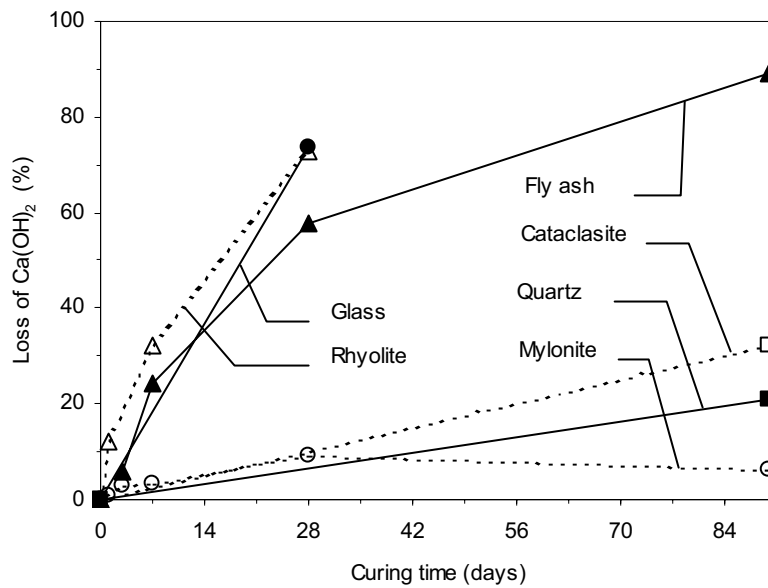


Figure 6.1 Pozzolanic reactivity of fillers expressed as % loss of $\text{Ca}(\text{OH})_2$ determined by TGA. Particle size of fillers 0-20 μm (0-125 μm for quartz filler), pH of mixing water was 13.5, all mixes cured at 20°C. The weight proportion of filler, water and CH was 50:35:15 (the water content was adjusted for some mixes, see Section 5.4.2 for details). Extra water was added to the top of the curing glasses after 2 days of curing.

The effect of changing the alkalinity, as well as changing the particle size, has been tested for the mylonite, see results in Appendix B1. It was expected that the pozzolanic reactivity should increase with increasing pH and with decreasing particle sizes. However, all these tests did show very low pozzolanic reactivity. Consequently, no reliable conclusions concerning the effects of alkalinity and particle size can be drawn based on these experiments.

6.2.3 Temperature effect on pozzolanic reactivity

The testing environment of the concrete prism test (CPT) and the accelerated mortar bar test (AMBT) both include elevated temperatures to accelerate the alkali-silica reaction, 38°C and 80°C, respectively. Details of the CPT and the AMBT are given in Section 5.2.2 and Section 5.2.3, respectively. To investigate the temperature effect on the pozzolanic reactivity of fillers, some of these were tested at different temperatures. Figure 6.2 shows the loss of CH on mixes with rhyolite and mylonite filler due to different temperatures and curing time. Note that the temperature has a significant influence on the pozzolanic reactivity of both the tested fillers. This was an expected effect because solubility of silica increases with increasing temperature. The pozzolanic reactivity was close to zero for the mylonite filler at temperatures of

20°C and 38°C. However, the pozzolanic reactivity was significantly increased at 80°C, as shown in Figure 6.2. Note that the pozzolanic reactivity of the granite filler was identical to the pozzolanic reactivity of the mylonite filler, when both of these were tested at 80°C. The pozzolanic reactivity of the granite filler has not been tested at other temperatures than 80°C.

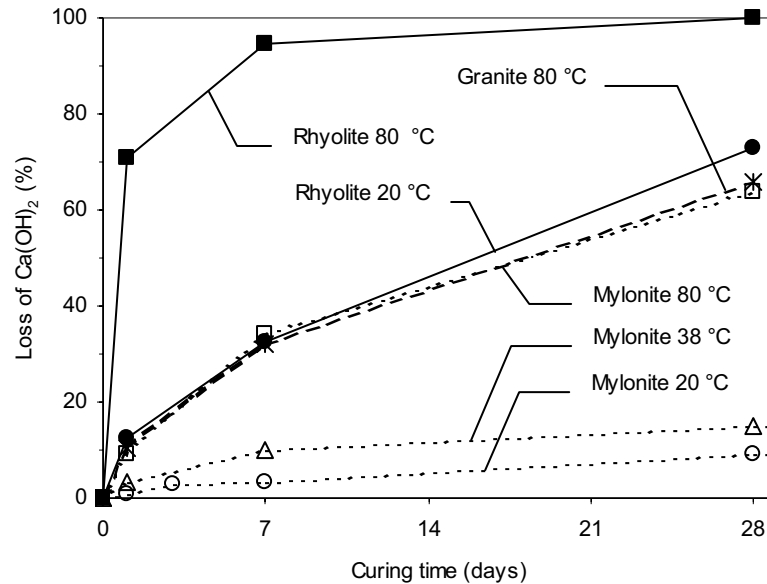


Figure 6.2 Temperature effect on pozzolanic reactivity. Particle size of fillers 0-20 μm , pH of mixing water was 13.5. The weight proportion of filler, water and CH was 50:35:15 (the water content was adjusted to 40 for the mix with rhyolite filler). Extra water was added to the top of the curing glasses after 2 days of curing.

Extended testing up to 90 days (results given in Appendix B1) gave a more pronounced difference in pozzolanic reactivity between 20°C and 38°C for the mylonite filler. The loss of CH was 28% at 90 days for the mylonite cured at 38°C, and only 6 % for the same filler cured at 20°C. The temperature effect was apparent also for the rhyolite filler. An increase in temperature from 20°C to 80°C gave an increase in loss of CH from 12 % to 71 % at one-day curing time. At 28 days of curing at 80°C, the reaction was completed as all the CH was consumed.

6.2.4 Concluding discussion on pozzolanic reactivity

The granite/gneiss filler of equal particle size as the mylonite filler gave the same pozzolanic reactivity as the mylonite filler at a temperature of 80°C, see Figure 6.2. The semi-quantitative analyses of the fillers, reported in Section 5.3.4.2, have

indicated a lower quantity of quartz in the granite/gneiss filler compared to the mylonite filler. The quartz in the mylonite is less stable than the quartz in the granite/gneiss due to cataclasis. It was therefore expected that the mylonite filler should give a slightly higher pozzolanic reactivity than the granite/gneiss filler. However, it seems like the pozzolanic reactivity of crystalline quartz is more or less similar, and that cataclasis does not increase the pozzolanic reactivity significantly.

The results on pozzolanic reactivity from the present study show that the materials with a distinct amorphous silica phase, i.e. fly ash, bottle glass and Icelandic rhyolite, gave a clearly pozzolanic behaviour at a temperature of 20°C. The Norwegian cataclastic rocks known to be alkali-reactive, as well as the non-reactive granite/gneiss, gave no or very low pozzolanic reactivity at this temperature. The effect of increasing the temperature was significant, and at a temperature of 80°C also the mylonite and the granite/gneiss showed a clear pozzolanic behaviour. The increase in pozzolanic reactivity with increasing temperature is believed to be due to the higher solubility of silica caused by the elevated temperature (in contrast to the solubility of CH that decreases with rising temperature). This strong temperature effect on pozzolanic reactivity is probably of high importance concerning testing of fillers by methods involving high temperatures.

There is obviously a clear distinction between fillers containing amorphous silica and fillers with crystalline silica. The mylonite and the cataclasite are known to be alkali-reactive due to the cataclasis caused by dynamic metamorphism (see also Section 2.5.1). A general effect of the cataclasis is a reduction of the grain sizes, and the formation of so-called subgrains. According to Wigum (1995a), the alkali-reactivity of cataclastic rocks, such as the mylonite and the cataclasite in the present study, is clearly related to the total grain boundary area of quartz. However, the quartz in the mylonite and the cataclasite are still crystalline. Even though these rocks are alkali-reactive due to the cataclasis, the pozzolanic reactivity is not significantly higher than for the granite/gneiss rock, which is known to be non-reactive. Based on these rather limited tests on the temperature effect, it can be suggested that all rocks containing silica, whether crystalline or amorphous, will be more or less pozzolanic at high temperatures, i.e. 80°C. This may be of large significance when tested by methods involving high temperatures, such as the AMBT. This will be further discussed in Section 6.3.

6.3 Alkali-silica reactivity

6.3.1 Introduction

The slow nature of the expansion phenomena caused by the alkali-silica reaction makes it necessary to rely on accelerated testing methods. The concrete prism test (CPT gives a moderate acceleration due to elevated temperature (38°C) and high relative humidity (see description of the method in Section 5.2.2). A normal acceptance criterion when testing aggregates is an expansion limit of 0.04 % after one year of storing, both according to the Canadian and the Norwegian practice

(Jensen & Fournier 2000). When specific mix designs involving pozzolanic additives like silica fume and fly ash are evaluated, an acceptance criterion of 0.03 % is used according to the Norwegian guidelines (Norwegian Concrete Association 1996). Alternatively, the acceptance criterion is 0.04 % after two years of storing. The 0.04 % limit after two years of storing is also used in Canada according to Bleszynski et al. (2000).

Due to the long time needed to evaluate aggregates or concrete mix designs by the CPT, faster methods like the accelerated mortar bar test (AMBT) are of great interest. In this method, the mortar bars are stored in 1 N NaOH solution at 80°C, see Section 5.2.3 for further description of the method. Even though the AMBT (also referred to as the NBRI method) was originally designed to evaluate aggregates only, it has been used extensively around the world to evaluate the effect of pozzolanic additives. There have been carried out several studies describing the general suitability of the AMBT for the prediction of supplementary cementing materials such as silica fume, fly ash and slag (Bérubé et al. 1995, Fournier & Malhotra 1999, Bleszynski et al. 2000). Because of this, the method was believed to give adequate information also when testing fillers. The AMBT was therefore used as a screening test prior to the testing in the concrete prism test. One important aspect has been to investigate if there is a general correlation between the two methods when using filler as additive.

Bleszynski et al. (2000) found the correlation between the accelerated mortar bar test (AMBT) and the concrete prism test (CPT) to be acceptable when testing the effect of fly ash and silica fume, when these materials replaced equal parts of cement by weight. They found an acceptance criterion of 0.1% expansion in the AMBT to correspond well to the 0.04% limit at two years of storing by the CPT. The exception from this was one mix with 35% slag, which passed the CPT but clearly failed the AMBT. According to Jensen & Fournier (2000), the longer and thinner bars used in the Canadian version of the AMBT (CSA A23.2-25A 1993), 25 mm x 25 mm x 250 mm, give higher expansions than the shorter and thicker bars (40 mm x 40 mm x 160 mm) used in the Norwegian version (Lindgård et al. 1993). This difference is believed to be caused mainly by the faster diffusion of NaOH into the thinner bars than into the thicker bars. Jensen & Fournier (2000) suggested a correlation factor of 0.6 between the Canadian and the Norwegian versions of the AMBT. According to this, the Canadian acceptance criterion of 0.1% when testing pozzolanic materials by the AMBT corresponds to an expansion of 0.06 % at 14 days by the Norwegian version of the method.

The following sections present the most important findings from studies using the concrete prism test and the accelerated mortar bar test. A comprehensive list of results is given in Appendix B2 and B3.

6.3.2 Expansions due to ASR depending on the type of filler

6.3.2.1 Expansions by the concrete prism test (CPT)

Figure 6.3 shows the influence of different fillers of 0-125 μm grading on the expansion by the CPT. Fly ash and silica fume concretes are also shown in the figure. In all these mixes, the fillers replaced non-reactive sand, while the w/c ratio, as well as the quantity of cement, was kept constant.

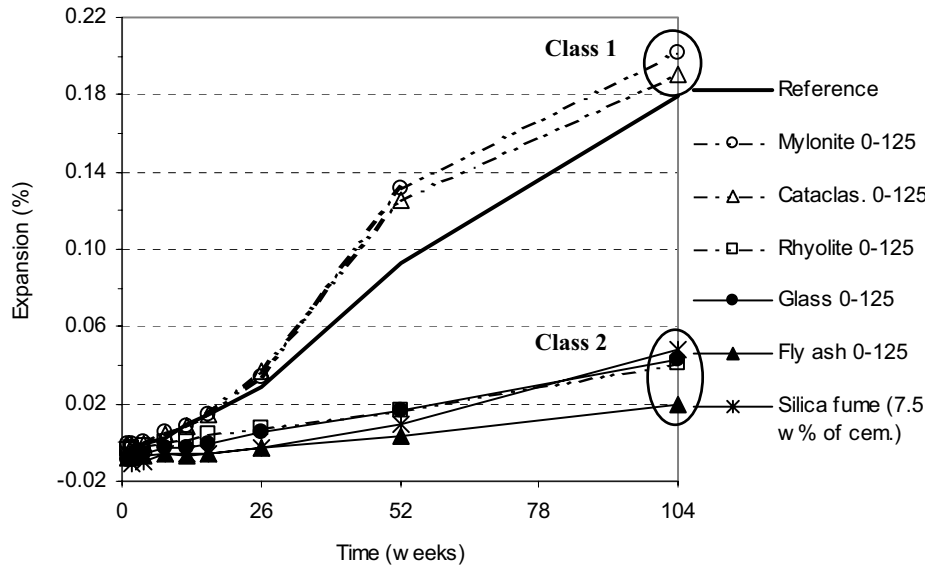


Figure 6.3 CPT: Effect of fillers on concrete expansions up to two years. Constant w/c ratio = 0.45 and quantity of cement (400 kg/m^3) in all mixes. Filler/total aggregate ratio was 5.15 % (by volume) for all fillers, including fly ash. Addition level of silica fume was 7.5 % of cement weight.

Note in Figure 6.3 that the supplementary materials can be divided into two classes based on the effect in concrete: 1) Both the mylonite and the cataclasite fillers gave an increased expansion compared to the reference concrete. The relative difference was at a maximum at one year of exposure, while the difference was smaller at two years of exposure. 2) The effect of the other fillers (glass, rhyolite, fly ash), including silica fume, was the opposite with respect to expansion, as they all gave a distinct inhibiting effect. The fly ash resulted in the lowest expansion, while the glass and rhyolite fillers gave a slightly higher expansion. The addition of silica fume gave approximately the same behaviour as the addition of glass and rhyolite filler. But the quantity of silica fume was much lower than the quantity of rhyolite and fly ash in these experiments (10.4 % silica fume versus 27 % glass filler and fly

ash, all amounts in volume % of cement). Consequently, silica fume was much more effective in controlling the expansions than fly ash and glass filler. The much higher specific surface area of the silica fume compared to the glass filler and the fly ash is probably of significance in this respect. Silica fume is well known to be a highly reactive pozzolan, and some of the research in this area has been summarized by Justnes (1996).

The Norwegian guidelines (Norwegian Concrete Association 1996) allows concrete mixes containing pozzolans to be used if the expansion is less than 0.03 % after one year, or alternatively 0.04 % after two years. The concretes containing fly ash, silica fume, rhyolite and glass filler all clearly qualified the one-year criterion. However, the glass, rhyolite and silica fume concretes reached values on the border or slightly above the two-year criterion.

The inclination of the curves for reference concrete and concrete incorporating mylonite and cataclasite filler indicates lower expansion rates for these concretes after one year of storing compared to the expansion rate up to one year; see Figure 6.3. This indicates that the potential of expansion was reaching a limit. On the other hand, the expansion rates for the concretes giving small expansions (class 2) seem to be constant over time, or with a slight tendency towards an increase in the expansion rate after one year. One of the concerns when using pozzolanic additives is whether the alkali-silica reaction is being eliminated (fully or partly), or if the effect is a postponing of the reaction. By looking at the inclinations of the expansion curves, it could be concluded that there was a weak tendency towards that the relative effect of the expansion inhibiting materials was larger at one year than at two years of exposure. Especially was this the case for the silica fume concrete. This gives evidence to the conclusion that at least some of the observed positive effect may be due to a postponing, and not a true elimination of the expansive reactions. Prolonged testing may clarify this better. However, according to Duchesne & Bérubé (2000), one weakness of this test method is the tendency of loss of alkalis due to leaching from the prisms. This fact makes it difficult to draw absolutely reliable conclusions based on long-term testing by the CPT.

Figure 6.4 shows expansion results when non-reactive granite/gneiss filler was replaced with reactive mylonite-filler. Note that in these two particular experiments, the fine aggregate fraction (< 5 mm) consisted of reactive mylonite, while non-reactive granite/gneiss was used as coarse aggregate.

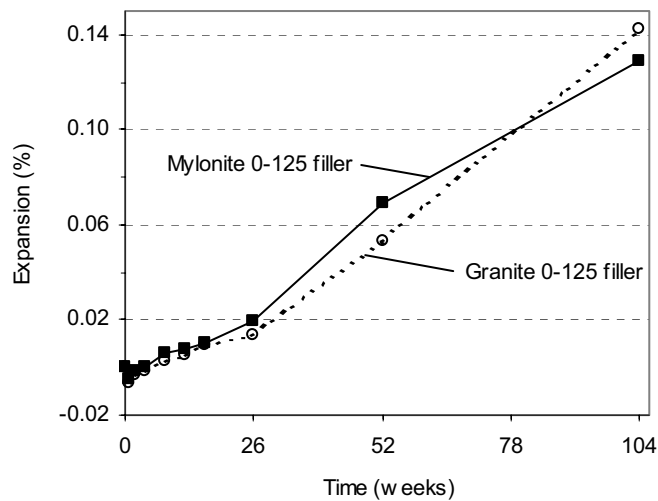


Figure 6.4 CPT: Effect of replacing mylonite filler by granite filler by the CPT. Mylonite sand (< 5 mm), granite/gneiss coarse aggregate. The filler amount was 6 % of the total aggregate volume.

The differences at both one and two years of expansion are not significant on a 5 % significance level².

6.3.2.2 Expansions by the accelerated mortar bar test (AMBT)

Figure 6.5 shows the influence of different fillers of 0-125 µm grading on the expansion by the AMBT compared to a reference mortar with no filler. Note that the amount of filler was 20 % of the total aggregate volume in these mixes, except the fly ash and silica fume, which were added in lower amounts. The amount of fillers corresponds to 54 % of the cement volume. Note the lower addition levels of fly ash (10 volume % of aggregates, corresponding to 27 % of the cement volume) and silica fume (7.5 % of the cement weight, corresponding to 10.4 volume % of the cement).

² This conclusion is based on calculations of 95 % confidence intervals. Overlapping confidence intervals give evidence to that no reliable conclusion can be drawn whether there are differences between the fillers or not. The confidence limits were calculated using the formula: $\bar{x} \pm z_{\alpha/2} SE(\bar{x})$, according to Walpole et al. (1998). The standard error is the ratio between the standard deviation and the square root of the number of experiments (3 prisms of each mix combination). An estimate of the standard deviation for both one and two years of expansion by the CPT is 0.01 %; see Section 4.2.2.

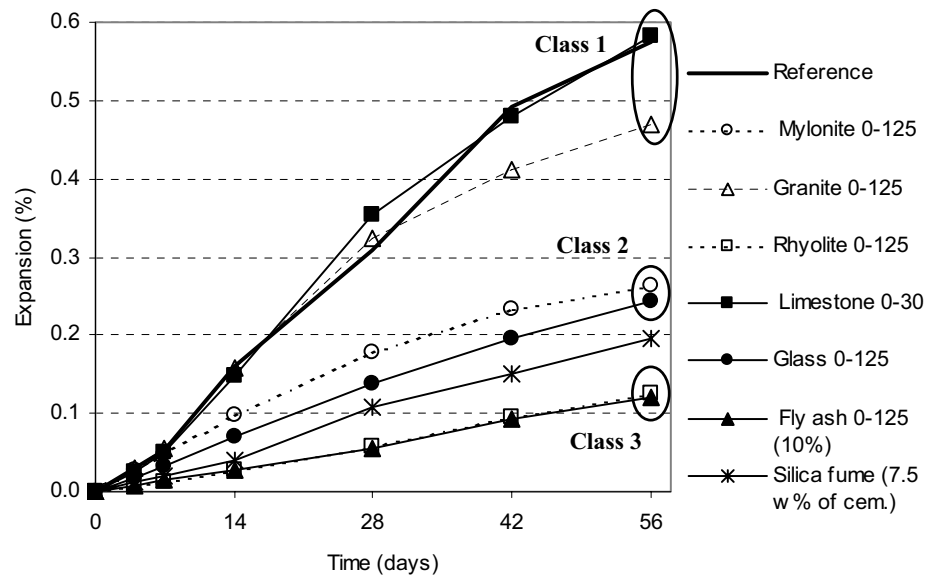


Figure 6.5 AMBT: Effect of fillers on expansions. Amount of filler was 20 % (of total aggregate volume), 10% for fly ash. Amount of silica fume was 7.5 % of cement weight. Constant w/c ratio (0.47) and quantity of cement (600 kg/m^3) for all mixes.

Based on the results in Figure 6.5, the fillers can roughly be divided into three classes with respect to their effect on the mortar bar expansions:

1. Limestone and granite/gneiss fillers gave no significant effect on the expansion at 14 days.
2. The mylonite and glass fillers all gave a marked reduction, both at 14 and 56 days.
3. The rhyolite and fly ash reduced the expansion to 0.03 % at 14 days, and to about 0.12 % at 56 days.

The cataclasite filler is not shown in Figure 6.5, and was not tested as a 0-125 fraction by the AMBT. However, testing of the 0-20 fraction of cataclasite has shown that the effect caused by this filler was nearly identical to the effect of the mylonite 0-20 filler with respect to expansions measured by the AMBT.

The reduced expansion due to addition of silica fume was evident, though less distinct than for fly ash and rhyolite filler; see Figure 6.5. Silica fume is generally believed to be highly effective in reducing the expansions caused by ASR, and the

less distinct reduction seen in Figure 6.5 is believed to be due to the lower addition level of silica fume compared to the other fillers.

6.3.2.3 Discussion of the observed differences between the AMBT and the CPT results

This section will highlight some of the striking differences between the results obtained by the concrete prism test and the accelerated mortar bar test. But first, some important factors should be mentioned: The amount of added filler was much higher in the AMBT experiments presented in Figure 6.5 compared to the CPT results presented in Figure 6.3, 20 % and 5.15 % of the total aggregate volume, respectively. These levels correspond to 54 % and 27 % of the cement volume, respectively. The direct effect of different addition levels of filler will be discussed separately in Section 6.3.3. Also note that in the AMBT experiments, the filler replaced an equal volume of the reactive mylonite sand used in the reference mix. In the CPT experiments, only the coarse aggregates (> 5 mm) in the reference mix was reactive mylonite, while the sand fraction consisted of non-reactive granite/gneiss. In these experiments, the filler replaced a volume fraction of the non-reactive sand, meaning that the amount of reactive coarse aggregates remained unchanged when filler was added.

The accelerated mortar bar test showed a significant reduction in expansion for rhyolite filler, fly ash and silica fume. This was fully in agreement with the results obtained by the concrete prism method. Also the glass filler gave a significant reduction in expansion in agreement with the CPT experiments, even though the effect of glass filler was less pronounced in the AMBT experiment. However, the positive effects, in terms of reduced expansion, of the mylonite filler and the cataclasite filler contradict the results obtained by the concrete prism test. The CPT is believed to provide the most reliable prediction of the expected long-term behaviour in field due to its moderate temperature. Obviously, the AMBT may not always give reliable predictions of the effects of fillers. The temperature effect is believed to be the major reason why the effect of mylonite and cataclasite filler was totally different by the AMBT and the CPT. As shown in Section 6.2.3, the mylonite 0-20 filler did not give any significant pozzolanic reactivity at a temperature of 38°C, while the pozzolanic reactivity at 80°C was significant. This difference in pozzolanic reactivity was probably of crucial importance regarding the effect of alkali-reactive fillers. Pozzolanic materials are generally known to reduce the problems associated with alkali-silica reactions (see Section 2.9.2). It should be noted that the pozzolanic reactivity for the mylonite 0-20 and the granite/gneiss 0-20 filler was exactly the same. But the effect on the expansion by the AMBT differed a lot; see Figure 6.5. Mylonite 0-125 was much more effective in reducing the expansion than granite/gneiss 0-125. It is, however, important to note that there is a large difference in particle size distribution between these two fillers. The median particle size is 52.8 µm for the granite/gneiss but only 27.3 µm for the mylonite filler. As the pozzolanic reactivity is believed to increase with decreasing particle size, the mylonite 0-125 is believed to be much more pozzolanic than the

granite/gneiss 0-125. This difference in pozzolanic reactivity may be responsible for the large observed difference in expansion when tested by the AMBT.

The observed differences between the two methods will be treated further in the succeeding sections, also involving the effects of the alkali amount, the amount of added filler and the particle size distributions.

6.3.3 Expansions due to ASR depending on the particle size and the amount of filler

6.3.3.1 Expansions by the concrete prism test (CPT)

Figure 6.6 shows the effect of varying particle size distribution of fillers. A comprehensive list of results can be found in Appendix B2, while the details regarding particle size distribution of the fillers can be found in Appendix A2. Note that the effect of the particle size distribution was limited and barely significant. However, for the mylonite fillers, there was a tendency that the filler of finer grading gave higher expansion. The results of the rhyolite fillers indicated the opposite effect, i.e. the finer fraction gave a lower resulting expansion.

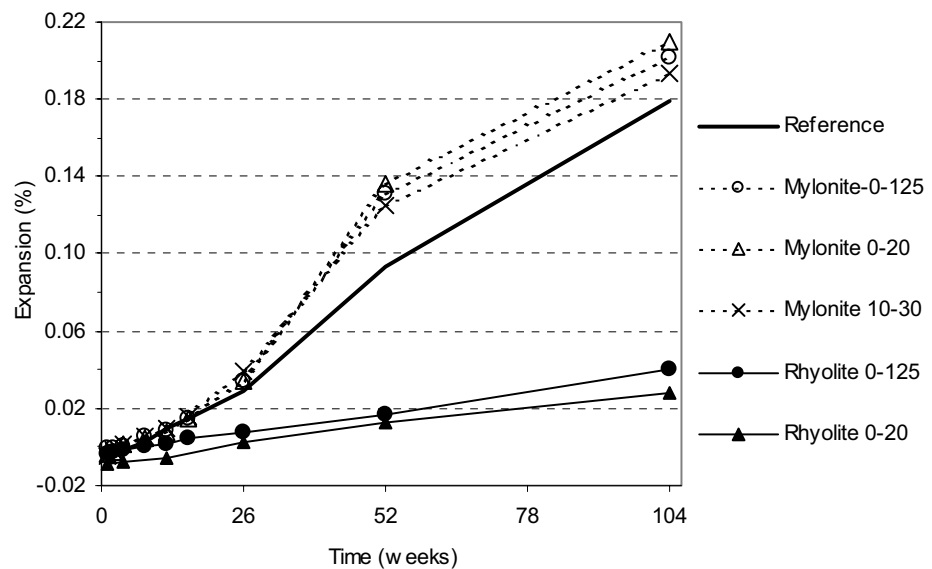


Figure 6.6 CPT: Effect of particle size on expansion. Constant w/c ratio (0.45) and quantity of cement (400 kg/m^3) for all mixes. Filler/total aggregate ratio was 5.15 % (by volume) for all mixes.

The larger inhibiting effect of the rhyolite 0-20 filler compared to the rhyolite 0-125 filler was an expected effect, because the pozzolanic reactivity is believed to increase with decreasing particle size. The mylonite filler did not give any

significant pozzolanic reactivity at a temperature of 38°C; see Section 6.2.3 for details. In this case where pozzolanicity is not apparent, the smaller particles may cause a faster expansion. Due to the smaller size, the reactive quartz may come more easily in contact with the alkali hydroxides, and thereby cause a quicker reaction. However, due to fracture mechanical effects, see Section 2.1.1.1, smaller particles could be expected to cause less expansion than larger particles. In this case, the increased speed of the alkali-silica reactions due to smaller particle sizes seems to dominate the net effect.

The effect of adding different amounts of mylonite 0-125 filler to the reactive system can be seen in Figure 6.7. Additions up to 5 % filler lead to increased expansion after one year, which also was confirmed by the two years expansion results. Further addition gave no increase in expansion. This may possibly be due to a pessimum effect. The concept of pessimum proportion of reactive aggregate, or more precisely a pessimum reactive aggregate to alkali ratio is well known in the literature. However, it has not been documented any tendency of pessimum behaviour for Norwegian alkali-reactive aggregates to the author's knowledge.

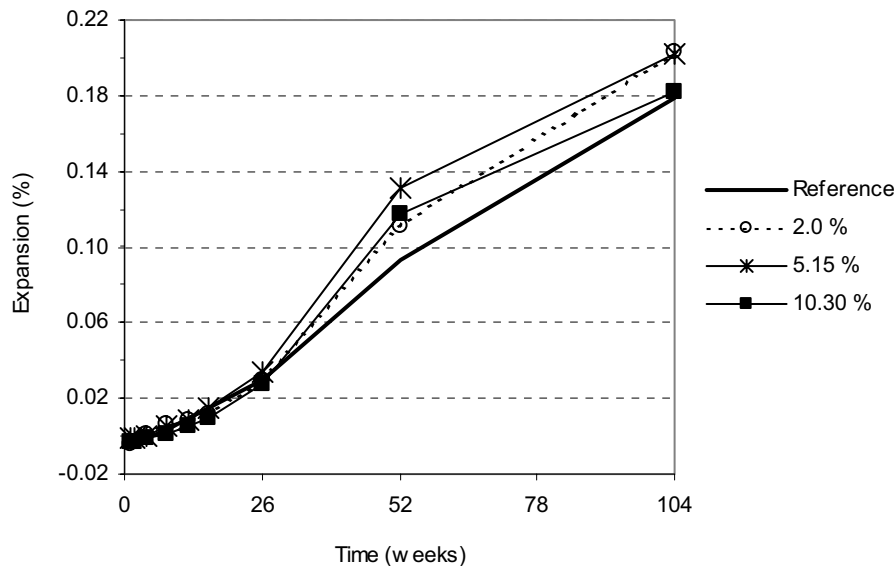


Figure 6.7 CPT: Effect of content of mylonite 0-125 filler on expansion of concrete prisms. Constant w/c ratio (0.45) and quantity of cement (400 kg/m³) for all mixes. Addition level of fillers given in % of total aggregate volume.

The results from Figure 6.7 indicate that the addition of reactive mylonite filler has caused a small additional expansion compared to the reference mix. The quantity of reactive filler does, however, not seem to be a critical factor in this case. The amount of reactive silica in the mylonite was obviously large enough to cause relatively

large expansion even before the reactive filler was added. The limited effect on expansion from addition of reactive filler has previously been shown in Figure 6.4, showing that replacing non-reactive filler with reactive mylonite filler caused no significant increase in expansion. The effect of adding reactive mylonite filler to a system of non-reactive aggregates has not been tested, but this will probably cause expansion.

6.3.3.2 Expansions by the accelerated mortar bar test (AMBT)

In Figure 6.8, the effect of different particle size distributions of mylonite and rhyolite is presented. The trend seen in the figure is that a smaller particle size gave larger reduction in expansion at all ages of testing. It should be noted that the fillers labelled 10-30 and 20-125 also contain some amount of very small particles, see details of the particle size distributions in Section 5.3.4. This trend of obtaining a reduced expansion when the particle size decreased was evident also for the cataclaste, glass and fly ash, see comprehensive results in Appendix B3. This may be explained by increasing pozzolanic reactivity with decreasing particle size.

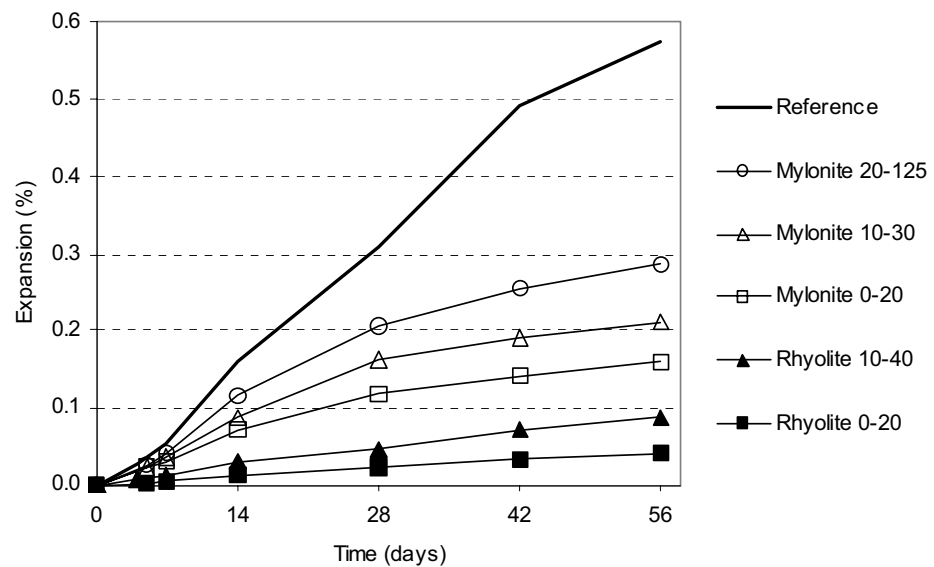


Figure 6.8 AMBT: Effects of particle size on expansion of mortar prisms. 20 volume % filler of total aggregate, corresponding to 54 volume % of cement. Constant w/c ratio (0.47) and quantity of cement (600 kg/m^3) for all mixes.

In Table 6.1, the combined effect of different addition levels of filler and particle size distributions can be observed for the 14-days expansions.

Table 6.1 Effect of 10 and 20 % filler replacement (by volume of total aggregates).

Filler type/ Amount	Expansion at 14 days (%)		
	Ref. (0 %)	10 %	20 %
Mylonite 0-20	0.16	0.12	0.07
Mylonite 0-125		0.15	0.11
Rhyolite 0-20		-	0.01
Rhyolite 0-125		0.07	0.03
Glass 0-20		-	0.06
Glas 0-125		0.16	0.07
Fly ash 0-20		0.02	-
Fly ash 0-125		0.03	-
Granite 0-125		-	0.16
Limestone 0-30		-	0.15
Silica fume*		0.04	

* Note that the amount of silica fume was 7.5 weight % of cement.

The overall tendency, as seen from Table 6.1, was a reduction in expansion with increasing amount of filler. Reduced particle size did also reduce the expansion. However, the differences in expansions for fillers of different particle sizes were small, and in most cases not significant on a 5 % significance level.

It should be remarked that the mortars tested at the 10 % levels of mylonite 0-125 and glass 0-125, as well as the 20 %-level of the granite 0-125, gave a significant reduction in expansion at an age of 56 days, while the limestone 0-20 filler gave no reduction in expansion at all at this age, see detailed results in Appendix B3.

The decrease in expansion for decreasing particle size for rhyolite filler was in agreement with the results obtained in the concrete prism method; see Figure 6.6. However, the decrease in particle size also gave a significant decrease in expansion for the mortars containing mylonite filler. This is in contrast to the results obtained by the concrete prism method. It confirms the conclusion from Section 6.3.2.3 that the AMBT does not give a reliable prediction of the effect of the cataclastic fillers (cataclasite and mylonite) due to the temperature effect on pozzolanicity.

6.3.4 Expansions due to ASR depending on the alkali content and the temperature

6.3.4.1 Effect of NaOH addition on the expansion of concrete prisms

As specified in the description of the method, addition of sodium hydroxide (NaOH) shall be used to increase the alkali content to 5 kg/m^3 Na_2O -equivalent. This increase in sodium hydroxide is generally believed to increase the expansions owing to alkali-silica reactions. Table 6.2 shows results of some mixes containing silica fume. Note that the expansions followed the expected pattern, as an increase in alkali content gave an increased expansion. This was evident also for the extreme alkali level of 10 kg/m^3 Na_2O -equivalent. Comprehensive test results are given in Appendix B2.

Table 6.2 Effect on alkali-load and quantity of silica on 2-years expansions.

Amount of silica fume (weight % of cement)	Na_2O eqv. (kg/m^3)		
	4	5	10
5 %	0.054 %	-	-
7.5 %	0.040 %	0.048 %	0.093 %

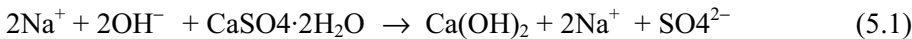
Table 6.3 shows results of some mixes containing mylonite 0-125 filler. Note that an increase in Na_2O -equivalent from 4 to 5 kg/m^3 did not result in the expected increase in expansion. The effect was the opposite of what was expected, as the expansion decreased when the Na_2O equivalent increased from 4 to 5 kg/m^3 . This was evident both at the 5 % and 10 % addition levels of filler. The effect was more pronounced when the alkali level increased to 10 kg/m^3 , as this extreme level gave a significantly lower expansion than the lower alkali levels.

Table 6.3. Effect of alkali-load and quantity of filler on 2-years expansions.

Amount of mylonite 0-125 filler (vol. % of cement)	Increase in reactive aggregates	Na_2O eqv. (kg/m^3)		
		4	5	10
No extra filler	-	-	0.179 %	-
2.0 %	3.8 %	-	0.203 %	-
5.15 %	11.4 %	0.227 %	0.202 %	-
10.30 %	22.8 %	0.209 %	0.182 %	0.135 %

According to Diamond (1997), the addition of NaOH leads to an immediate increase in sodium ions in the pore water. However, the hydroxide does not increase correspondingly to balance the cations on a short-term basis. Over longer time, the amount of hydroxide ions increase but never reach the expected content that balances the level of sodium ions.

The value of hydroxide ions does, however, never reach values that might have been expected based on the NaOH level. According to Diamond (1997), the consequence of adding NaOH is dissolution of gypsum and precipitation of calcium hydroxide according to (5.1):



Over longer time, the sulphate ions are removed from the pore solution by ettringite precipitation. The consequence of this is dissolution of hydroxide ions. Some sulphate may, however, stay solved over time. One practical consequence of adding NaOH is a weaker CSH-phase, as will be further discussed in Section 6.5.2. The addition of NaOH may not necessarily give an accelerated expansion rate as have been demonstrated here.

6.3.4.2 Effect of alkalinity on the expansion of mortar bars

In the AMBT, the supply of sodium and hydroxide from the solution where the prisms are stored may be regarded to be close to unlimited during the testing period. The mobility of the ions depends on the permeability of the mortar. One consequence of pozzolanic reactions is a reduced permeability, with decreased ion mobility. To investigate this effect relative to other possible controlling effects (e.g. binding of alkali hydroxides), a series of four mortars was exposed to careful drying (3 days at 50°C) after 28 days of storing in NaOH solution, followed by pressure saturation in NaOH solution (also see Section 5.2.3.2). After the pressure saturation in NaOH solution, storing in NaOH at 80°C was continued. The idea behind this experiment was that alkali hydroxides might be forced into the prisms to overcome the effect of reduced permeability. The methodology involves some uncertainty with respect to the irreversible alteration of the pore structure caused by drying of the mortar bars.

In Figure 6.9, PS means pressure saturated. As seen in Figure 6.9, there was no effect of pressure saturation on the reference mortar, indicating that in this case the available quantity of alkali hydroxides was no limiting factor. On the other hand, there can be observed a small effect regarding the mortar with added rhyolite filler, and a somewhat larger effect for the mylonite filler. The most pronounced change was observed for the mortar with silica fume. These observations indicate that a shortage of available sodium and hydroxide ions probably play some role while testing mineral additives in the AMBT method. But it is obviously not the only controlling factor, as the rhyolite filler being very effective in controlling the expansions, was not much affected by the process of pressure saturation. The mortar

with silica fume was, on the other hand, much affected and showed a pronounced increase in expansion compared to the standard method. Silica fume was generally very effective at early ages (up to 14 days) in controlling the expansion, while the inclination of the expansion curves seem to be constant for a long period of time, indicating that ASR is going on. The observations described might indicate that the effect of reduced ion mobility is of greater effect in the case with silica fume than in the case with rhyolite filler. Even though silica fume is a more effective pozzolan than rhyolite powder, the great difference in quantity (10.6 versus 27 % of cement volume) might be responsible for this. While the effect of lower ion mobility may be of some importance, it looks obvious that other mechanisms than this are of importance.

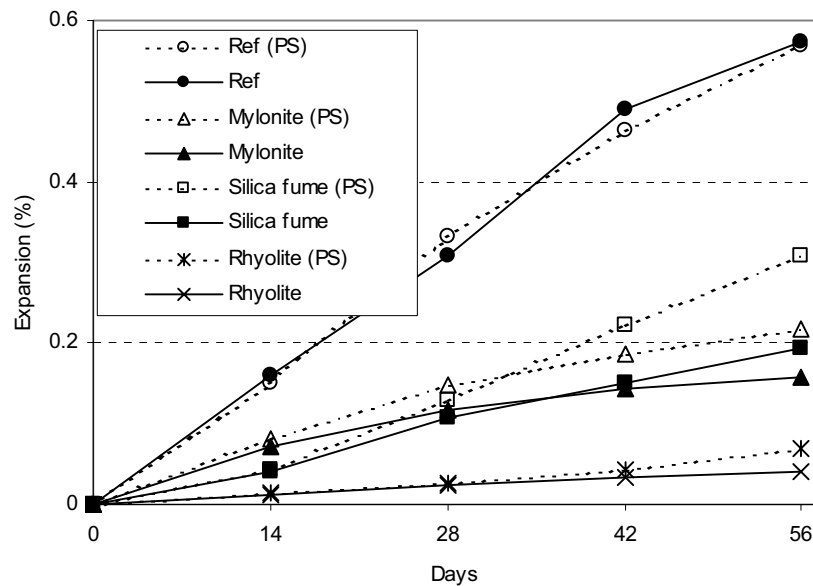


Figure 6.9. Effect of drying and pressure saturation (after 28 days) in NaOH-solution. 10 % fillers (% of total aggregate volume), 7.5 % silica fume (% of cement weight). Time scale for specimens having been pressure saturated (labelled PS) has been adjusted.

Bérubé et al. (1995) have documented that the alkali concentration of the pore solution inside the mortar bars has a major influence on the expansion of mortar bars. Based on a study of mortar bars with silica fume and fly ash, they concluded that the most critical mechanism to reduce the expansion was the reduction of alkalis and pH. This reduction is caused by alkali dilution, or by entrapping of alkalis in the CSH-gel produced by the pozzolanic reaction. They further concluded that the suitability of using the AMBT method for testing of silica fume and fly ash is evident, as long as the testing period is restricted to 14 days. After this period, they reported the alkali concentration, as well as the expansions, to increase, no matter

the amount and quality of the supplementary materials. The results from the present study indicates that this is also the case for silica fume, while the mortars containing fly ash and rhyolite filler in the amounts of 10 and 20 %, respectively, did show an expansion below 0.05 % at 56 days. As the availability of alkali hydroxides should be high in this case, it is difficult to understand that the only explanation for the reduced expansion is the reduced availability of alkali hydroxide.

The effect of the alkalinity in the NaOH storing solution has been studied for four different mortar recipes. A set of experiments with storing of the specimens in a solution of artificial pore water was carried out (solution with Na, K, Ca and OH ions in approximately the same amounts as in the pore water of the mortars, see Section 5.2.3.2 for details). By using artificial pore water, the idea was that the net transport of ions between the storing solution and the mortar bar should be limited. These results are plotted in Figure 6.11, while the result of the similar mortar bars stored according to the standard storing conditions are plotted in Figure 6.10. Comprehensive results can be found in Appendix B3.

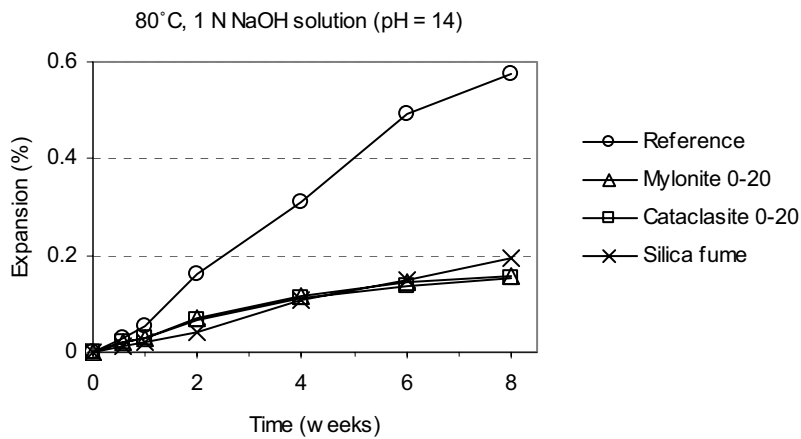


Figure 6.10. Expansion by standard AMBT. 20 % filler (of total aggregate volume), 7.5% silica fume (of cement weight).

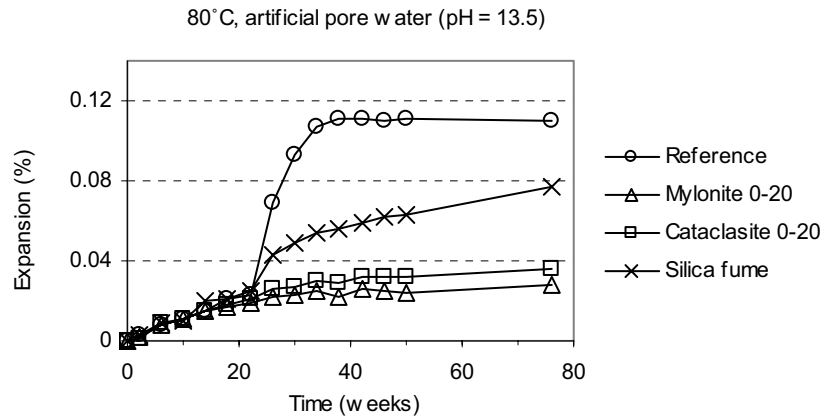


Figure 6.11. Expansion by modified AMBT, storing at 80°C in artificial pore water of pH = 13.5. 20 % filler (of total aggregate volume), 7.5% silica fume (of cement weight).

Note the large difference in time scale and expansion scale between Figure 6.10 and Figure 6.11. The buffer of sodium and hydroxide ions in the storing solutions used in the standard conditions of the method was, as expected, of large importance for the kinetics of the alkali-silica reaction. The external supply of sodium and hydroxide ions made the reaction continue to much higher expansions than obtained at 14 days. When the experiments were stopped at 8 weeks of storing, the expansion of the reference mortar was 0.57. The reference mortar stored in the artificial pore water solution reach a maximum expansion of only 0.11% after 38 weeks of storing. The reason why no higher expansion than 0.11 was reached might be due to a reduction of alkali hydroxides below a critical limit, due to consumption of alkali hydroxides by the alkali-silica reaction. However, it should be mentioned that some scientists has pointed at the opportunity that alkalis might be regenerated due to an exchange of calcium ions for alkali ions (Powers & Steinour 1955 a, b and Chatterji et al. 1986, 1992).

The replacement of aggregate with 20 % rock fillers (mylonite and cataclasite) reduced the expansion to approximately one third of the expansion from the reference mortar without filler addition; see Figure 6.10 and Figure 6.11. However, the silica fume seems to be less effective in reducing the expansion than the rock filler when the mortar bars were stored in the artificial pore water solution, see Figure 6.11. The increase in expansion for the mortar bars containing silica fume indicates that at least some of the inhibiting of silica fume is due to a postponing of the expansion, and not a true elimination of the alkali-silica reaction.

6.3.4.3 Effect of temperature on the expansion of mortar bars

The pure accelerating effect due to the temperature used by the AMBT has been studied separately using the standard 1 N NaOH solution in combination with temperatures of 38°C and 20°C. Comprehensive results can be found in Appendix B3.

Figure 6.12 and Figure 6.13 show expansions after storing at 38°C and 20°C, respectively. Note the large difference in expansion scale and time scale of these figures compared to Figure 6.10, which shows expansions after storing at 80°C.

Figure 6.12 shows that at an age of approximately one year of storing, the expansion of the reference mortar bars stored at 38°C was roughly the same as for the mortar bars stored at 80°C in artificial pore water solution. Due to lack of measuring points between 24 and 48 weeks, it is not possible to give any reliable estimates regarding the expansion trend. However, a further increase in expansions would be expected in prolonged testing due to the large availability of alkali hydroxide.

The results show a clear difference in the effect of the rock fillers (mylonite and cataclasite) at a temperature of 38°C compared to the effect of the same fillers at a temperature of 80°C. This may be seen by comparing Figure 6.10 with Figure 6.12. The expansion inhibiting effect of these fillers was obvious at a temperature of 80°C, while the effect was less significant at 38°C. This could be due to the low pozzolanic reactivity for the mylonite filler at 38°C; see Figure 6.2. Even though the inhibiting effect of mylonite and cataclasite was drastically reduced when the temperature was lowered to 38°C, the inhibiting effect was still significant. This contradicts the results obtained by the CPT; see results in Figure 6.3, where the same fillers caused increased expansion. However, the fillers replaced non-reactive sand in the CPT experiments, and thereby increased the total content of reactive aggregate. In the AMBT experiments, the fillers replaced reactive sand. This difference may explain some of the observed difference in effect from the cataclastic rock fillers between the two methods. The expansion inhibiting effect of silica fume was evident also at the temperature of 38°C. This was expected since silica fume is known to be highly pozzolanic at any temperature > 20°C. According to data reported by Justnes (1996), the 7.5 % amount of silica is presumably consumed by the pozzolanic reaction after 28 days even at 20°C.

Figure 6.13 presents the results of mortar bars stored at 20°C. At this temperature there was hardly any expansion at all for any of the mix combinations at 52 weeks.

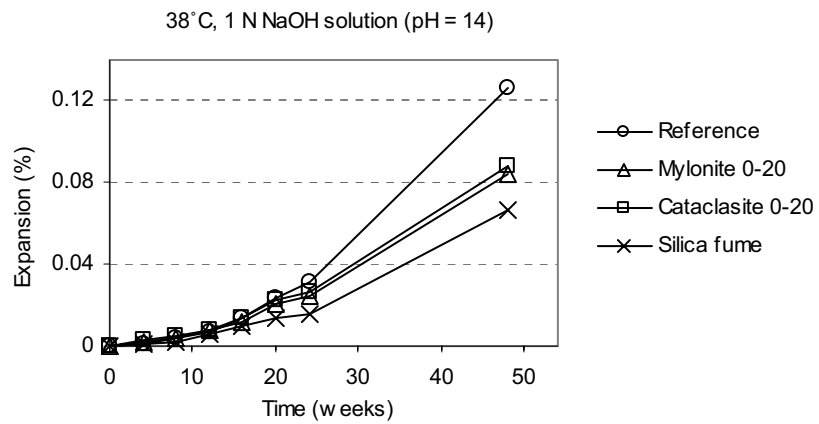


Figure 6.12. Expansion by modified AMBT, storing at 38°C. 20 % filler (of total aggregate volume), 7.5% silica fume (of cement weight).

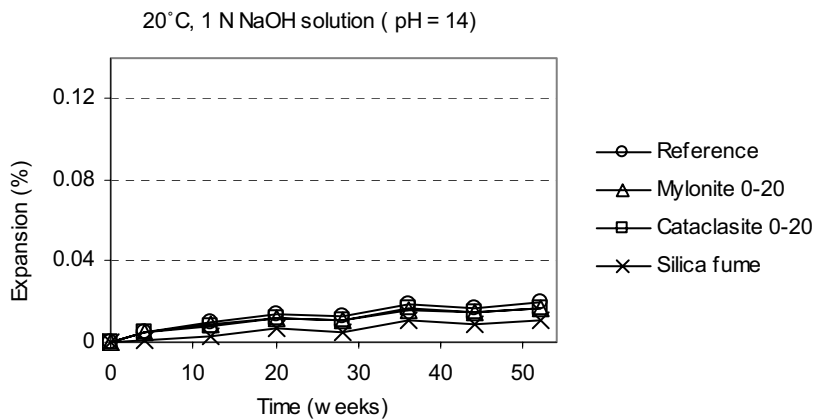


Figure 6.13. Expansion by modified AMBT, storing at 20°C. 20 % filler (of total aggregate volume), 7.5 % silica fume (of cement weight).

6.3.5 A limited study of the expansion in an early phase

The normal procedure of the AMBT involves measurements of expansion after the reference length of the prisms has been recorded. Normally, this is done after storing one day in a NaOH-solution while the temperature rises from 20°C to 80°C. To investigate the possible influence of expansions happening in this very early phase, a few experiments to investigate the early phases have been performed, where the mortar bars were measured as soon as possible, i.e. at the time when the specimens could be removed from the moulds without being damaged (6-8 hours after casting).

The bars were then measured, followed by storage in 20°C up to 1 day (at 100 RH), and then heated up to 80°C in NaOH solution from one to two days. The bars were cooled down to 20°C before they were measured.

Table 6.4. Early phase expansions of mortar bars.

Time / mortar	Expansions (%)	
	Reference	20 % mylonite 0-20
1 day	-0.002	-0.011
2 days	0.003	-0.003

As can be seen from Table 6.4, there was no significant difference between the expansions of the reference mix and the mortar with mylonite filler. Consequently, no significant changes of length have taken place in this early phase.

Most of the mortar bars tested in the present study have been measured both at the time of de-moulding, and at the second day when a temperature of 80°C was established. The measure at 2 days and 80°C has been used as reference, because all subsequent measurement was performed at this temperature. However, the general conclusion is that there is no significant effect of using the 2-days values as reference lengths, compared to using the 1-day length values. Based on this limited study, the argument that the effect of inhibiting materials on reduced expansion is caused by expansions in a very early plastic phase of the concrete or mortar does not seem to be valid.

It should, however, be noted that some of the mortars containing high amounts of very fine fillers, have shown a tendency of swelling during the first day. This was observed as swelling on top of the bars at the time of de-moulding. The reason for this phenomenon is not known, but is believed to be of minor significance for the expansion results presented here. However, this effect needs to be further investigated.

6.4 Micro structure depending on the type of filler

6.4.1 General

The aim of the micro-structural analyses has been to examine and describe the textural changes and reaction products due to ASR. Parallel testing of specimens stored one year according to conditions by the CPT has been performed by optical microscopy and by electron probe microanalyzer (EPMA). The polished sections and thin sections are complementary in the way that the polished sections cover a rather large area, while the thin sections give possibilities of detailed studies. In Table 6.5, the compositions of the examined concretes are given, together with the expansions after one and two years of exposure according to the CPT.

Table 6.5 Description and expansion data for concretes examined by micro- structural analyses. Na_2O -equivalent was 5 kg/m^3 for all mixes. Constant w/c ratio (0.45) and quantity of cement (400 kg/m^3) for all mixes.

Concrete	1 year expansion (%)	2 years expansion (%)
Reference*	0.093	0.179
5.15 % mylonite 0-125 filler	0.136	0.202
5.15 % rhyolite 0-125 filler	0.017	0.041
5.15 % glass 0-125 filler	0.017	0.043

* Only optical microscopy

Two specimens from accelerated mortar bar testing was examined by optical microscopy. Expansions after 14 days and 56 days of storing are given in Table 6.6. The specimens were examined after 56 days of storing.

Table 6.6. Description of specimens and expansion data for mortars examined by optical microscopy. Constant w/c ratio (0.47) and quantity of cement(600 kg/m^3) for both mixes.

Mortar	14 days expansion (%)	56 days expansion (%)
Reference	0.16	0.57
20 % mylonite 0-20 filler	0.07	0.16

The investigation was carried out by the use of fluorescent impregnated thin sections (TS) and fluorescent impregnated polished section (PS), examined by polarising microscope, stereo microscope and UV – light, see Section 5.2.5. The dimensions of the thin sections were 30 mm x 48 mm, and the polished sections 100 mm x 70 – 75

mm. In the following, observations of the textural changes and the reaction products caused by alkali-silica reactions (ASR) are described. The preparation of thin sections is a sensitive process, involving possibilities of disturbance of the original cut surface. During the preparation process, it has been observed that in some cases, alkali-silica gel visible by the naked eye was lost in the process. Consequently, the amount of gel found on the thin sections should not qualify as an indicator of the degree of reaction. The number of cracks running from aggregates into the cement paste is a better indication of the damage of the concrete, while observation of alkali-silica gel is important as a qualitative indication whether the damages is caused by alkali-silica reaction, or by other mechanisms.

6.4.2 Observations of textural changes and reaction products by optical microscopy

6.4.2.1 Specimens from concrete prism testing

The investigation has been carried out and reported separately by Viggo Jensen. The full report, including micro photos, can be found in Appendix D. In the following, the major findings from this study are summarized.

Table 6.7 summarizes the result of the investigations by optical microscopy. Note that the degree of damage in reference concrete and the mylonite filler concrete is described as deleterious. On the other hand, no or very few signs of damage was found in the concretes with glass and rhyolite filler.

Table 6.7 Summarised observations on polished sections and thin sections

Type of filler	Cracks	Gel	Degree of damage	Observed filler particles	w/c ratio by optical judgement
Reference	many	yes*	deleterious**	none	w/c \approx 0.45
Mylonite filler	many	yes	deleterious**	not observed	slightly reduced
Rhyolite filler	few	no	none	few/ 0.13 –0.03 mm	significantly reduced
Glass filler	few	yes	minor**	many/ 0.13 -0.002 mm	significantly reduced

* Gel occurred only in polished section and not in the thin section, probably because the gel was washed out during preparation of the polished TS.

** Deleterious when ASR causes cracks in the cement paste. Minor when ASR not causes cracks.

The effects of glass filler, rhyolite filler and mylonite filler in terms of expansion have been confirmed by the qualitative observations done by optical microscopy. Also note that the optical judgement of porosity or w/c ratio (see Table 6.7) has indicated a denser paste for the concretes with glass and rhyolite filler (and to a lesser extent also mylonite filler) compared to the reference concrete. This is most

likely due to pozzolanic reactions between CH and glass and rhyolite fillers, as well as a contribution towards more homogeneously distributed reaction products (CSH).

6.4.2.2 Specimens from accelerated mortar bar besting

The investigation was carried out and reported separately by Marit Haugen. The full report, including micro photos, can be found in Appendix E. The major findings from this study are summarized in the following.

The investigation showed extensive cracking in the reference mortar containing no filler. Partly dissolved aggregate grains and cracks running from the aggregates into the surrounding cement paste were observed. Alkali-silica gel was observed in cracks and air voids. The cracking occurred throughout the whole section. The specimen from the mortar with 20 % mylonite 0-20 filler had significantly less air voids than the reference mortar. The cement paste in the specimen containing filler was denser than in the reference specimen. Cracking, partly dissolution of aggregate grains and alkali-silica gel was also observed in this specimen. However, these signs of alkali-silica reactions were mainly observed near the exposed surfaces, in a zone of about six mm thickness. It seems likely that the denser mortar caused by the mylonite filler has reduced the rate of ingress of alkali hydroxides from the storing solution. The denser mortar is presumably caused by the pozzolanic reactivity of the mylonite filler possibly in combination with a general filler effect giving more homogeneously distributed reaction products. In addition to the lower ion mobility caused by the denser cement paste, alkali hydroxides may be bound in the CSH resulting from the pozzolanic reaction.

6.4.3 Observations and chemical analyses by the electron probe micro analyser (EPMA)

Concretes containing mylonite filler, rhyolite filler and glass filler (see details in Table 6.5) have been examined by EPMA. Some qualitative and quantitative observations are given below, while comprehensive results including SEM micrographs are given in Appendix B4.

One observation was that the concrete with mylonite filler was significantly cracked, with gel-filled cracks running from aggregates into the cement paste; see Figure 6.14. Chemical analyses of the reaction products have been performed using wavelength dispersive X-ray spectrometer (WDS). Table 6.8 shows the mean composition of ASR gel found in cracks in the cement paste. Ettringite has also been found in one crack (see photo SEM 1 in Appendix B4), the chemical composition is given in Table 6.8.

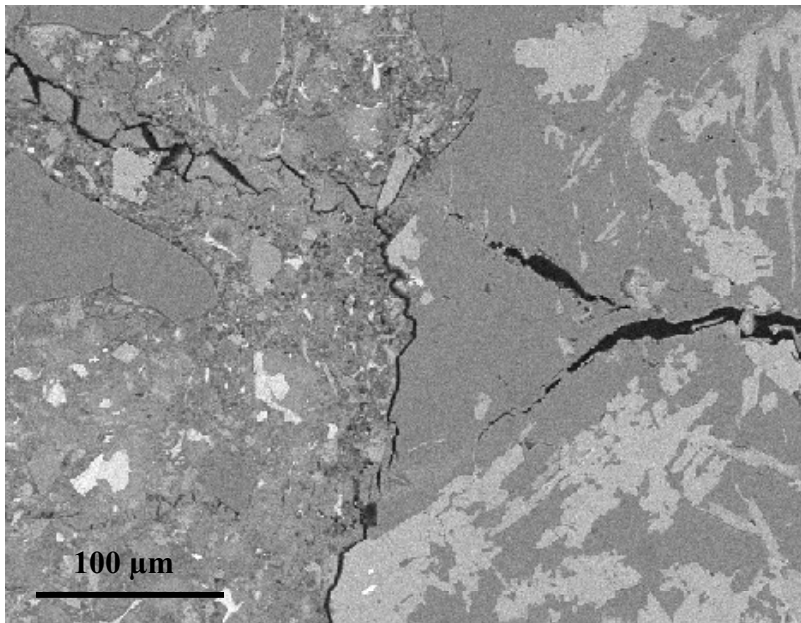


Figure 6.14. Crack with ASR gel running from large aggregate and out into the cement paste. Backscatter SEM micrograph.

Table 6.8. Chemical composition of reaction products in cracks, concrete with mylonite filler. Mean values and standard deviations (seven analyses of alkali-silica gel, three analyses of ettringite).

	Na ₂ O	K ₂ O	SiO ₂	CaO	SO ₃	Al ₂ O ₃	MgO	FeO	Total	Product
Mean	3.44	3.36	34.69	36.12	0.14	1.21	0.05	0.00	79.01	A-S gel
St. dev	1.64	1.36	4.71	4.31	0.07	0.80	0.07	0.00		
Mean	2.85	0.63	0.26	55.57	15.80	16.98	0.02	0.00	92.11	Ettringite
St. dev	3.51	0.07	0.12	1.31	0.46	1.21	0.01	0.00		

As discussed in Section 2.4.2, ettringite are commonly found in association with alkali-silica gel. According to Jensen (1993), ettringite may succeed alkali-silica gel in cracks, or grow together with the gel. The formation of ettringite may contribute to the expansion in concrete. It should be noted that the formation of ettringite are very common also in old concrete with no ASR, as has been reported by Jensen (1993) also for Norwegian concretes.

The chemical composition of the alkali-silica gel observed in cracks in the cement paste was high in calcium; see Table 6.8. The chemical composition of alkali-silica

gel is known to vary widely, and calcium amount in the same order as measured in this study has been reported earlier (Poole 1992). Jensen (1993) has reported chemical data of gel in the cement paste of field concrete. The chemical composition of his analyses is rather similar to the data of the present study. However, one exception is that the amount of Na_2O was lower and the amount of K_2O was higher in the data of Jensen (1993).

The concrete with glass filler did generally show few signs of ASR. However, gel was observed in one air void. Glass particles in the size range from $< 10 \mu\text{m}$ to $> 100 \mu\text{m}$ could be observed in the cement paste. Most of the glass particles showed clear signs of zonation, indicating some kind of chemical reaction with the cement paste. To investigate this possible chemical reaction between the glass particles and the cement paste or cement pore fluid, element mapping was carried out. The element mapping, which can be found in Appendix B4, have shown a distinct decrease in Na and Si, and a less distinct increase in Ca in the boundary zone of the glass particles. However, no signs indicating that the glass particles had lead to formation of alkali-silica gel or cracking was found. It is possible that released alkalis from the glass particles could react with other reactive aggregate particles in the long run. However, test results from CPT up to two years, see Table 6.5, have clearly shown that the addition of glass filler reduced the expansion significantly compared to the reference concrete, and no signs of negative effects of the glass filler have been found.

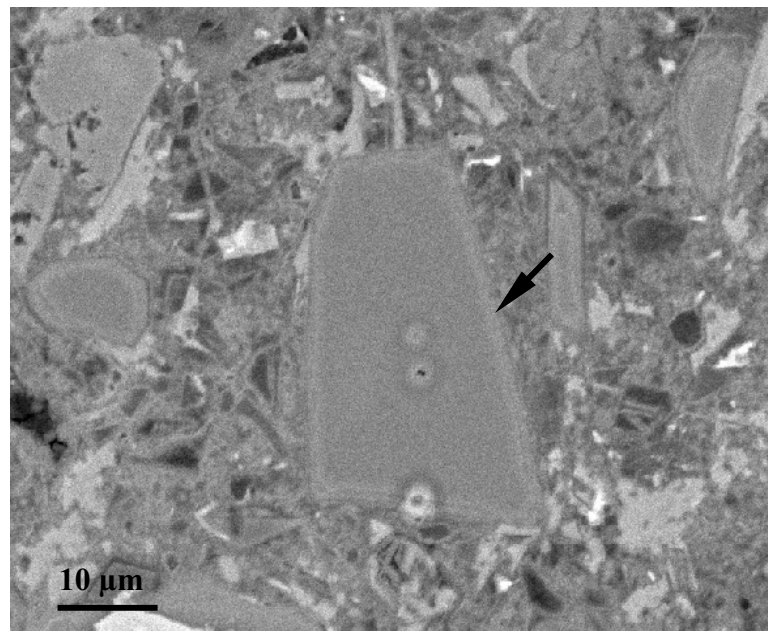


Figure 6.15. Zonation of glass particles, shown as a distinct light grey rim in the contact zone between the glass particle and the cement paste. Backscatter SEM-micrograph.

Table 6.9 shows some examples of chemical composition of alkali-silica gel found in air voids of glass filler concrete and mylonite filler concrete.

Table 6.9. Chemical composition of residue of reaction products in air voids in concretes with mylonite and glass filler. Inner part of pore: towards the centre of the pore, outer part: towards boundary between pore and cement paste. (Single analyses).

Na ₂ O	K ₂ O	SiO ₂	CaO	SO ₃	Al ₂ O ₃	MgO	FeO	Total	Filler
3.73	10.70	43.13	21.89	0.00	0.04	0.00	0.00	79.50	Mylonite
10.49	8.19	70.50	2.75	0.39	0.09	0.00	0.02	92.43	Glass, inner
6.08	6.35	41.98	25.19	0.13	0.25	0.00	0.06	80.03	Glass, outer

The gel found in the air void in the mylonite filler concrete differs significantly from the gel found in the cracks; see Table 6.8. The S/C ratio was significantly higher, and the amount of K₂O was also much higher. The reaction products observed in the air voids in the glass filler concrete was of two distinct compositions, see Table 6.9 and figure 3 and 4 in Appendix B4. The composition of the outer part of the pore was in the same range with respect to S/C ratio as noted for the mylonite concrete, while the product of the inner part (towards the centre) was very low in Ca and high in Si. The relatively high amount of Na₂O in the gel within the glass filler concrete is probably due to the very high amount of Na₂O in the glass. The difference between the gel of the inner part and the outer part may be caused by reaction between the outer part of the gel and the surrounding cement paste. It is well known from the literature that the composition of alkali-silica gel may vary much within the same concrete. The variation in calcium content is often related to the location of the gel in the concrete, and probably also to the age of the concrete. As discussed by Diamond (2000), many scientists have observed that the gel inside or close to reacted aggregate grains is very low in calcium, while the gel very often will pick up calcium from the cement paste as it moves away from the reactive grain. The swelling potential may vary much, and many scientists consider gels very rich in calcium non-swelling, possible towards an alkali rich CSH. However, this view on the role of calcium is disputed by some scientists, e.g. Chatterji et al. (1986, 1992), as previously discussed in Section 2.5.4.

The specimen from the rhyolite concrete has also been studied by the EPMA. No reaction products or other signs of ASR were found in this specimen.

6.5 Compressive strength and capillary suction depending on the type of filler

6.5.1 General

The following sections give results from routine testing of compressive strength and capillary suction. A comprehensive list of results is given in Appendix B2, while the most relevant results are shown and discussed below.

6.5.2 Influence of fillers on the compressive strength

The effect of added filler on compressive strength can be seen in Figure 6.16 and Figure 6.17 for 28 and 365 days of curing, respectively. Mean values and 95 % confidence intervals are given in both figures. Comprehensive results on compressive strength are given in Appendix B2. The compressive strength tests were performed according to NS 3668. (The amounts of 5.15 and 10.3 % are abridged to 5 and 10 %, respectively in Figure 6.16 and 6.17).

The presented results are all from concretes with 5 kg Na₂O equivalent, which mean that NaOH equivalent to approximately 1 kg Na₂O-equivalent was added in order to increase the alkali level. Some results from concretes where no NaOH was added will be presented later.

Figure 6.16 shows the compressive strength after 28 days of curing. All fillers gave increased 28-days compressive strength compared to the reference. The trend for the mylonite filler was an increase with increasing amount of filler. A decrease in particle size did also give an increase in strength for the mylonite filler. The opposite effect was observed for the rhyolite filler, where the finest fraction (0-20) gave lower compressive strength than the coarser (0-125) one. However, the difference between the levels of strength of the 0-20 and the 0-125 rhyolite filler concretes are not significant on a 5 % level.

The situation is somewhat changed when the compressive strength after one year is plotted, as seen in Figure 6.17. The differences were generally less pronounced at one year of curing compared to 28 days of curing. All concretes containing 5.15 % or higher amounts of mylonite and cataclasite filler, except the concrete with 2 % mylonite filler, obtained increased, but not statistically higher, compressive strength. The mix with only 2 % added mylonite filler gave a remarkable and unexpected rise from 28 to 365 days.

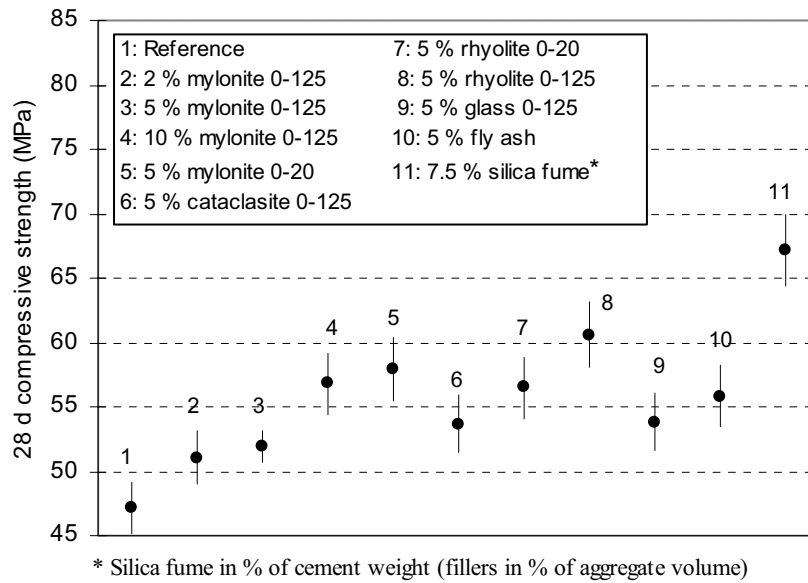


Figure 6.16 Compressive strength after 28 days of curing in water at 20 °C. Mean values and 95 % confidence intervals. All concretes with NaOH addition to 5 kg Na₂O equivalent. Constant w/c ratio (0.45) and quantity of cement (400 kg/m³) for all mixes.

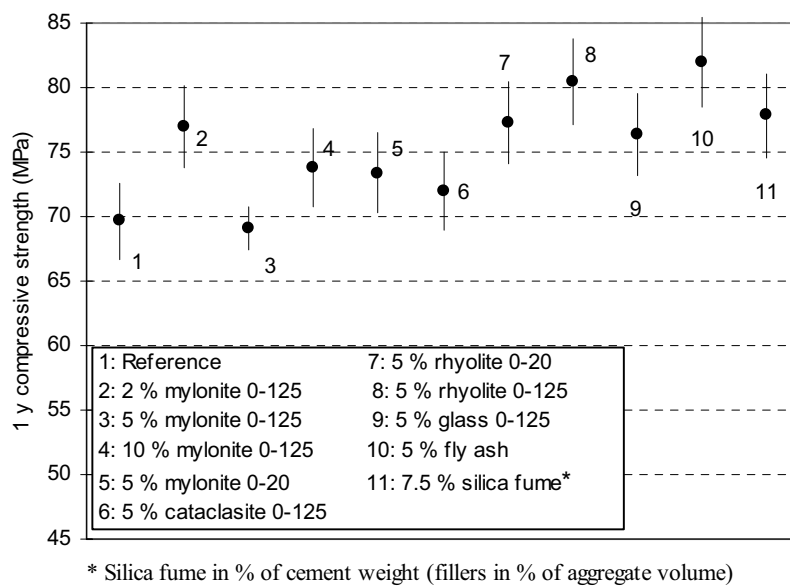


Figure 6.17 Compressive strength after 365 days of curing in water at 20 °C. Mean values and 95 % confidence intervals. All concretes with NaOH-addition 5 kg Na₂O equivalent. Constant w/c ratio (0.45) and quantity of cement (400 kg/m³) for all mixes.

A striking observation can be made by comparing the 28 days results with those of 365 days of curing. At the age of 28 days of curing, the compressive strength of the silica fume concrete was significantly higher than concretes with glass, rhyolite and fly ash. The compressive strengths of the concretes containing rhyolite, glass and fly ash was all in the same range as the silica fume concrete at an age of one year. Obviously, only a fraction of the total potential of strength increase was achieved at 28 days of curing for these mixes containing rhyolite, glass and fly ash. The quicker growth in compressive strength is caused by a quicker pozzolanic reaction due to the high fineness of the silica fume, which is practically consumed at 28 days of curing (Justnes 1996). Consequently, the increase in compressive strength from 28 days to one year because of the silica fume is insignificant.

The addition of NaOH seems to alter the compressive strength. This can be observed in Table 6.10, where compressive strengths and resistance numbers are tabulated for some concretes with different alkali levels. Note that an addition of NaOH gave a decrease in compressive strength for all the concretes except the one with mylonite of size fraction 0-20. Some of the differences in compressive strength between the 4 and 5 kg levels are small and not significant.

Table 6.10. Differences in compressive strength and resistance number for concrete with 4 and 5 kg Na_2O -equivalent. No addition of NaOH at the 4-kg level. Filler amount in % of total aggregate volume. Constant w/c ratio (0.45) and quantity of cement (400 kg/m^3) for all mixes.

Filler / Na_2O -equiv.	28 d. compr. strength (MPa)		1 y. compr. strength (MPa)		1 y. resistance nr. * E7 (s/m^2)	
	4 kg/m^3	5 kg/m^3	4 kg/m^3	5 kg/m^3	4 kg/m^3	5 kg/m^3
Reference	53.0	47.2	70.6	69.7	4.37	4.26
5.15 % mylon. 0-125	56.7	51.9	72.4	69.0	6.40	5.11
10.30 % mylon. 0-125	64.6	56.8	80.1	73.8	7.16	5.62
5.15 % mylon. 0-20	55.2	57.9	66.9	73.4	4.33	7.70
5.15 % rhyolite 0-125	62.2	60.6	82.3	80.5	6.88	9.30
5.15 % granite 0-20	55.1	-	69.6	-	4.28	-
7.5 % silica fume*	73.5	67.1	86.6	77.8	11.20	9.99

*Silica fume amount in % of cement weight.

Note from Table 6.10 that silica fume and rhyolite filler increased the compressive strength as expected due to the high pozzolanic reactivity of these materials. However, the granite and mylonite filler, being non-pozzolanic at the curing temperature, gave no significant increase in compressive strength, except at the highest addition level (10.3 %) of mylonite.

6.5.3 Influence of fillers on the capillary suction

A description of the method is given in Section 5.2.10. Comprehensive test results are given in Appendix B2.

It is believed to be a general correlation between the resistance number and the water/cement ratio, and Smeplass & Skjølsvold (1996) have reported data based on national experience using the capillary suction method. However, silica fume is known to increase the resistance number considerably, as have been reported by Isaksen et al. (1996). The resistance number indicates the resistance to water ingress, and consequently the fineness of the pore system of the concrete. Hence, any effects of the fillers with respect to refining the pore system may cause an increase in the resistance number.

In Figure 6.18, the resistance number is plotted versus compressive strength.

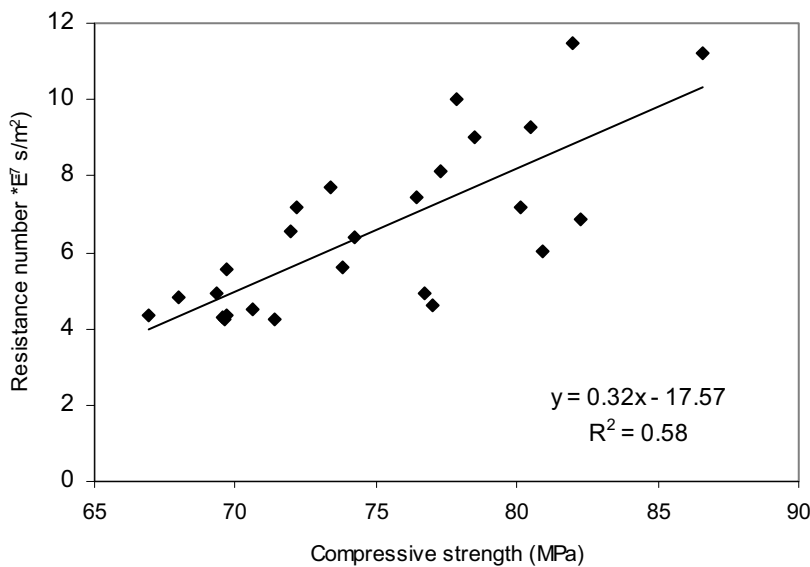


Figure 6.18. Resistance number versus compressive strength. Granite sand, mylonite coarse aggregate, OPC and w/c-ratio 0.45 for all mixes. Varying alkali levels (4 or 5 kg Na₂O-equiv./m³), varying types and amounts of filler addition. Constant w/c ratio (0.45) and quantity of cement (400 kg/m³) for all mixes.

Note that the trend obtained in the present study, see Figure 6.18, was that the resistance number increased with increasing compressive strength, as could be expected. But the correlation between the resistance number and the compressive strength is rather weak. Isaksen et al. (1996) reported that the resistance number is

highly dependent on the amount of silica fume. Based on this, also taking into consideration the large differences in pozzolanic reactivity between the different fillers, there could not be expected to be a straightforward correlation between the resistance number and the compressive strength.

6.5.4 Concluding remarks on the compressive strength and the capillary suction

Based on the present results it is concluded that the effect of granite/gneiss filler and mylonite filler is insignificant with respect to compressive strength at the 5 % addition level; see Table 6.10. On the other hand, addition of rhyolite and 10 % mylonite filler have been documented to give a significant increase in compressive strength, both at 28 days and 1 year of curing. The effects of the other fillers (cataclasite, glass and fly ash) are uncertain due to the disturbing effect of the added NaOH, as have been discussed in Section 6.5.2. But the effect on compressive strength from the cataclasite filler seems to be fairly low, and hardly significant. On the other hand, both glass filler and fly ash seem to give a significant increase in compressive strength.

As could be expected, there seem to be a general connection between the pozzolanic reactivity of the fillers and the potential of increasing the compressive strength. The fillers being chemically inert seem to give little or no effect on compressive strength, unless very high amounts are added. It is noteworthy that 5 % addition of the very fine filler fraction 0-20 μm of mylonite and granite/gneiss gave no significant effect on the compressive strength. This contradicts the results reported by Kronlöf (1994, 1997) where quartz filler believed to be chemically inert increased the compressive strength by roughly 4 MPa. Kronlöf (1994, 1997) reported that the strength increase was clearest in the leanest mixes (with cement amounts of less than 250 kg/m^3). In the present study, the w/c ratio was 0.45 for all mixes, and the cement amount was 400 kg/m^3 . The addition of inert fillers may reduce internal bleeding more in lean mixes than in mixes with such high cement amounts as in the present study, a fact that might explain some of the difference.

6.6 Summary and concluding discussion

Direct testing of pozzolanic reactivity, by mixing CH, fillers and an alkaline solution simulating the pore water in concrete, has been carried out. The remaining CH at different times of curing is then a measure of the pozzolanic reactivity. All fillers (in the particle range of 0-20 μm) with a distinct amorphous phase gave high pozzolanic reactivity when cured at 20°C. The Norwegian alkali-reactive rock fillers (mylonite and cataclasite) gave low pozzolanic reactivity at 28 days of curing. The temperature effect on the pozzolanic reactivity has been shown to be large, with a pronounced increase for both the mylonite and rhyolite fillers when the temperature increased from 20°C to 80°C. No significant difference in pozzolanic reactivity between 20°C and 38°C was noted for the mylonite filler. Consequently, the pozzolanic reactivity for mylonite was close to zero both at 20°C and 38°C, while it was significant at 80°C.

All fillers with a pronounced pozzolanic reactivity at low temperatures reduced the expansions significantly in concrete tested by the CPT. On the other hand, the Norwegian alkali reactive rock fillers with low pozzolanic reactivity did not give any difference, or gave a small increase in expansion. The effect of changing the particle size was generally very low, though a weak tendency towards an increase in expansion as the particle size decreased was observed for the mylonite filler. The effect of particle size reduction was the opposite for the rhyolite filler, as the finer grading reduced the expansion more than the coarse grading.

The micro-structural analyses of four concrete samples, exposed one year according to conditions of the CPT, have confirmed the expansion results. Extensive cracking and gel products were observed in the reference sample and in the sample with mylonite filler. The concrete with glass filler showed minor signs of ASR, which is in accordance to the low expansions obtained by the CPT. Glass particles from a few microns up to the largest sizes was easily observed by both optical microscopy and SEM. Most of the glass particles showed clear signs of zonation, indicating chemical reaction with the cement paste/pore fluid. The dissolution of the outer part of the glass particles has also been verified by element mapping in the micro probe study. There is a concern about the large alkali amounts within the glass particles, and to what extent this might be of significance for the long-term behaviour. However, the micro-structural analyses after one year of storing, and the expansion data up to two years of storing, indicate that the inhibiting effect of the glass particles is stable over time. For the concrete containing rhyolite filler, a few cracks was observed, but no indications of alkali-silica reactions could be observed. The capillary porosity, as measured by optical microscopy, was significantly reduced for both the concretes containing glass filler and rhyolite filler. This gives evidence of a denser CSH-phase caused by pozzolanic reactivity, possibly in combination with a general filler effect. A reduction in the capillary porosity caused by the mylonite filler, though being smaller, was also observed.

The increase in compressive strength was obvious and significant for the rhyolite filler, but insignificant for the other rock fillers unless very high amounts of filler were added. No significant difference between natural granite/gneiss filler and alkali reactive crushed mylonite filler was found. Fly ash and glass filler also gave a significant increase in compressive strength as expected. These fillers were tested only in concretes with added NaOH.

Extensive testing of fillers using the AMBT has been performed. While the natural granite/gneiss and the limestone fillers had no or very low effect on the expansion at all ages, the effect was pronounced for the alkali-reactive rock fillers, as well as for glass filler, fly ash and silica fume. A general correlation between the amount of filler and the particle size on one side, and the inhibiting effect on the other, has been found. Both finer fractions, and higher amounts, gave an increased inhibiting effect. A general observation of these experiments is that the addition of pozzolanic materials implies reduced expansion.

The effect of adding mylonite and cataclasite fillers was not truly predicted by the AMBT. Increasing amount of filler and decreasing particle size gave increasing inhibiting effect. This is believed to be due to the pozzolanic reactivity of the fillers at the elevated temperature of this method as shown in Section 6.2.3. As the true field situation does not involve prolonged elevated temperatures, the pozzolanic reactivity of these fillers is too low to play a dominant role. This has been demonstrated by testing the cataclastic fillers by the CPT, where these fillers rather tended to give higher expansions than to inhibit the expansions.

It has been clearly shown that all the alkali-reactive fillers tested within the present study may react pozzolanic, at least when grown down to particles $< 20 \mu\text{m}$. However, the Norwegian rock fillers mylonite and cataclasite being clearly pozzolanic at the temperature of 80°C showed an insignificant pozzolanic reactivity at 20°C and 38° . Hence, these materials should not be considered pozzolanic in real field concrete because the pozzolanic reactivity at temperatures of 38°C and lower is too low to play a dominant role. The results obtained by CPT indicate that the mylonite and cataclasite fillers are potentially alkali-reactive in concrete. When utilizing such materials, normal precautions with respect to alkali loads and use of efficient pozzolanic materials as inhibiting agents should be taken. The AMBT should not be used to test the effect of rock fillers in concrete unless the fillers have been documented to be pozzolanic at temperatures relevant in field conditions, because the method may give an unreliable prediction of the inhibiting effect.

The effects of the different fillers on expansions measured by the AMBT and the CPT have been measured in combination with mylonite aggregate, and the effects have been related to reference mortar and concrete with no reactive filler. Only a few experiments using other reference materials have been carried out. The combination of cataclasite aggregate and mylonite filler gave the same kind of performance as the combination of mylonite aggregate and mylonite filler when tested by the AMBT, see results in Appendix B3. The combination of Spratt limestone coarse aggregate and mylonite filler gave the same kind of performance as the combination of Mylonite coarse aggregate and mylonite filler when tested by the CPT, see results in Appendix B2. These results indicate that the methodology of testing is relevant, but it cannot be excluded that the effects of the different fillers would be different in combination with other alkali-reactive coarse aggregates.

It should also be noted that one test with reactive mylonite fine aggregate ($< 5 \text{ mm}$) and non-reactive granite/gneiss coarse aggregate ($> 5 \text{ mm}$) have been carried out. When non-reactive granite/gneiss filler replaced the reactive mylonite filler in the sand, there was no significant effect caused by this replacement. This indicates that the mylonite filler may not contribute much to expansions. The mylonite filler may cause small expansions in combination with non-reactive aggregate, but due to the low amounts of filler normally added, it may not be deleterious. However, the mylonite filler as well as the cataclasite filler should be treated as potentially harmful in concrete, and normal precautions according to national regulations with

respect to amount of potentially deleterious aggregates, alkali level and pozzolanic additions should be taken when utilizing such materials.

The present study has given valuable information concerning the practical implications of using alkali-reactive fillers. However, some of the more fundamental issues concerning the paradox of alkali-silica reactions and pozzolanic reactions are still far from being fully understood. It is clear that factors such as temperature, alkalinity and particle size, and off course the structure of the silica, all have a very large effect on the solubility of silica. And solubility has obviously a large influence on both the alkali-silica reaction and the pozzolanic reaction. It seems clear that grinding of alkali-reactive materials to fine powder in many cases favours the pozzolanic reaction. This is presumably due to the much higher surface area, which promotes quicker reactions with the surrounding pore water and cement paste. There is much evidence in the literature that calcium has a crucial influence on the reaction products, and high availability of calcium seems to favour the desirable pozzolanic reaction. In the cases of very fine powders evenly distributed in the cement paste it is reasonable to assume that calcium ions may come more easily in contact with the dissolving silica and thereby contribute to a “safe” reaction according to the terminology of Powers & Steinour (1995a,b). This is the case for fillers of such materials as bottle glass and Icelandic rhyolite. However, the opposite effect, i.e. increased expansion with decreasing particle size, both observed within the present study for slowly reacting mylonites, as well as for highly reactive opal as reported by Diamond & Thaulow (1974), makes the picture very complicated. It is clear that more fundamental research on the mechanisms of the alkali-silica reaction is necessary to understand this.

7 Effects of fillers on the rheological properties of fresh concrete - results and discussion

7.1 Introduction

The experimental investigations of the effect of filler materials on fresh concrete have been carried out by matrix tests within the present study. The Particle Matrix (PM) model (Mørtzell et al. 1995, Mørtzell 1996) gives the workability of concrete, in terms of the empirical slump measure, as a function of the matrix and particle properties and their relative volume fraction. The PM model is then used to predict the effects of fillers on fresh concrete, based on the measured effects in the matrix. A description of the particle-matrix model is given in Section 3.6. The FlowCyl test, which is the single-parameter test used to characterise the matrix paste within the PM model, is described in Section 5.2.6.2.

At a constant grading of the aggregates, as for the concretes tested within the present study, the PM model predicts the workability of the concrete to be a unique function of the flow resistance ratio (λ_Q) and the volume fraction of the matrix phase. However, a recent study reported by Smeplass & Mørtzell (2001) indicated that the flow resistance ratio, obtained by the FlowCyl, is insufficient to characterise the rheological properties of the matrix. An earlier study by Pedersen & Mørtzell (2001) indicated that the flow resistance ratio (λ_Q) obtained by the FlowCyl is basically controlled by the plastic viscosity. In the study of Pedersen & Mørtzell (2001), the yield stress (τ_0) and the plastic viscosity (μ) of the matrix were measured by a Fann viscometer. The correlation between the plastic viscosity and the flow resistance ratio has been confirmed by the present study. As seen in Figure 7.1, the correlation between the plastic viscosity and the flow resistance ratio seems obvious. The points can be fitted with an exponential function, as indicated in the figure, or alternatively by a power-law function. The correlation between the yield stress and the flow resistance ratio is less obvious. The present results indicate that the FlowCyl viscometer gives relevant information about the plastic viscosity. But it does not distinguish very well at flow resistance ratios above 0.8 because relatively large variations in plastic viscosity seem to give rather small variations in flow resistance λ_Q .

In the work of Mørtzell (1996), only one type of cement was used (an ordinary Portland cement with performance close to the OPC used in the present study) to correlate the matrix rheology towards concrete rheology. Mørtzell (1996) also used only one type of plasticizer. The parameter study included variations in w/c ratio, filler type and filler amount. Consequently, the correlation between the rheological properties of the concrete and the corresponding matrix phase was only verified for a limited spectre of materials. The more recent work discussed above indicates that there is a need for a better characterisation of the rheological properties of the matrix, and in particular that the yield stress must be taken into account by using a

more sensitive characterisation method than FlowCyl. In this study the fundamental rheological parameters of the matrix, yield stress and plastic viscosity, have been characterized using a Physica rheometer with parallel plate configuration; see Section 5.2.6.3 for further description of the methodology.

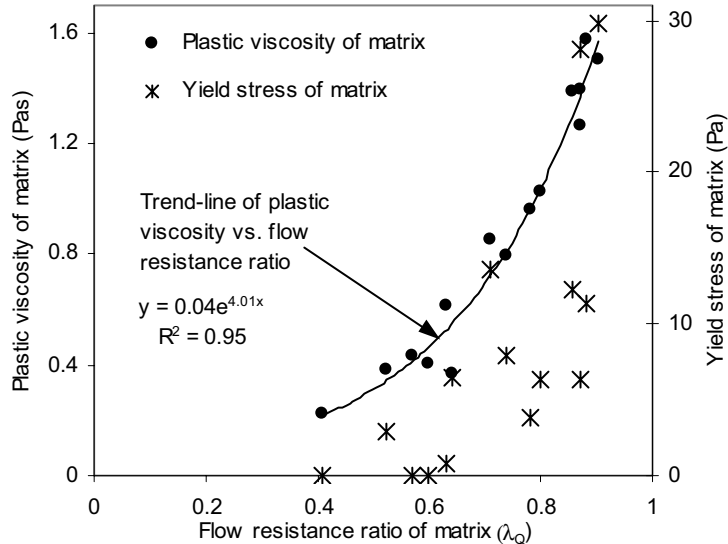


Figure 7.1. Relationship between λ_Q measured by the FlowCyl tube viscometer and the fundamental rheological parameters plastic viscosity and yield stress of the matrix phase measured by the Physica rheometer.

In the present study, the fillers were tested in different mix combinations, using both the FlowCyl tube viscometer and the Physica rheometer. A study of the relationship between the rheological properties of matrix and self-compacting concrete (SCC) has also been carried out. The results are treated in the following section.

7.2 Influence of fillers on the rheological properties of the matrix

7.2.1 Introduction

The parameter study by the FlowCyl viscometer involved testing of different fillers at different w/c ratios and filler addition levels. The parameter study using the more fundamental characterisation by the Physica rheometer also involved different plasticizers in combination with the tested fillers. A limited study of the effects of different cement types is also reported in this section. Note that the test programmes of the two parameter studies differ significantly (outlines of the test programmes are given in Section 5.4.6 and 5.4.7). The mix design of the matrices tested within the

Physica parameter study aimed towards very stable mixes, meaning relatively low w/c ratios or/and high filler addition levels. The mixes tested by the FlowCyl had generally higher w/c ratios and/or lower filler additions. Generally, stability is a precondition if the rheological properties are to be tested. However, testing by the Physica rheometer is believed to be more sensitive with respect to the stability of the matrices than testing by the FlowCyl viscometer.

Descriptions of all the tested fillers are given in Section 5.3.4. Note that the particle size distribution varied much for the tested fillers, see Table 5.16 in Section 5.3.4.3 and Appendix A2 for details.

7.2.2 Influence of fillers on the flow resistance ratio λ_Q

7.2.2.1 General

In this section, results from the rheological investigations performed using the FlowCyl viscometer are presented. A comprehensive list of results can be found in Appendix C1.

7.2.2.2 Effects of addition of fillers

Figure 7.2 presents the effect of adding filler at a constant w/c- ratio. Note that the results of the matrices containing carbonate filler and limestone filler are totally overlapping at the two highest filler addition levels.

The addition of filler at a constant w/c ratio gave an increase in λ_Q for all the tested fillers. The granite filler gave the lowest λ_Q , while fly ash gave the highest. The ranking of the fillers was constant over the tested range of filler addition. According to Figure 7.2, the difference in λ_Q between the granite filler and the fly ash was larger at the intermediate addition level than at the highest addition level. Bearing in mind the exponential relationship between the flow resistance ratio and the plastic viscosity presented in Figure 7.1, the difference in plastic viscosity between the granite filler and the fly ash may be higher at the highest addition level.

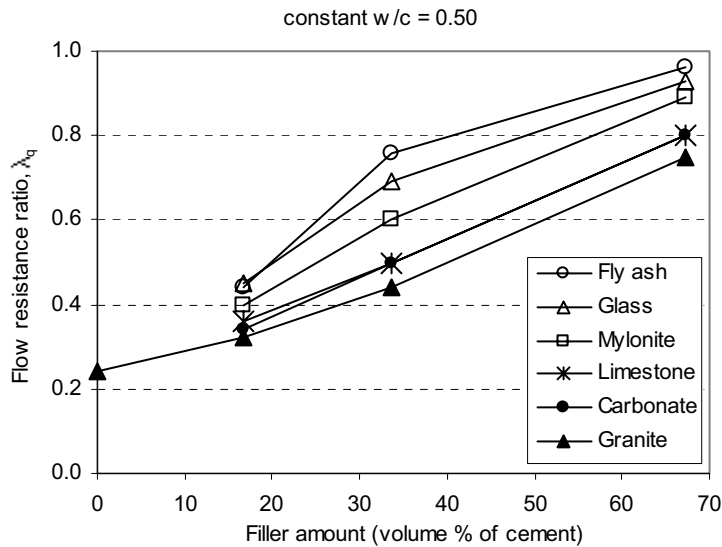


Figure 7.2. Flow resistance ratio as a function of filler type and filler amount at constant w/c = 0.5. Filler amount in volume % of cement. The amount of plasticizer (SSP 2000) was 1.0 % of the cement weight for the mixes with 33.6 % filler, while the amounts were equal relative to the powder (including both cement and filler) volume for the other addition levels (1.6 % of total powder volume for all mixes). All fillers were 0-125 fractions.

7.2.2.3 Replacement of cement by filler

In Figure 7.3, the effect of replacing cement by filler is presented. In this set of experiments, the filler dosage increased as the w/c ratio increased from 0.40 to 0.60, to compensate for the decreasing cement amount. The w/p ratios of the different fillers were kept constant as the w/c increased, meaning that filler replaced cement by weight. Consequently, the total powder volume increased some with increasing filler addition due to the lower density of filler compared to cement. However, all the amounts of fillers were identical on a volume basis.

According to Figure 7.3, fly ash and glass filler gave increasing flow resistance with increasing filler amount. All the other fillers gave lower flow resistance ratios when the filler replaced cement.

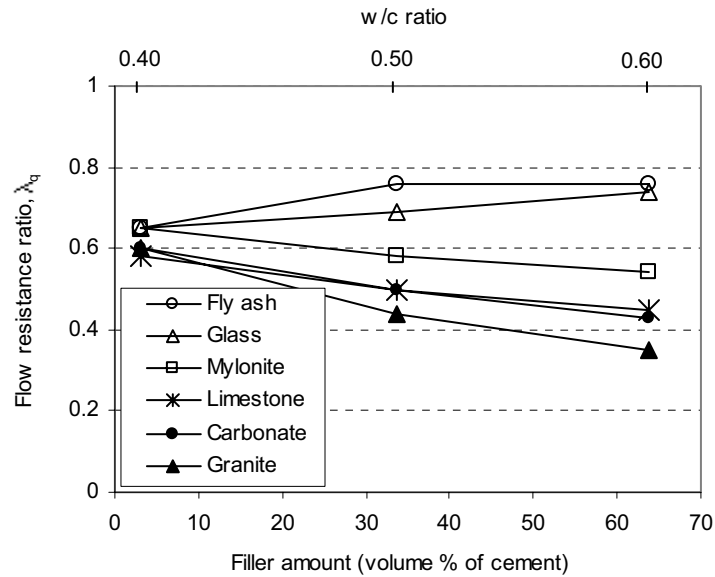


Figure 7.3. Flow resistance ratio as a function of filler type and filler amount when filler replaced cement. The amount of plasticizer (SSP 2000) was 1.0 % of the cement weight for the mixes with 33.6 % filler, while the amounts were equal relative to the powder (including both cement and filler) volume for the other addition levels (1.6 % of total powder volume for all mixes). All fillers were 0-125 fractions.

The relatively large differences in flow resistance ratio caused by different fillers, as presented in Figure 7.2 and Figure 7.3, were caused by differences in physical and surface chemical characteristics of the fillers. The physical characteristics include particle size distribution, shape and roughness of the particles, while the surface chemical properties are dominated by the mineralogy. The span in mineralogy and physical properties is wide for the tested fillers; see Chapter four, Section 5.3.4 for descriptions of the filler materials.

The total matrix grading curves, combining both cement and filler at the 34 % filler addition level, are plotted in Figure 7.4. At this level of filler addition, the total grading of the powders are dominated by the larger cement amount. However, the influence of the fillers on the total grading is evident.

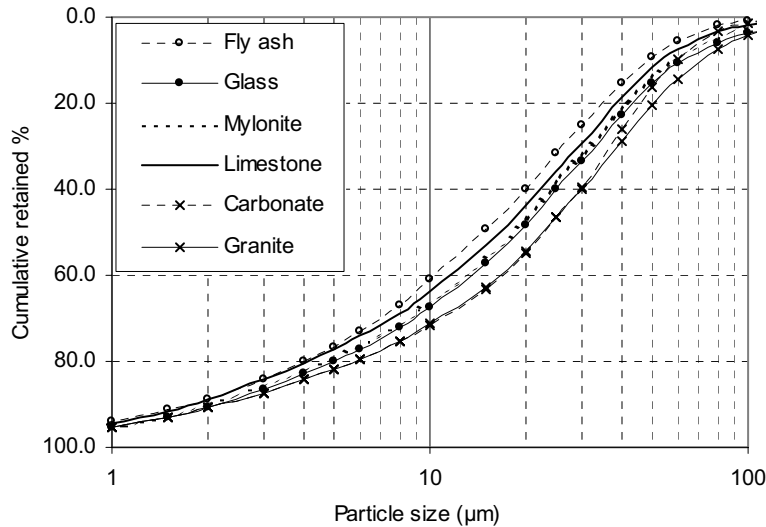


Figure 7.4. Total grading curves, including both cement and addition of 34 volume % of 0-125 fillers (addition in % of cement volume).

The granite filler, which gave the lowest flow resistance ratio at all tested addition levels, has the coarsest grading curve in combinations with cement as can be seen in Figure 7.4. On the other hand, the fly ash, which gave the highest flow resistance ratio, has the finest grading. However, there are some striking points regarding the correlation between grading and flow resistance ratio to be pointed at. The total grading curve of limestone/cement is only slightly different from the fly ash/cement curve, while the limestone filler gave a much lower flow resistance ratio than the fly ash. This indicates that other properties than particle size distribution is of importance, as could be expected. Further, there is a striking difference in particle size distribution between the carbonate filler and the limestone filler. These fillers, both being pure calcite fillers, gave equal flow resistance ratios at all tested levels, despite the difference in grading between them. This indicates that the straighter grading of the limestone/cement curve is more favourable than the grading curve of the carbonate/cement system.

An earlier study by Skjølsvold & Pedersen (1997) has indicated a strong influence from the specific surface area on the flow resistance ratio. Calculations of specific surface area based on grading curves involve some amount of uncertainty. The method used in this study (SediGraph), assumes spherical shape of all the particles, while the real shape of the particles may differ a lot from perfect spheres. Additionally, the detection of the finest parts of the curve, which is the most difficult part to measure, gives a very strong influence on the calculated surface area. In the present study, the correlation between the calculated surface area of the fillers and the corresponding plastic viscosity was rather weak.

Billberg (1999) found that the median particle size (D_{50}) may serve as a good indicator of the fineness, and he found a general dependence on both yield stress and plastic viscosity from the D_{50} . This was based on studies on limestone fillers of varying grading. He found both the yield stress and the plastic viscosity to increase with a decrease in D_{50} . It could, however, not be expected that it possible to predict the effect of different fillers on the rheological properties based on the single parameter characterisation D_{50} . It is obvious that also surface chemical effects caused by different mineralogy is of great importance. Additionally, the total grading curve of the filler is obviously important. Generally, the total grading curves, like those presented in Figure 7.4, are expected to be of importance. The influence of the grading curve is probably higher at lower w/c ratios and higher filler addition levels due to the increase in particle concentration.

In the following, the flow resistance ratio is plotted versus the D_{50} . Based on the above discussion, it was not expected to the author to be a straightforward correlation between the rheological properties and the D_{50} . However, such plots may be convenient as a basis to sort out the effects caused by other characteristics than the D_{50} .

In Figure 7.5, the flow resistance ratio is plotted versus the median particle size for matrix mixes containing equal amounts of filler on a volume basis. Limestone fillers of three varying gradings have been included in the plot in addition to the 0-125 fillers presented previously.

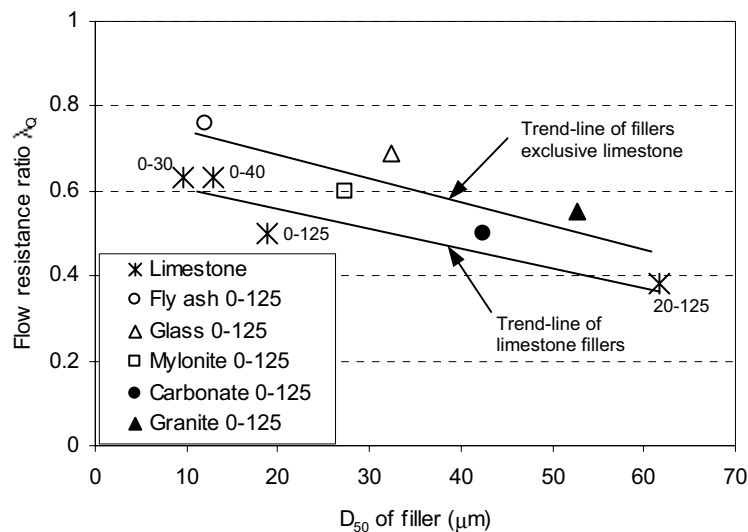


Figure 7.5. Flow resistance ratio versus D_{50} of fillers. w/c ratio = 0.5, 34 volume % filler. The Amount of SSP 2000 was 1.63 volume % of total powder amount for all mixes.

If the results are evaluated relative to the trend line, then it appears that the limestone filler gave significantly lower flow resistance ratio than the fineness should indicate. Thus, mineralogy of limestone, possibly in combination with effects of shape and roughness, appears to be favourable. This positive effect of limestone is known from the literature (Danielsen & Wallevik 1989). It should also be noted that the fly ash gave a surprisingly high flow resistance ratio, since fly ash is generally regarded to increase the workability of concrete when replacing cement. The effects caused by differences in mineralogy are believed to be sensitive to differences in the type and dosage of plasticizer. This aspect will be treated further in Section 7.2.5.

7.2.3 Influence of fillers on the plastic viscosity and the yield stress

7.2.3.1 General

The parameter study performed by the Physica rheometer is presented in the following sections. For details of the Physica instrument and the methodology of testing, see Chapter 5, Section 5.2.6.3. An outline of the test programme is presented in Section 5.4.8. Most of the results within this parameter study will only be presented graphically in this chapter. All results are given in tabulated form in Appendix C2.

7.2.3.2 Influence of different filler types

A plot of the effects of the tested fillers at a w/c ratio of 0.4 and 34 volume % added filler is presented in Figure 7.6. The range in both yield stress and plastic viscosity is large, showing that the rheological behaviour strongly depends of the type of filler. The ranking of fillers in terms of the effect on the plastic viscosity is basically equal to the ranking in flow resistance ratio obtained by the FlowCyl testing; this may be seen by comparing the results shown in Figure 7.6 with the results shown in Figure 7.2. However, the carbonate filler caused a significantly lower plastic viscosity compared to the limestone filler, while the FlowCyl results indicated no difference in flow resistance ratio between these two fillers. The carbonate filler also gave a significantly lower yield stress compared to the limestone filler. Note that the w/c ratio of the matrices plotted in Figure 7.6 was 0.4, while the matrices tested by the FlowCyl with equal filler amount (34 %) had a w/c ratio of 0.5. A possible explanation for the different behaviour at w/c ratio of 0.4 compared to 0.5, might be that the effect of particles being close to perfect spheres, as is the case for the carbonate filler due to its origin as chemically precipitated filler, is more important at lower w/c ratios due to the higher particle concentration.

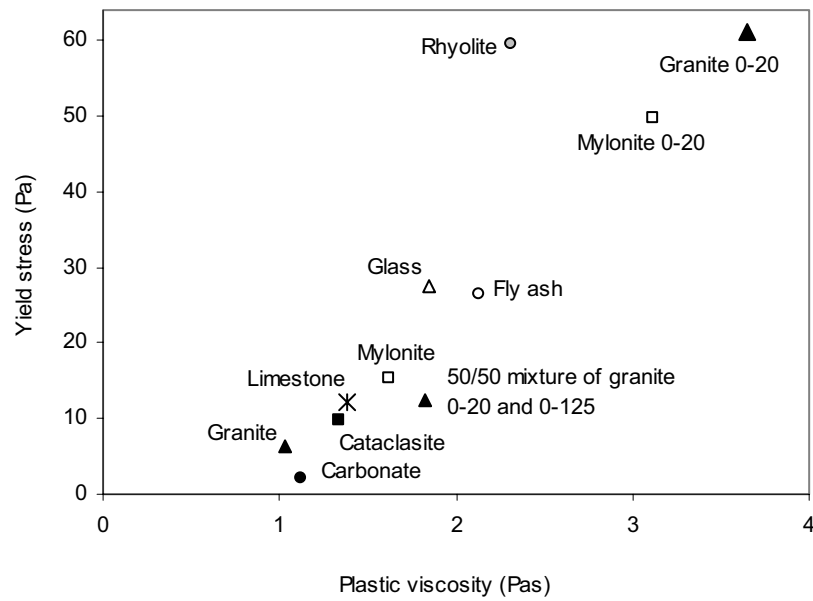


Figure 7.6. Rheological properties of matrices with $w/c=0.4$ and 34 % added filler (by the cement volume). Addition of 0.8 % SSP 2000 (by weight of cement) for all mixes. The fillers marked 0-20 consisted of particles below 20 μm , the others were 0- 125 μm fillers.

In Figure 7.7 and Figure 7.8, the plastic viscosity and the yield stress are plotted versus the median particle size of the fillers.

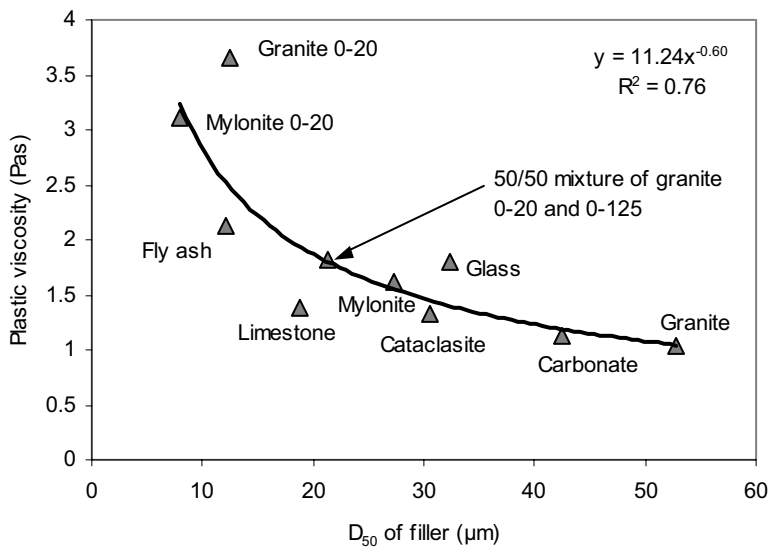


Figure 7.7. Plastic viscosity as a function of the median particle size (D_{50}) of the fillers. w/c -ratio= 0.4, 34 volume % of filler. All fillers utilized as 0-125 fractions, except those marked 0-20.

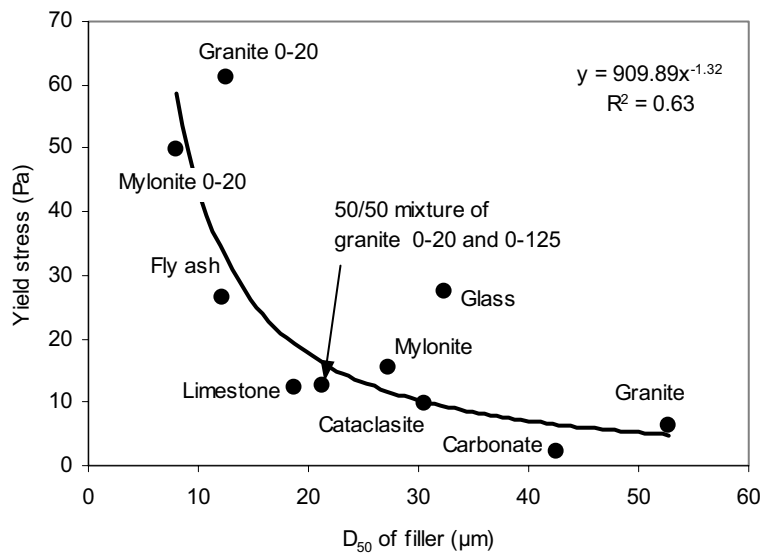


Figure 7.8. Yield stress as a function of the median particle size (D_{50}) of the fillers. w/c -ratio= 0.4, 34 volume % of filler. All fillers utilized as 0-125 fractions, except those marked 0-20.

The general trend is an increase in plastic viscosity with decreasing median particle size (see Figure 7.7). Likewise, the general trend is an increase in yield stress with decreasing median particle size (see Figure 7.8).

The higher value of plastic viscosity and yield stress of the matrix with mylonite filler compared to the matrix with granite filler may to a great extent be explained by the finer grading of the granite filler. The fact that the mylonite filler is crushed, while the granite filler is of glaciofluvial origin may also be of some importance. However, a study by Skjølvold & Pedersen (1997) has shown that the difference in shape and surface texture between the glaciofluvial granite filler and the crushed mylonite filler is limited. The amount of mica was in the same order for these fillers. According to Danielsen & Wallevik (1989), mica has a negative effect in concrete, as it reduces the workability. They further reported weathered mica to be less deleterious with respect to workability. The weathering of the mica in the glaciofluvial granite filler may consequently be of importance for the low values of plastic viscosity and yield stress obtained for matrices containing this filler.

The observed difference in plastic viscosity and yield stress between the matrices containing cataclasite filler and mylonite filler may not be explained by difference in grading, as the grading of these fillers are rather close to each other. The difference in mineralogy may explain the difference in rheological properties. According to the semi-quantitative analysis presented in Table 4.14, the cataclasite filler contains no mica, while the amount of mica is between 5 and 8 % for the mylonite filler.

Note the very high values of plastic viscosity and yield stress obtained in the matrices containing mylonite 0-20 and granite 0-20 filler, apparently caused by the very high surface areas of these fine fillers. The combination of granite 0-20 with granite 0-125 gave considerably lower yield stress and plastic viscosity. The rhyolite 0-125 filler resulted in high yield stress relative to the other 0-125 fillers. The rhyolite filler is unusual for concrete purposes, and contains some amounts of alteration minerals like zeolite and smectite. The amount of particles of colloidal size is relatively high compared to the other fillers, a fact that might partly explain the high yield stress.

A noteworthy fact from Figure 7.6 is that the granite 0-20 gave higher plastic viscosity and yield stress compared to the mylonite 0-20 filler, in contrast to the results for the coarser 0-125 as discussed above. Due to the finer grading of the mylonite 0-20 filler compared to the granite 0-20 filler, this was unexpected and is difficult to explain based on the physical and mineralogical characteristic.

The fly ash generated high values of plastic viscosity and yield stress. As discussed in Section 7.2.2.3, this was unexpected since fly ash is generally considered to be very beneficial to improve the workability. But compared to the (0-20) fillers of granite and mylonite, the values of yield stress and plastic viscosity for the fly ash matrix were low. The high value of yield stress obtained for the mix containing glass filler, relative to the D_{50} of this filler, is noteworthy. The yield stress was in the same

range as the value obtained by fly ash, in spite of the large difference in particle size distribution between the glass filler and the fly ash.

7.2.3.3 Replacement of cement by filler

Normally, filler will be added to the concrete to increase the matrix volume and/or to increase the stability. The replacement of cement by filler may not be a very common practice. However, when speaking of SCC, it may be of relevance to know the rheological effects caused by filler compared to the effects by cement since rather high amounts of filler may be used. In addition, it may be highly useful when designing new cement types. The general trend in the cement business is a large reduction in the amount of cement clinker, which must be replaced by materials such as slag, fly ash, limestone filler or other inert or pozzolanic materials.

Results of seven of the fillers presented in Figure 7.6 are shown graphically in Figure 7.9, as the starting points of each arrow. The end points of each arrow show the rheological parameters caused by the same filler at an equal w/p-ratio (on a volume basis) at a w/c ratio of 0.5. This means that filler replaced an equal volume of cement when going in the arrow's direction.

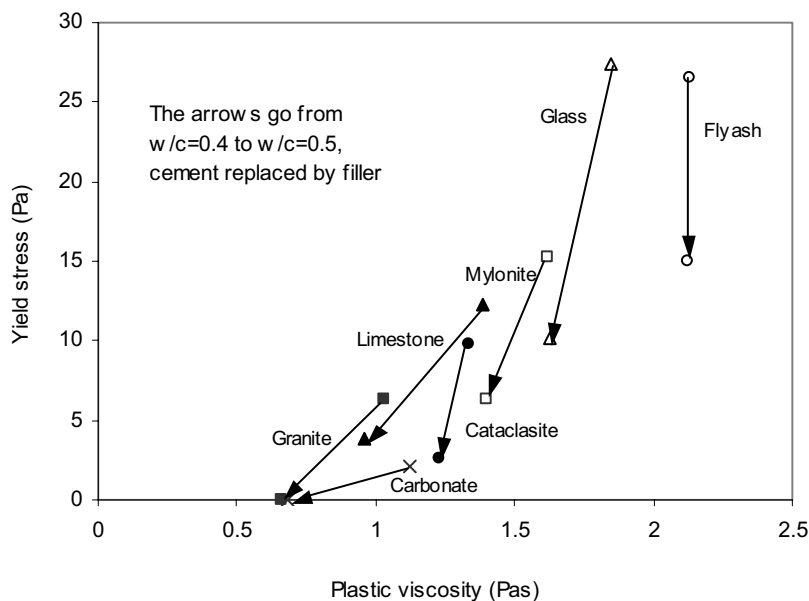


Figure 7.9. Effect of replacing cement with filler. The arrows go from w/c=0.4, 34 % filler, to w/c = 0.5, 67 % of filler. Addition of SSP 2000 was 0.8 % at w/c=0.4 and 1.0 % at w/c = 0.5, giving the same amount of plasticizer per volume powder for all the mixes. Note that the particle concentration (by volume) was identical for all mixes at both w/c ratios.

The replacement of cement by fillers, as showed in Figure 7.9, was generally effective in reducing the yield stress as well as the plastic viscosity of the matrices. This was an expected effect for all the fillers with higher median particle size than the cement, i.e. all the fillers in Figure 7.9 except the fly ash. The fly ash gave a different kind of performance, as it did not significantly change the plastic viscosity of the matrix when replacing the cement. Based on the present results, fillers in general tend to reduce the yield stress when replacing cement.

7.2.4 Influence of different types and amounts of plasticizers on the rheological properties of the matrix

In Figure 7.10, the effect of different types and addition levels of plasticizers are shown. The co-polymers showed a high effect in reducing the yield stress compared to the naphthalene and lignosulphonate, as also observed by Maedler and Kusterle (1999) in mortar. For the given matrix mix design, the yield stress was practically zero at a dosage of 0.8 % for all the tested co-polymers, while the values for the naphthalene-based plasticizer was somewhat higher. The different effects of a co-polymer and a naphthalene are, however, believed to be dependent on the type of cement, type of filler, particle concentration etc, this will be discussed in section 7.2.5. Even though all the tested co-polymers showed more or less equal behaviour with respect to yield stress, there was nearly a three-fold difference in the effect on plastic viscosity. The significance for practical applications, like for instance SCC, from the observed differences in plastic viscosity, could be expected to be large, especially in terms of resistance to segregation and bleeding.

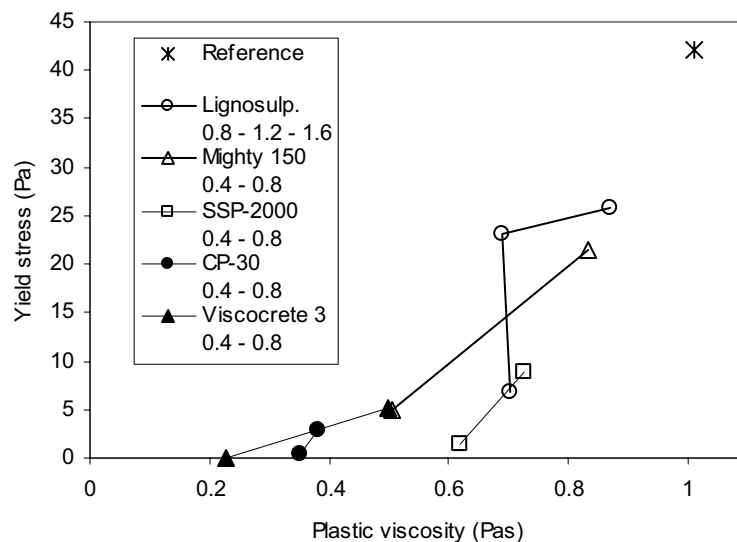


Figure 7.10. Effect of different types of plasticizers on the rheological properties of the matrix. $w/c = 0.5$, 30 weight % mylonite filler for all mixes. Amount of plasticizer is given in weight % of cement.

7.2.5 Combined effects of fillers and plasticizers on the rheological properties of the matrix

The effects of fillers presented earlier in this chapter are strictly speaking only valid for one type of plasticizer (SSP 2000), and in combination with one type of cement (OPC). As have been presented in Figure 7.10, there are great variations with respect to the efficiency of the different types of plasticizers. While the new generation of plasticizers, the so-called co-polymers, are said to basically rely on steric hindrance, the mechanisms of the highly efficient Mighty 150 is based on electrostatic repulsion. In the following sections, a study aiming to look into the combined effects, or the interaction effects, between plasticizer and filler is reported.

In Figure 7.11, the combined effect of the filler type and the type of plasticizer is shown. The co-polymer (SSP 2000) gave significantly lower yield stresses for all the mixes. However, the effect regarding plastic viscosity was not consistent. For the mixes containing fly ash and mylonite filler, there was no significant effect on plastic viscosity, while the effect was an increase in plastic viscosity for the mixes with granite, limestone and glass filler.

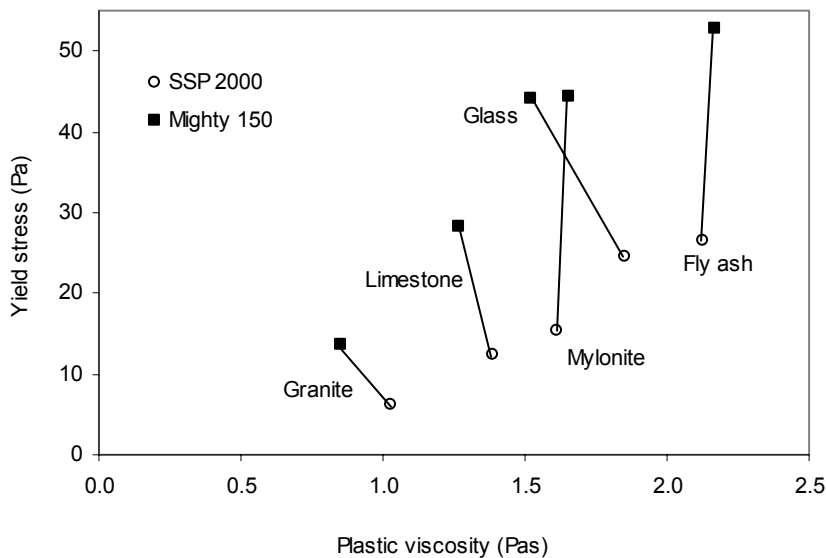


Figure 7.11. Plastic viscosity as a function of filler type and type of plasticizer. OPC, $w/c=0.4$, 34 volume % filler, 0.8 % plasticizer.

The effect of replacing some part of cement with an equal volume of filler has already been demonstrated, see Figure 7.9. This effect is demonstrated in Figure 7.12 for mylonite and limestone filler, also introducing the type of plasticizer as a new parameter. There was no distinct difference in the effect on plastic viscosity; the

tendency is rather that the results involving Mighty 150 and SSP 2000 were very close to each other. On the other hand, there can be observed a distinct interaction effect between the type of filler and the type of plasticizer regarding the yield stress. The yield stress values of the corresponding mylonite and limestone mixes were rather close to each other with addition of SSP 2000, while the differences were distinct when Mighty 150 was used as plasticizer. The difference was clearest at a w/c-ratio of 0.5, which means at the highest addition level of filler.

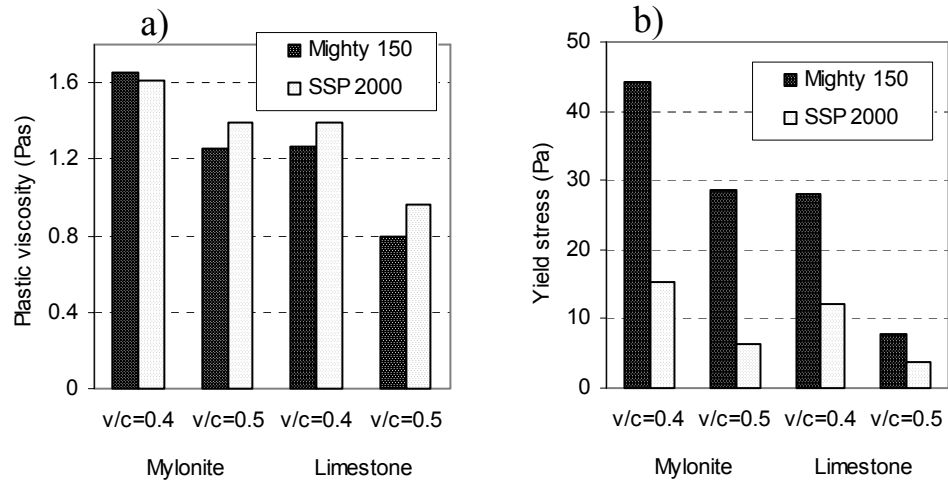


Figure 7.12 a) and b) The combined effect of replacing cement by filler and change in type of plasticizer for two different fillers. 34 volume % filler for the mixes with w/c = 0.4, and 67 % for the mixes with w/c = 0.5. Addition of SSP 2000 was 0.8 % at w/c=0.4 and 1.0 % at w/c = 0.5, giving the same amount of plasticizer per volume powder for all the mixes. Note that the particle concentration (by volume) was equal for all mixes at both w/c ratios.

Figure 7.13 a and b presents the effect of increasing the filler concentration at a constant w/c-ratio of 0.5. The plastic viscosity increased as the filler concentration increased for all combinations. The difference between the two plasticizers was not very marked with respect to plastic viscosity for any of the mix combinations. However, the Mighty 150 gave a slightly lower plastic viscosity than the SSP 2000 at the highest addition levels of filler, while there were no significant differences at the lower addition levels.

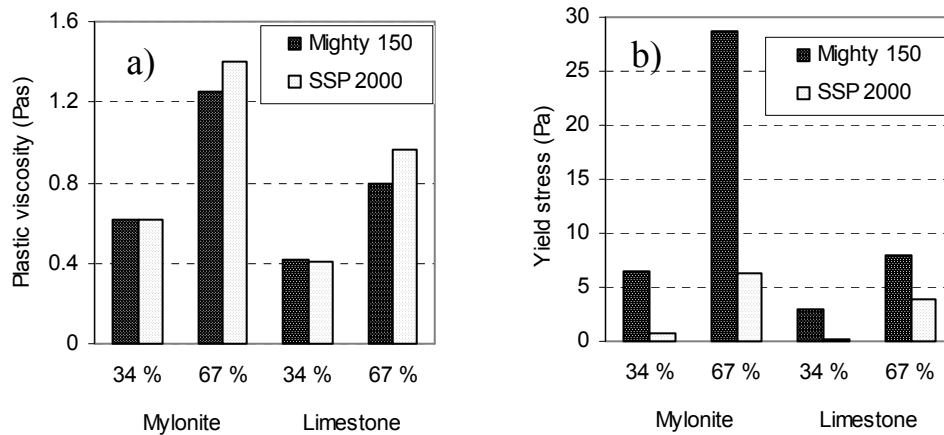


Figure 7.13. a) and b) The combined effect of adding filler and changing the type of plasticizer for two different fillers. The addition of SSP 2000 was 0.8 % at 33.6 % filler and 1.0 % at 67.2 % filler, giving the same amount of plasticizer per volume powder for all the mixes. The w/c ratio was 0.5 for all mixes.

The highest dosage of mylonite filler gave a significantly higher yield stress than the equal mix with limestone filler while Mighty 150 was used, while the difference was rather small when SSP 2000 was used. This indicates a high degree of interaction effect between the type of filler, the filler concentration and the type of plasticizer. It may be concluded that the combination of Mighty 150 and limestone filler is beneficial in reducing the yield stress, while the combination of Mighty 150 and mylonite filler is less beneficial.

In general, the SSP 2000 seems to be very effective in reducing the yield stress compared to Mighty 150. On the other hand, the effects on plastic viscosity are more or less equal for the two plasticizers. In addition, SSP 2000 seems to reduce the differences in yield stress between matrices with low and high filler amount, as well as differences between different types of fillers. This means that the effect of SSP 2000 is less sensitive to changes in filler type and filler concentration than the effect of Mighty 150.

7.2.6 Combined effects of cements and plasticizers on the rheological properties of the matrix

A few examples of the impact of the type of cement and plasticizer are presented below. Figure 7.14 a) and b) gives a graphical presentation of the combined effect of changing the type of cement and the type of plasticizer. All the three cements are ordinary Portland cements, but differ in chemical composition and fineness. See Section 5.3.1 for details of the physical and chemical properties.

When changing from OPC to HSOPC, a distinct interaction effect between the cement and the plasticizer can be seen. A change from OPC to HSOPC gave a decrease in both the plastic viscosity and yield stress with SSP 2000 as plasticizer. The opposite effect, i.e. an increase in both plastic viscosity and yield stress, can be observed with Mighty 150 as plasticizer. The mix with ROPC and Mighty 150 was too stiff to be tested by the Physica rheometer. It may be concluded that Mighty 150 is less favourable in combination with HSOPC than in combination with OPS, while the situation is the opposite for SSP 2000.

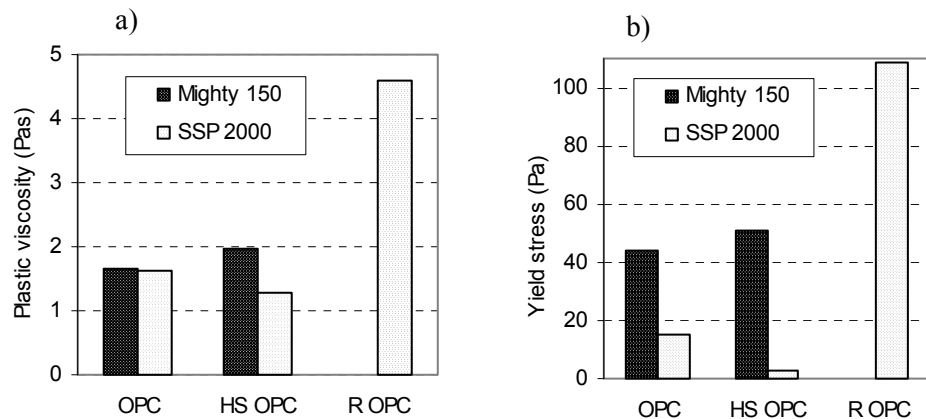


Figure 7.14 a) and b). Plastic viscosity and yield stress for matrices with OPC, HSOPC and ROPC. $w/c = 0.4$, 34 volume % mylonite filler and 0.8 weight % plasticizer all mixes. The mix with ROPC and Mighty 150 was too stiff to be tested.

7.3 Correlation between the rheological properties of SCC and the corresponding matrix phase

7.3.1 Introduction

So far in this chapter, the influence of different constituents that have been presented, were obtained by rheological characterisation of the matrix phase only. This kind of testing is particularly valuable to study the effects of different constituents of the matrix phase, and the interactions effects between the constituents. However, to gain full utilization of the matrix results, there is a need to establish the relationship between the rheological properties of the matrix phase and the rheological properties of the concrete. The particle matrix model gives a general relationship between the properties of the matrix phase and the concrete. However, some of the limitations of the particle matrix model discussed in Section 7.1 and Section 3.6.3 have raised the need for a better characterisation of the matrix phase than given by the flow resistance ratio. A set of experiments of effects of different

constituents characterised by the fundamental parameters yield stress and plastic viscosity has already been reported. In the following sections, a study of ten series of self-compacting concretes and their corresponding matrices is reported. Both concretes and matrices were tested by viscometers to get the fundamental rheological values yield stress and plastic viscosity. Additionally, the self-compacting concretes were tested using the empirical slump-flow measure. All matrices were also characterised using the FlowCyl viscometer, giving the flow resistance ratios. The aim of this study was basically to investigate if the characterisation of the matrices by the Physica rheometer was suitable as input to predict the behaviour of SCC. In particular, it was important to investigate the hypothesis that the yield stress of the matrix is an important controlling parameter. This study has involved ten series of SCC with three or four matrix volumes in each series. A total of 38 concrete mixes are included in the study.

Note that the grading of the aggregates was kept constant for all concretes, meaning that all the observed differences in concrete rheology was due to either the matrix composition or the matrix volume. The matrix volume varied throughout the test programme; consequently the volume of the aggregate varied correspondingly. This causes a minor variation of aggregate fines contributing to the matrix volume. This effect has been minimised by using the average matrix volume within the series. The total effect of the resulting variation in filler amount is believed to be small compared to other possible sources of error. It should be noted that the total grading of mix 7-10 differed some from the grading of mix 1-6 due to differences in the 8-11 mm fractions, this may be seen in Appendix A5 where the details in mix design are given. This difference may have contributed to some of the scatter of the results, but is probably of relatively low significance. It should also be noted that cement of the batch of OPC used in the SCC mixes nr. 7 and 8 was not available at the time the matrices corresponding to these concretes were tested. Consequently, OPC from a different batch (of the same type of cement produced at the same plant) was used when the rheological properties of the matrices were tested. This might also have contributed to some of the scatter of the results. However, the fineness (Blaine) was identical for these two batches of cement, and the difference in rheological properties is believed to be small.

The matrices were designed to cover a wide range of rheological properties in order to give large variations in the matrix volumes necessary to reach self-compacting concrete (here defined as slump-flow 650 mm or larger). This was achieved using different types of cement and varying water/cement ratios. Filler and silica fume was added to most of the concrete mixes, see Table 7.1 for information regarding mix design of the concretes. Emphasis was laid on designing concretes being sufficiently stable, and all the concrete series were stable at the normal self compacting criteria of 650 mm slump flow.

The most relevant results of the examinations of the self-compacting concretes and their corresponding matrices are shown in Table 7.1. A more comprehensive list of the results, also including parameters such as air content and 28 days compressive

strength, is given in Appendix C3. An outline of the test programme is given in Chapter 5; see Section 5.4.8.

Table 7.1. Results of the rheological properties of concrete and matrix.

Mix design of concretes						Rheology of concrete			Rheology of matrix			Series nr.
Cement	w/b w/p	Filler	Silica-fume	Plasti-cizer	Matrix vol. (l)	τ_0 (Pa)	μ (Pas)	SF (mm)	τ_0 (Pa)	μ (Pas)	λ_0	
HSOPC	0.40 0.30	20 % limest.	5 %	1.0 % CP30	325	53.2	57.9	550	3.9	0.88	0.74	1
					340	9.6	19.4	740				
					355	4.6	15.9	765				
HSOPC	0.40 0.30	20 % mylon.	5 %	1.0 % CP30	325	193.9	36.5	540	4.6	1.00	0.78	2
					340	31.8	37.2	635				
					355	24.5	25.2	660				
					370	4.0	15.9	760				
ROPC	0.50 0.37	20 % limest.	5 %	1.0 % CP30	355	38.7	17.7	540	8.8	0.70	0.60	3
					370	23.3	14.1	650				
					385	14.8	10.1	640				
					400	9.5	7.3	670				
ROPC	0.50 0.37	20 % mylon.	5 %	1.0 % CP30	355	52.3	20.2	535	9.5	0.81	0.63	4
					370	23.0	14.5	620				
					385	16.8	10.5	660				
					400	15.1	8.3	680				
OPC	0.5 0.37	20 % limest.	5 %	1.0 % CP30	325	58.1	38.7	435	2.0	0.38	0.45	5
					340	23.1	21.5	615				
					355	13.3	11.6	675				
					370	22.9	7.6	760				
OPC	0.50 0.37	20 % mylon.	5 %	1.0 % CP30	325	77.2	36.9	480	3.8	0.47	0.49	6
					340	33.9	22.8	580				
					355	18.2	14.5	670				
					370	10.0	7.9	750				
OPC*	0.60 0.32	60 % limest.	0	1.2 % SSP2000	340	289.0	46.6	470	5.6	0.71	0.73	7
					350	143.6	30.4	570				
					360	94.8	25.5	615				
					370	26.5	21.8	670				
OPC*	0.40 0.35	0 %	0	1.0 % SSP2000	340	113.0	44.6	440	10.7	0.85	0.82	8
					360	65.0	29.7	518				
					380	59.0	21.3	580				
					400	23.0	17.0	650				
SROPC*	0.50 0.36	15 % limest.	5 %	0.7 % CP30	310	56.8	21.3	540	0.5	0.32	0.49	9
					325	32.7	12.6	670				
					340	2.5	7.5	715				
ROPC*	0.50 0.42	0 %	5 %	1.0 % CP 30	325	48.6	16.6	540	6.0	0.35	0.51	10
					340	26.8	11.5	600				
					355	18.6	8.2	620				
					370	13.7	6.4	670				

*Results of rheological properties of concrete from a national SCC project, see Section 5.4.8.

7.3.2 Rheological properties of SCC

An increased matrix volume gave a unique increase in slump-flow within each series, with one exception in the series with rapid OPC and limestone filler; see the plotted results in Figure 7.15. This unexpected result is believed to be due to an experimental error. There is a great span in curvatures between the result of the 10 series, and generally the ones with lower initial matrix volumes have steeper curves in the matrix volume – slump-flow diagram. This is in totally in agreement with the particle-matrix model.

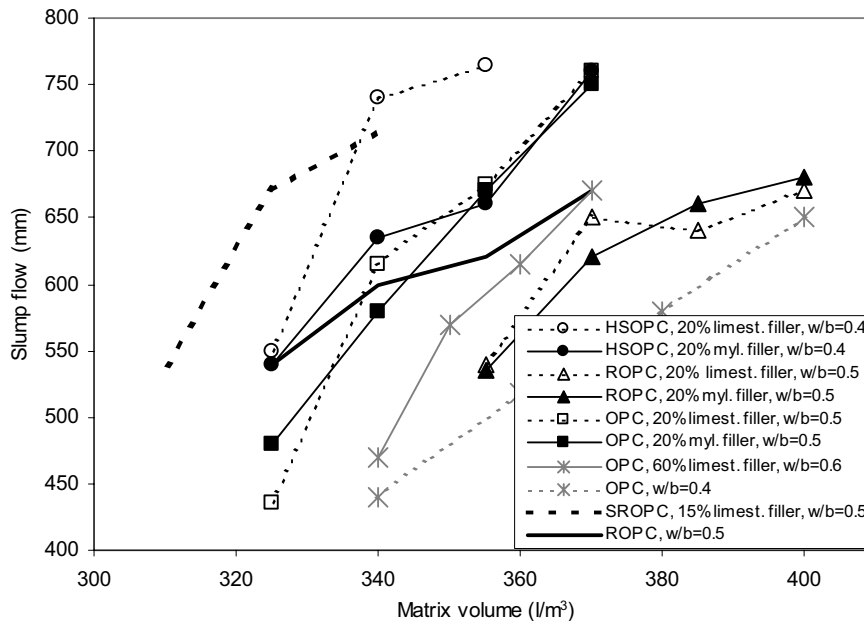


Figure 7.15. Slump-flow depending on matrix volume, type of cement, type of filler and w/b-ratio.

Plots of yield stress and plastic viscosity are presented in Figure 7.16 and Figure 7.17, respectively. An increased matrix volume gave a decrease in both the yield stress and the plastic viscosity within each series. Generally, the behaviour of the concretes being self-compacting (defined as a slump-flow of 650 mm or higher) was close to Newtonian, with yield stresses below 30 Pa. As the yield stress is a measure of the stress needed to initiate flow of the concrete, this was in agreement with the expectations.

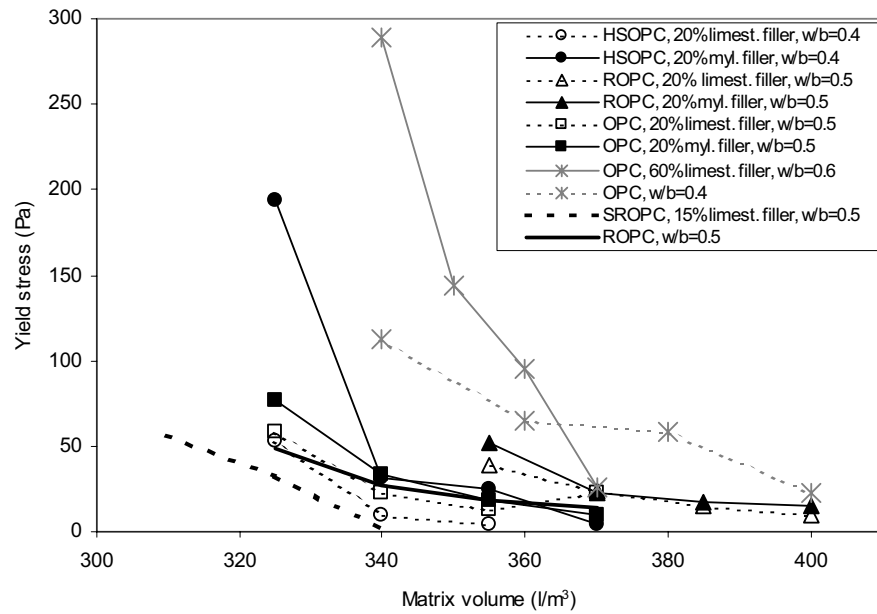


Figure 7.16. Yield stress depending on matrix volume, type of cement, type of filler and w/b-ratio.

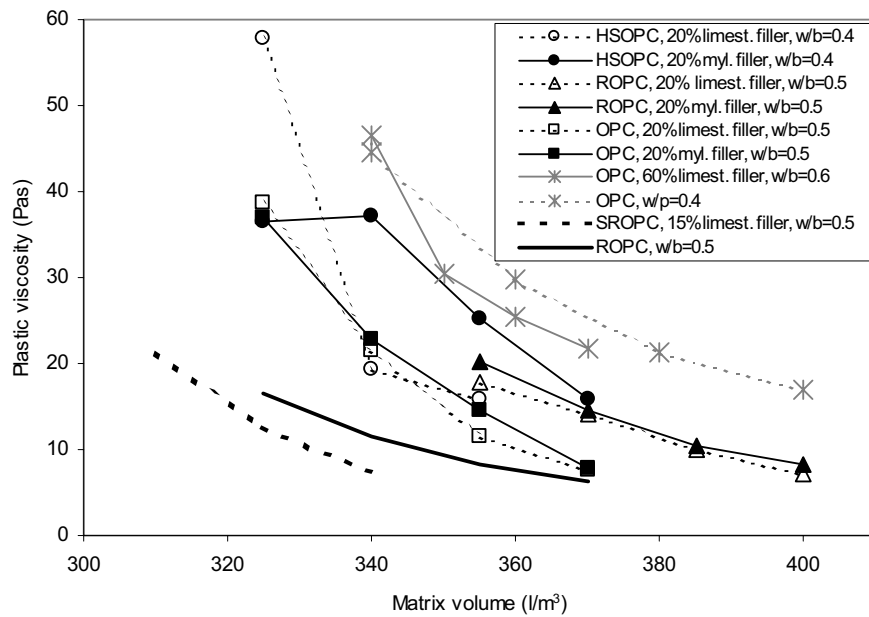


Figure 7.17. Plastic viscosity depending on on matrix volume, type of cement, type of filler and w/b-ratio.

An increased matrix volume gave a decrease in both yield stress and plastic viscosity within each series; see Figure 7.16 and Figure 7.17. The differences in yield stress were generally small at high matrix volumes, while the differences at low matrix volumes were more marked; see Figure 7.16. Based on these plots, it may be concluded that both plastic viscosity and yield stress influence the slump-flow measure. However, the correlations of slump flow versus plastic viscosity, and the correlation of slump flow versus yield stress are weak.

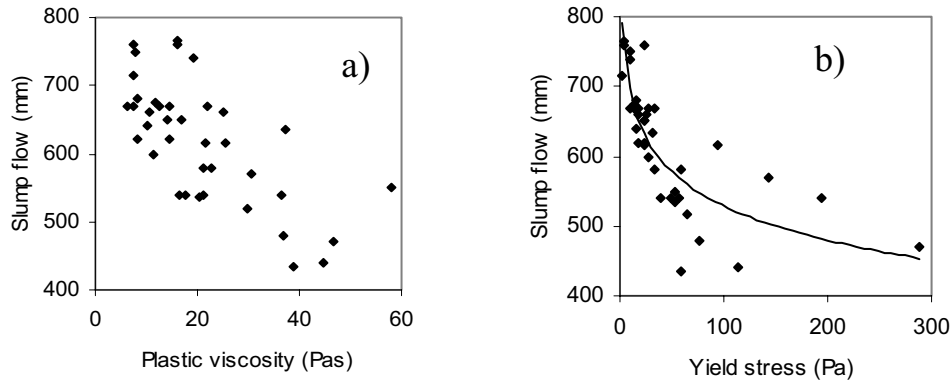


Figure 7.18. a) SF versus plastic viscosity. b) SF versus yield stress.

At slump-flow values below 600 mm, i.e. for concretes not being “self-compacting” the scatter was very high. Some mixes gave very high values of slump flow despite a yield stress above 100 Pa. It could have been expected that the plastic viscosity for these concretes reaching high slump flows despite the high yield stress were low to give a “compensation” for the high yield stress, but this was not the case. Based on the present results, it was not possible to model the slump flow in terms of the more fundamental rheological parameters yield stress and/or plastic viscosity. A major reason why this was not possible is believed to be due to the interaction between the flow table and the concrete. When measuring the slump flow of highly flowable mixes, there is only a thin layer of matrix holding the greater aggregates suspended as they slide across the table. The friction between the concrete and the flow table must consequently be of great importance compared to the pure material parameters expressed in terms of yield stress and plastic viscosity. It could be expected that the friction is greatly influenced by the coarse aggregates, and to what extent these are “floating” in the matrix or being “dragged” by it. This is believed to be mostly controlled by the stability of the SCC, a parameter that has not been quantified within the present study. It may be concluded that the slump-flow method does not reflect the rheological properties of SCC fully, and it is obvious that such a method has many limitations in describing the workability of SCC for practical purposes. However, the method is much in use due to its simplicity. When used with care, preferably in combination with a trained eye, it may give very useful information concerning workability of SCC. In addition, it is very useful in the production

control at the mixing plant, where sophisticated rheological measurements are not available.

The plastic viscosity of the concrete is believed to be of high importance when it comes to resistance against segregation of the larger particles. As expected, there seems to be a correlation between the velocity of the concrete front when it spreads over the table and the plastic viscosity of the concrete, see Figure 7.19.

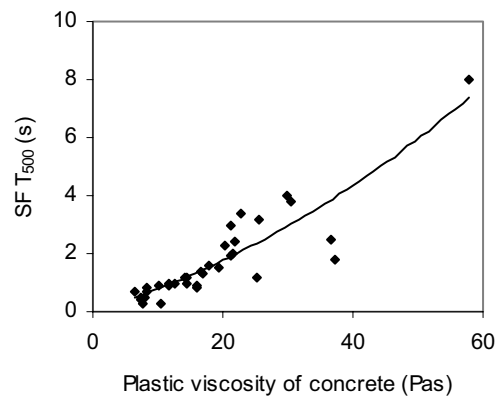


Figure 7.19. Correlation between SF-T₅₀₀ and plastic viscosity of the concrete.

The SF-T₅₀₀, which is the time needed to reach a spread diameter of 500 mm, is basically controlled by the plastic viscosity of the concrete. The SF-T₅₀₀ may then serve as an indicator of the plastic viscosity as confirmed in Figure 7.19. However, accurate measures of the values are difficult to obtain due to the low values of SF-T₅₀₀ for typical Norwegian SCCs, which are often below 2 seconds.

7.3.3 Influence of the constituent materials on the rheological properties of concrete

The major purpose of this study was to test the relationship between the rheological properties of concretes and matrices, respectively. However, some conclusions regarding the effects of the constituents in the SCCs can be drawn based on the concrete results and will be discussed in the following.

The influence of the type of cement was large. This can be observed in Figure 7.20. The original idea of the six concrete series presented in Figure 7.20 was to test all combinations of three different types of cement and two types of filler. A w/c-ratio of 0.5 was chosen for these mixes. The tests of matrices run prior to the concrete series did, however, indicate a need to lower the w/c-ratio for the mixes of the high

strength cement (HSOPC) in order to attain a sufficient stability of the matrix phase. The w/c-ratios of the two concrete series with HSOPC were therefore lowered to 0.4. Even at this lower w/c-ratio, the HSOPC resulted in a much higher slump-flow than the corresponding series with ROPC of equal matrix volume, and equal to, or higher than for the OPC series of equal matrix volume. The SCC series with SROPC, see Figure 7.15, also caused high slump-flows at low matrix volumes. The effect of the SROPC cannot be directly compared to the HSOPC due to the different w/c-ratios. Also note that the dosage of plasticizer was lower in the SROPC series than in the HSOPC series, see Table 7.1 for details.

The effect of changing from mylonite to limestone filler can also be observed in Figure 7.20. The differences were small and not significant for the OPC and ROPC concretes. However, the limestone filler gave a significantly higher slump-flow than the mylonite filler within the two series of HSOPC. The particle size distribution of the limestone filler is finer than for the mylonite filler. This gives evidence to that the mineralogy of the limestone is more favourable than the mineralogy of the mylonite filler, and is in agreement with the matrix investigations presented in Section 7.2.3, see Figure 7.6, where limestone filler gave lower values of both yield stress and plastic viscosity compared to mylonite filler.

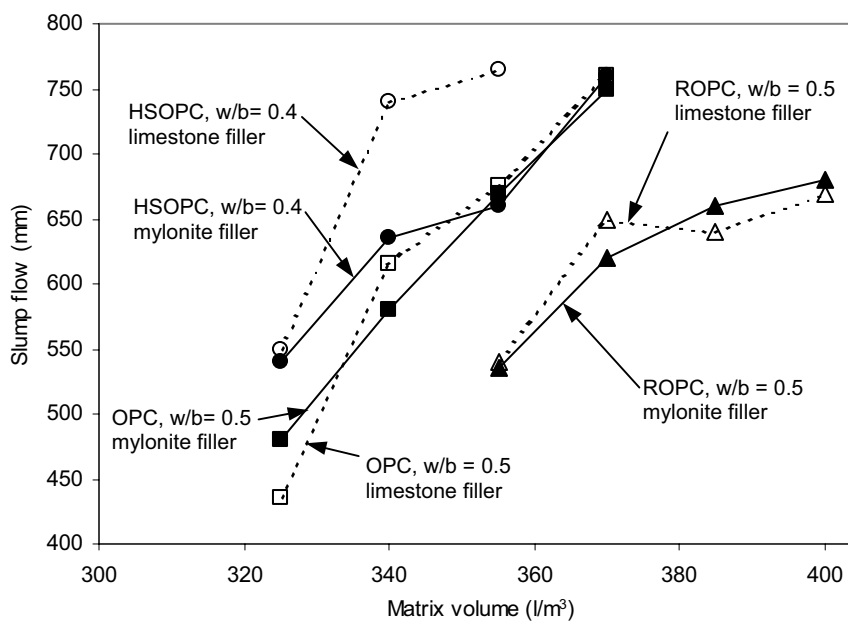


Figure 7.20. Effect of type of cement and type of filler on the rheological properties of concrete expressed as slump-flow. Limestone 0-125 (Norcem) filler and mylonite 0-125 filler.

The effect of changing the mix design within the series of ROPC, $w/b = 0.5$ and no additional filler, by adding 20 % limestone filler, can be observed in Figure 7.21. The addition of filler at a constant w/c -ratio and constant amount of plasticizer (based on the cement weight) gave a decrease in slump-flow for equal matrix volumes.

The effect of increasing the w/c -ratio from 0.4 to 0.6 for the series of OPC, replacing the cement by limestone filler, can also be observed in Figure 7.21. This change caused a significant increase in slump-flow for equal matrix volumes of the two mix designs. The w/p -ratio was lower in the series with 60 % filler addition; see details in Table 7.1. The amount of plasticizer was higher in the series with 60 % filler relative to the cement amount (1.2 % versus 1.0 % within the series with no filler), but significantly lower per m^3 concrete. The overall effect of replacing cement with limestone filler was an increase in slump-flow at equal matrix volume, and a lowering of the matrix volume needed to reach a specified limit of slump-flow. Both the SCC with OPC at a w/b -ratio of 0.4, as well as the concrete with w/v -ratio of 0.6 with 60 % addition of filler, gave appropriate stability. However, the stability of the SCC has not been quantified in this study.

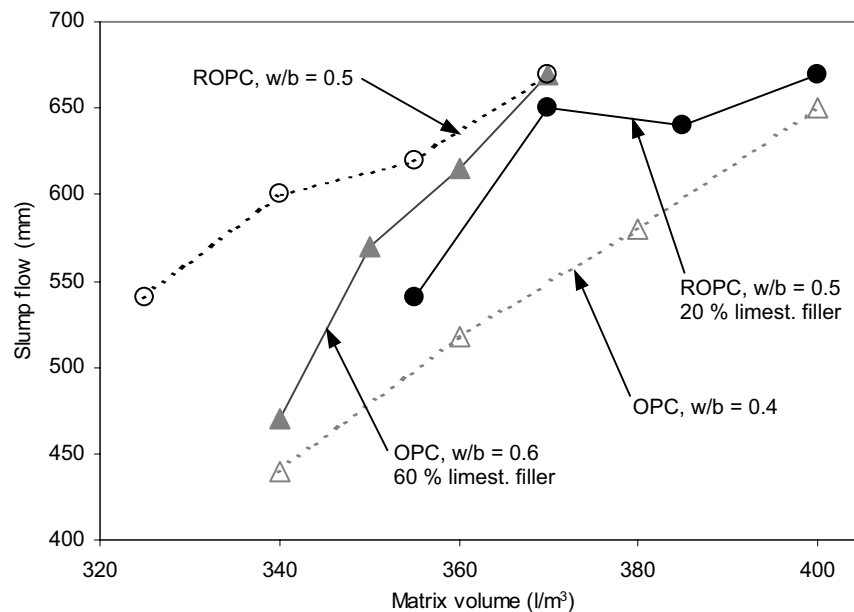


Figure 7.21. Effect of filler addition on the rheological properties of SCC, expressed as slump-flow. Limestone 0-125 (Norcem) filler.

7.3.4 Relationship between the rheological properties of concrete and matrix

At a constant composition and grading of the aggregates, the PM model predicts the matrix volume needed to reach a given workability to be a unique function of the matrix rheology. Mørtzell (1996) used the slump measure to describe the workability of ordinary vibrated concrete. In the same way, the slump-flow measure may be used as a measure of the workability of SCC. The fact that empirical one-parameter methods such as the slump measure for vibrated concrete, and the slump-flow measure for SCC, are not able to fully describe the rheological properties of concrete have already been discussed; see Section 3.2. Consequently, there is a need for a more fundamental characterisation of the fresh concrete. Rheological measurements performed by a concrete viscometer, e.g. the BML viscometer, is generally believed to give a more covering characterisation of the fresh concrete than the one-parameter empirical methods described above. As shown in the present study (see Section 7.3.2), there is no straightforward correlation between the slump-flow measure and the more fundamental rheological parameters yields stress and plastic viscosity. Measuring methods such as the BML viscometer are not available at the mixing plants, and we need simpler methods like slump-flow to rely on. Despite the limitations of the slump-flow measure, it is certainly useful for practical purposes, and it gives useful information regarding the workability of SCC. In the following, result of the correlation between concrete and matrix rheology are presented. The SCC was characterised both using the empirical slump-flow measure and the more fundamental characterisation by the BML viscometer.

In Figure 7.22 a) and b) and Figure 7.23, the matrix volume needed to reach the common self-compacting criteria of slump-flow equal to 650 mm is plotted versus the plastic viscosity, the yield stress and the flow resistance ratio of the matrix, respectively.

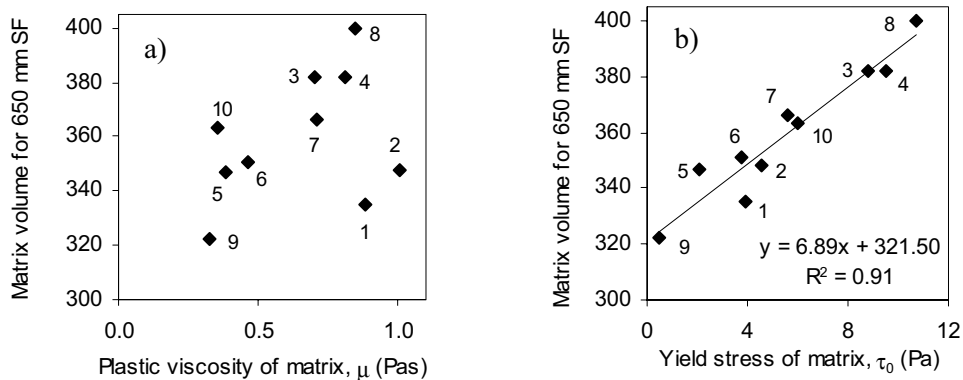


Figure 7.22. Matrix volume necessary to reach a slump flow of 650 mm versus plastic viscosity a) and yield stress b) in the matrix. Series numbers according to Table 7.1.

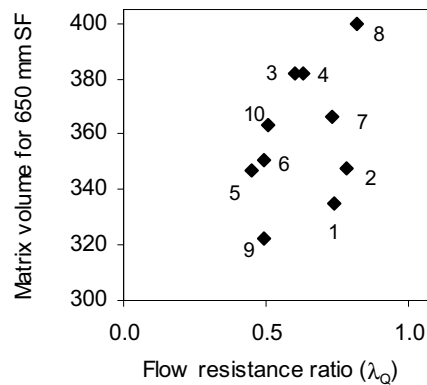


Figure 7.23. Matrix volume necessary to reach a slump flow of 650 mm versus flow resistance ratio. Series numbers according to Table 7.1.

As shown in Figure 7.22 b, the matrix volume needed to make the concrete self-compacting (using a criteria of slump-flow equal to 650 mm) was highly dependent on the yield stress of the matrix, with a correlation coefficient of 0.91. No obvious correlation is present in the plot of the matrix volume to reach a slump flow of 650 mm versus the plastic viscosity (see Figure 7.22 a, nor is it in the equivalent plot involving the flow resistance ratio (see Figure 7.23).

The direct correlation between the rheology of the matrix and the rheology of the concrete at a fixed matrix volume has been analysed. Seven of the ten concrete series within the present study has been measured at a matrix volume of exactly 355 litres, while values for two more concrete series have been obtained by interpolation. Plots of the correlation between the rheological parameters of the concretes and the corresponding matrices, at a matrix volume of 355 litres, are shown in Figure 7.24. Equally, the correlation between the rheological properties of the concrete and the corresponding matrix at a fixed matrix volume of 370 litres are plotted in Figure 7.25. The plastic viscosity of the matrix seems to have an influence on the plastic viscosity of the concrete, but the correlation is not very strong. The influence of the yield stress of the matrix on the concrete yield stress seems less obvious. Note that the change from 355 to 370 litres matrix volume had a much higher influence on the yield stress than on the plastic viscosity.

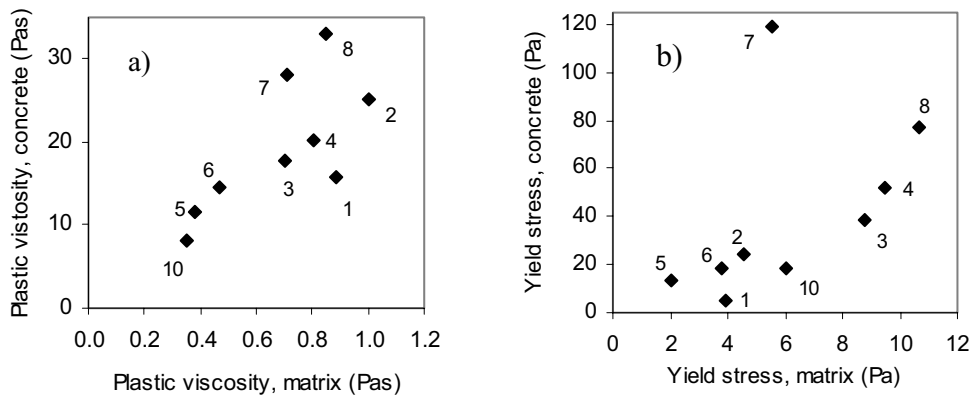


Figure 7.24 Correlation between a): plastic viscosity of concrete and corresponding matrix and b): yield stress of concrete and corresponding matrix. Fixed matrix volume of 355 litres/m³. Series numbers according to Table 7.1.

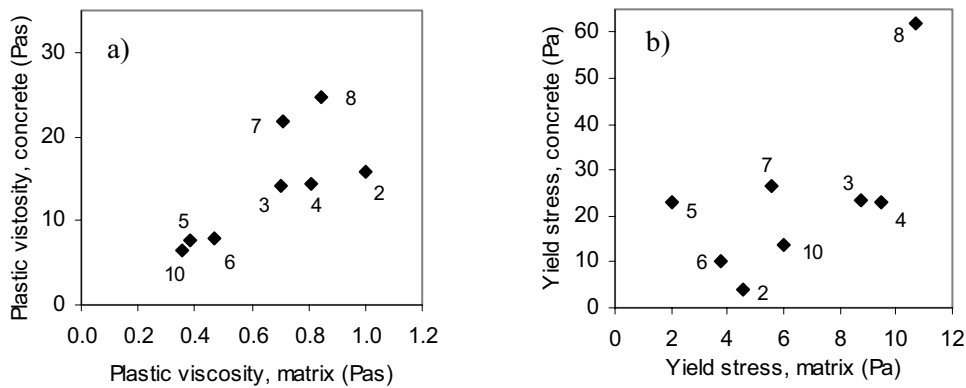


Figure 7.25 Correlation between a): plastic viscosity of concrete and corresponding matrix and b): yield stress of concrete and corresponding matrix. Fixed matrix volume of 370 litres/m³. Note the large difference between Figure 6.24 b and Figure 6.25 b regarding the scale on the ordinate (concrete yield stress). Series numbers according to Table 7.1.

Wallevik & Hammer (2003) studied the correlation between the rheological properties of mortar with two different matrix volumes and the corresponding matrix using the two different cement types OPC and HSOPC. Measurements were done at four different times (10, 40, 70 and 100 minutes). The correlation between the mortar yield stress and the matrix yield stress was strong within each series. As expected, the ratio of the yield stress in mortar and matrix ($\tau_{\text{mortar}}/\tau_{\text{matrix}}$) was much higher at the lowest matrix volume. Also the ratio between plastic viscosity in

mortar and matrix ($\mu_{\text{mortar}}/\mu_{\text{matrix}}$) was much higher at the lowest matrix volume. At the highest matrix volume (80 volume %), the correlation between mortar and matrix rheology was strong even when the results involving both OPC and HSOPC was plotted together. However, at the lowest matrix volume (60 volume %), the trend line of OPC results was far from the trend line of HSOPC results. This trend was evident both for yields stress, plastic viscosity, as well as for “gels strength”.

The results of Wallevik & Hammer (2003) basically agree with the results of the present study. Due to the much higher matrix volumes in the mortar series performed by Wallevik & Hammer (2003) than in the concretes performed within the present study, we would expect the correlation to be stronger in the mortar series. Even though it is obvious that the matrix rheology influences the concrete rheology much, there cannot be found any straightforward correlation between concrete and matrix rheology. There might be interaction effects between the matrix phase and the concrete phase that are not found by the characterization methods currently used.

7.3.5 Concluding discussion regarding the relationship between concrete and matrix rheology

The results of the present study have confirmed the basic principles of the PM model for self-compacting concrete. The workability of the concrete, in terms of the slump-flow measure, is a unique function of the matrix volume within each series of concrete. In addition, the yield stress of the matrix seems to be a very important parameter controlling the workability of the concrete. However, there has not been found any straightforward correlation between the fundamental rheological properties of concrete and matrix at a fixed matrix volume. Despite this, there seems to be a correlation between the fundamental matrix parameter yield stress and the empirical concrete parameter slump flow.

In the thesis of Mørtzell (1996), the workability of normal concrete, in terms of slump, was reported to be a unique function of the air voids space modulus of the aggregate, the flow resistance ratio of the matrix and their relative volume fraction. The results from the present study, together with the results of Smeplass & Mørtzell (2001), have indicated that the flow resistance ratio is insensitive to important properties of the matrix phase.

The yield stress of the matrix seems to be the most important matrix parameter to control the workability of SCC based on the present study. On the other hand, Mørtzell (1996) found the flow resistance ratio, a parameter being most influenced by the plastic viscosity, to be relevant as an input to describe the workability of ordinary vibrated concrete. Based on this, it may seem like SCC is more sensitive to small variations in the yield stress of the matrix phase than in vibrated concrete. From the study of Smeplass & Mørtzell (2001), and the present study, it is obvious that the cement type has a crucial influence on the concrete rheology. The present study has confirmed that the influence of the type of cement on the yield stress is

large. The HSOPC has given noteworthy low yield stresses compared to the other cements, especially related to the plastic viscosity of the matrix. This is illustrated in Figure 7.26, where the yield stress has been plotted versus the plastic viscosity. All numbers on the plot refer to the series numbers in Table 7.1. Note that the ratio between yield stress and plastic viscosity is relatively constant, when the matrices containing HSOPC are removed (series 1 and 2). It has been shown previously (see Figure 7.11) that the change from a naphthalene (Mighty 150) plasticizer to a copolymer (SSP 2000) may change the yield stress/plastic viscosity ratio considerably. It is likely that the ratio between the yield stress and the plastic viscosity did not vary much for the concrete series Mørtzell (1996) used to correlate the concrete rheology versus matrix rheology. This may explain some of the difference between the results of SCC in the present study and the results of ordinary concrete of Mørtzell (1996).

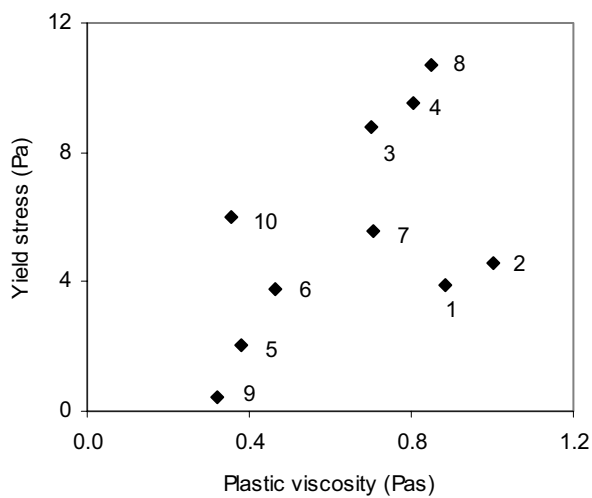


Figure 7.26. Relationship between plastic viscosity and yield stress of the matrices. The numbers refer to the series number; see full description of the mix design in Table 7.1

To conclude, it should be clear that the particle matrix model needs further development. Some problems related to the SCC have been highlighted in this work. But still, the testing of matrix rheology should be regarded highly useful. Especially, it is highly useful to investigate the effects of the different constituents in filler modified cement paste. The rheological behaviour of the matrix may be used to give an indication of the rheological behaviour of concrete. However, it is clear that the issue of the particle - matrix model is an uncharted domain relative to SCC, and some substantial work is required to better understand the interactions between the particles and the matrix for such systems. Such a work is out of scope of this thesis.

7.4 Summary and concluding discussion

The study has shown that the basic principles of the PM model are relevant also for self-compacting concrete. Testing of the rheological properties of the matrix should be considered useful to analyse the effects of different constituents on the rheological properties of concrete. However, the model has some limitations, especially when it comes to the characterisation of the matrix phase. A methodology to perform a more fundamental characterisation of the matrix phase than the FlowCyl gives has been developed in the present study. By using the Physica rheometer with a parallel plate configuration, it was possible to attain the rheological properties in terms of the fundamental parameters plastic viscosity and yield stress.

The relevance of the results obtained by the Physica rheometer has been verified through a study of the correlation between SCC and the corresponding matrix. This study has indicated that the yield stress of the matrix has a crucial influence in controlling the workability of the SCC, expressed as slump-flow, while the influence of the plastic viscosity is less obvious. This contradicts the results of Mørtzell (1996) for ordinary concrete. He found the workability of the concrete, in terms of slump, to be controlled by the flow resistance ratio, given that the aggregate grading was kept constant. In the present study, the flow resistance ratio was found to be directly correlated to the plastic viscosity. The yield stress seemed to have no, or very low, influence on the flow resistance ratio. Hence, the flow resistance ratio and the plastic viscosity are more or less equivalent measures. The observed difference between the study of Mørtzell (1996) and the present study may indicate that the yield stress of the matrix is more important in SCC than in ordinary concrete. However, it is also likely that the ratio between the yield stress and the plastic viscosity varied within a rather limited spectre in the study of Mørtzell (1996) compared to within the present study, a fact that might explain at least some of the difference.

The parameter studies performed on the matrix phase have shown great variations in effects of the different fillers. The particle size distribution of the fillers has been shown to be highly important. Finer fillers tend to induce higher plastic viscosity and yield stress than the coarser fillers. But surface effects related to different mineralogy are also highly important. In combination with OPC and SSP 2000, the limestone filler and the fly ash generated relatively low values of plastic viscosity and yield stress relative to their particle size distribution. The glass filler and the rhyolite filler generated, on the other hand, relatively high values of plastic viscosity and yield stress.

The co-polymer SSP 2000, which basic dispersion mechanism is believed to rely on steric hindrance, has been shown to be much more effective in reducing the yield stress compared to Mighty 150. Mighty 150 is a sulphonated naphthalene, and is believed to basically act as a dispersant by electrostatic repulsion. The SSP 2000 also seems to reduce the differences in yield stress between matrices with low and high filler amount, as well as differences between different types of fillers. This means that the effect of SSP 2000 is less sensitive to changes in filler type and filler

concentration than the effect of Mighty 150. Consequently, the dispersion agent based on steric hindrance seems to be more robust and less dependent on the surface chemistry of the mineral particles than the dispersion agent based on electrostatic repulsion.

Replacement of cement by filler is shown to be effective to reduce the yield stress of the matrix. This effect has also been confirmed in concrete for limestone filler.

A limited study of cements has shown that the great variations in concrete workability caused by the cement are reflected by the rheological properties of the matrix. The present study has also highlighted some interaction effects between cements, plasticizers and fillers. More research is needed within this area to in order to be able to choose the optimum combinations of cements, fillers and plasticizers.

8 Conclusions of the experimental work

8.1 Effects of fillers on the pozzolanic reactivity and alkali-silica reactivity

The pozzolanic reactivity of the 0-20 μm fractions of the fillers has been tested at a curing temperature of 20°C. The tested fillers can be divided into two distinct classes with respect to pozzolanity:

- The pozzolanic reactivity of fly ash, glass and rhyolite filler was distinct
- The pozzolanic reactivity of mylonite, cataclasite and quartz fillers was insignificant at the age of 28 days

The mylonite filler has also been tested at curing temperatures of 38°C and 80°C, corresponding to the temperatures used by the CPT and the AMBT, respectively. The difference in pozzolanic reactivity between 20°C and 38°C was very small. However, the pozzolanic reactivity at 80°C was significant. The pozzolanic reactivity for non-reactive granite/gneiss filler was identical to the reactivity of the mylonite filler at 80°C. It may be suggested that all fillers of rocks containing silica, whether well crystalline or not, will be more or less pozzolanic at such high temperatures as 80°C.

The effect of adding alkali-reactive filler to a reference concrete containing reactive coarse aggregate has been tested both using the CPT and the AMBT. Based on testing by the CPT, the fillers can be divided into two distinct classes:

- Fly ash, silica fume, glass filler and rhyolite filler significantly reduced the expansions compared to the reference concrete.
- Mylonite and cataclasite fillers had no effect or gave increased expansions compared to the reference concrete.

The effect of the particle size distribution was rather small. But the 0-20 fraction of mylonite filler gave higher expansions at all ages than the 0-125 fraction. The effect of reducing the particle size was the opposite for the rhyolite filler, as the 0-20 fraction gave lower expansion than the 0-125 fraction.

Micro structural analyses, using optical microscopy and electron probe micro analyser, have given additional information regarding the performance of glass filler, mylonite filler and rhyolite filler. The results obtained from the micro structural analyses have confirmed that the judgment of the effect of these fillers based on the CPT expansion results are reliable.

The AMBT seems to give reliable predictions of long-term effects when fillers being clearly pozzolanic are tested. However, the AMBT may give unreliable predictions of the effect of fillers containing well crystalline quartz. The large influence of temperature on the pozzolanic reactivity is presumably the major reason why the effect of materials such as Norwegian cataclastic rock fillers is not truly predicted by this method. Test methods using very high temperatures, such as the AMBT, should not be recommended to test the effects of rock fillers containing silica, unless their pozzolanic reactivity are evident also at lower temperatures.

8.2 Effects of fillers on the compressive strength

The effect of adding the Norwegian reactive rock fillers mylonite and cataclasite, as well as the non-reactive granite/gneiss filler, was insignificant at normal addition levels. No effect of reducing the particle size distribution from 0-125 μm to 0-20 μm was observed. Addition of Icelandic rhyolite filler increased the compressive strength significantly. Also fly ash and glass filler gave a significant increase in compressive strength.

8.3 Effects of fillers, plasticizers and cements on the rheological properties of the matrix

Addition of filler at a constant w/c ratio increased the flow resistance ratio for all the tested fillers. Replacement of cement by filler decreased the flow resistance ratio for most fillers. The exception from this was glass filler and fly ash, which increased the flow resistance ratio when replacing cement. A large part of the differences between the fillers can be directly related to the particle size distribution of the fillers. Finer fillers tend to give higher flow resistance ratios. But other physical parameters seem to be of importance. A well-graded particle distribution curve, meaning a straight curve with particles evenly distributed over the whole spectre, seems to give lower flow resistance ratios compared to a less well-graded curve. The mineralogy seems to have some influence. For the given set of experiments, using the co-polymer SSP 2000 as plasticizer, the limestone filler gave low flow resistance ratios in relation to its fine particle size distribution.

A laboratory program using a more sophisticated matrix characterisation than the FlowCyl has been carried out. The Physica rheometer, with parallel plate configuration, gives the opportunity to measure the fundamental rheological parameters yield stress and plastic viscosity. It has been shown that the flow resistance ratio, as measured by the FlowCyl, is mostly influenced by the plastic viscosity. Hence, the flow resistance ratio and the plastic viscosity are more or less equivalent measures.

The ratio between yield stress and plastic viscosity was relatively constant for most of the mixes when using a co-polymer based plasticizer (SSP 2000). However, when the co-polymer plasticizer (SSP 2000) was replaced by the naphthalene plasticizer (Mighty 150), these ratios were changed significantly. At the same dosage, Mighty 150 gave a significantly higher yield stress compared to SSP 2000. The replacement

of SSP 2000 with Mighty 150 reduced the plastic viscosity for the matrices containing granite/gneiss filler, limestone filler and glass filler, while it was slightly increased for fly ash and mylonite filler. The new generation of plasticizers, such as the SSP 2000, seems to reduce the yield stress of the matrix to a much higher extent than the older generations of plasticizers. Further, the co-polymers seem to level out the large differences due to different fillers, which may be apparent when using other types of plasticizers. Hence, the dispersion agent based on steric hindrance seems to be more robust and less dependent on the surface chemistry of the mineral particles than the dispersion agent based on electrostatic repulsion.

The replacement of cement by fillers reduced the yield stress significantly. The reduction in plastic viscosity was also significant, unless for the fly ash matrix.

8.4 Correlation between the rheological properties of matrix and concrete

The basic principles of the PM model are believed to be relevant for ordinary concrete, as well as for self-compacting concrete. At a fixed grading and matrix volume, all differences in the rheological properties of the concrete due to changes in cement type, type and dosage and plasticizer, and type and amount of filler, must be reflected by the rheological properties of the matrix. However, the present study, as well as earlier studies discussed within this work, has highlighted some of the limitations of the PM model. The matrix properties in terms of the empirical flow resistance ratio do not give a covering characterisation of this phase regarding SCC. The yield stress values for a typical matrix of Norwegian SCC are very low, with typical values below 10 Pa. Despite such low values, it has been shown that the yield stress of the matrix seems to have a crucial influence on the slump flow measure. Further, the plastic viscosity of the matrix seems to have a large influence on the plastic viscosity of the concrete. The correlation between the yield stress of the matrix and the concrete are less obvious.

The study of the rheological properties of the matrix is believed to be of great value to increase the knowledge of the pure effects or the interaction effects of different constituents. To gain full utilization of the results, there is a need to establish the relationship between the rheological properties of matrix and concrete. Based on the characterisation methods used in this work, there does not seem to be a straightforward correlation between the rheological properties of concrete and matrix. It seems clear that substantial work on this topic is needed to achieve a better understanding of the very complex interactions between the matrix phase and the particle phase of concrete.

9 References

Alexandridis, A. and Gardner, N. J. (1980): "Mechanical behaviours of fresh concrete", *Cement and Concrete Research*, vol. 11, pp 323-339.

ASTM C227-81 (1996): "Standard test method for potential alkali reactivity of cement-aggregate combinations (mortar-bar method)", The American Society for Testing Materials.

Bache, H. H. (1984): "Brudmekanik" ("Fracture mechanics"), *Beton-Teknik*, Aalborg Portland, Aalborg, Denmark, 15 pp. In Danish.

Banfill P. F. G. (1990): "The rheology of cement paste: progress since 1973", *Proceedings from the Rilem colloquium on properties of fresh concrete*, Chapman and Hall, Hannover, pp 3-9.

Barnes H. A. and Walters K. (1985): "The yield stress myth?", *Rheologica Acta*, vol. 24, Nr 4, pp 323-326.

Barnes, H. A., Hutton, J. F. and Walters, K. (1989): "An introduction to rheology", ISBN 0 444 87469-0, Elsevier Science, Amsterdam, The Netherlands.

Bathey, M.H. and Pring, A. (1997): "Mineralogy for students", Addison Wesley Longman, ISBN 0-582-08848-8, Essex, England.

Bažant, Z.P., Zi, G. and Meyer, C. (2000): "Fracture mechanics of ASR in concretes with waste glass of different sizes", *Journal of Engineering Mechanics*, vol. 126, pp 226-232.

Bérubé, M.A., Dorion, J.F. (2000): "Distribution of alkalis in concrete structures affected by alkali-silica reactivity and contribution by aggregates", *Proceedings of the 11th International Conference of Alkali-Aggregate Reaction*, Quebec, Canada, pp 139-148.

Bérubé, M.A., Duchesne, J. and Chouinard, D. (1995): "Why the accelerated mortar method ASTM 1260 is reliable for evaluating the effectiveness of supplementary cementing materials in suppressing expansion due to alkali-silica reactivity", *Cement, Concrete and Aggregates*, vol. 17, pp 26-34.

Biernacki, J. J., Williams, J. and Stutzman, P. (2001): "Kinetics of reaction of calcium hydroxide and fly ash", *ACI Materials Journal*, vol. 98, pp 340-349.

- Billberg P. (1999): "Fine Mortar Rheology in Mix Design of SCC", Proceedings of The 1st International RILEM Symposium on Self-Compacting Concrete, Stockholm, Sweden.
- Bleszynski, R., Thomas, M. and Hooton, M. (2000): "The efficacy of ternary cementitious systems for controlling expansion due to alkali-silica reaction in concrete", Proceedings of the 11th International Conference of Alkali-Aggregate Reaction, Quebec, Canada, pp 583-592.
- Bonavetti, V. L. And Irassar, E. F. (1994): "The effect of stone dust content in sand", Cement and Concrete Research, vol. 24, pp 580-590.
- Box, G. E. P., Hunter, W. G. and Hunter, J. S. (1978): "Statistics for experimenters. An introduction to design, data analysis, and model building", John Wiley & Sons, Inc., ISBN 0-471-09315-7, New York, USA.
- Boyd, S., Bremner, T.W. and Holm, T.A. (2000): "Addition of lightweight aggregate reduces expansion in concrete containing a highly reactive normal weight aggregate", Proceedings of the 11th International Conference of Alkali-Aggregate Reaction, Quebec, Canada, pp 593-602.
- Bremseth, S.K. (2003) "Testing av tilslag av sandstein og kataklasitt etter kanadisk betongprismemetode" ("Testing of sandstone and cataclasite aggregates by the Canadian concrete prism test"), Norcem report 9D4/R03050, Brevik, Norway. In Norwegian.
- Broekmans, M.A.T.M. (1999): "Classification of the alkali-silica reaction in geochemical terms of silica dissolution", Proceedings of the 7th Euroseminar on microscopy applied on building materials, Delft, The Netherlands, pp 155-170.
- Broekmans, M.A.T.M. (2002): "The alkali-silica reaction: Mineralogical and geochemical aspects of some Dutch concretes and Norwegian mylonites", PhD thesis, Utrecht University, The Netherlands.
- Çelik, T. and Marar, K. (1996): "Effects of crushed stone dust on some properties of concrete", Cement and Concrete Research, vol. 26, pp 1121-1130.
- Chatterji, S. and Thaulow, N. (2000): "Some fundamental aspects of alkali-silica reaction", Proceedings of the 11th International Conference of Alkali-Aggregate Reaction, Quebec, Canada, pp 21-29.
- Chatterji, S., Fördös, Z. and Thaulow, N. (1992): "Alkali-silica reaction – Danish experience", in "The alkali-silica reaction in concrete", R .N. Swamy, ed., Blackie and Son Ltd., ISBN 0-216-92691-2, London, UK.

Chatterji, S., Jensen, A.D., Thaulow, N and Christensen, P. (1986): "Studies of alkali-silica reaction. Part 3. Mechanism by which NaCl and Ca(OH)₂ affect the reaction." Cement and Concrete Research, vol. 16, pp 246-254.

Chmelar, J. (2003): Personal e-mail communication.

Colleparidi, M. (2003): "A state-of-the-art review on delayed ettringite attack on concrete", Cement and Concrete Composites, vol. 25, pp 401-407.

Cross, C.W., Iddings, J.P., Pirsson, L.V., and Washington, H.S. (1902): "A quantitative chemico-mineralogical classification and nomenclature of igneous rocks", Journal of Geology, v. 10, p. 555-690.

CSA A23.2-14A (1994): "Potential expansivity of aggregates (procedures for length change due to ASR in concrete prisms)", CSA A23-94 – Methods of test for concrete. Canadian Standard Association (CSA), Rexdale, Ontario, Canada, pp 205-214.

CSA A23.2-25A (1994): "Test method for detection of alkali-silica reactive aggregate by accelerated expansion of mortar bars", CSA A23-94 – Methods of test for concrete. Canadian Standard Association (CSA), Rexdale, Ontario, Canada, pp 236-242.

Cyr, M., Legrand, C. and Mouret, M. (2000): "Study of the shear thickening effect of superplasticizers on the rheological behaviour of cement pastes containing or not mineral additives", Cement and Concrete Research, vol. 30, pp. 1477-1483.

Dahl, P. A., Meland, I. and Jensen, V. (1992): "Norwegian experience with different test methods for alkali-aggregate reactivity", Proceeding of the 9th International Conference on Alkali-Aggregate Reaction in Concrete, London, UK, pp 224-230.

Danielsen, S. W. and Wallevik, O. (1989): „Tilslag og fersk betongs egenskaper – statusrapport“ ("Aggregates and properties of fresh concrete – state-of-the-art"), Materialutvikling Høyfast betong, delrapport 1.1, 75 pp. In Norwegian.

Danielsen, S.W. (2003): "Sand-/grusressurser i Årdal, Ryfylke - samfunnsmessig betydning som byggeråstoff" ("Sand-/gravel resources in Årdal, Ryfylke - social importance as raw material in construction"), NorStone internal memo, Sandnes, Norway. In Norwegian.

de Larrard, F., Ferraris, C.F. and Sedran, T. (1998): "Fresh concrete: A Herschel-Bulkley material", Materials and Structures, vol. 31, pp. 494-498.

Dent Glasser, L. S. and Kataoka, N. (1981): "The chemistry of alkali-silica reactions", Proceedings of the 5th International Conference on Alkali-Silica Reactions, Cape Town, South Africa.

Dent Glasser, L. S. and Kataoka, N. (1982): "On the role of calcium in the alkali-aggregate reaction", *Cement and Concrete Research*, vol. 12, pp 321-331.

Diamond, S. (1997): "Alkali-silica reactions – some paradoxes", *Cement and Concrete Composites*, vol. 19, pp 391-401.

Diamond, S. (2000): "Chemistry and other characteristics of ASR gels", *Proceedings of the 11th International Conference of Alkali-Aggregate Reaction*, Quebec, Canada, pp 31-40.

Diamond, S. (2002): Personal e-mail communication.

Diamond, S. and Thaulow, N. (1974): "A study of expansion due to alkali-silica reactions as conditioned by the grain size of the reactive aggregate", *Cement and Concrete Research*, vol. 4, pp 591-607.

Diamond, S., Barneyback, R. S. jr., and Struble, L. J.(1981): "On the physics and chemistry of alkali silica reactions", *Proceedings of the 5th International Conference on Alkali-Silica Reactions*, Cape Town, South Africa.

Dove, P.M. and Rimstidt, J.D. (1994): "Silica-water interactions", in *Reviews in Mineralogy* vol. 29: *Silica: Physical behavior, geochemistry and materials applications*, Mineralogical Society of America, ISBN 0-939950-35-9, Washington DC, USA.

Duchesne, J. and Bérubé, M. A. (2000): "Long-term effectiveness of supplementary cementing materials against ASR", *Proceedings of the 11th International Conference of Alkali-Aggregate Reaction*, Quebec, Canada, pp 613-619.

Duchesne, J. and Bérubé, M. A. (2001): "Long-term effectiveness of supplementary cementing materials against alkali-silica reaction", *Cement and Concrete Research*, vol 31, pp 1057-1063.

Ferraris C.F., Obla K. H. and Hill R. (2001a): "The influence of mineral admixtures on the rheology of cement paste and concrete", *Cement and Concrete Research*, vol. 31, pp 245-255.

Ferraris, C.F., de Larrard, F. and Martys, N. (2001b): "Fresh concrete rheology: Recent developments", *Materials Science of Concrete VI*, The American Ceramic Society, Westerville, OH, USA, pp. 215-251.

Ferraris, C. F. (1999): "Measurement of the rheological properties of high performance concrete: State of the art report", *Journal of Research of the National Institute of Standards and Technology*, vol. 104, pp 461-478.

- Ferraris, C. F. and Gaidis, J. (1992): "Connection between the rheology of concrete and rheology of cement paste", *ACI Materials Journal*, vol. 88, pp 388-393.
- Flatt, R. J., Houst, Y. F., Bowen, P. and Hofman, H. (2000): "Electrosteric repulsion by superplasticisers between cement particles – and overlooked mechanism?", *Proceedings of the 6th CANMET/ACI International Conference on Superplasticizers and Other Chemical Admixtures in Concrete*, Nice, France, pp 1159-1165.
- Fournier, B. and Malhotra, V.M. (1996): "Inter-laboratory Study on the CSA A23.2-14A Concrete prism Test for Alkali-Silica Reactivity in Concrete", *Proceedings of the 10th International Conference on Alkali-Aggregate Reaction in Concrete*, Melbourne, Australia, pp. 302-309.
- Fournier, B. and Malhotra, V.M. (1999): "Evaluation of laboratory test methods for alkali-silica reactivity", *Cement, Concrete and Aggregates*, vol. 21, pp 173-184
- Geiker, M.R., Brandl, M., Thrane, L.N., Bager, D.H. and Wallevik, O. (2002a): "The effect of measuring procedure on the apparent rheological properties of self-compacting concrete", *Cement and Concrete Research*, vol. 32, pp. 1791-1795.
- Geiker, M.R., Brandl, M., Thrane, L.N. and Nielsen, L.F. (2002b): "On the effect of coarse aggregate fraction and shape on the rheological properties of self-compacting concrete", *Cement, Concrete and Aggregates*, vol. 24, pp. 3-6.
- Glasser, F.P.(1992): "Chemistry of the alkali-aggregate reaction", in "The alkali-silica reaction in concrete", R .N. Swamy, ed., Blackie and Son ltd., ISBN 0-216-92691-2, London, UK.
- Golterman, P. (1995): "Mechanical predictions of concrete deterioration – part 2: classification of crack patterns", *ACI Materials Journal*, vol. 92, pp 58-63.
- Granerud, D.R. (2002): „Selvkomprimerende betong – reologiske egenskaper for matriks og betong“ ("Self-compacting concrete – rheological properties of matrix and concrete") M.Sc. thesis, NTNU, Trondheim, Norway. (In Norwegian).
- Grattan-Bellew, P.E. (1992): "Alkali-silica reaction – Canadian experience", in "The alkali-silica reaction in concrete", R .N. Swamy, ed., Blackie and Son ltd., ISBN 0-216-92691-2, London, UK.
- Gudmundsson G., Halfdanarson, J. and Möller, J. (2000): "Effect of silica fume properties on mitigation of ASR reactivity in concrete". *Proceedings of the 11th International Conference on Alkali-Aggregate reactions in Concrete*, Quebec, Canada, pp 643-652.

- Gudmundsson, G. and Asgeirsson, H. (1983): "Parameters affecting alkali expansion in Icelandic concretes", Proceedings of the 6th International Congress on Alkali-Silica Reactions, 1983, Copenhagen, Denmark.
- Gudmundsson, G. and Olafsson, H. (1999): "Alkali-silica reactions and silica fume, 20 years of experience in Iceland", Cement and Concrete Research, vol. 29, pp 1289-1297.
- Gudmundsson, G. (1975): "Investigations on Icelandic pozzolans", Proceedings of the Symposium on Alkali-Aggregate Reactions, preventive measures, Reykjavik, Iceland.
- Helgason, T. (1981) "Alkalivirkni nokkurra íslenskra bergtegunda" ("Alkali reactions in some Icelandic rocks"). Report, Rb-V-150, 38 pp. In Icelandic.
- Ho, D. W. S., Shein, A. M. M., Ng, C. C. and Tam, C. T. (2002): "The use of quarry dust for SCC applications", Cement and Concrete Research, vol. 32, pp 505-511.
- Hobbs, D. W. and Gutteridge, W. A. (1979): "Particle size of aggregate and its influence upon the expansion caused by the alkali-silica reaction", Magazine of Concrete Research, vol. 31, pp 235-242.
- Hólmgeirsdóttir, Þ. (2001): "Rhyolite from Hvalfjörður, Iceland – Thin section analysis", report, University of Iceland and ERGO Engineering Geology, Reykjavik, Iceland.
- Hou, X, Kirkpatrick, R.J., Struble, L.J., Shin, J. and Monteiro, P.J.M. (2003): "The structure of ASR gel and its relationship to C-S-H", Proceeding of the Engineering Conference on Advances in Cement and Concrete IX: Volume Changes, Cracking, and Durability, Copper Mountain, Colorado, USA
- Hu, C., de Larrard, F., Sedran, T., Boulay, F., Bosck, F. And Deflorenne, F. (1996): "Validation of BTRHEOM, the new rheometer for soft-to-fluid concrete", Materials and Structures, vol. 29, pp 620-631.
- Hudec, P.P. and Cyrus Chamari, R. (2000): "Ground waste glass as an alkali-silica reactivity inhibitor", Proceedings of the 11th International Conference of Alkali-Aggregate Reaction, Quebec, Canada, pp 663-672.
- Irgens, F. (1998): "Reologi og ikke-Newtonske fluider" ("Rheology and non-Newtonian fluids"), forelesningsnotater, Institutt for mekanikk, termo- og fluiddynamikk, NTNU, Trondheim, Norway.
- Isaksen, H.R., Sellevold, E.J., Liestøl, G. and Kompen, R. (1996): "Utvikling av kloridbestandig betong. Akselererte kloridtester ved 90 døgns alder" ("Development

of concrete sustainable to chloride ingress. Accelerated chloride tests at 90 days maturity”). Report Statens Vegvesen Vegdirektoratet 96-08-BRU, Oslo, Norway, 54 pp. In Norwegian.

Jensen, J., Jensen, V., Schouenborg, B., Sibbick, R.C., Nixon, P., Thøgersen, F., Lorenzi, G. and Soares, I. (1998): “Standard Test for Alkali-reactive Rock; STAR Project Final Report, European Commission, DG XII, contract nr. SMT4-CT96-2128, 148 pp.

Jensen, V. (1993) ”Alkali aggregate reactions in southern Norway”, Doctor Technicae-theses, Technical University of Trondheim, Norway.

Jensen, V. (1996): “Present experience with aggregate testing in Norway”, Proceeding of the 10th International Conference on Alkali-Aggregate Reaction in Concrete, Melbourne, Australia, pp 133-142.

Jensen, V. (2000): “In-situ measurements of relative humidity and expansion of cracks in structures damaged by ASR”, Proceedings of the 11th International Conference on Alkali-Aggregate Reaction in Concrete, Quebec, Canada, pp 849-858.

Jensen, V. (2003): “Elgseter Bridge in Trondheim damaged by alkali silica reaction: Microscopy, expansion and relative humidity measurements, treatments with mono silanes and repair”, Proceedings of the 9th Euroseminar on Microscopy Applied to Building Materials, Trondheim, Norway.

Jensen, V. and Fournier, B. (2000): “ Influence of different procedures on accelerated mortar bar and concrete prism tests: Assessment of seven Norwegian alkali-reactive aggregates”, Proceedings of the 11th International Conference on Alkali-Aggregate Reaction in Concrete, Quebec, Canada, pp 345-354.

Johansen, A.C. (2000): ”Fillerens betydning på betongens reologi” (“The impact of the aggregate filler on the concrete rheology”, M.Sc. thesis, NTNU, Trondheim, Norway. In Norwegian.

Johansen, K., Meland, I., Lindgård, J., Wallevik, O., Skjeggerud, K., Lindevall, G and Hauck, C. (1992): ”Effekt av ulike fillertyper i sementbasert materialer” (“Effects of different fillers on cement based materials”), Materialutvikling Høyfast Betong, delrapport 3.7., 13 pp. In Norwegian

Jones, A.E.K. and Clark, L.A. (1997): “The effects of ASR on the properties of concrete and the implications for assessment”, Engineering Structures, vol. 20, no 9, 99 785-791.

Justnes, H. (1992): "Hydraulic binders based on condensed silica fume and slaked lime", Proceedings of the 9th International Congress on the Chemistry of Cement, New Delhi, India, pp 284-290.

Justnes, H. (2003): "Rheology of cement based binders – State-of-the-art", Sintef report STF22 A02617, Trondheim, Norway.

Justnes, H., Østnor, T. (2001): "Pozzolanic, amorphous silica produced from the mineral olivine", Proceedings of the 7th CANMET/ACI International Conference on Fly Ash, Silica Fume, Slag and Natural Pozzolans in Concrete, Chennai, India, pp769-781.

Justnes, H., Sellevold, E. J. and Lundevall, G. (1992): "High strength concrete binders, Part A: Reactivity and composition of cement pastes with and without condensed silica fume", Proceedings of the 4th International Conference on Fly Ash, Silica Fume, Slag and Natural Pozzolans in Concrete, Istanbul, Turkey, pp 873-889.

Kawamura, M., Takamoto, K. and Hasaba, S. (1986): "Effect of silica fume on alkali-silica expansion in mortars. Fly ash, Silica fume, Slag and Natural Pozzolans in Concrete. Proceedings of the 2nd International Conference, Madrid, Spain, pp 999-1012.

Kjellsen, K. and Lagerblad, B. (1995): "Influence of natural minerals in the filler fraction on hydration and properties of mortars", CBI report, Stockholm, Sweden.

Kjellsen, K., Rønning, T. F. and Meland, I. (2001): "Prevention of deleterious alkali aggregate reactions by use of Norwegian Portland-fly ash cement", NCR seminar, Hirtshals, Denmark.

Krogh, H.: (1975): "Examination of alkali-silica gels", report, Danmarks Ingeniørakademi.

Kronlöf, A. (1994): "Effect of very fine aggregate on concrete strength", Materials and Structures, vol. 27, pp 15-25.

Kronlöf, A. (1997): "The effect of inert mineral powder in concrete", Doctor of Technology thesis, Helsinki University of Technology, Finland.

Lagerblad, B. and Trägårdh, J. (1992): "Slowly reacting aggregates in Sweden – mechanism and conditions for reactivity in concrete", Proceedings from the 9th International Conference on Alkali-Aggregates Reaction in Concrete, London, pp 570-578.

Lawrence, C.D. (1998) "The constitution and specification of Portland cements", in Lea's chemistry of cement and concrete, P.C Hewlett, ed., Arnold, ISBN 0 340 56589 6, London, UK.

- Lindgård, J. and Wigum, B. (2003): "Alkalireaksjoner i betong – felterfaringer" ("Alkali-reactions in concrete – field experience"), Sintef report, Trondheim, Norway. In Norwegian.
- Lindgård, J., Dahl, P. A. and Jensen, V. (1993): "Bergartssammensetning – alkalireaktive tilslag. Beskrivelse av prøvingsmetoder og krav til laboratorier" ("Rock types - reactive aggregates. Description of methods and laboratory requirements"), SINTEF report STF70 A93030, Trondheim, Norway. In Norwegian.
- Maedler, U. and Kuesterle, W. (1999): "The rheological behaviour of cementitious materials with chemically different superplasticizers", Proceedings of the International symposium: The role of admixtures in high performance concrete, Monterrey, Mexico 1999.
- Massazza, F. (1998): "Pozzolana and pozzolanic cements", in Lea's chemistry of cement and concrete, P.C Hewlett, ed., Arnold, ISBN 0 340 56589 6, London, UK.
- Mather, B.L. (1999): "How to make concrete that will not suffer deleterious alkali-silica reaction", Cement and Concrete Research, vol. 29, pp 1277-1280.
- Meland, I. (1999): "Alkalireaksjoner, forsøksserie nr. 2" ("Alkali-reactions, test series nr. 2"), SINTEF report STF22 F99725 (Ressursvennlig kvalitetsbetong, DP Bestandighet), Trondheim, Norway. In Norwegian.
- Micromeritics Instrument Corporation (1998): "SediGraph 5100, Windows software, Operator's manual", Norcross, USA.
- Minitab (2000): www.minitab.com
- Mørtzell E. (1996): „Modellering av delmaterialenes betydning for betongens konsistens“ ("Modelling of the effect of the constituents on the concrete workability"), Dr.ing. thesis, Department of Structural Engineering, Norwegian Institute of Technology, Trondheim. In Norwegian.
- Mørtzell E., Maage M. and Smepllass S. (1995): "A Particle-Matrix Model for Prediction of Workability of Concrete", Proceedings from the International Conference on Production Methods and Workability of Fresh Concrete", Glasgow, Scotland.
- Mørtzell E., Smepllass S., Hammer T.A. and Maage M. (1996): "FLOWCYL – How to Determine the Flow Properties of the Matrix Phase of High Performance Concrete", Proceedings of the 4th International Symposium on Utilization of High-strength/ High-performance Concrete, Paris, France.

- Nehdi, M. (2000): "Why some carbonate fillers cause rapid increases of viscosity in dispersed cement-based materials", *Cement and Concrete Research*, vol. 30, pp. 1663-1669.
- Nehdi, M, Mindess, S. and Aitcin, P.C (1997): "Statistical modelling of the microfiller effect on the rheology of composite cement pastes", *Advances in Cement Research*, vol. 9, pp. 37-46.
- Nehdi, M., Mindess, S and Aitcin, P .C. (1998): "Rheology of high-performance concrete: Effect of ultrafine particles", *Cement and Concrete Research*, vol. 28, pp. 687-697.
- Nielsen, A. (1983): "Sorptions properties of concrete with alkali-silica reactive aggregate", *Proceedings of the 6th International Congress on Alkali-Silica Reactions*, Copenhagen, Denmark, pp. 195-200.
- Nilsson, L. O. (1983): *Moisture Effects on the Alkali-Silica Reaction*, *Proceedings of the 6th International Congress on Alkali-Silica Reactions*, 1983, Copenhagen, Denmark, pp. 201-208.
- Nishibiyashi, S. and Yamamura, K. (1992): "Effect of reactive fine aggregate on expansion characteristics of concrete due to alkali aggregate reaction", *Proceedings of the 9th International Conference on Alkali-Aggregates Reaction in Concrete*, London, pp. 723-730.
- Normin 2000 (1999): "Alkalireaksjoner i betong", Hovedprosjektrapport, in Norwegian ("Alkali aggregate reactions in concrete – main project report") Oslo, Norway, 166 pp.
- Norwegian Concrete Association (1996): "Bestendig betong med alkalireaktivt tilslag" ("Durable concrete with alkali reactive aggregates"), Publication nr. 21, Oslo, Norway. In Norwegian.
- Norwegian Concrete Association (2002): "Guidelines for production and use of self-compacting concrete", Publication nr. 29, Oslo, Norway.
- Norwegian Control Council for Concrete Products (2003): "Metoder for prøving av tilslag – del 2" ("Methods for aggregate testing – part 2"), Oslo, Norway. In Norwegian).
- NS 3086 (2003): "Sement med spesielle egenskaper" ("Cements with special properties"). In Norwegian.
- NS 3659 (1987): "Betongprøving. Fersk betong - Luftinnhold" ("Concrete testing - Fresh concrete - Air content"). In Norwegian.

NS 3660, (1987): "Betongprøving - Fersk betong - Densitet" ("Concrete testing - Fresh concrete - Density.") In Norwegian.

NS 3662 (1987): "Betongprøving - Fersk betong - Konsistens og synkmål". ("Concrete testing - Fresh concrete - Slump test.") In Norwegian.

NS 3668 (1987): "Betongprøving - Herdet betong - Prøvelegemers trykkfasthet." ("Concrete testing - Hardened concrete - Compressive strength of test specimens.") In Norwegian.

NS 3669, (1987): "Betongprøving – Herdet betong – Støping og lagring av prøvelegemer til å bestemme fasthet." ("Concrete testing - Hardened concrete - Making and curing of test specimens for strength tests.") In Norwegian.

NS-EN 197-1 (2000): "Cemen, part 1: Composition, specifications and conformity criteria for common cements".

Oberholster, R. E. and Davis, G. (1986): "An accelerated method for testing the potential alkali reactivity of siliceous aggregates", Cement and Concrete Research, vol. 16, pp 181-189.

Odler, I. (1998): "Hydration, setting and hardening of Portland cement", in Lea's chemistry of cement and concrete, P.C Hewlett, ed., Arnold, ISBN 0 340 56589 6, London, UK, 1998.

Olafsson, H. (1992): "Alkali-silica reaction- Icelandic experience", in The alkali-silica reaction in concrete, R .N. Swamy, ed., Blackie and Son ltd., ISBN 0-216-92691-2, London, UK.

Pedersen, B. and Mørtzell. E (2001): "Characterisation of fillers for SCC", Proceedings of the 2nd International Symposium on Self-Compacting Concrete, Tokyo, Japan.

Poole, A.B. (1992) "Introduction to alkali-aggregate reaction in concrete", in The alkali-silica reaction in concrete, R .N. Swamy, ed., Blackie and Son ltd., ISBN 0-216-92691-2, London, UK.

Poulsen, E., Hansen, T.S. and Sørensen, H.E. (2000): "Release of alkalis from feldspar in concrete and mortar", Proceedings of the Canmet/ACI International Conference on Durability of Concrete, Barcelona, Spain.

Powers, T.C. (1958): "Structure and physical properties of hardened Portland cement paste", Journal of the American Ceramic Society, vol. 41, pp. 1-6.

Powers, T. C. and Steinour, H. H. (1955a): "An interpretation of some published researches on the alkali-aggregate reaction, part 1: The chemical reactions and

mechanisms of expansion”, *Journal of the American Concrete Institute*, vol. 51, pp. 497-516.

Powers, T. C. and Steinour, H. H. (1955b): “An interpretation of some published researches on the alkali-aggregate reaction, part 2: A hypotheses concerning safe and unsafe reactions with reactive silica in concrete”, *Journal of the American Concrete Institute*, vol. 26, pp. 785-811.

Prezzi, M., Monteiri, J.M. and Sposito, G. (1997): “The alkali-silica reaction, Part 1: Use of the double-layer theory to explain the behaviour of reactions-product gels”, *ACI Materials Journal*, vol. 94, pp 10-17.

Qingham, B., Xuequan, W., Mingshu, T., Nishibayashi, S., Kuroda, T. and Tiecheng, W. (1996): “Effect of reactive aggregate powder on suppressing expansion due to alkali-silica reaction”, *Proceedings of the 10th International Conference on Alkali-Aggregates Reaction in Concrete*, Melbourne, Australia, pp 546-553.

Ramachandran, V.S. (1998): “Alkali-aggregate expansion inhibiting admixtures”, *Cement and Concrete Research*, vol. 20, pp 149-161.

Rangaraju, P.R. and Olek, J. (2000): “Evaluation of the potential of densified silica fume to cause alkali-silica reaction in cementitious matrices using a modified ASTM 1260 test procedure”, *Cement, Concrete and Aggregates*, vol. 22, pp 150-159.

Relling, R.H. (1999): “Coastal Concrete Bridges: Moisture State, Chloride Permeability and Aging Effects”, Dr. ing. thesis, Norwegian University of Science and Technology, Trondheim.

Rilem TC 106-ASR (2000): “A-TC 10-2- Detection of potential alkali-reactivity of aggregates – The ultra accelerated mortar-bar-test”, *Materials and Structures*, vol. 33, pp 283-293.

Rimstidt, J.D. (1997): “Quartz solubility at low temperatures”, *Geochimica et Cosmochimica Acta*, vol. 61, pp. 2553-2558.

Rodrigues, F.A., Monteiro, P.J.M. and Sposito, G. (1999): “The alkali silica reaction. The surface charge density of silica and its effect on expansive pressure”, *Cement and Concrete Research*, vol. 29, pp 527-530.

Rogers, C.A. (1988): “General information on standard alkali-reactive aggregates from Ontario, Canada”, Engineering materials office, Ministry of transportation, Ontario, Canada.

Rowland, I.D. and Howe, T.N. (1999): "Vitruvius, Ten books on architecture", Cambridge University Press.

Sellevold, E.J. (1997): "Resistivity and humidity measurements of repaired and non-repaired areas in Gimsøystraumen bridge, International Conference: Repair of concrete structures. From theory to practice in a marine environment, Svolvær, Norway.

Sellevold, E. (1993): "Sementpasta porøsitet. Powers model, volumberegninger" ("Porosity of cement paste. Powers' model, volumetric calculations"), compendium at the Norwegian University of Science and Technology, Trondheim, Norway. In Norwegian.

Sellevold, E.J., Bager, D.H., Klitgaard Jensen, E. and Knudsen, T. (1982): "Silica fume-cement pastes: hydration and pore structure", Report BML 82.610, Norwegian Institute of Technology, Trondheim, Norway.

Shao, Y., Lefort, T. Moras, S. and Rodriguez, D. (2000): "Studies on concrete containing ground waste glass", Cement and Concrete Research, vol. 30, pp 91-100.

Shaw, D. J. (1991): "Introduction to colloid & surface chemistry", ISBN 0 75061182 0, Butterworth-Heinemann, Oxford, UK.

Shayan, A. and Ivanusec, I. (1995): "An experimental clarification of the association of delayed ettringite formation with alkali-aggregate reaction", Cement and Concrete Composites, vol. 18, pp 161-170.

Shehata, M.H. and Thomas, M.D.A. (2002): "Use of ternary blends containing silica fume and fly ash to suppress expansion due to alkali-silica reaction in concrete", Cement and Concrete Research, vol. 32, pp 341-349.

Skjølvold, O. and Pedersen, B. (1997): "Crushed sand in concrete. A study on fillers", project report, Norwegian University of Science and Technology, Trondheim, Norway. In Norwegian.

Smeplass S. (2002): "Effekt av sementtype på betongens støpelighet" ("The influence of the cement type on the workability of concrete") Norcem report, Brevik, Norway. In Norwegian.

Smeplass S. and Fredvik T. (2001): "Selvkomprimerende betong. Tilpasning av partikkel-matriksmodellen" ("Self-compacting concrete. Implementation of the particle-matrix model"), Norcem report, Brevik, Norway. In Norwegian.

Smeplass S. and Mørtzell E. (2001). The particle matrix model applied on SCC, Proceedings of the 2nd International Symposium on Self-Compacting Concrete, Tokyo, Japan.

Smeplass, S. and Skjølvold, O. (1996): "Betongprøving. Kapillær sugsevne og porøsitet" ("Concrete testing. Capillary suction and porosity"), SINTEF Quality manual KS70 110, 9 pp. In Norwegian.

Stark, D. (1991): "The moisture condition of field concrete exhibiting alkali-silica reactivity", Proceedings of the 2nd International Conference on Durability of Concrete, Canada, ACI Publication SP 126/52, pp 973-987.

Struble, L. (2002): "Colloidal suspensions", compendium at the PhD-course: Rheology of Fresh Cementitious Materials - Self-Compacting Concrete, Lyngby, Denmark.

Swamy, R.N. and Al-Asali, M.M. (1988): "Engineering properties of concrete affected by alkali-silica reaction", ACI Materials Journal, vol. 85, pp 367-374.

Tattersall G.H. and Banfill P.F.G. (1983). The rheology of fresh concrete, Pitman Adv. Pub. Program, London.

Thomas, M.D.A., Hooper, R. and Stokes, D.B. (2000): "Use of lithium-containing compounds to control expansion in concrete due to alkali-silica reaction", Proceedings of the 11th International Conference of Alkali-Aggregate Reaction, Quebec, Canada, pp 783-792.

TI-B 51, Test method (1985): "The alkali-silica reactivity of sand", Teknologisk Institut, Denmark. In Danish.

Urhan, S. (1986): "Alkali silica and pozzolanic reactions in concrete. Part 1: Interpretation of published results and a hypothesis concerning the mechanism", Cement and Concrete Research, vol. 17, pp 141-152.

Wallevik J. E. (2003): "Rheology of particle suspensions; fresh concrete, mortar and cement paste with various types of lignosulphonate", Dr. ing. thesis, Department of Structural Engineering, The Norwegian University of Science and Technology, Trondheim, Norway.

Wallevik, J.E. and Hammer, T.A. (2003): "Sammenligning av Norcem Standard og Norcem Anlegg ved bruk av ConTec 4" ("Relationship between Norcem Standard cement and Norcem Anlegg cement tested by the ConTec 4"), internt notat i KMB-prosjektet "Reologiske egenskaper for sementbaserte bindemidler", Sintef, Trondheim, Norway. In Norwegian.

Wallevik O. and Gjörv O. (1990): "Development of a coaxial cylinder viscosimeter for fresh concrete", Proceedings of the Rilem colloquium on properties of fresh concrete, Chapman and Hall, Hannover, pp 213-224.

- Wallevik, O. (2002): "IBRI At your service; The Rheology of fresh concrete", Reykjavik, Iceland.
- Wallevik, O. H. (1990): "Den ferske betongens reologi og anvendelse på betong med og uten tilsetning av silikastøv" ("The rheology of fresh concrete and its application on concrete with and without silica fume"), Dr.ing. thesis, Department of building Materials, Norwegian Institute of Technology, Trondheim. In Norwegian.
- Wallevik, O., Saasen, A. and Gjørsv, O. E. "Effect of filler materials on the rheological properties of fresh concrete", *ACI Materials Journal*, vol. 92, pp524-528.
- Wang, H. and Gillott, J.E. (1991): "Mechanism of alkali-silica reaction and the significance of calcium hydroxide", *Cement and Concrete Research*, vol. 21, pp 647-654.
- Wang, H. and Gillott, J.E. (1992): "Competitive nature of alkali-silica fume and alkali-aggregate (silica) reaction", *Magazine of Concrete Research*, vol. 44, pp 235-239.
- Wigum B. J. and Thorenfeldt E. (2003): "Carbon fibre reinforced polymers (*CFRP*) sheets to repair bridge pillars damaged by Alkali Aggregate Reaction (*ASR*), Elgeseter bridge, Trondheim, Norway", SINTEF report, Trondheim, Norway.
- Wigum B.J., Hagelia, P., Haugen, M. and Broekmans, M.A.T. (2000): "Alkali aggregate reactivity of Norwegian aggregates assessed by quantitative petrography", *Proceedings of the 11th International Conference of Alkali-Aggregate Reaction*, Quebec, Canada, pp 533-542.
- Wigum, B.J. (1995a): "Examination of microstructural features of Norwegian cataclastic rocks and their use for predicting alkali-reactivity in concrete", *Engineering Geology*, vol. 40, pp 195-214.
- Wigum, B.J. (1995b): "Alkali-aggregate reactions in concrete; Properties, classification and testing of Norwegian cataclastic rocks", Dr.ing. thesis, The Norwegian Institute of Technology, Trondheim, Norway.
- Wigum, B.J. and French, W.J. (1996): "Sequential examination of slowly expanding alkali-reactive aggregates in accelerated mortar bar testing", *Magazine of Concrete Research*, vol. 48, pp 281-292.
- Williams, D. A., Saak, A. W. and Jennings, H. M. (1999): "The influence of mixing on the rheology of fresh cement paste", *Cement and Concrete Research*, vol. 29, pp 1491-1496.

Xu, G.J.Z., Watt, D.F. and Hudec, P.P. (1995): "Effectiveness of mineral admixtures in reducing ASR expansion", *Cement and Concrete Research*, vol. 25, pp 1225-1236.

Zhang, X, and Han, J. (2000): "The effect of ultra-fine admixture on the rheological property of cement paste", *Cement and Concrete Research*, vol. 30, pp. 827-830.

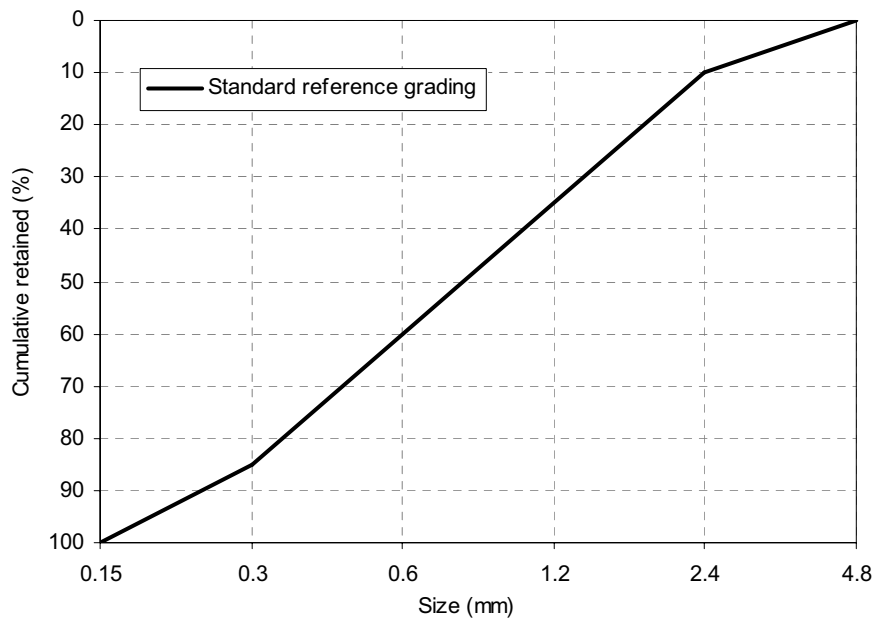
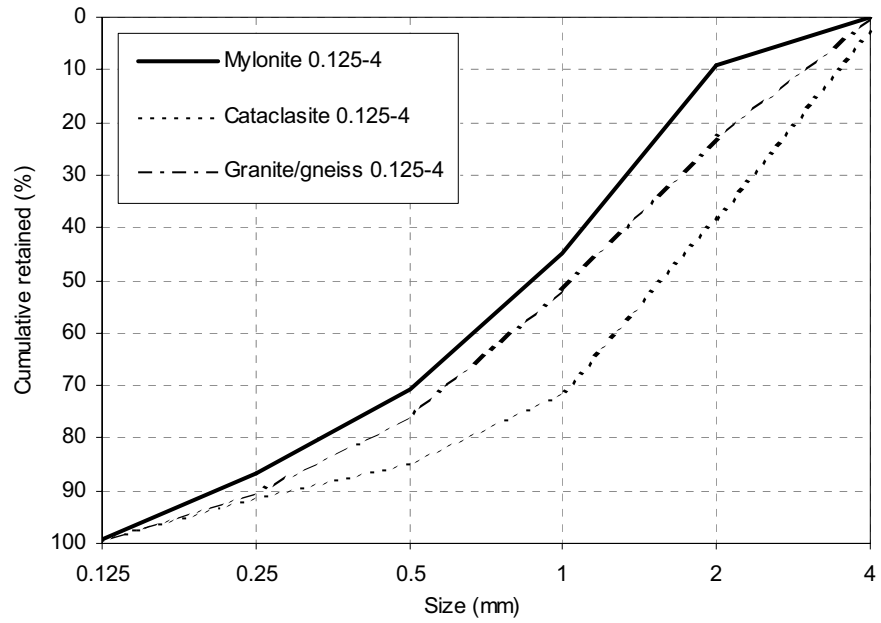
Zhang, C., Wang A., Tang, M. and Zhang, N. (1999): "Influence of aggregate size and aggregate grading on ASR expansion", *Cement and Concrete Research*, vol. 29, pp 1393-139.

Appendix A

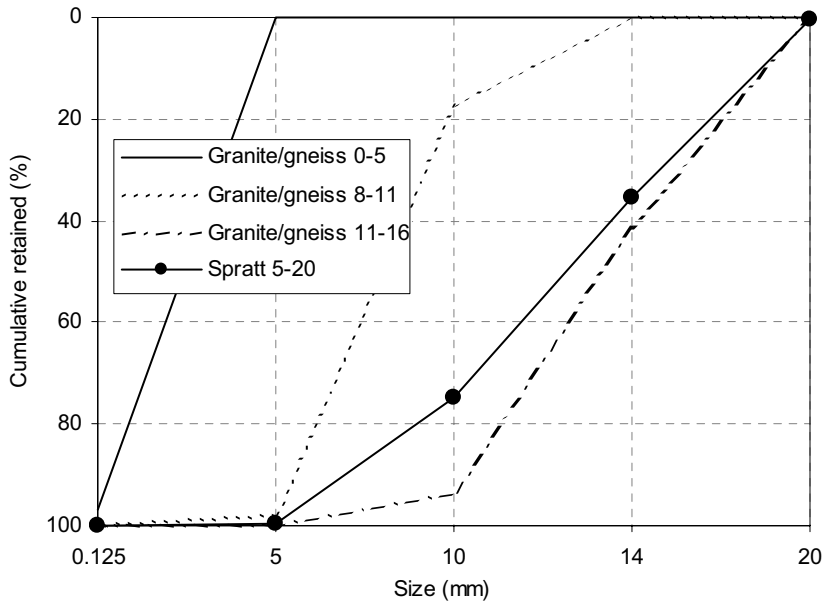
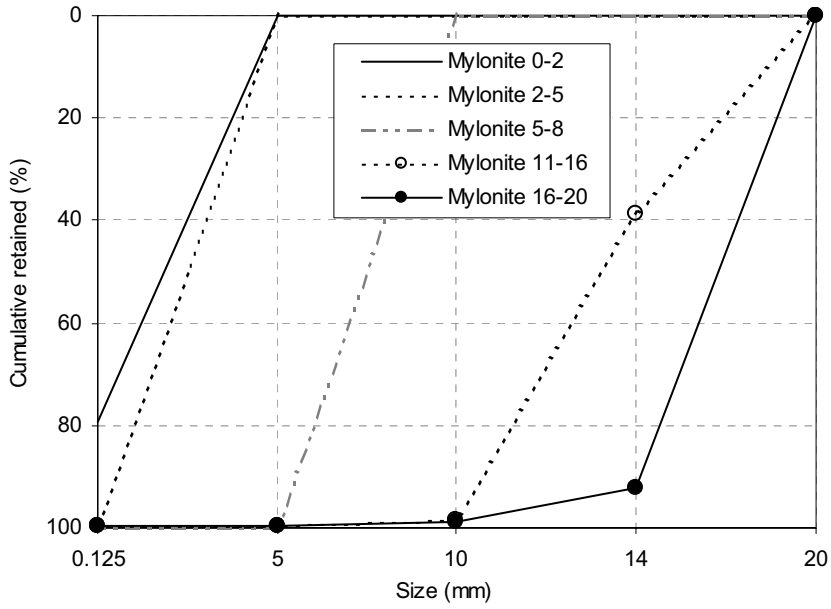
- A1 Particle size distributions of fine and coarse aggregates
- A2 Particle size distributions of filler
- A3 Mix design of concretes tested by the CPT
- A4 Mix design of mortars tested by the AMBT
- A5 Mix design of self-compacting concretes

A1: Particle size distribution of fine and coarse aggregates

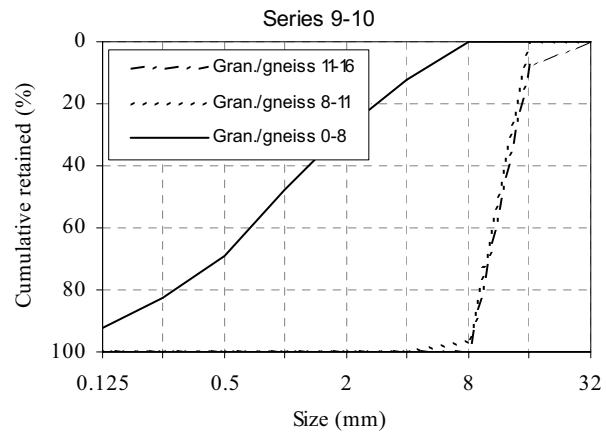
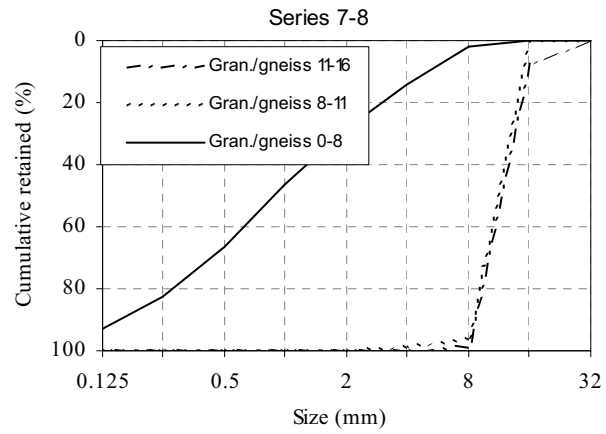
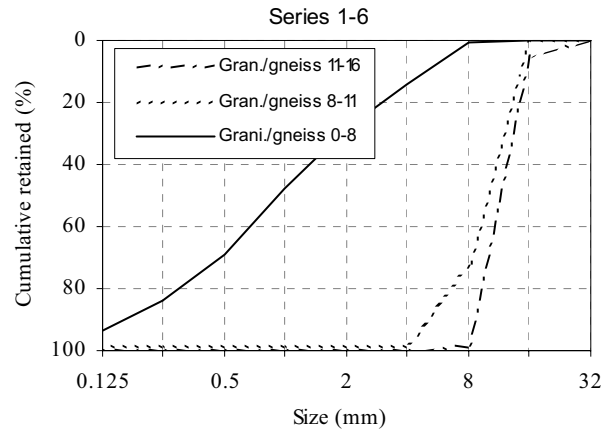
Particle size distributions of aggregates used in mortars tested by the accelerated mortar bar test (AMBT)



Particle size distributions of aggregates used in concretes tested by the concrete prism test (CPT)

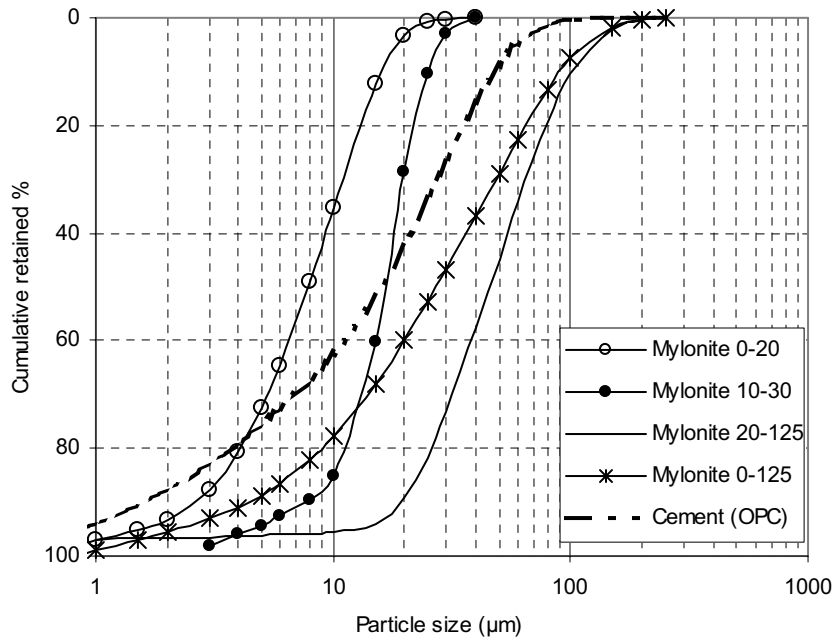


Particle size distribution of aggregates used in self-compacting concretes

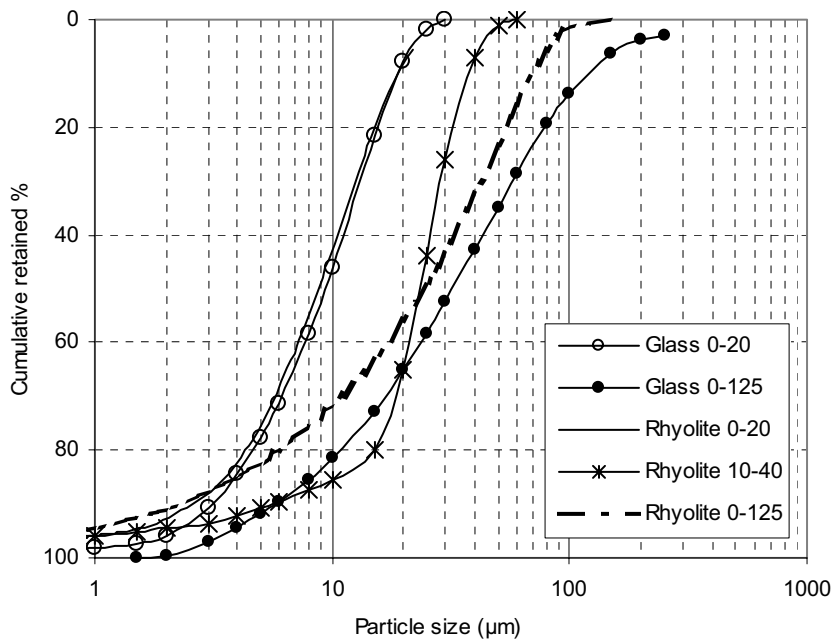


A2: Particle size distribution of fillers

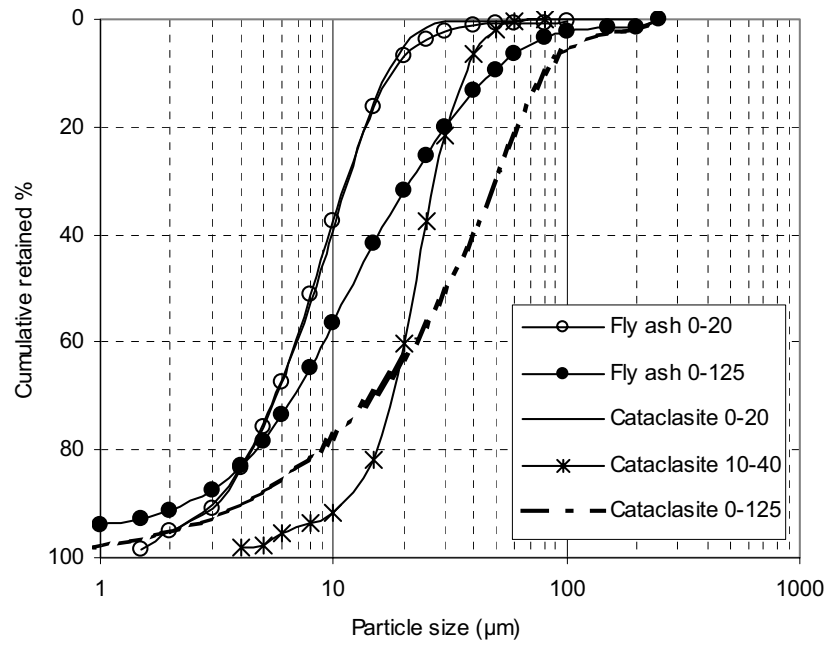
mylonite fillers and cement



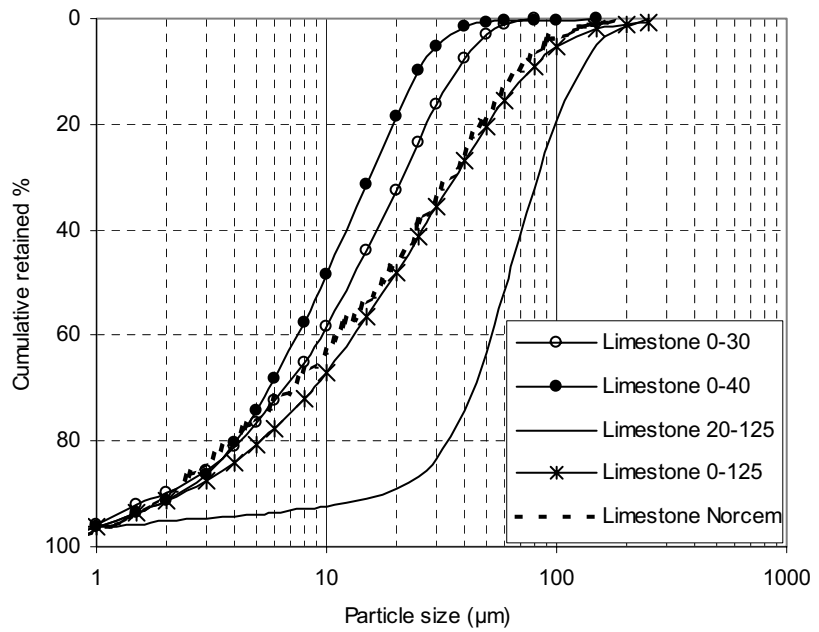
glass and rhyolite fillers



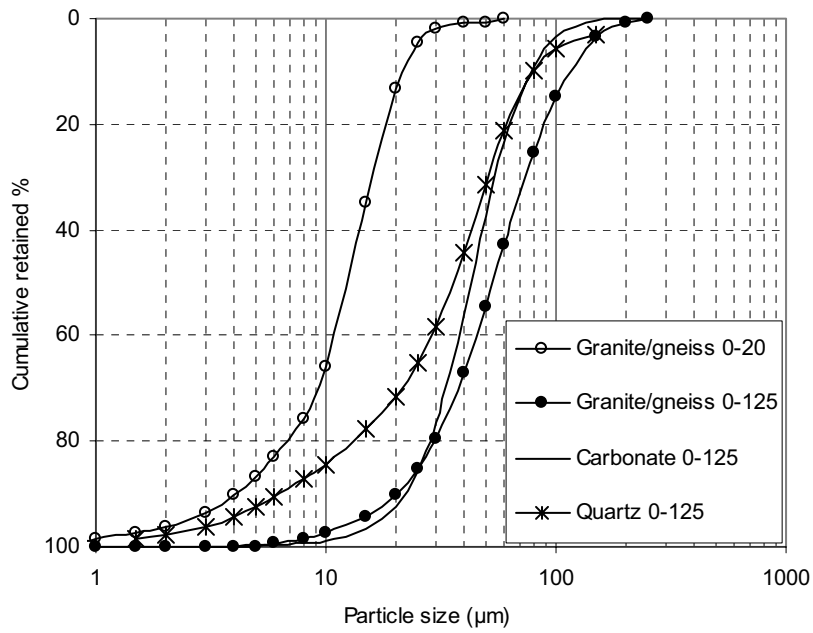
fly ash and cataclasite fillers



limestone fillers



granite/gneiss, carbonate and quartz fillers



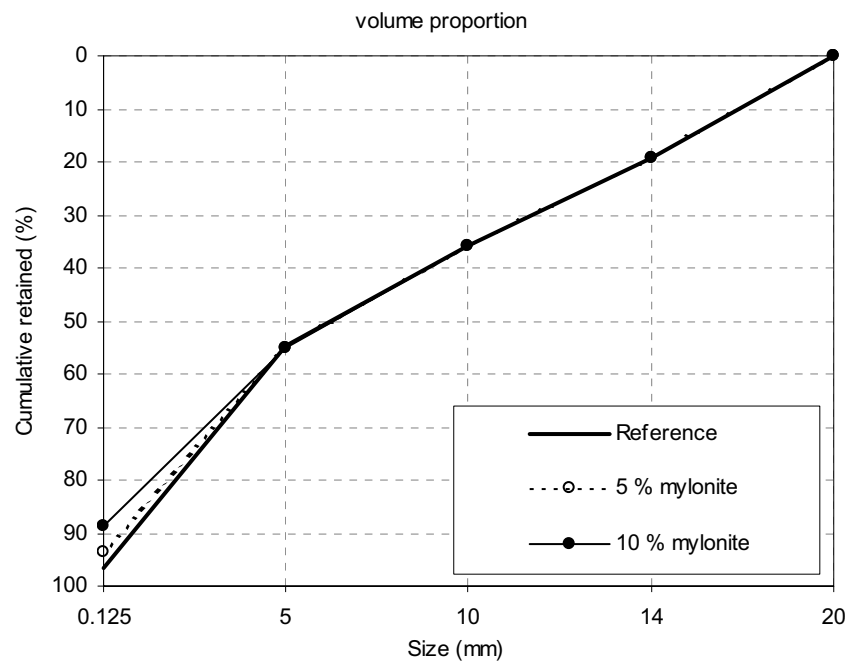
Density of fillers: (kg/m³)

Mylonite	2.78
Cataclasite	2.76
Granite/ gneiss	2.67
Limestone	2.70
Carbonate	2.71
Glass	2.49
Rhyolite	2.51
Fly ash	2.24
Quartz	2.65

A3: Mix design of concretes tested by the concrete prism test (CPT)

Recipes and gradings for the reference mix and the mixes with 5.15 and 10.3 volume % mylonite 0-125 filler. The other fillers were tested at the same amounts as mylonite 0-125 filler on a volume basis.

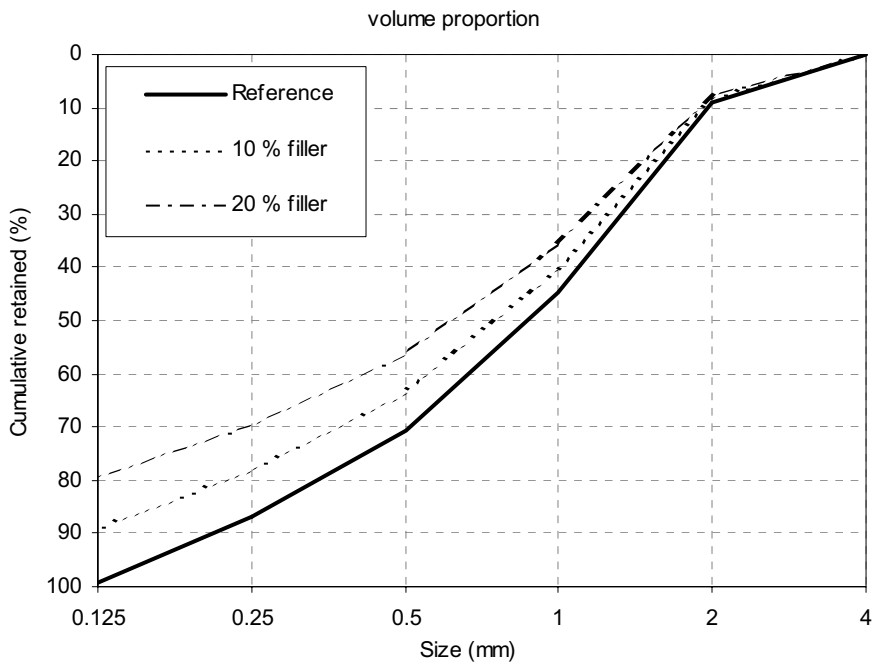
Materials (amounts in kg/m ³)	Reference	5.15 % mylonite filler	10.3 % mylonite filler
OPC	400	400	400
Water	180	180	180
Granite 0-125 filler	36.4	-	-
Mylonite 0-125 filler	-	95.7	191.6
Granite 0-5	764.1	704.4	613.1
Mylonite 5-8	345.7	346.4	346.7
Mylonite 11-16	491.2	492.2	492.7
Mylonite 16-20	181.9	182.3	191.6
SSP 2000	0.8	1.2	4.0
NaOH	1.17	1.17	1.17
w/c ratio	0.45	0.45	0.45



A4: Mix design of mortars tested by the accelerated mortar bar test (AMBT)

Recipes and gradings for the reference mix and the mixes with 10 and 20 volume % mylonite 0-125 filler. The other fillers were tested at the same amounts as mylonite 0-125 filler on a volume basis.

Materials (amounts in kg/m ³)	Reference no filler	10 % mylonite 0-125 filler	20 % mylonite 0-125 filler
OPC	596.5	596.5	596.5
Water	280.4	280.4	280.4
Mylonite 0 - 125 filler	-	143.1	286.2
Mylonite 0 - 4 mm	1431.7	1288.3	1144.7
SSP 2000 (15 %)	2.4	3.4	4.7
w/c ratio	0.47	0.47	0.47

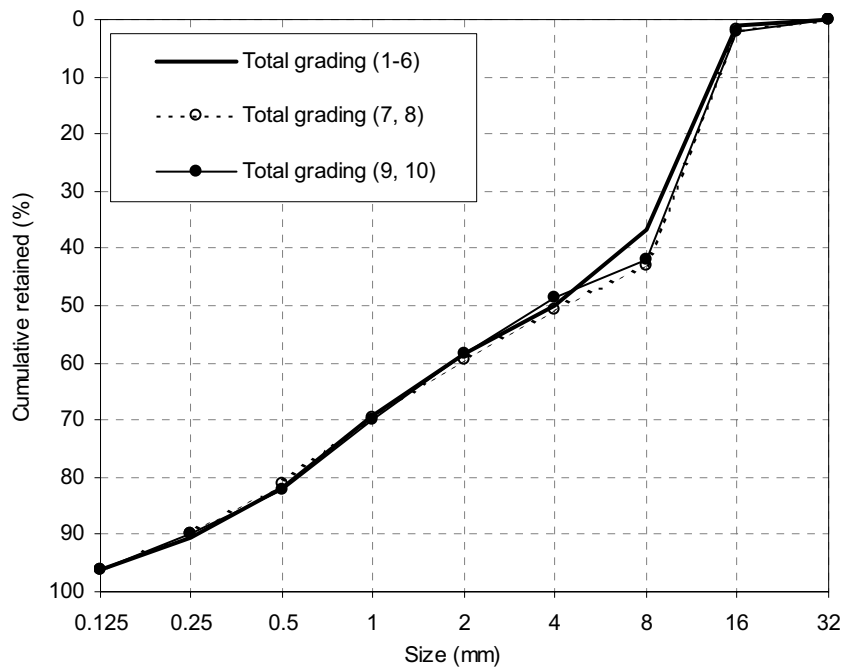


A5: Mix design of self-compacting concretes

Example of recipe for series 1, 325 litres matrix volume/m³. Amounts in kg/m³.

HSOPC	355.9
Silica fume	17.8
Limestone filler	71.2
Water	149.5
Granite 0-8	1047.0
Granite 8-11	361.0
Granite 11-16	397.1
Scanflux CP 30	4.12
Matrix volume	325
w/c ratio	0.40
w/p ratio	0.29

Total aggregate grading (Årdal granite/gneiss). The grading was kept constant independently of the matrix volume. Note that the retained amount at the 8 mm sieve differed for series 7-10 due to different gradings of the 8-11 fractions.



Appendix B

- B1 Results of pozzolanic reactivity
- B2 Concrete results – alkali-silica reactions, compressive strength and capillary suction
- B3 Mortar results
- B4 Electron probe microanalyzer, chemical data and photos

B1: Results pozzolanic reactivity

Description	days	weight loss due to CH decomposition (mg)	weight loss 105-1000°C (mg)	remaining CH (mg)	loss of CH (%)
Mylonite 0-20 pH = 13.5, 5°C	0	6.50	13.31	26.75	0.0
	90	6.38	12.92	26.26	1.8
Mylonite 0-20 pH = 13.0 20°C	0	6.50	13.31	26.75	0.0
	28	6.23	13.08	25.64	4.2
	90	6.04	13.32	24.86	7.1
Mylonite 0-20 pH = 13.5 20°C	0	6.84	12.34	28.15	0.0
	1	6.79	12.90	27.94	0.7
	3	6.64	13.53	27.33	2.9
	7	6.62	14.18	27.24	3.2
	28	6.22	13.67	25.60	9.1
	90	6.42	14.68	26.42	6.1
Mylonite 0-20 pH = 14.0 20°C	0	6.79	13.00	27.94	0.0
	1	6.60	13.05	27.16	2.8
	7	6.44	13.57	26.50	5.2
	28	6.64	14.31	27.33	2.2
90	6.02	13.69	24.78	11.3	
Mylonite 10-30 pH = 13.5, 20°C	0	7.32	13.19	30.13	0.0
90	6.18	12.81	25.43	15.6	
Mylonite 20-125 pH = 13.5, 20°C	0	7.35	13.09	30.25	0.0
	90	6.48	11.98	26.67	11.8
Mylonite 0-20 pH = 13.5 38°C	0	6.84	12.34	28.15	0.0
	1	6.62	12.92	27.24	3.2
	7	6.15	13.21	25.31	10.1
	28	5.81	13.04	23.91	15.1
90	4.93	13.77	20.29	27.9	
Mylonite 0-20 pH = 13.5 80°C	0	6.73	12.83	27.70	0.0
	1	6.12	12.82	25.19	9.1
	7	4.44	13.03	18.27	34.0
28	2.43	13.75	10.00	63.9	
Rhyolite 0-20* pH = 13.5 20°C	0	6.75	16.73	27.78	0.0
	1	5.92	14.58	24.36	12.3
	7	4.89	17.17	20.13	27.6
	28	1.83	17.01	7.53	72.9
Rhyolite 0-20* pH = 13.5 20°C	0	7.10	14.60	29.22	0.0
	7	5.01	14.25	20.62	29.4
	7	4.51	14.71	18.56	36.5
	7	4.56	12.53	18.77	35.8
28	2.47	14.88	10.17	65.2	
Rhyolite 0-20 pH = 13.5 80°C	0	7.10	14.60	29.22	0.0
	1	2.06	15.33	8.48	71.0
	7	0.37	14.37	1.52	94.8
	28	0.00	15.32	0.00	100.0

* Identical recipes and test conditions, different batches.

Description	days	weight loss due to CH decomposition (mg)	weight loss 105-1000°C (mg)	remaining CH (mg)	loss of CH (%)
Fly ash 0-20 pH = 13.5 80°C	0	6.87	10.93	28.3	0.0
	1	7.25	12.34	29.8	-5.5
	3	6.47	12.15	26.6	5.8
	7	5.21	11.88	21.4	24.2
	28	2.89	12.92	11.9	57.9
	90	0.74	14.66	3.0	89.2
Glass 0-20 pH = 13.5, 20°C	0	6.53	12.53	26.9	0.0
	28	1.73	13.24	7.1	73.5
Cataclasite 0-20 pH = 13.5, 20°C	0	6.99	12.78	28.8	0.0
	90	4.74	12.81	19.5	32.2
Quartz 0-125 pH = 13.5, 20°C	0	7.81	11.00	32.1	0.0
	90	6.18	9.05	25.4	20.9
Granite 0-20 pH = 13.5 80°C	0	6.88	10.45	28.3	0.0
	1	6.15	10.35	25.3	10.6
	7	4.67	10.46	19.2	32.1
	28	2.34	11.21	9.6	66.0

B2: Concrete results - fresh properties, compressive strength, capillary suction

Mix nr.	Mix design					
	cement	fine aggreg. (< 5 mm)	coarse aggreg. (> 5 mm)	filler type	filler amount (vol. % of aggr.)	Na ₂ O eqv. (kg/m ³)
1 (ref)	OPC	granite	mylonite	granite 0-125	2.00	5.00
2	OPC	granite	mylonite	mylonite 0-125	5.15	5.00
24	OPC	granite	mylonite	mylonite 0-125	5.15	5.00
27	OPC	granite	mylonite	mylonite 0-125	5.15	5.00
Mean of 2, 24 and 27						
3	OPC	granite	mylonite	mylonite 0-125	10.30	5.00
4	OPC	granite	mylonite	cataclasite 0-125	5.15	5.00
5	OPC	granite	mylonite	rhyolite 0-125	5.15	5.00
6	OPC	granite	mylonite	mylonite 0-20	5.15	5.00
7	OPC	granite	mylonite	mylonite 10-30	5.15	5.00
8	OPC	granite	mylonite	mylonite 0-125	5.15	4.08
9	OPC	granite	mylonite	mylonite 0-125	10.30	4.08
10	OPC	granite	mylonite	fly ash 0-125	5.15	5.00
11	OPC	granite	mylonite	silica fume	5.00*	4.08
25	OPC	granite	mylonite	silica fume	5.00*	4.08
28	OPC	granite	mylonite	silica fume	5.00*	4.08
Mean of 11, 25 and 28						
12	OPC	granite	mylonite	silica fume	7.50*	4.08
13	OPC	granite	mylonite	silica fume	7.50*	5.00
14	ROPC	granite	mylonite	mylonite 0-125	5.15	5.00
15	HSOPC	granite	mylonite	mylonite 0-125	5.15	5.00
16	OPC	granite	mylonite	mylonite 0-125	10.30	10.00
17	OPC	granite	mylonite	silica fume	7.50*	10.00
18	OPC	granite	mylonite	glass 0-125	5.15	5.00
19	OPC	granite	mylonite	mylonite 0-125	2.00	5.00
20	OPC	mylonite	granite	mylonite 0-125	6.00	5.00
21	OPC	mylonite**	granite	granite 0-125	6.00	5.00
22	OPC	granite	spratt	granite 0-125	2.00	5.00
23	OPC	granite	spratt	mylonite 0-20	5.15	5.00
26 (ref)	OPC	granite	mylonite	granite 0-125	2.00	4.08
29	OPC	granite	mylonite	rhyolite 0-20	5.15	5.00
91	OPC	granite	mylonite	granite 0-125	2.00	4.08
92	OPC	granite	mylonite	mylonite 0-125	5.15	4.08
93	OPC	granite	mylonite	mylonite 0-20	5.15	4.08
94	OPC	granite	mylonite	rhyolite 0-125	5.15	4.08
95	OPC	granite	mylonite	granite 0-20	5.15	4.08
Mean of 26 and 91						
Mean of 8 and 92						

*Amount of silica fume in weight % of cement

** Filler removed by sieving

Mix 91-95: only compressive strength and capillary suction testing

Mix nr.	Compressive strength (MPa)											
	1 day				28 days				1 year			
				Mean				Mean				Mean
1	28.7	28.7	28.9	28.8	46.9	45.2	49.4	47.2	70.9	68.6	69.5	69.7
2	30.6	31.2	30.5	30.8	50.9	48.9	50.3	50.0	67.8	68.0	68.3	68.0
24	33.8	33.0	33.5	33.4	53.6	53.9	53.3	53.6	63.7	73.3	72.1	69.7
27	32.1	32.8	33.0	32.6	52.8	51.5	51.8	52.0	70.0	68.7	69.4	69.4
2, 24, 27				32.3				51.9				69.0
3	31.3	31.6	32.0	31.6	56.8	57.0	56.7	56.8	73.8	73.8	73.9	73.8
4	31.5	31.1	32.7	31.8	52.3	54.1	54.5	53.6	71.8	72.5	71.7	72.0
5	34.9	34.6	34.7	34.7	61.8	60.8	59.1	60.6	80.8	80.3	80.3	80.5
6	34.0	35.9	35.0	35.0	57.7	57.9	58.1	57.9	72.9	73.5	73.8	73.4
7	35.9	35.7	35.6	35.7	56.0	55.2	56.7	56.0	69.9	72.1	74.6	72.2
8	32.0	33.2	33.5	32.9	57.3	57.3	58.6	57.7	74.7	73.4	74.7	74.2
9	34.5	35.2	34.8	34.8	64.3	64.8	64.8	64.6	80.5	79.7	80.2	80.1
10	35.2	35.9	35.8	35.6	56.2	54.2	57.1	55.8	80.7	81.2	84.0	82.0
11	35.0	36.9	35.6	35.8	68.7	68.2	62.3	66.4	76.7	80.1	78.7	78.5
25	32.6	33.6	33.9	33.4	66.6	66.2	64.3	65.7	80.3	81.3	81.1	80.9
28	32.4	32.7	32.0	32.3	64.3	63.8	63.5	63.8	77.2	75.8	77.2	76.7
11, 25, 28				33.8				65.3				78.7
12	37.1	37.7	37.4	37.4	73.7	73.6	73.1	73.5	88.3	85.7	85.6	86.6
13	35.3	34.5	34.5	34.8	68.1	68.3	65.0	67.1	77.6	77.3	78.6	77.8
14	47.2	46.2	47.3	46.9	66.3	65.7	63.2	65.1	80.5	80.3	84.5	81.8
15	24.9	25.7	25.6	25.4	43.4	41.6	39.2	41.4	61.2	62.2	62.3	61.9
16	20.6	20.6	20.4	20.5	30.8	34.1	36.4	33.8	53.1	52.6	54.5	53.4
17	26.8	26.8	26.4	26.7	55.5	55.9	54.9	55.4	66.9	67.8	67.1	67.3
18	34.7	33.9	33.3	34.0	53.6	53.6	54.3	53.8	74.2	76.3	78.8	76.4
19	32.0	31.6	31.6	31.7	51.6	51.0	50.6	51.1	77.2	76.9	76.8	77.0
20	35.9	35.0	35.5	35.5	60.9	60.6	59.4	60.3	77.2	76.9	76.8	77.0
21	38.1	38.9	39.2	38.7	52.7	52.0	53.3	52.7	78.0	76.7	77.1	77.3
22	30.7	30.4	29.1	30.1	50.9	50.1	50.9	50.6	62.2	62.1	63.2	62.5
23	30.6	30.6	32.3	31.2	59.7	66.5	61.2	62.5	63.4	65.0	62.9	63.8
26	26.8	28.0	27.8	27.5	51.0	50.7	51.4	51.0	70.0	69.2	70.0	69.7
29	33.2	33.7	34.5	33.8	56.2	56.3	56.9	56.5	78.9	78.6	74.4	77.3
91	32.2	32.3	31.6	32.0	55.4	55.5	53.9	54.9	70.7	70.7	72.8	71.4
92	34.6	34.1	34.1	34.3	55.7	54.7	56.3	55.6	69.4	70.7	71.8	70.6
93	34.8	33.6	34.5	34.3	53.4	55.4	56.7	55.2	63.9	67.5	69.4	66.9
94	34.9	36.9	36.4	36.1	61.7	62.5	62.3	62.2	82.6	83.5	80.7	82.3
95	34.4	35.1	33.9	34.5	57.7	57.3	50.2	55.1	70.6	68.1	70.0	69.6
26, 91				29.8				53.0				70.6
8, 92				33.6				56.7				72.4

Mix nr.	Fresh properties			Capillary suction testing				
	slump (cm)	air (%)	density (kg/m ³)	k (*E ⁻²) (s/m ²)	m (*E ⁷) (kg/m ² *s ^{0.5})	suction porosity (%)	macro porosity (%)	total porosity (%)
1	14.0	1.8	2446	1.75	4.26	11.7	1.1	12.8
2	13.5	2.0	2446	1.85	4.84	13.1	1.3	14.4
24	15.0	2.1	2446	1.62	5.54	12.2	1.2	13.4
27	10.5	2.7	2424	1.79	4.95	12.5	1.6	14.1
2, 24, 27	13.0	2.3	2439	1.75	5.11	12.6	1.4	14.0
3	12.0	1.9	2447	1.73	5.62	13.2	1.3	14.5
4	16.0	2.6	2426	1.46	6.57	12.0	1.7	13.7
5	7.0	2.0	2441	1.26	9.30	13.4	2.0	15.4
6	23.0	1.3	2448	1.27	7.70	11.3	0.9	12.2
7	11.5	1.9	2441	1.38	7.16	12.0	1.1	13.1
8	18.0	1.8	2437	1.43	6.40	11.6	1.1	12.7
9	24.0	1.0	2445	1.38	7.16	12.0	1.1	13.1
10	13.5	2.2	2421	1.15	11.50	12.8	1.6	14.4
11	14.0	2.7	2417	1.29	9.02	12.5	2.1	14.6
25	16.0	2.5	2419	1.65	6.02	12.8	1.6	14.4
28	16.0	2.6	2400	1.80	4.90	12.8	1.4	14.2
11, 25, 28	15.3	2.6	2412	1.58	6.65	12.7	1.7	14.4
12	13.5	2.6	2413	1.15	11.20	12.4	2.1	14.5
13	6.0	2.3	2427	1.31	9.99	13.3	1.6	14.9
14	14.5	2.5	2424	1.50	5.98	11.8	1.6	13.4
15	14.0	3.1	2409	1.68	5.27	12.6	2.0	14.6
16	3.0	2.1	2439	1.52	7.63	13.7	1.3	15.0
17	3.5	2.0	2445	1.66	6.58	13.9	1.6	15.5
18	15.0	3.1	2406	1.45	7.43	12.8	2.4	15.2
19	15.5	2.8	2415	1.67	4.62	11.6	1.2	12.8
20	13.5	1.7	2443	1.80	4.96	12.9	1.3	14.2
21	7.5	1.8	2443	1.75	4.84	12.4	1.2	13.6
22	14.0	2.3	2397	1.90	4.12	12.7	1.4	14.1
23	19.0	1.3	2418	1.85	4.86	13.3	1.1	14.4
26	16.0	2.7	2408	1.79	4.37	11.9	1.5	13.4
29	16.0	2.6	2411	1.43	8.12	13.0	1.8	14.8
91	14.5	2.1	2448	1.76	4.24	11.7	1.4	13.1
92	17.5	1.7	2441	1.87	4.52	12.8	1.2	14.0
93	19.0	1.3	2433	1.97	4.33	13.1	1.1	14.2
94	11.0	1.9	2424	1.50	6.88	12.8	1.8	14.6
95	22.0	1.0	2444	1.69	4.28	11.2	0.7	11.9
26, 91	15.3	2.4	2428	1.78	4.31	11.8	1.5	13.3
8, 92	17.8	1.8	2439	1.65	5.46	12.2	1.2	13.4

Concrete prism test – expansion and weight data

Mix nr.		Weeks								
		1	2	4	8	12	16	26	52	104
1	Expansion (%)	-0.004	-0.003	0.000	0.005	0.012	0.016	0.032	0.088	
		-0.003	-0.003	-0.002	0.002	0.009	0.015	0.03	0.104	0.189
		-0.003	-0.003	-0.002	0.002	0.007	0.012	0.026	0.088	0.169
	Mean (%)	-0.003	-0.003	-0.001	0.003	0.009	0.015	0.029	0.093	0.179
	St. deviation	0.001	0.000	0.001	0.002	0.002	0.002	0.003	0.009	0.014
	Weight increase (%)	0.063	0.117	0.162	0.225	0.315	0.342	0.424	0.595	-
		0.054	0.108	0.154	0.199	0.289	0.316	0.398	0.605	0.840
	Mean (%)	0.057	0.111	0.153	0.210	0.294	0.324	0.396	0.594	0.827
St. deviation	0.005	0.005	0.010	0.014	0.020	0.016	0.028	0.012	0.019	
2	Expansion (%)	0.000	-0.001	0.001	0.006	0.009	0.014	0.035	0.139	
		-0.001	-0.001	0.000	0.005	0.008	0.016	0.033	0.128	0.21
		-0.001	0.000	0.000	0.006	0.008	0.014	0.034	0.126	0.194
	Mean (%)	-0.001	-0.001	0.000	0.005	0.008	0.015	0.034	0.131	0.202
	St. deviation	0.000	0.001	0.001	0.000	0.000	0.001	0.001	0.007	0.011
	Weight increase (%)	0.108	0.162	0.216	0.287	0.368	0.404	0.503	0.728	
		0.082	0.136	0.191	0.273	0.355	0.391	0.464	0.691	0.973
	Mean (%)	0.096	0.151	0.205	0.283	0.365	0.404	0.491	0.715	0.976
St. deviation	0.013	0.013	0.013	0.009	0.009	0.013	0.024	0.020	0.004	
3	Expansion (%)	-0.002	-0.002	-0.001	0.001	0.006	0.011	0.03	0.114	0.183
		-0.003	-0.002	-0.001	0.002	0.006	0.009	0.028	0.128	0.194
		-0.003	-0.003	0.000	0.002	0.006	0.009	0.026	0.11	0.168
	Mean (%)	-0.003	-0.003	-0.001	0.002	0.006	0.010	0.028	0.117	0.182
	St. deviation	0.000	0.000	0.000	0.000	0.000	0.001	0.002	0.010	0.013
	Weight increase (%)	0.126	0.189	0.243	0.306	0.396	0.441	0.531	0.783	1.062
		0.106	0.159	0.220	0.291	0.379	0.405	0.493	0.766	1.004
	Mean (%)	0.113	0.173	0.233	0.298	0.382	0.415	0.501	0.763	1.017
St. deviation	0.011	0.015	0.012	0.008	0.013	0.023	0.027	0.021	0.040	
4	Expansion (%)	-0.001	-0.001	0.001	0.005	0.009	0.016	0.037	0.125	0.191
		-0.002	-0.003	0.000	0.004	0.009	0.016	0.035	0.118	0.183
		-0.003	-0.002	-0.002	0.005	0.007	0.014	0.039	0.134	0.199
	Mean (%)	-0.002	-0.002	0.000	0.005	0.009	0.015	0.037	0.126	0.191
	St. deviation	0.001	0.001	0.001	0.000	0.001	0.001	0.002	0.008	0.008
	Weight increase (%)	0.127	0.172	0.236	0.309	0.39	0.417	0.544	0.708	0.989
		0.098	0.152	0.214	0.286	0.366	0.402	0.500	0.724	1.018
	Mean (%)	0.102	0.153	0.213	0.282	0.363	0.396	0.508	0.697	0.979
St. deviation	0.023	0.019	0.023	0.028	0.028	0.024	0.034	0.034	0.045	

Mix nr.		Weeks								
		1	2	4	8	12	16	26	52	104
5	Expansion (%)	-0.003	-0.003	-0.001	0.001	0.002	0.004	0.008	0.018	-
		-0.004	-0.003	-0.003	0.000	0.001	0.003	0.007	0.016	0.039
		-0.004	-0.003	-0.001	0.001	0.002	0.005	0.008	0.017	0.042
	Mean (%)	-0.004	-0.003	-0.002	0.001	0.002	0.004	0.007	0.017	0.041
	St. deviation	0.001	0.001	0.001	0.001	0.001	0.001	0.001	0.001	0.002
	Weight increase (%)	0.127	0.154	0.181	0.236	0.272	0.281	0.317	0.390	-
0.098		0.134	0.170	0.214	0.250	0.259	0.286	0.375	0.527	
0.109		0.146	0.182	0.237	0.255	0.282	0.310	0.364	0.537	
Mean (%)	0.111	0.145	0.178	0.229	0.259	0.274	0.304	0.376	0.532	
St. deviation	0.014	0.010	0.007	0.013	0.011	0.013	0.017	0.013	0.008	
6	Expansion (%)	-0.003	-0.001	0.004	0.006	0.010	0.016	0.035	0.133	0.204
		-0.004	-0.003	0.000	0.004	0.007	0.014	0.033	0.132	0.189
		-0.003	-0.003	-0.001	0.003	0.007	0.014	0.034	0.142	0.238
	Mean (%)	-0.003	-0.002	0.001	0.005	0.008	0.014	0.034	0.136	0.210
	St. deviation	0.000	0.001	0.002	0.002	0.002	0.002	0.001	0.006	0.025
	Weight increase (%)	0.146	0.201	0.265	0.347	0.411	0.456	0.511	0.739	0.995
0.137		0.183	0.256	0.339	0.403	0.439	0.503	0.750	0.970	
0.133		0.195	0.266	0.355	0.417	0.471	0.533	0.728	1.057	
Mean (%)	0.139	0.193	0.262	0.347	0.410	0.455	0.516	0.739	1.007	
St. deviation	0.007	0.009	0.005	0.008	0.007	0.016	0.015	0.011	0.045	
7	Expansion (%)	-0.003	0.000	0.004	0.008	0.012	0.018	0.039	0.110	0.174
		-0.005	-0.003	0.000	0.004	0.010	0.015	0.040	0.129	0.202
		-0.006	-0.003	0.000	0.005	0.008	0.014	0.039	0.135	0.205
	Mean (%)	-0.005	-0.002	0.001	0.005	0.010	0.016	0.040	0.125	0.193
	St. deviation	0.002	0.002	0.002	0.002	0.002	0.002	0.001	0.013	0.017
	Weight increase (%)	0.127	0.190	0.254	0.362	0.426	0.453	0.580	0.788	1.023
0.097		0.168	0.220	0.318	0.379	0.415	0.529	0.723	0.988	
0.099		0.163	0.217	0.316	0.370	0.415	0.515	0.723	0.966	
Mean (%)	0.108	0.173	0.230	0.332	0.392	0.428	0.541	0.745	0.992	
St. deviation	0.017	0.015	0.020	0.026	0.030	0.022	0.034	0.037	0.029	
8	Expansion (%)	-0.004	-0.002	0.001	0.005	0.007	0.011	0.024	0.131	0.238
		-0.003	0.000	0.005	0.008	0.010	0.014	0.026	0.121	0.217
		-0.003	-0.002	0.001	0.004	0.007	0.008	0.022	0.133	0.226
	Mean (%)	-0.003	-0.001	0.002	0.006	0.008	0.011	0.024	0.129	0.227
	St. deviation	0.001	0.001	0.003	0.002	0.002	0.003	0.002	0.006	0.010
	Weight increase (%)	0.100	0.200	0.264	0.391	0.473	0.537	0.582	0.764	1.056
0.089		0.170	0.224	0.331	0.394	0.438	0.492	0.662	0.966	
0.100		0.173	0.227	0.345	0.400	0.454	0.509	0.663	0.927	
Mean (%)	0.097	0.181	0.238	0.356	0.422	0.477	0.528	0.697	0.983	
St. deviation	0.006	0.017	0.022	0.032	0.044	0.053	0.048	0.059	0.066	

Mix nr.		Weeks								
		1	2	4	8	12	16	26	52	104
9	Expansion (%)	-0.005	-0.003	-0.001	0.004	0.006	0.008	0.023	0.112	0.220
		-0.005	-0.003	-0.002	0.003	0.005	0.007	0.020	0.122	0.190
		-0.005	-0.003	0.000	0.004	0.006	0.008	0.023	0.119	0.216
	Mean (%)	-0.005	-0.003	-0.001	0.003	0.006	0.008	0.022	0.118	0.209
	St. deviation	0.000	0.000	0.001	0.001	0.001	0.001	0.001	0.005	0.017
	Weight increase (%)	0.118	0.199	0.253	0.362	0.416	0.443	0.524	0.678	0.976
		0.133	0.240	0.302	0.426	0.488	0.524	0.612	0.808	1.021
		0.090	0.199	0.253	0.370	0.425	0.452	0.533	0.750	1.003
Mean (%)	0.114	0.212	0.269	0.386	0.443	0.473	0.557	0.745	1.000	
St. deviation	0.022	0.024	0.028	0.035	0.040	0.044	0.049	0.065	0.022	
10	Expansion (%)	-0.007	-0.007	-0.006	-0.006	-0.006	-0.005	-0.002	0.003	-
		-0.008	-0.008	-0.006	-0.007	-0.007	-0.007	-0.004	0.004	0.020
		-0.008	-0.008	-0.007	-0.006	-0.006	-0.006	-0.001	0.004	0.019
	Mean (%)	-0.008	-0.008	-0.006	-0.006	-0.006	-0.006	-0.002	0.004	0.020
	St. deviation	0.001	0.001	0.000	0.001	0.001	0.001	0.001	0.001	0.001
	Weight increase (%)	0.174	0.229	0.265	0.330	0.348	0.375	0.412	0.467	-
		0.144	0.189	0.234	0.288	0.306	0.333	0.351	0.423	0.566
		0.118	0.181	0.226	0.281	0.290	0.317	0.344	0.417	0.561
Mean (%)	0.145	0.200	0.242	0.299	0.314	0.342	0.369	0.435	0.564	
St. deviation	0.028	0.026	0.021	0.026	0.030	0.030	0.037	0.027	0.003	
11	Expansion (%)	-0.005	-0.005	-0.002	0.002	-0.001	0.000	0.005	0.017	0.053
		-0.005	-0.005	-0.005	-0.002	-0.002	-0.004	0.003	0.016	0.052
		-0.006	-0.006	-0.003	-0.002	-0.002	-0.003	0.003	0.018	0.058
	Mean (%)	-0.005	-0.005	-0.003	-0.001	-0.002	-0.002	0.004	0.017	0.054
	St. deviation	0.001	0.001	0.002	0.002	0.001	0.002	0.001	0.001	0.003
	Weight increase (%)	0.129	0.157	0.194	0.249	0.277	0.323	0.379	0.508	0.775
		0.116	0.143	0.170	0.233	0.260	0.295	0.340	0.483	0.752
		0.118	0.146	0.173	0.218	0.255	0.282	0.337	0.491	0.774
Mean (%)	0.121	0.149	0.179	0.233	0.264	0.300	0.352	0.494	0.767	
St. deviation	0.007	0.007	0.013	0.015	0.012	0.021	0.023	0.012	0.013	
12	Expansion (%)	-0.008	-0.008	-0.008	-0.004	-0.003	-0.004	-0.003	0.008	0.041
		-0.009	-0.009	-0.010	-0.006	-0.006	-0.005	-0.006	0.007	0.043
		-0.009	-0.009	-0.009	-0.006	-0.004	-0.005	-0.004	0.007	0.037
	Mean (%)	-0.009	-0.009	-0.009	-0.005	-0.004	-0.005	-0.005	0.007	0.040
	St. deviation	0.001	0.001	0.001	0.001	0.001	0.001	0.001	0.000	0.003
	Weight increase (%)	0.118	0.146	0.164	0.209	0.246	0.255	0.300	0.428	0.719
		0.110	0.146	0.165	0.210	0.247	0.265	0.311	0.448	0.750
		0.100	0.118	0.145	0.190	0.227	0.227	0.281	0.408	0.644
Mean (%)	0.109	0.137	0.158	0.203	0.240	0.249	0.297	0.428	0.704	
St. deviation	0.009	0.016	0.011	0.011	0.011	0.020	0.015	0.020	0.055	

Mix nr.		Weeks								
		1	2	4	8	12	16	26	52	104
13	Expansion (%)	-0.009	-0.012	-0.011	-0.006	-0.006	-0.005	-0.003	0.011	0.049
		-0.008	-0.010	-0.009	-0.005	-0.004	-0.005	-0.001	0.010	0.051
		-0.007	-0.011	-0.009	-0.006	-0.006	-0.007	-0.004	0.008	0.042
	Mean (%)	-0.008	-0.011	-0.010	-0.006	-0.005	-0.005	-0.003	0.009	0.048
	St. deviation	0.001	0.001	0.001	0.001	0.001	0.001	0.002	0.001	0.005
	Weight increase (%)	0.120	0.148	0.175	0.212	0.249	0.277	0.314	0.470	0.756
		0.100	0.137	0.164	0.200	0.237	0.255	0.301	0.447	0.766
		0.100	0.127	0.154	0.200	0.227	0.254	0.300	0.436	0.699
Mean (%)	0.107	0.137	0.165	0.204	0.238	0.262	0.305	0.451	0.740	
St. deviation	0.011	0.010	0.010	0.007	0.011	0.013	0.008	0.018	0.036	
14	Expansion (%)	-0.003	-0.004	-0.001	0.005	0.010	0.014	0.038	0.142	0.209
		-0.004	-0.004	0.001	0.008	0.009	0.014	0.042	0.166	0.261
		-0.004	-0.004	0.000	0.006	0.009	0.014	0.037	0.149	0.224
	Mean (%)	-0.004	-0.004	0.000	0.006	0.009	0.014	0.039	0.153	0.231
	St. deviation	0.000	0.000	0.001	0.001	0.001	0.001	0.003	0.013	0.026
	Weight increase (%)	0.175	0.230	0.303	0.432	0.505	0.542	0.661	0.873	1.121
		0.152	0.215	0.286	0.403	0.474	0.510	0.626	0.886	1.190
		0.145	0.208	0.280	0.380	0.452	0.488	0.588	0.841	1.121
Mean (%)	0.157	0.217	0.290	0.405	0.477	0.513	0.625	0.866	1.144	
St. deviation	0.016	0.011	0.012	0.026	0.027	0.027	0.037	0.023	0.040	
15	Expansion (%)	-0.004	-0.002	-0.002	0.002	0.004	0.009	0.021	0.094	0.131
		-0.002	-0.001	0.000	0.004	0.006	0.009	0.021	0.090	0.124
		-0.003	-0.001	-0.001	0.004	0.006	0.009	0.021	0.095	0.142
	Mean (%)	-0.003	-0.002	-0.001	0.003	0.006	0.009	0.021	0.093	0.132
	St. deviation	0.001	0.001	0.001	0.001	0.001	0.000	0.000	0.003	0.009
	Weight increase (%)	0.111	0.176	0.222	0.296	0.343	0.380	0.454	0.723	0.899
		0.081	0.145	0.208	0.280	0.343	0.370	0.461	0.741	0.921
		0.055	0.118	0.182	0.245	0.300	0.327	0.391	0.673	0.900
Mean (%)	0.082	0.146	0.204	0.274	0.329	0.359	0.435	0.712	0.907	
St. deviation	0.028	0.029	0.021	0.026	0.025	0.028	0.039	0.035	0.013	
16	Expansion (%)	-0.002	-0.001	-0.001	0.004	0.009	0.015	0.032	0.069	0.135
		-0.003	-0.001	-0.001	0.005	0.009	0.015	0.030	0.073	0.143
		-0.001	0.000	-0.001	0.005	0.009	0.015	0.029	0.070	0.127
	Mean (%)	-0.002	-0.001	-0.001	0.004	0.009	0.015	0.030	0.071	0.135
	St. deviation	0.001	0.001	0.000	0.001	0.000	0.000	0.001	0.002	0.008
	Weight increase (%)	0.081	0.109	0.154	0.208	0.254	0.281	0.362	0.589	0.833
		0.071	0.079	0.124	0.176	0.238	0.247	0.344	0.582	0.803
		0.062	0.080	0.124	0.186	0.221	0.248	0.337	0.576	0.788
Mean (%)	0.071	0.089	0.134	0.190	0.238	0.259	0.348	0.582	0.808	
St. deviation	0.010	0.017	0.017	0.016	0.016	0.019	0.013	0.006	0.023	

Mix nr.		Weeks								
		1	2	4	8	12	16	26	52	104
17	Expansion (%)	-0.010	-0.012	-0.010	-0.005	-0.002	-0.002	0.010	0.039	0.085
		-0.012	-0.011	-0.010	-0.004	0.000	-0.001	0.010	0.034	0.094
		-0.013	-0.012	-0.010	-0.005	-0.001	-0.001	0.009	0.039	0.098
	Mean (%)	-0.012	-0.012	-0.010	-0.005	-0.001	-0.001	0.010	0.037	0.093
	St. deviation	0.002	0.000	0.000	0.000	0.001	0.001	0.001	0.003	0.007
	Weight increase (%)	0.081	0.099	0.144	0.189	0.225	0.243	0.333	0.549	0.854
		0.091	0.109	0.154	0.200	0.236	0.254	0.336	0.563	0.926
		0.081	0.100	0.136	0.181	0.226	0.235	0.326	0.570	0.869
Mean (%)	0.084	0.102	0.145	0.190	0.229	0.244	0.332	0.561	0.883	
St. deviation	0.006	0.006	0.009	0.009	0.006	0.010	0.005	0.011	0.038	
18	Expansion (%)	-0.008	-0.008	-0.006	-0.003	-0.001	0.001	0.006	0.018	-
		-0.009	-0.009	-0.006	-0.003	-0.003	-0.001	0.004	0.016	0.044
		-0.009	-0.009	-0.006	-0.004	-0.003	-0.001	0.005	0.018	0.043
	Mean (%)	-0.009	-0.008	-0.006	-0.003	-0.002	0.000	0.005	0.017	0.043
	St. deviation	0.001	0.001	0.000	0.001	0.001	0.001	0.001	0.001	0.000
	Weight increase (%)	0.137	0.192	0.229	0.293	0.321	0.339	0.376	0.495	-
		0.100	0.163	0.200	0.254	0.281	0.290	0.327	0.445	0.644
		0.117	0.171	0.216	0.262	0.289	0.307	0.343	0.460	0.667
Mean (%)	0.118	0.176	0.215	0.270	0.297	0.312	0.348	0.467	0.656	
St. deviation	0.019	0.015	0.015	0.021	0.021	0.025	0.025	0.026	0.016	
19	Expansion (%)	-0.004	-0.004	0.001	0.006	0.008	0.012	0.028	0.103	0.198
		-0.004	-0.003	0.001	0.006	0.009	0.013	0.029	0.106	0.198
		-0.005	-0.004	0.001	0.006	0.007	0.011	0.031	0.125	0.212
	Mean (%)	-0.004	-0.003	0.001	0.006	0.008	0.012	0.029	0.111	0.203
	St. deviation	0.000	0.001	0.000	0.000	0.001	0.001	0.001	0.012	0.008
	Weight increase (%)	0.138	0.203	0.276	0.396	0.461	0.497	0.599	0.829	1.105
		0.081	0.154	0.217	0.317	0.398	0.416	0.488	0.742	1.004
		0.082	0.145	0.199	0.299	0.363	0.399	0.481	0.716	0.943
Mean (%)	0.100	0.167	0.231	0.337	0.407	0.437	0.523	0.762	1.017	
St. deviation	0.033	0.031	0.040	0.052	0.050	0.053	0.066	0.059	0.082	
20	Expansion (%)	-0.005	-0.002	0.001	0.005	0.007	0.010	0.019	0.066	-
		-0.006	-0.001	0.000	0.005	0.008	0.010	0.020	0.071	0.122
		-0.004	-0.001	0.000	0.007	0.008	0.011	0.019	0.070	0.136
	Mean (%)	-0.005	-0.001	0.000	0.006	0.008	0.010	0.020	0.069	0.129
	St. deviation	0.001	0.000	0.001	0.001	0.001	0.000	0.000	0.003	0.009
	Weight increase (%)	0.145	0.217	0.290	0.399	0.444	0.471	0.516	0.616	-
		0.118	0.200	0.291	0.410	0.455	0.482	0.528	0.637	0.801
		0.144	0.207	0.279	0.396	0.441	0.468	0.495	0.594	0.828
Mean (%)	0.136	0.208	0.287	0.401	0.447	0.474	0.513	0.616	0.814	
St. deviation	0.015	0.009	0.007	0.007	0.007	0.008	0.017	0.022	0.019	

Mix nr.		Weeks								
		1	2	4	8	12	16	26	52	104
21	Expansion (%)	-0.007	-0.004	-0.002	0.002	0.005	0.009	0.015	0.050	0.149
		-0.007	-0.003	0.000	0.003	0.005	0.009	0.014	0.055	0.147
		-0.007	-0.003	-0.001	0.003	0.005	0.009	0.011	0.055	0.131
	Mean (%)	-0.007	-0.003	-0.001	0.003	0.005	0.009	0.013	0.053	0.142
		St. deviation	0.000	0.001	0.001	0.001	0.000	0.000	0.002	0.003
	Weight increase (%)	0.124	0.213	0.275	0.390	0.426	0.488	0.497	0.612	0.852
		0.109	0.192	0.255	0.374	0.410	0.447	0.492	0.620	0.821
		0.118	0.199	0.272	0.381	0.426	0.462	0.517	0.634	0.807
Mean (%)	0.117	0.201	0.267	0.382	0.421	0.466	0.502	0.622	0.826	
	St. deviation	0.007	0.011	0.011	0.008	0.009	0.021	0.013	0.011	0.023
22	Expansion (%)	0.000	-0.003	0.003	0.021	0.038	0.073	0.123	0.184	0.226
		-0.004	-0.002	0.003	0.024	0.046	0.083	0.134	0.200	0.236
		-0.002	-0.001	0.004	0.024	0.047	0.079	0.116	0.178	0.208
	Mean (%)	-0.002	-0.002	0.003	0.023	0.043	0.078	0.124	0.188	0.223
		St. deviation	0.002	0.001	0.001	0.001	0.005	0.005	0.009	0.011
	Weight increase (%)	0.065	0.159	0.243	0.393	0.486	0.608	0.739	0.870	0.991
		0.074	0.166	0.250	0.407	0.527	0.656	0.767	0.906	1.035
		0.064	0.156	0.229	0.376	0.495	0.596	0.715	0.806	0.935
Mean (%)	0.068	0.160	0.241	0.392	0.503	0.620	0.740	0.861	0.987	
	St. deviation	0.005	0.005	0.010	0.016	0.021	0.032	0.026	0.050	0.051
23	Expansion (%)	-0.005	-0.002	0.001	0.024	0.050	0.092	0.139	0.189	0.241
		-0.003	-0.002	0.001	0.025	0.056	0.095	0.140	0.200	0.238
		-0.005	-0.003	0.002	0.026	0.057	0.099	0.145	0.207	0.248
	Mean (%)	-0.004	-0.002	0.002	0.025	0.055	0.095	0.141	0.199	0.242
		St. deviation	0.001	0.000	0.001	0.001	0.004	0.003	0.003	0.009
	Weight increase (%)	0.103	0.205	0.289	0.448	0.578	0.718	0.793	0.896	1.148
		0.108	0.190	0.262	0.416	0.524	0.642	0.714	0.858	1.012
		0.111	0.222	0.305	0.471	0.600	0.739	0.822	0.942	1.117
Mean (%)	0.107	0.206	0.285	0.445	0.568	0.700	0.776	0.899	1.092	
	St. deviation	0.004	0.016	0.022	0.028	0.039	0.051	0.056	0.042	0.071
24	Expansion (%)	-0.006	-	-0.003	-	0.012	-	0.076	0.139	-
		-0.006	-	-0.004	-	0.012	-	0.079	0.131	-
		-0.006	-	-0.003	-	0.013	-	0.090	0.156	-
	Mean (%)	-0.006	-	-0.003	-	0.013	-	0.082	0.142	-
		St. deviation	0.000	-	0.000	-	0.000	-	0.007	0.013
	Weight increase (%)	0.100	-	0.246	-	0.446	-	0.719	0.937	-
		0.072	-	0.224	-	0.429	-	0.734	0.930	-
		0.073	-	0.238	-	0.412	-	0.677	0.879	-
Mean (%)	0.082	-	0.236	-	0.429	-	0.710	0.916	-	
	St. deviation	0.016	-	0.011	-	0.017	-	0.029	0.032	-

Mix nr.		Weeks								
		1	2	4	8	12	16	26	52	104
25	Expansion (%)	-0.011	-	-0.012	-	-0.007	-	0.010	0.038	0.082
		-0.013	-	-0.014	-	-0.009	-	0.009	0.038	0.097
		-0.014	-	-0.014	-	-0.008	-	0.008	0.033	0.083
	Mean (%)	-0.013	-	-0.013	-	-0.008	-	0.009	0.036	0.087
	St. deviation	0.001	-	0.001	-	0.001	-	0.001	0.003	0.009
	Weight increase (%)	0.080	-	0.143	-	0.250	-	0.385	0.689	0.930
		0.046	-	0.119	-	0.219	-	0.356	0.666	0.948
		0.046	-	0.130	-	0.242	-	0.390	0.687	1.013
Mean (%)	0.058	-	0.131	-	0.237	-	0.377	0.681	0.964	
St. deviation	0.020	-	0.012	-	0.016	-	0.019	0.013	0.043	
26	Expansion (%)	-0.011	-	-0.007	-	0.004	-	0.053	0.109	0.179
		-0.011	-	-0.009	-	0.002	-	0.053	0.114	0.236
		-0.011	-	-0.007	-	0.004	-	0.048	0.102	0.197
	Mean (%)	-0.011	-	-0.008	-	0.003	-	0.051	0.109	0.204
	St. deviation	0.000	-	0.001	-	0.001	-	0.003	0.006	0.029
	Weight increase (%)	-0.027	-	0.234	-	0.478	-	0.703	0.901	1.001
		-0.036	-	0.172	-	0.381	-	0.599	0.808	1.062
		0.000	-	0.267	-	0.452	-	0.673	0.875	1.041
Mean (%)	-0.021	-	0.225	-	0.437	-	0.658	0.862	1.035	
St. deviation	0.019	-	0.048	-	0.050	-	0.054	0.048	0.031	
27	Expansion (%)	-0.006	-	-0.003	-	0.008	-	0.072	0.131	-
		-0.007	-	-0.003	-	0.010	-	0.074	0.133	-
		-0.007	-	-0.003	-	0.010	-	0.072	0.144	-
	Mean (%)	-0.007	-	-0.003	-	0.009	-	0.073	0.136	-
	St. deviation	0.000	-	0.000	-	0.001	-	0.002	0.007	-
	Weight increase (%)	0.100	-	0.265	-	0.438	-	0.748	0.967	-
		0.073	-	0.245	-	0.436	-	0.717	0.917	-
		0.090	-	0.280	-	0.498	-	0.769	0.995	-
Mean (%)	0.088	-	0.263	-	0.457	-	0.745	0.960	-	
St. deviation	0.014	-	0.018	-	0.035	-	0.026	0.040	-	
28	Expansion (%)	-0.010	-	-0.010	-	-0.006	-	0.010	0.037	0.106
		-0.010	-	-0.010	-	-0.008	-	0.010	0.038	0.107
		-0.011	-	-0.011	-	-0.008	-	0.009	0.033	0.094
	Mean (%)	-0.010	-	-0.010	-	-0.007	-	0.010	0.036	0.102
	St. deviation	0.000	-	0.000	-	0.001	-	0.000	0.003	0.007
	Weight increase (%)	0.083	-	0.139	-	0.241	-	0.361	0.629	1.008
		0.072	-	0.145	-	0.235	-	0.362	0.643	1.050
		0.072	-	0.144	-	0.243	-	0.386	0.629	1.033
Mean (%)	0.076	-	0.142	-	0.239	-	0.370	0.634	1.030	
St. deviation	0.006	-	0.003	-	0.004	-	0.014	0.008	0.021	

Mix nr.		Weeks								
		1	2	4	8	12	16	26	52	104
29	Expansion (%)	-0.008	-	-0.008	-	-0.005	-	0.003	0.014	0.030
		-0.009	-	-0.008	-	-0.006	-	0.003	0.014	0.030
		-0.009	-	-0.008	-	-0.006	-	0.003	0.011	0.025
	Mean (%)	-0.009	-	-0.008	-	-0.006	-	0.003	0.013	0.028
	St. deviation	0.001	-	0.000	-	0.001	-	0.000	0.001	0.003
	Weight increase (%)	0.099	-	0.171	-	0.252	-	0.297	0.387	0.504
		0.063	-	0.145	-	0.226	-	0.290	0.362	0.489
		0.071	-	0.151	-	0.230	-	0.275	0.354	0.478
	Mean (%)	0.078	-	0.155	-	0.236	-	0.287	0.368	0.490
	St. deviation	0.019	-	0.014	-	0.014	-	0.011	0.017	0.013

B3: Accelerated mortar bar test – expansion and weight data

a) Normal storing conditions

Description of mix		Days						
		4	5	7	14	28	42	56
mylonite aggregate reference (0.125 - 4.0 mm)	Expansion (%)	0.030	-	0.051	0.153	0.342	0.469	0.548
		0.030	-	0.054	0.162	0.363	0.496	0.58
		0.029	-	0.054	0.166	0.223	0.508	0.594
	Mean (%)	0.030	-	0.053	0.161	0.309	0.491	0.574
	St. deviation	0.000	-	0.002	0.006	0.076	0.020	0.024
	Weigth increase (%)	0.290	-	0.341	0.971	1.772	2.130	2.385
		0.306	-	0.390	0.934	1.748	2.139	2.292
		0.289	-	0.306	0.918	1.768	2.107	2.294
Mean (%)	0.295	-	0.346	0.941	1.763	2.125	2.324	
St. deviation	0.009	-	0.042	0.027	0.013	0.016	0.053	
mylonite aggregate ref. standard grading (0.15 - 4.8 mm) w/c 0.45	Expansion (%)	0.029	-	0.064	0.158	0.343	0.473	0.566
		0.028	-	0.061	0.150	0.334	0.463	0.554
		0.028	-	0.063	0.158	0.351	0.485	0.583
	Mean (%)	0.028	-	0.063	0.155	0.343	0.473	0.568
	St. deviation	0.001	-	0.002	0.005	0.009	0.011	0.014
	Weigth increase (%)	0.241	-	0.567	1.426	2.199	2.543	2.749
		0.292	-	0.584	1.426	2.251	2.612	2.852
		0.360	-	0.582	1.353	2.140	2.517	2.740
Mean (%)	0.297	-	0.578	1.402	2.197	2.557	2.780	
St. deviation	0.060	-	0.009	0.042	0.055	0.049	0.063	
cataclasite aggr. reference (0.125 - 4.0 mm)	Expansion (%)	-	0.098	0.132	0.238	0.374	0.451	0.523
		-	0.094	0.131	0.235	0.365	0.440	0.508
		-	0.096	0.133	0.240	0.371	0.448	0.515
	Mean (%)	-	0.096	0.132	0.238	0.370	0.446	0.515
	St. deviation	-	0.002	0.001	0.003	0.005	0.005	0.008
	Weigth increase (%)	-	-	-	1.374	1.458	1.391	1.307
		-	-	-	1.311	1.393	1.327	1.344
		-	-	-	1.433	1.450	1.400	1.416
Mean (%)	-	-	-	1.373	1.434	1.373	1.356	
St. deviation	-	-	-	0.061	0.035	0.040	0.055	
rhyolite reference ref. standard grading (0.15 - 4.8 mm) w/c 0.45	Expansion (%)	0.019	-	0.028	0.059	0.239	0.428	0.586
		0.017	-	0.030	0.058	0.228	0.432	0.605
		0.018	-	0.028	0.058	0.222	0.412	0.575
	Mean (%)	0.018	-	0.029	0.059	0.230	0.424	0.589
	St. deviation	0.001	-	0.001	0.001	0.009	0.011	0.015
	Weigth increase (%)	1.039	-	1.093	1.403	1.950	2.406	2.880
		1.033	-	1.106	1.396	1.903	2.429	2.918
		0.960	-	1.051	1.304	1.884	2.373	2.826
Mean (%)	1.011	-	1.083	1.368	1.912	2.403	2.875	
St. deviation	0.044	-	0.029	0.055	0.034	0.028	0.046	

Description of mix		Days						
		4	5	7	14	28	42	56
granite/gneiss aggr. (0.125 - 4.0 mm) reference (v/c = 0.42)	Expansion (%)	-	0.010	0.010	0.037	0.108	0.166	0.218
		-	0.007	0.008	0.037	0.108	0.170	0.223
		-	0.009	0.010	0.036	0.109	0.171	0.224
	Mean (%)	-	0.009	0.009	0.037	0.108	0.169	0.221
	St. deviation	-	0.001	0.001	0.000	0.001	0.002	0.003
	Weigh increase (%)	-	0.084	0.135	0.185	0.572	0.841	1.076
		-	0.083	0.116	0.198	0.446	0.792	1.056
		-	0.117	0.167	0.234	0.551	0.801	1.034
Mean (%)	-	0.094	0.139	0.206	0.523	0.811	1.056	
St. deviation	-	0.019	0.026	0.025	0.068	0.026	0.021	
mylonite aggregate (0.125 - 4.0 mm) 10 % mylonite 0-20 filler	Expansion (%)	-	0.028	0.049	0.129	0.228	0.282	0.319
		-	0.026	0.046	0.120	0.214	0.268	0.303
		-	0.028	0.049	0.125	0.221	0.275	0.311
	Mean (%)	-	0.028	0.048	0.125	0.221	0.275	0.311
	St. deviation	-	0.001	0.002	0.004	0.007	0.007	0.008
	Weigh increase (%)	-	0.233	0.416	-	1.181	1.431	1.581
		-	0.234	0.384	-	1.119	1.419	1.536
		-	0.183	0.365	-	1.129	1.395	1.511
Mean (%)	-	-	0.388	-	1.143	1.415	1.542	
St. deviation	-	-	0.026	-	0.034	0.019	0.035	
mylonite aggregate (0.125 - 4.0 mm) 10 % mylonite 0-125 filler	Expansion (%)	0.023	-	0.054	0.161	0.284	0.370	0.430
		0.023	-	0.052	0.151	0.291	0.380	0.442
		0.020	-	0.050	0.142	0.272	0.354	0.411
	Mean (%)	0.022	-	0.052	0.151	0.282	0.368	0.427
	St. deviation	0.002	-	0.002	0.010	0.010	0.013	0.016
	Weigh increase (%)	0.269	-	0.471	1.093	1.581	1.783	1.850
		0.219	-	0.456	1.080	1.502	1.755	1.755
		0.254	-	0.473	1.048	1.606	1.809	1.758
Mean (%)	0.247	-	0.467	1.074	1.563	1.782	1.788	
St. deviation	0.025	-	0.010	0.023	0.054	0.027	0.054	
mylonite aggregate (0.125 - 4.0 mm) 20 % mylonite 0-20 filler	Expansion (%)	-	0.021	0.031	0.074	0.122	0.151	0.166
		-	0.022	0.031	0.072	0.119	0.143	0.161
		-	0.023	0.030	0.068	0.111	0.134	0.149
	Mean (%)	-	0.022	0.031	0.071	0.117	0.143	0.158
	St. deviation	-	0.001	0.001	0.003	0.006	0.008	0.008
	Weigh increase (%)	-	0.231	0.329	-	0.939	1.169	1.268
		-	0.264	0.380	-	1.057	1.271	1.403
		-	0.297	0.363	-	0.991	1.255	1.338
Mean (%)	-	0.264	0.358	-	0.995	1.232	1.336	
St. deviation	-	0.033	0.026	-	0.059	0.055	0.068	

Description of mix		Days						
		4	5	7	14	28	42	56
mylonite aggregate (0.125 - 4.0 mm) 20 % mylonite 10-30 filler	Expansion (%)	-	0.021	0.034	0.082	0.146	0.180	0.200
		-	0.025	0.039	0.091	0.157	0.191	0.213
		-	0.023	0.038	0.092	0.181	0.199	0.222
	Mean (%)	-	0.023	0.037	0.088	0.161	0.190	0.212
	St. deviation	-	0.002	0.003	0.005	0.018	0.010	0.011
	Weigth increase (%)	-	0.284	0.418	-	1.322	1.439	1.522
		-	0.252	0.370	-	1.295	1.379	1.496
		-	0.267	0.367	-	1.285	1.335	1.485
Mean (%)	-	0.268	0.385	-	1.300	1.384	1.501	
St. deviation	-	0.016	0.029	-	0.019	0.052	0.019	
mylonite aggregate (0.125 - 4.0 mm) 20% mylonite 20-125 filler	Expansion (%)	-	0.026	0.044	0.117	0.210	0.257	0.289
		-	0.026	0.041	0.114	0.205	0.253	0.285
		-	0.027	0.043	0.114	0.204	0.253	0.285
	Mean (%)	-	0.026	0.042	0.115	0.206	0.254	0.286
	St. deviation	-	0.000	0.002	0.002	0.003	0.002	0.003
	Weigth increase (%)	-	0.287	0.422	-	1.367	1.451	1.552
		-	0.249	0.382	-	1.196	1.462	1.562
		-	0.268	0.452	-	1.190	1.441	1.625
Mean (%)	-	0.268	0.419	-	1.251	1.451	1.580	
St. deviation	-	0.019	0.035	-	0.100	0.011	0.040	
mylonite aggregate (0.125 - 4.0 mm) 20 % mylonite 0-125 filler (a)	Expansion (%)	0.028	-	0.049	0.104	0.185	0.249	0.271
		0.026	-	0.045	0.096	0.173	0.224	0.258
		0.026	-	0.045	0.095	0.173	0.225	0.259
	Mean (%)	0.027	-	0.047	0.098	0.177	0.233	0.263
	St. deviation	0.001	-	0.002	0.005	0.007	0.014	0.007
	Weigth increase (%)	0.184	-	0.401	0.736	1.188	1.422	1.506
		0.149	-	0.365	0.747	1.163	1.379	1.478
		0.15	-	0.334	0.684	1.084	1.267	1.417
Mean (%)	0.161	-	0.367	0.722	1.145	1.356	1.467	
St. deviation	0.020	-	0.034	0.034	0.054	0.080	0.045	
mylonite aggregate (0.125 - 4.0 mm) 20 % mylonite 0-125 filler (b)	Expansion (%)	0.027	-	0.047	0.108	0.189	0.241	0.278
		0.025	-	0.046	0.098	0.181	0.232	0.267
		0.026	-	0.047	0.098	0.182	0.236	0.271
	Mean (%)	0.026	-	0.047	0.101	0.184	0.236	0.272
	St. deviation	0.001	-	0.000	0.006	0.004	0.005	0.006
	Weigth increase (%)	0.117	-	0.302	0.688	1.040	1.308	1.426
		0.134	-	0.369	0.755	1.124	1.309	1.477
		0.219	-	0.370	0.758	1.145	1.313	1.414
Mean (%)	0.157	-	0.347	0.733	1.103	1.310	1.439	
St. deviation	0.054	-	0.039	0.040	0.056	0.003	0.033	

Description mix nr.		Days						
		4	5	7	14	28	42	56
mylonite aggregate (0.125 - 4.0 mm) 20 % mylonite 0-125 filler (c)	Expansion (%)	0.026	-	0.047	0.102	0.181	0.230	0.266
		0.027	-	0.047	0.098	0.180	0.235	0.271
		0.025	-	0.046	0.098	0.177	0.231	0.266
	Mean (%)	0.026	-	0.046	0.099	0.179	0.232	0.268
		St. deviation	0.001	-	0.001	0.002	0.002	0.002
	Weigth increase (%)	0.202	-	0.388	0.775	1.197	1.382	1.517
		0.184	-	0.384	0.718	1.102	1.352	1.436
		0.201	-	0.419	0.754	1.172	1.373	1.491
	Mean (%)	0.196	-	0.397	0.749	1.157	1.369	1.481
		St. deviation	0.010	-	0.019	0.029	0.049	0.015
mylonite aggregate (0.125 - 4.0 mm) 7.5 % silica fume (w. % of cement)	Expansion (%)	0.013	-	0.020	0.039	0.103	0.146	0.188
		0.011	-	0.020	0.040	0.108	0.149	0.193
		0.011	-	0.019	0.043	0.111	0.157	0.203
	Mean (%)	0.012	-	0.020	0.041	0.108	0.151	0.195
		St. deviation	0.001	-	0.000	0.002	0.004	0.006
	Weigth increase (%)	0.105	-	0.279	-	1.291	1.622	1.866
		0.052	-	0.242	-	1.246	1.557	1.903
		0.086	-	0.242	-	1.245	1.574	1.868
	Mean (%)	0.081	-	0.254	-	1.260	1.584	1.879
		St. deviation	0.027	-	0.021	-	0.026	0.034
mylonite aggregate (0.125 - 4.0 mm) 10% mylonite 0-20 filler 4 % silica fume (w. % of cement)	Expansion (%)	-	0.008	0.011	0.020	0.032	0.052	0.067
		-	0.007	0.011	0.019	0.032	0.050	0.064
		-	0.008	0.011	0.020	0.037	0.056	0.070
	Mean (%)	-	0.008	0.011	0.020	0.034	0.053	0.067
		St. deviation	-	0.000	0.000	0.001	0.003	0.003
	Weigth increase (%)	-	0.153	0.324	0.494	0.903	1.074	1.142
		-	0.135	0.321	0.472	0.928	1.012	1.130
		-	0.152	0.305	0.474	0.914	1.033	1.168
	Mean (%)	-	0.147	0.316	0.480	0.915	1.040	1.147
		St. deviation	-	0.010	0.010	0.012	0.012	0.031
mylonite aggregate (0.125 - 4.0 mm) 10% Fly ash 0-20	Expansion (%)	0.007	-	0.012	0.019	0.034	0.041	0.048
		0.006	-	0.011	0.018	0.034	0.042	0.052
		0.006	-	0.012	0.018	0.034	0.042	0.053
	Mean (%)	0.006	-	0.011	0.019	0.034	0.042	0.051
		St. deviation	0.000	-	0.000	0.001	0.000	0.000
	Weigth increase (%)	0.252	-	0.370	-	0.824	0.941	1.093
		0.220	-	0.355	-	0.845	0.963	1.098
		0.253	-	0.337	-	0.825	0.943	1.078
	Mean (%)	0.241	-	0.354	-	0.831	0.949	1.090
		St. deviation	0.019	-	0.016	-	0.012	0.012

Description of mix		Days						
		4	5	7	14	28	42	56
mylonite aggregate (0.125 - 4.0 mm) 10% Fly ash 0-125	Expansion (%)	0.009	-	0.017	0.028	0.052	0.086	0.112
		0.007	-	0.016	0.028	0.059	0.098	0.125
		0.008	-	0.015	0.029	0.057	0.097	0.125
	Mean (%)	0.008	-	0.016	0.028	0.056	0.094	0.121
		St. deviation	0.001	-	0.001	0.000	0.004	0.007
	Weigth increase (%)	0.403	-	0.487	0.806	1.025	1.176	1.209
		0.388	-	0.506	0.826	1.096	1.247	1.298
		0.352	-	0.503	0.771	1.055	1.156	1.240
Mean (%)	0.381	-	0.498	0.801	1.058	1.193	1.249	
	St. deviation	0.026	-	0.010	0.028	0.036	0.048	0.045
mylonite aggregate (0.125 - 4.0 mm) 20% limestone 0-30 filler	Expansion (%)	0.027	-	0.051	0.147	0.350	0.477	0.575
		0.027	-	0.053	0.151	0.358	0.484	0.591
		0.025	-	0.051	0.147	0.351	0.477	0.578
	Mean (%)	0.026	-	0.051	0.148	0.353	0.480	0.581
		St. deviation	0.001	-	0.001	0.002	0.005	0.004
	Weigth increase (%)	0.151	-	0.269	-	1.477	1.914	2.199
		0.100	-	0.249	-	1.479	1.828	2.077
		0.117	-	0.268	-	1.510	1.929	2.214
Mean (%)	0.123	-	0.262	-	1.489	1.890	2.163	
	St. deviation	0.026	-	0.011	-	0.018	0.054	0.075
mylonite aggregate (0.125 - 4.0 mm) 20% granite 0-125 filler	Expansion (%)	0.028	-	0.054	0.160	0.328	0.415	0.474
		0.030	-	0.053	0.156	0.316	0.400	0.455
		0.030	-	0.056	0.162	0.330	0.420	0.479
	Mean (%)	0.029	-	0.054	0.159	0.325	0.412	0.469
		St. deviation	0.001	-	0.001	0.003	0.008	0.010
	Weigth increase (%)	0.180	-	0.261	0.702	1.191	1.518	1.665
		0.229	-	0.262	0.654	1.259	1.521	1.701
		0.147	-	0.244	0.652	1.173	1.450	1.597
Mean (%)	0.185	-	0.256	0.669	1.208	1.496	1.654	
	St. deviation	0.041	-	0.010	0.028	0.045	0.040	0.053
mylonite aggregate (0.125 - 4.0 mm) 10% glass 0-125 filler	Expansion (%)	0.037	-	0.075	0.157	0.277	0.354	0.434
		0.038	-	0.078	0.160	0.284	0.365	0.449
		0.035	-	0.076	0.158	0.279	0.362	0.443
	Mean (%)	0.037	-	0.076	0.158	0.280	0.361	0.442
		St. deviation	0.002	-	0.001	0.002	0.004	0.006
	Weigth increase (%)	0.401	-	0.697	1.203	1.866	2.180	2.371
		0.327	-	0.602	1.152	1.771	2.098	2.339
		0.329	-	0.519	1.107	1.695	2.058	2.231
Mean (%)	0.352	-	0.606	1.154	1.777	2.112	2.314	
	St. deviation	0.042	-	0.089	0.048	0.086	0.062	0.074

Description of mix		Days						
		4	5	7	14	28	42	56
mylonite aggregate (0.125 - 4.0 mm) 20% glass 0-20 filler	Expansion (%)	0.013	-	0.029	0.057	0.118	0.175	0.228
		0.013	-	0.028	0.053	0.114	0.169	0.220
		0.014	-	0.029	0.056	0.118	0.174	0.228
	Mean (%)	0.013	-	0.029	0.055	0.117	0.173	0.225
		St. deviation	0.001	-	0.001	0.002	0.002	0.004
	Weigth increase (%)	0.186	-	0.254	-	0.813	0.983	1.237
		0.152	-	0.254	-	0.796	1.050	1.253
		0.186	-	0.237	-	0.794	1.031	1.268
Mean (%)	0.175	-	0.248	-	0.801	1.021	1.253	
	St. deviation	0.019	-	0.010	-	0.010	0.035	0.016
mylonite aggregate (0.125 - 4.0 mm) 20% glass 0-125 filler	Expansion (%)	0.017	-	0.033	0.073	0.140	0.198	0.244
		0.016	-	0.031	0.070	0.136	0.193	0.241
		0.017	-	0.031	0.070	0.138	0.196	0.244
	Mean (%)	0.017	-	0.032	0.071	0.138	0.196	0.243
		St. deviation	0.001	-	0.001	0.001	0.002	0.002
	Weigth increase (%)	0.224	-	0.481	0.791	1.272	1.547	1.651
		0.255	-	0.408	0.766	1.242	1.498	1.617
		0.222	-	0.445	0.804	1.266	1.523	1.643
Mean (%)	0.234	-	0.445	0.787	1.260	1.523	1.637	
	St. deviation	0.019	-	0.036	0.020	0.016	0.025	0.018
mylonite aggregate (0.125 - 4.0 mm) 20% cataclasite 0-20 filler	Expansion (%)	-	0.020	0.031	0.067	0.110	0.138	0.153
		-	0.021	0.032	0.069	0.115	0.145	0.161
		-	0.020	0.030	0.063	0.106	0.132	0.146
	Mean (%)	-	0.020	0.031	0.066	0.110	0.138	0.153
		St. deviation	-	0.001	0.001	0.003	0.004	0.006
	Weigth increase (%)	-	0.218	0.336	0.605	0.975	1.126	1.210
		-	0.269	0.404	0.657	1.010	1.178	1.263
		-	0.249	0.332	0.597	0.945	1.128	1.211
Mean (%)	-	0.246	0.357	0.620	0.977	1.144	1.228	
	St. deviation	-	0.026	0.041	0.032	0.032	0.030	0.030
mylonite aggregate (0.125 - 4.0 mm) 20% cataclasite 10-40 filler	Expansion (%)	-	0.028	0.043	0.102	0.180	0.232	0.265
		-	0.028	0.042	0.098	0.179	0.230	0.265
		-	0.027	0.042	0.101	0.179	0.230	0.266
	Mean (%)	-	0.027	0.042	0.100	0.180	0.231	0.265
		St. deviation	-	0.001	0.000	0.002	0.000	0.001
	Weigth increase (%)	-	0.252	0.319	0.689	1.160	1.379	1.513
		-	0.251	0.351	0.669	1.138	1.339	1.473
		-	0.235	0.285	0.687	1.173	1.324	1.525
Mean (%)	-	0.246	0.319	0.682	1.157	1.347	1.504	
	St. deviation	-	0.010	0.033	0.011	0.018	0.028	0.028

Description mix nr.		Days						
		4	5	7	14	28	42	56
mylonite aggregate (0.125 - 4.0 mm) 10% rhyolite 0-125 filler	Expansion (%)	0.024	-	0.036	0.071	0.153	0.220	0.272
		0.022	-	0.033	0.067	0.144	0.210	0.258
		0.020	-	0.031	0.066	0.146	0.211	0.263
	Mean (%)	0.022	-	0.033	0.068	0.148	0.214	0.264
		St. deviation	0.002	-	0.002	0.003	0.004	0.006
	Weigth increase (%)	0.270	-	0.472	0.793	1.231	1.467	1.551
		0.235	-	0.420	0.740	1.127	1.379	1.514
		0.267	-	0.468	0.752	1.236	1.403	1.487
Mean (%)	0.258	-	0.453	0.761	1.198	1.416	1.517	
	St. deviation	0.019	-	0.029	0.028	0.062	0.046	0.033
mylonite aggregate (0.125 - 4.0 mm) 20% rhyolite 0-20 filler	Expansion (%)	-	0.003	0.007	0.013	0.023	0.034	0.040
		-	0.002	0.005	0.013	0.022	0.033	0.041
		-	0.003	0.006	0.013	0.024	0.035	0.043
	Mean (%)	-	0.002	0.006	0.013	0.023	0.034	0.041
		St. deviation	-	0.001	0.001	0.001	0.001	0.001
	Weigth increase (%)	-	0.345	0.465	0.534	0.861	1.034	1.189
		-	0.414	0.569	0.637	0.948	1.137	1.172
		-	0.398	0.726	0.622	0.951	1.107	1.245
Mean (%)	-	0.385	0.587	0.598	0.920	1.092	1.202	
	St. deviation	-	0.036	0.131	0.056	0.051	0.053	0.038
mylonite aggregate (0.125 - 4.0 mm) 20% rhyolite 10-40 filler	Expansion (%)	0.009	-	0.013	0.031	0.047	0.071	0.088
		0.007	-	0.013	0.030	0.045	0.068	0.087
		0.007	-	0.014	0.030	0.047	0.075	0.090
	Mean (%)	0.008	-	0.014	0.030	0.046	0.071	0.088
		St. deviation	0.001	-	0.001	0.001	0.001	0.003
	Weigth increase (%)	0.507	-	0.577	0.839	1.066	1.293	1.416
		0.436	-	0.559	0.768	1.030	1.274	1.397
		0.469	-	0.590	0.747	1.024	1.302	1.389
Mean (%)	0.471	-	0.575	0.785	1.040	1.290	1.400	
	St. deviation	0.035	-	0.016	0.048	0.023	0.014	0.014
mylonite aggregate (0.125 - 4.0 mm) 20% rhyolite 0-125 filler	Expansion (%)	0.008	-	0.015	0.028	0.058	0.098	0.128
		0.008	-	0.013	0.027	0.058	0.092	0.121
		0.007	-	0.012	0.027	0.060	0.096	0.128
	Mean (%)	0.007	-	0.014	0.027	0.059	0.095	0.126
		St. deviation	0.000	-	0.002	0.001	0.001	0.003
	Weigth increase (%)	0.347	-	0.486	0.660	0.990	1.199	1.303
		0.327	-	0.465	0.602	0.895	1.136	1.187
		0.346	-	0.502	0.709	1.003	1.194	1.263
Mean (%)	0.340	-	0.484	0.657	0.963	1.176	1.251	
	St. deviation	0.011	-	0.019	0.054	0.059	0.035	0.059

Description mix nr.		Days						
		4	5	7	14	28	42	56
mylonite aggregate (0.125 - 4.0 mm) 20% quartz 0-125 filler	Expansion (%)	0.012	-	0.023	0.082	0.140	0.180	0.204
		0.011	-	0.023	0.084	0.149	0.192	0.215
		0.011	-	0.021	0.086	0.153	0.196	0.220
	Mean (%)	0.011	-	0.022	0.084	0.148	0.189	0.213
		St. deviation	0.001	-	0.001	0.002	0.007	0.008
	Weigth increase (%)	0.219	-	0.405	0.776	1.096	1.316	1.349
		0.269	-	0.404	0.757	1.094	1.329	1.346
		0.321	-	0.457	0.795	1.168	1.320	1.387
Mean (%)	0.270	-	0.422	0.776	1.119	1.321	1.361	
	St. deviation	0.051	-	0.030	0.019	0.042	0.007	0.023
mylonite aggregate (0.125 - 4.0 mm) 10 % cataclasite 0-20 filler	Expansion (%)	-	0.070	0.098	0.168	0.239	0.279	0.318
		-	0.067	0.093	0.160	0.233	0.276	0.312
		-	0.067	0.093	0.162	0.234	0.279	0.312
	Mean (%)	-	0.068	0.094	0.163	0.235	0.278	0.314
		St. deviation	-	0.002	0.003	0.004	0.003	0.002
	Weigth increase (%)	-	-	-	0.917	0.950	0.850	0.933
		-	-	-	0.986	0.919	0.835	0.835
		-	-	-	0.965	0.965	0.915	0.915
Mean (%)	-	-	-	0.956	0.945	0.867	0.895	
	St. deviation	-	-	-	0.035	0.024	0.042	0.052
mylonite aggregate (0.125 - 4.0 mm) 20 % cataclasite 0-20 filler	Expansion (%)	-	0.040	0.050	0.077	0.103	0.118	0.132
		-	0.039	0.048	0.075	0.100	0.114	0.127
		-	0.038	0.047	0.073	0.099	0.114	0.128
	Mean (%)	-	0.039	0.048	0.075	0.100	0.115	0.129
		St. deviation	-	0.001	0.002	0.002	0.002	0.002
	Weigth increase (%)	-	-	-	0.779	0.829	0.779	0.779
		-	-	-	0.809	0.793	0.760	0.760
		-	-	-	0.803	0.786	0.719	0.786
Mean (%)	-	-	-	0.797	0.803	0.753	0.775	
	St. deviation	-	-	-	0.016	0.023	0.031	0.014
cataclasite aggregate (0.125 - 4.0 mm) 20 % mylonite 0-20 filler	Expansion (%)	-	0.048	0.063	0.099	0.133	0.152	0.169
		-	0.047	0.063	0.097	0.129	0.147	0.161
		-	0.051	0.065	0.103	0.136	0.154	0.169
	Mean (%)	-	0.049	0.064	0.100	0.133	0.151	0.166
		St. deviation	-	0.002	0.001	0.003	0.003	0.004
	Weigth increase (%)	-	-	-	0.919	0.952	0.919	0.885
		-	-	-	0.953	1.020	0.970	1.004
		-	-	-	1.033	1.016	0.999	1.049
Mean (%)	-	-	-	0.968	0.996	0.963	0.979	
	St. deviation	-	-	-	0.058	0.038	0.041	0.085

Description mix nr.		Days						
		4	5	7	14	28	42	56
granite/gneiss aggr. (0.125 - 4.0 mm) 20 % mylonite 0-125 filler (v/c = 0.42)	Expansion (%)	-	0.008	0.008	0.023	0.056	0.081	0.105
		-	0.008	0.007	0.024	0.056	0.082	0.107
		-	0.009	0.008	0.025	0.057	0.085	0.114
	Mean (%)	-	0.008	0.008	0.024	0.056	0.083	0.109
	St. deviation	-	0.000	0.000	0.001	0.001	0.002	0.005
	Weigth increase (%)	-	0.098	0.163	0.277	0.473	0.946	0.750
		-	0.099	0.214	0.330	0.511	0.659	0.824
		-	0.082	0.198	0.297	0.462	0.561	0.758
	Mean (%)	-	0.093	0.192	0.301	0.482	0.722	0.778
	St. deviation	-	0.009	0.026	0.026	0.026	0.200	0.040

b) Modified storing conditions

Storing in 1 N NaOH-solution at 20°C

Mix	weeks	Expansion (%)			Mean	St.dev.	Weight increase (%)			Mean	St.dev.
Reference (no filler)	4	0.005	0.005	0.006	0.005	0.000	0.17	0.168	0.169	0.169	0.001
	12	0.010	0.010	0.010	0.010	0.000	0.373	0.353	0.304	0.343	0.035
	20	0.014	0.014	0.015	0.014	0.001	0.356	0.336	0.338	0.343	0.011
	28	0.012	0.013	0.013	0.013	0.000	0.373	0.336	0.355	0.355	0.019
	36	0.018	0.018	0.019	0.019	0.000	0.407	0.386	0.389	0.394	0.011
	44	0.017	0.017	0.017	0.017	0.000	0.424	0.386	0.389	0.400	0.021
	52	0.019	0.019	0.019	0.019	0.000	0.424	0.386	0.405	0.405	0.019
20 % mylonite 0-20 filler	4	0.006	0.005	0.005	0.005	0.000	0.181	0.183	0.181	0.181	0.001
	12	0.009	0.008	0.008	0.008	0.001	0.361	0.332	0.346	0.346	0.015
	20	0.012	0.012	0.012	0.012	0.000	0.427	0.415	0.444	0.429	0.015
	28	0.012	0.011	0.011	0.011	0.000	0.477	0.448	0.461	0.462	0.014
	36	0.016	0.016	0.016	0.016	0.000	0.526	0.531	0.526	0.528	0.003
	44	0.015	0.015	0.014	0.015	0.000	0.559	0.548	0.559	0.555	0.007
	52	0.017	0.017	0.016	0.017	0.001	0.592	0.581	0.576	0.583	0.008
20 % cataclasite 0-20 filler	4	0.005	0.006	0.005	0.005	0.000	0.165	0.181	0.149	0.165	0.016
	12	0.008	0.009	0.008	0.008	0.001	0.296	0.312	0.298	0.302	0.009
	20	0.011	0.013	0.012	0.012	0.001	0.346	0.361	0.364	0.357	0.010
	28	0.010	0.012	0.011	0.011	0.001	0.362	0.378	0.364	0.368	0.008
	36	0.016	0.018	0.016	0.017	0.001	0.428	0.443	0.430	0.434	0.008
	44	0.014	0.016	0.015	0.015	0.001	0.428	0.443	0.430	0.434	0.008
	52	0.016	0.018	0.017	0.017	0.001	0.444	0.443	0.447	0.445	0.002
7.5 % silica fume	4	0.001	0.001	0.000	0.001	0.000	0.118	0.118	0.118	0.118	0.000
	12	0.004	0.003	0.003	0.003	0.000	0.186	0.203	0.219	0.202	0.017
	20	0.008	0.007	0.007	0.007	0.001	0.219	0.236	0.236	0.231	0.010
	28	0.005	0.005	0.005	0.005	0.000	0.219	0.236	0.219	0.225	0.010
	36	0.011	0.011	0.011	0.011	0.000	0.304	0.270	0.287	0.287	0.017
	44	0.010	0.009	0.009	0.009	0.000	0.287	0.270	0.287	0.281	0.010
	52	0.011	0.011	0.011	0.011	0.000	0.287	0.287	0.304	0.292	0.010

Storing in 1 N NaOH-solution at 38°C

Mix	weeks	Expansion (%)			Mean	St.dev.	Weight increase (%)			Mean	St.dev
Reference (no filler)	4	0.001	0.002	-0.001	0.001	0.001	0.169	0.201	0.167	0.179	0.019
	8	0.005	0.005	0.003	0.004	0.001	0.203	0.201	0.217	0.207	0.009
	12	0.008	0.008	0.006	0.007	0.001	0.321	0.368	0.368	0.352	0.027
	16	0.014	0.014	0.012	0.013	0.001	0.27	0.318	0.301	0.297	0.024
	20	0.024	0.025	0.023	0.024	0.001	0.338	0.385	0.351	0.358	0.024
	24	0.032	0.033	0.030	0.032	0.001	0.355	0.368	0.368	0.364	0.008
	48	0.126	0.127	0.125	0.126	0.001	0.573	0.619	0.569	0.587	0.028
20 % mylonite 0-20 filler	4	0.002	0.002	0.002	0.002	0.000	0.216	0.233	0.249	0.233	0.016
	8	0.004	0.005	0.004	0.004	0.001	0.333	0.333	0.316	0.327	0.010
	12	0.007	0.008	0.007	0.007	0.001	0.483	0.483	0.416	0.460	0.039
	16	0.011	0.012	0.012	0.012	0.001	0.45	0.466	0.466	0.460	0.009
	20	0.020	0.022	0.020	0.021	0.001	0.483	0.499	0.515	0.499	0.016
	24	0.024	0.026	0.025	0.025	0.001	0.533	0.549	0.549	0.544	0.009
	48	0.085	0.084	0.085	0.085	0.001	0.696	0.707	0.547	0.650	0.089
20 % cataclasite 0-20 filler	4	0.003	0.003	0.003	0.003	0.000	0.167	0.185	0.184	0.179	0.010
	8	0.004	0.005	0.004	0.005	0.001	0.201	0.219	0.200	0.207	0.010
	12	0.008	0.008	0.007	0.008	0.001	0.268	0.269	0.267	0.268	0.001
	16	0.013	0.014	0.014	0.014	0.000	0.301	0.286	0.284	0.290	0.010
	20	0.022	0.022	0.023	0.022	0.000	0.335	0.353	0.334	0.341	0.011
	24	0.027	0.027	0.027	0.027	0.000	0.385	0.370	0.350	0.369	0.017
	48	0.087	0.088	0.090	0.088	0.002	0.551	0.532	0.517	0.533	0.017
7.5 % silica fume	4	0.002	0.001	0.001	0.001	0.000	0.156	0.155	0.155	0.155	0.001
	8	0.003	0.002	0.002	0.002	0.000	0.173	0.138	0.172	0.161	0.020
	12	0.006	0.005	0.006	0.006	0.000	0.225	0.224	0.223	0.224	0.001
	16	0.010	0.009	0.010	0.010	0.000	0.225	0.207	0.206	0.213	0.011
	20	0.014	0.014	0.015	0.014	0.001	0.277	0.258	0.275	0.270	0.010
	24	0.016	0.015	0.016	0.015	0.001	0.312	0.275	0.292	0.293	0.018
	48	0.067	0.065	0.068	0.066	0.001	0.507	0.490	0.481	0.493	0.014

Storing in artificial pore water solution at 80°C

Mix	weeks	Expansion (%)			Mean	St.dev.	Weight increase (%)			Mean	St.dev.
Reference (no filler)	2	0.004	0.003	0.003	0.003	0.001	0.068	0.119	0.102	0.096	0.026
	6	0.009	0.007	0.008	0.008	0.001	0.171	0.221	0.288	0.227	0.059
	10	0.009	0.012	0.012	0.011	0.002	0.223	0.357	0.322	0.300	0.070
	14	0.016	0.015	0.016	0.015	0.001	0.291	0.272	0.339	0.301	0.035
	18	0.021	0.022	0.020	0.021	0.001	0.342	0.390	0.373	0.369	0.024
	22	0.021	0.024	0.023	0.023	0.001	0.411	0.390	0.509	0.437	0.063
	26	0.068	0.07	0.069	0.069	0.001	0.736	0.747	0.780	0.755	0.023
	30	0.092	0.094	0.094	0.093	0.001	0.873	0.866	0.848	0.862	0.013
	34	0.105	0.107	0.108	0.107	0.001	0.942	0.900	0.950	0.930	0.027
	38	0.108	0.111	0.113	0.111	0.003	0.942	0.934	0.950	0.942	0.008
	42	0.108	0.112	0.114	0.111	0.003	0.925	0.917	0.950	0.930	0.017
	46	0.108	0.111	0.113	0.110	0.003	0.925	0.900	0.916	0.913	0.013
	50	0.108	0.113	0.113	0.111	0.003	0.993	0.985	0.984	0.987	0.005
76	0.108	0.111	0.111	0.110	0.002	1.010	0.985	1.001	0.999	0.013	
20 % mylonite 0-20 filler	2	-0.002	0.008	0.000	0.002	0.005	0.217	0.235	0.100	0.184	0.074
	6	0.007	0.011	0.006	0.008	0.003	0.484	0.352	0.365	0.400	0.073
	10	0.009	0.014	0.008	0.011	0.003	0.501	0.487	0.464	0.484	0.018
	14	0.013	0.020	0.014	0.015	0.004	0.568	0.537	0.564	0.556	0.017
	18	0.015	0.021	0.014	0.017	0.004	0.568	0.604	0.581	0.584	0.019
	22	0.016	0.024	0.018	0.019	0.005	0.618	0.621	0.581	0.606	0.022
	26	0.02	0.025	0.02	0.022	0.003	0.634	0.638	0.614	0.629	0.013
	30	0.022	0.026	0.021	0.023	0.003	0.668	0.671	0.647	0.662	0.013
	34	0.023	0.028	0.023	0.025	0.003	0.718	0.621	0.647	0.662	0.050
	38	0.021	0.027	0.02	0.023	0.004	0.701	0.688	0.664	0.684	0.019
	42	0.023	0.029	0.025	0.026	0.003	0.701	0.705	0.630	0.679	0.042
	46	0.023	0.028	0.023	0.025	0.003	0.751	0.688	0.680	0.706	0.039
	50	0.022	0.028	0.022	0.024	0.004	0.768	0.772	0.763	0.768	0.004
76	0.028	0.031	0.026	0.028	0.002	0.868	0.856	0.846	0.857	0.011	

Mix	weeks	Expansion (%)			Mean	St.dev.	Weight increase (%)			Mean	St.dev
20 % cataclasite 0-20 filler	2	0.005	-0.001	-0.002	0.001	0.004	0.117	0.168	0.149	0.145	0.026
	6	0.013	0.008	0.007	0.009	0.003	0.351	0.336	0.315	0.334	0.018
	10	0.013	0.009	0.009	0.011	0.003	0.401	0.403	0.365	0.390	0.021
	14	0.020	0.013	0.013	0.015	0.004	0.501	0.504	0.481	0.495	0.012
	18	0.022	0.016	0.016	0.018	0.003	0.484	0.487	0.498	0.490	0.007
	22	0.028	0.018	0.019	0.021	0.006	0.518	0.521	0.531	0.523	0.007
	26	0.032	0.024	0.024	0.026	0.004	0.651	0.621	0.663	0.645	0.022
	30	0.033	0.025	0.024	0.027	0.005	0.635	0.705	0.697	0.679	0.039
	34	0.036	0.029	0.027	0.030	0.005	0.718	0.722	0.663	0.701	0.033
	38	0.032	0.028	0.028	0.029	0.002	0.718	0.722	0.697	0.712	0.014
	42	0.037	0.03	0.029	0.032	0.004	0.718	0.739	0.730	0.729	0.010
	46	0.035	0.03	0.03	0.032	0.003	0.701	0.773	0.746	0.740	0.036
	50	0.038	0.029	0.029	0.032	0.005	0.818	0.840	0.829	0.829	0.011
76	0.041	0.034	0.034	0.036	0.004	0.935	0.974	0.929	0.946	0.025	
Mix	weeks	Expansion (%)			Mean	St.dev.	Weight increase (%)			Mean	St.dev
7.5 % silica fume	2	0.000	0.002	0.007	0.003	0.004	0.069	0.000	0.069	0.046	0.040
	6	0.006	0.008	0.013	0.009	0.004	0.155	0.173	0.189	0.172	0.017
	10	0.008	0.009	0.013	0.010	0.003	0.189	0.190	0.189	0.189	0.000
	14	0.018	0.019	0.023	0.020	0.002	0.344	0.328	0.326	0.333	0.010
	18	0.019	0.020	0.024	0.021	0.003	0.292	0.259	0.326	0.293	0.034
	22	0.023	0.023	0.029	0.025	0.004	0.310	0.345	0.309	0.321	0.021
	26	0.042	0.041	0.046	0.043	0.003	0.533	0.570	0.550	0.551	0.018
	30	0.047	0.047	0.052	0.049	0.003	0.482	0.501	0.533	0.505	0.026
	34	0.052	0.052	0.057	0.054	0.003	0.533	0.570	0.498	0.534	0.036
	38	0.054	0.054	0.059	0.056	0.003	0.516	0.501	0.481	0.499	0.017
	42	0.058	0.058	0.062	0.059	0.002	0.482	0.518	0.515	0.505	0.020
	46	0.061	0.061	0.065	0.062	0.003	0.550	0.501	0.498	0.516	0.029
	50	0.062	0.061	0.066	0.063	0.003	0.585	0.570	0.584	0.579	0.009
76	0.076	0.075	0.081	0.077	0.003	0.000	0.604	0.601	0.402	0.348	

Pressure saturation of mortar bars

(Only bars nr. 2 and 3 pressure saturated in NaOH solution, bar nr. 1 dried and stored dry until further storing in NaOH-solution for all 3 bars)

Mix	Days	Expansion (%)			Weight increase (%)		
		1	2	3	1	2	3
Reference (no filler)	14	0.150	0.152	0.151	1.296	1.213	1.058
	28	0.326	0.334	0.339	2.143	2.050	1.928
	After drying (20°C)	0.242	0.251	0.255	-1.901	-2.050	-2.047
	After PS (20°C)	0.258	0.283	0.287	0.311	2.016	1.860
	PS + 14	0.445	0.462	0.467	1.849	2.255	2.133
	PS + 28	0.544	0.566	0.573	1.918	2.323	2.201
20 % mylonite filler	14	0.091	0.089	0.061	0.804	0.771	0.785
	28	0.153	0.142	0.148	1.223	1.173	1.118
	After drying (20°C)	0.070	0.059	0.065	-0.85	-0.82	-0.85
	After PS (20°C)	0.076	0.065	0.073	0.201	0.654	0.634
	PS + 14	0.194	0.182	0.192	1.006	1.207	1.152
	PS + 28	0.227	0.213	0.223	1.207	1.290	1.269
20 % rhyolite filler	14	0.014	0.015	0.015	0.600	0.582	0.622
	28	0.027	0.026	0.026	0.772	0.805	0.777
	After drying (20°C)	-0.053	-0.053	-0.053	-1.543	-1.489	-1.537
	After PS (20°C)	-0.045	-0.041	-0.041	-0.189	0.514	0.363
	PS + 14	0.043	0.044	0.043	0.669	0.959	0.846
	PS + 28	0.060	0.068	0.071	0.875	1.061	1.019
7.5 % silica fume	14	0.041	0.043	0.043	1.033	0.879	0.897
	28	0.131	0.126	0.132	1.481	1.533	1.415
	After drying (20°C)	0.043	0.038	0.043	-1.826	-1.929	-1.932
	After PS (20°C)	0.061	0.068	0.069	0.086	1.102	0.983
	PS + 14	0.223	0.218	0.224	1.516	1.637	1.656
	PS + 28	0.308	0.304	0.313	1.705	1.809	1.777

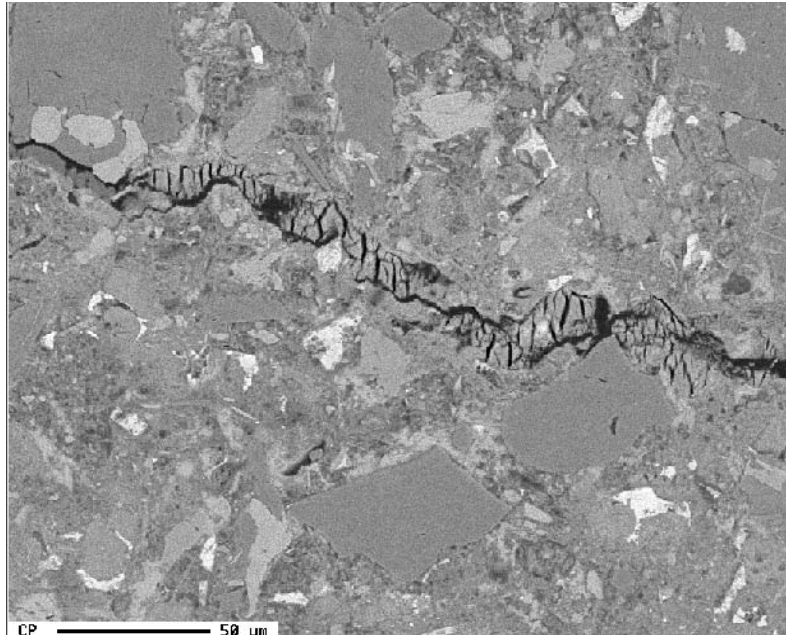
B4: Electron probe microanalyzer: chemical data, backscatter SEM micro photos and element mapping

Chemical analyses of alkali-silica gel in crack in mylonite-filler concrete

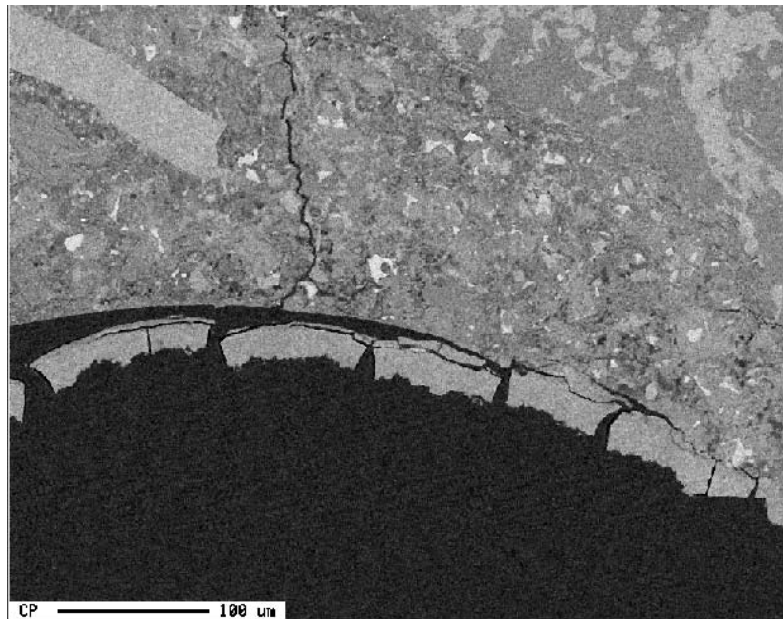
Nr.	Na ₂ O	K ₂ O	SiO ₂	CaO	SO ₃	Al ₂ O ₃	MgO	FeO	Total
1	2.91	1.84	31.47	38.89	0.21	1.43	0.02	0.00	76.27
2	0.94	1.44	31.16	41.07	0.19	1.42	0.05	0.00	81.18
3	2.16	2.86	34.25	39.58	0.25	2.04	0.04	0.00	76.34
4	3.04	4.22	30.82	36.97	0.12	1.14	0.03	0.00	78.16
5	4.47	3.69	32.53	35.05	0.10	2.12	0.20	0.00	82.82
6	5.24	5.07	39.97	32.34	0.07	0.13	0.00	0.00	81.54
7	5.35	4.41	42.60	28.95	0.06	0.17	0.01	0.00	79.01
Mean	3.44	3.36	34.69	36.12	0.14	1.21	0.05	0.00	79.33
St.dev.	1.64	1.36	4.71	4.31	0.07	0.80	0.07	0.00	2.59

Chemical analyses of ettringite in crack in mylonite-filler concrete

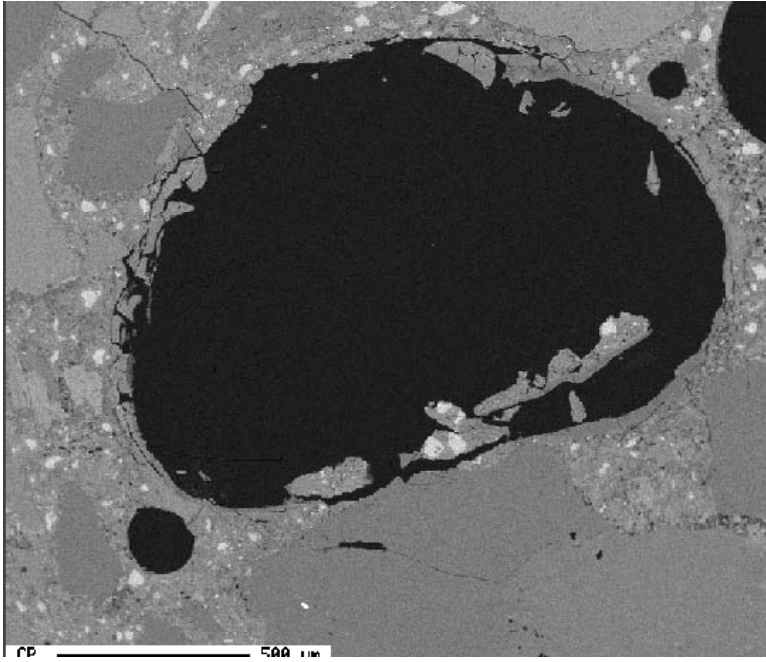
Nr.	Na ₂ O	K ₂ O	SiO ₂	CaO	SO ₃	Al ₂ O ₃	MgO	FeO	Total
1	1.08	0.59	0.39	54.64	15.76	15.66	0.01	0.00	89.13
2	0.58	0.58	0.15	57.07	16.28	18.03	0.02	0.00	94.70
3	6.90	0.71	0.24	55.01	15.36	17.26	0.02	0.00	98.50
mean	2.85	0.63	0.26	55.57	15.80	16.98	0.02	0.00	94.11
st.dev.	3.51	0.07	0.12	1.31	0.46	1.21	0.01	0.00	4.72



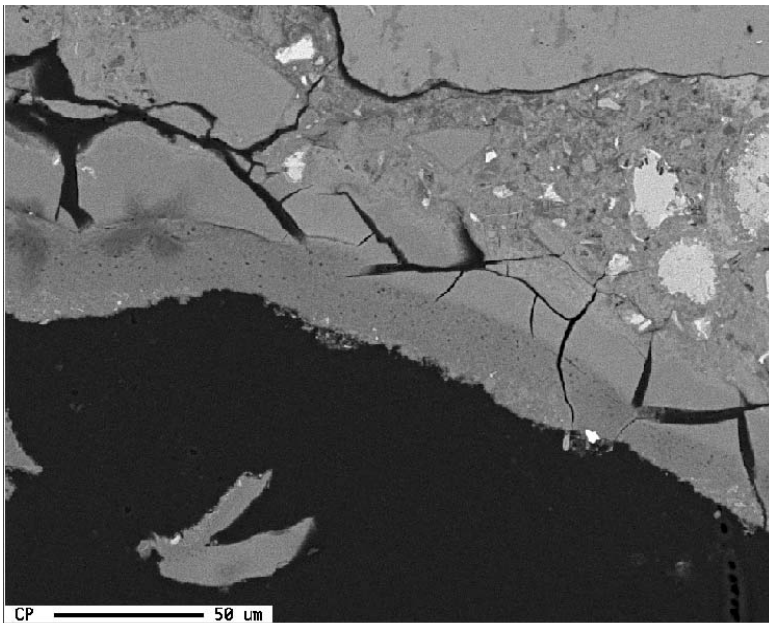
SEM 1. Crack filled with ettringite. (Mylonite filler concrete).



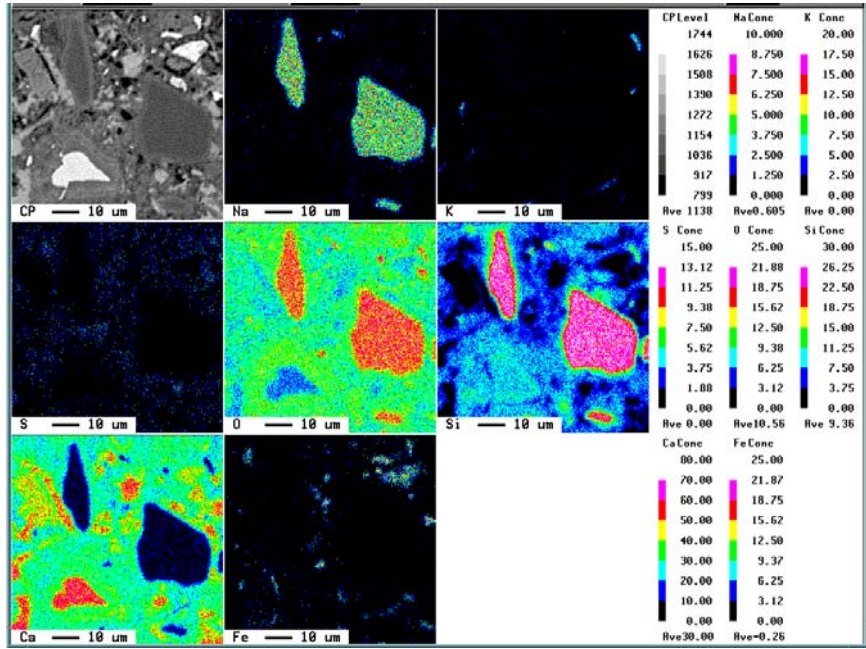
SEM 2. Air void with residue of alkali silica gel. (Mylonite filler concrete)



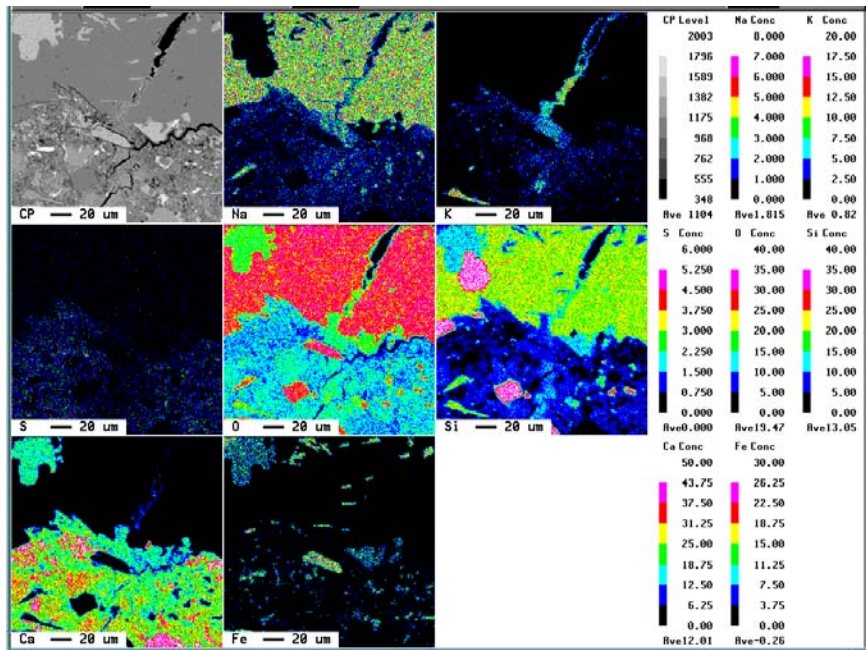
SEM 3. Air void with residue of alkali silica gel. (Glass filler concrete).



SEM 4. Detail of air void in photo 3.



Map 1. Element mapping of glass particles in concrete. (glass filler concrete).



Map 2. Element mapping of crack running from aggregate into cement paste (mylonite filler concrete).

Appendix C

- C1 Results of the matrix testing by the FlowCyl viscometer
- C2 Results of the matrix testing by the Physica rheometer
- C3 Self-compacting concrete – test results

C1: Matrix rheology by the FlowCyl viscometer

All mixes with Norcem Standardsement (OPC) and SSP 2000 plasticizer.

filler type	w/c	filler amount % of cement weight	plasticizer % of cement weight	λ_Q
no filler	0.5	0.0	0.64	0.24
granite/gneiss 0-125	0.5	14.3	0.73	0.32
granite/gneiss 0-125	0.5	28.6	0.82	0.44
granite/gneiss 0-125	0.5	57.1	1.00	0.75
granite/gneiss 0-125	0.4	2.7	0.65	0.60
granite/gneiss 0-125	0.6	54.1	0.98	0.35
mylonite 0-125	0.5	15.0	0.73	0.40
mylonite 0-125	0.5	30.0	0.82	0.60
mylonite 0-125	0.5	59.9	1.00	0.89
mylonite 0-125	0.4	2.9	0.65	0.65
mylonite 0-125	0.6	56.8	0.98	0.54
limestone 0-125	0.5	14.6	0.73	0.36
limestone 0-125	0.5	29.1	0.82	0.50
limestone 0-125	0.5	58.2	1.00	0.80
limestone 0-125	0.4	2.8	0.65	0.58
limestone 0-125	0.6	55.1	0.98	0.45
limestone 0-30	0.5	29.1	0.82	0.63
limestone 0-40	0.5	29.1	0.82	0.63
limestone 20-125	0.5	29.1	0.82	0.38
glass 0-125	0.5	13.4	0.73	0.45
glass 0-125	0.5	26.9	0.82	0.69
glass 0-125	0.5	53.7	1.00	0.93
glass 0-125	0.4	2.6	0.65	0.65
glass 0-125	0.6	50.8	0.98	0.74
fly ash 0-125	0.5	11.9	0.73	0.44
fly ash 0-125	0.5	23.7	0.82	0.76
fly ash 0-125	0.5	47.4	1.00	0.96
fly ash 0-125	0.4	2.3	0.65	0.65
fly ash 0-125	0.6	44.9	0.98	0.76
carbonate 0-125	0.5	14.6	0.73	0.34
carbonate 0-125	0.5	29.2	0.82	0.50
carbonate 0-125	0.5	58.4	1.00	0.80
carbonate 0-125	0.4	2.8	0.65	0.6
carbonate 0-125	0.6	55.3	0.98	0.43

λ_Q = flow resistance ratio measured by the FlowCyl viscometer

C2: Matric rheology by the Physica rheometer

All proportions in weight % of cement.

Cement	w/c	plasticizer type	plasticizer amount (% of cem.)	filler type	filler amount (% of cem.)	μ (Pas)	τ_0 (Pa)
OPC	0.4	SSP2000	0.80	Mylonite 0-20	30.0	3.12	49.8
OPC	0.4	SSP2000	0.80	Mylonite 0-125	30.0	1.62	15.3
OPC	0.4	Mighty 150	0.80	Mylonite 0-125	30.0	1.65	44.2
OPC	0.4	SSP2000	0.80	Limestone 0-125	29.1	1.39	12.3
OPC	0.4	Mighty 150	0.80	Limestone 0-125	29.1	1.22	28.7
OPC	0.4	SSP2000	0.80	Fly ash 0-125	24.2	2.13	26.6
OPC	0.4	Mighty 150	0.80	Fly ash 0-125	24.2	2.17	52.8
OPC	0.4	SSP2000	0.80	Glass 0-125	26.9	1.85	27.4
OPC	0.4	Mighty 150	0.80	Glass 0-125	26.9	1.52	44.1
OPC	0.4	Mighty 150	0.80	Granite 0-125	28.6	0.85	13.6
OPC	0.4	SSP2000	0.80	Granite 0-125	28.6	1.03	6.3
OPC	0.4	SSP2000	0.80	Granite 0-20	28.6	3.65	61.0
OPC	0.4	SSP2000	0.80	Granite 0-20/0-125	28.6	1.82	12.5
OPC	0.4	SSP2000	0.80	Rhyolite 0-125	27.0	2.32	59.5
OPC	0.4	SSP2000	0.80	Carbonate 0-125	29.2	1.12	2.1
OPC	0.4	SSP2000	0.80	Cataclasite 0-125	29.8	1.33	9.8
OPC	0.5	-	0.00	Mylonite 0-125	30.0	1.01	42.1
OPC	0.5	SSP2000	0.40	Mylonite 0-125	30.0	0.72	8.8
OPC	0.5	SSP2000	0.82	Mylonite 0-125	30.0	0.61	0.7
OPC	0.5	CP-30	0.40	Mylonite 0-125	30.0	0.38	3.0
OPC	0.5	CP-30	0.80	Mylonite 0-125	30.0	0.35	0.3
OPC	0.5	Viscocrete 3	0.40	Mylonite 0-125	30.0	0.50	5.1
OPC	0.5	Viscocrete 3	0.80	Mylonite 0-125	30.0	0.23	0.0
OPC	0.5	P	0.80	Mylonite 0-125	30.0	0.87	25.9
OPC	0.5	P	1.20	Mylonite 0-125	30.0	0.69	23.0
OPC	0.5	P	1.60	Mylonite 0-125	30.0	0.70	6.8
OPC	0.5	Mighty 150	0.40	Mylonite 0-125	30.0	0.83	21.5
OPC	0.5	Mighty 150	0.82	Mylonite 0-125	30.0	0.62	6.4
HSOPC	0.4	SSP2000	0.80	Mylonite 0-125	30.0	1.30	2.8
HSOPC	0.4	Mighty 150	0.80	Mylonite 0-125	30.0	1.98	50.7
ROPC	0.4	SSP2000	0.80	Mylonite 0-125	30.0	4.59	108.5
ROPC	0.4	Mighty 150	0.80	Mylonite 0-125	30.0	too stiff to test	
OPC	0.5	SSP2000	0.80	Limestone 0-125	29.1	0.41	0.2
OPC	0.5	Mighty 150	0.80	Limestone 0-125	29.1	0.42	3.0
OPC	0.5	SSP2000	0.80	Mylonite 0-125	59.9	1.37	11.2
OPC	0.5	SSP2000	1.00	Mylonite 0-125	60.0	1.40	6.4
OPC	0.5	Mighty 150	0.80	Mylonite 0-125	60.0	1.34	40.7
OPC	0.5	Mighty 150	1.00	Mylonite 0-125	60.0	1.25	28.6
OPC	0.5	SSP2000	0.80	Limestone 0-125	58.3	1.02	4.7
OPC	0.5	SSP2000	1.00	Limestone 0-125	58.3	0.96	3.8

μ = plastic viscosity

τ_0 = yield stress

Cement	v/c	plasticizer type	plasticizer amount (% of cem.)	filler type	filler amount (% of cem.)	μ (Pas)	τ_0 (Pa)
OPC	0.5	Mighty 150	0.80	Limestone 0-125	58.3	0.86	18.8
OPC	0.5	Mighty 150	1.00	Limestone 0-125	58.3	0.80	7.9
OPC	0.5	SSP2000	1.00	Granite 0-125	57.1	0.66	0.0
OPC	0.5	Mighty 150	1.00	Granite 0-125	57.1	0.58	2.0
OPC	0.5	SSP2000	1.00	Glass 0-125	53.7	1.63	10.1
OPC	0.5	Mighty 150	1.00	Glass 0-125	53.7	too stiff to test	
OPC	0.5	SSP2000	1.00	Cataclasite 0-125	59.6	1.23	2.6
OPC	0.5	SSP2000	1.00	Fly ash 0-125	48.4	2.13	15.1
OPC	0.5	SSP2000	1.00	Carbonate 0-125	58.4	0.68	0.0

C3: Self-compacting concrete – fresh properties and compressive strength

Series nr.	w/b	s/c	Cement	Plasticizer		Added filler		Matrix	Slump
				Type	Amount	Type	Amount	Amount (l/m ³)	(mm)
1	0.40	5 %	HSOPC	Scanflux CP30	1.00 %	Limestone	20 %	325	245
	0.40	5 %	HSOPC	Scanflux CP30	1.00 %	Limestone	20 %	340	280
	0.40	5 %	HSOPC	Scanflux CP30	1.00 %	Limestone	20 %	355	285
2	0.40	5 %	HSOPC	Scanflux CP30	1.00 %	Mylonite	20 %	325	255
	0.40	5 %	HSOPC	Scanflux CP30	1.00 %	Mylonite	20 %	340	270
	0.40	5 %	HSOPC	Scanflux CP30	1.00 %	Mylonite	20 %	355	270
	0.40	5 %	HSOPC	Scanflux CP30	1.00 %	Mylonite	20 %	370	285
3	0.50	5 %	ROPC	Scanflux CP30	1.00 %	Limestone	20 %	355	260
	0.50	5 %	ROPC	Scanflux CP30	1.00 %	Limestone	20 %	370	270
	0.50	5 %	ROPC	Scanflux CP30	1.00 %	Limestone	20 %	385	275
	0.50	5 %	ROPC	Scanflux CP30	1.00 %	Limestone	20 %	400	275
4	0.50	5 %	ROPC	Scanflux CP30	1.00 %	Mylonite	20 %	355	250
	0.50	5 %	ROPC	Scanflux CP30	1.00 %	Mylonite	20 %	370	260
	0.50	5 %	ROPC	Scanflux CP30	1.00 %	Mylonite	20 %	385	275
	0.50	5 %	ROPC	Scanflux CP30	1.00 %	Mylonite	20 %	400	270
5	0.50	5 %	OPC	Scanflux CP30	1.00 %	Limestone	20 %	325	230
	0.50	5 %	OPC	Scanflux CP30	1.00 %	Limestone	20 %	340	270
	0.50	5 %	OPC	Scanflux CP30	1.00 %	Limestone	20 %	355	275
	0.50	5 %	OPC	Scanflux CP30	1.00 %	Limestone	20 %	370	280
6	0.50	5 %	OPC	Scanflux CP30	1.00 %	Mylonite	20 %	325	240
	0.50	5 %	OPC	Scanflux CP30	1.00 %	Mylonite	20 %	340	255
	0.50	5 %	OPC	Scanflux CP30	1.00 %	Mylonite	20 %	355	275
	0.50	5 %	OPC	Scanflux CP30	1.00 %	Mylonite	20 %	370	275
7	0.60	0	OPC	SSP 2000+	1.20 %	Limestone	60 %	340	240
	0.60	0	OPC	SSP 2000+	1.20 %	Limestone	60 %	350	255
	0.60	0	OPC	SSP 2000+	1.20 %	Limestone	60 %	360	265
	0.60	0	OPC	SSP 2000+	1.20 %	Limestone	60 %	370	265
8	0.40	0	OPC	SSP 2000+	1.00 %	-	-	340	-
	0.40	0	OPC	SSP 2000+	1.00 %	-	-	360	-
	0.40	0	OPC	SSP 2000+	1.00 %	-	-	380	-
	0.40	0	OPC	SSP 2000+	1.00 %	-	-	400	-
9	0.50	5 %	SROPC	Scanflux CP30	0.70 %	Limestone	15 %	310	245
	0.50	5 %	SROPC	Scanflux CP30	0.70 %	Limestone	15 %	325	265
	0.50	5 %	SROPC	Scanflux CP30	0.70 %	Limestone	15 %	340	275
10	0.50	5 %	ROPC	Scanflux CP30	1.00 %	-	-	325	250
	0.50	5 %	ROPC	Scanflux CP30	1.00 %	-	-	340	265
	0.50	5 %	ROPC	Scanflux CP30	1.00 %	-	-	355	265
	0.50	5 %	ROPC	Scanflux CP30	1.00 %	-	-	370	270


Series 7: 0.6 % Scancem VMA (of cement weight) added

Series 8: 0.5 % Scancem VMA (of cement weight) added

Series nr.	SF	T ₅₀₀	Concrete rheology		Matrix rheology			Air	Density	Compr. strength	
	(mm)	(s)	τ_0 (Pa)	μ (Pas)	τ_0 (Pas)	μ (Pas)	λ_Q	(%)	(kg/m ³)	1 day (MPa)	28 days (MPa)
1	550	8.0	147.0	57.9	3.9	0.88	0.74	2.7	2431	28.6	89.4
	740	1.5	19.1	19.4				0.9	2400	24.4	84.0
	765	0.9	28.7	15.9				0.7	2407	21.6	82.3
2	540	2.5	193.9	36.5	4.6	1.00	0.78	2.5	2427	28.4	88.5
	635	1.8	31.8	37.2				1.8	2416	25.7	87.3
	660	1.2	24.5	25.2				1.2	2415	26.1	83.1
	760	0.8	4.0	15.9				0.7	2414	22.8	83.1
3	540	1.6	38.7	17.7	8.8	0.70	0.60	1.6	2413	39.7	73.8
	650	1.2	23.3	14.1				1.2	2382	41.7	74.9
	640	0.9	14.8	10.1				0.9	2375	40.8	71.6
	670	0.4	9.5	7.3				0.7	2384	38.6	70.9
4	535	2.3	52.3	20.2	9.5	0.81	0.63	2.6	2384	40.9	73.6
	620	1.2	23.0	14.5				1.0	2397	39.1	72.5
	660	0.3	16.8	10.5				0.7	2389	38.7	70.9
	680	0.7	15.1	8.3				0.7	2378	36.3	72.4
5	435	-	58.1	38.7	2.0	0.38	0.45	2.7	2366	27.4	70.8
	615	2.0	23.1	21.5				1.4	2411	23.8	66.7
	675	1.0	13.3	11.6				0.7	2404	22.6	65.6
	760	0.3	22.9	7.6				0.4	2387	19.5	65.8
6	480	-	77.2	36.9	3.8	0.47	0.49	2.5	2360	24.7	67.3
	580	3.4	33.9	22.8				2.7	2375	24.1	66.7
	670	1.0	18.2	14.5				1.0	2409	20.2	63.6
	750	0.5	10.0	7.9				0.5	2398	17.7	63.0
7	470	-	289.0	46.6	5.6	0.71	0.73	2.5	2386	-	45.6
	570	3.8	143.6	30.4				2.0	2399	-	45.5
	615	3.2	94.8	25.5				1.7	2375	-	44.8
	670	2.4	26.5	21.8				1.0	2395	-	44.3
8	440	-	113.0	44.6	10.7	0.85	0.82	-	-	-	-
	518	4.0	65.0	29.7				-	-	-	-
	580	1.9	59.0	21.3				-	-	-	-
	650	1.3	23.0	17.0				-	-	-	-
9	540	3.0	56.8	21.3	0.5	0.32	0.49	2.5	2404	-	66.9
	670	1.0	32.7	12.6				1.7	2389	-	64.0
	715	0.5	2.5	7.5				0.8	2394	-	61.8
10	540	1.4	48.6	16.6	6.0	0.35	0.51	2.0	2385	-	75.0
	600	0.9	26.8	11.5				1.4	2401	-	76.4
	620	0.8	18.6	8.2				1.0	2387	-	74.0
	670	0.7	13.7	6.4				0.6	2405	-	76.2

Appendix D

Optical microscopy report with photos – concrete specimens

		<h1>Rapport</h1>		Norsk betong - og tilslagslaboratorium AS
Tittel Micro structural analyses of Canadian concrete prisms with fillers		Osloveien 18 B 7018 Trondheim Telefon 73 531173 Telefax 73 531174 Mobil: 99712599 E-mail: viggo.jensen@nbt.no Web: www.nbt.no		
Oppdragsgiver(e) Bård Pedersen		Organisasjonsnr. NO 984 706 138		
Oppdragsgivers referanse				
Forfatter(e) Viggo Jensen		Ansvarlig signatur		
Rapportnummer R02004	Dato 2002-12-19	Gradering: Fortrolig	Antall sider og bilag (sider) 5 + 1 (9)	

Sammendrag

The aim of this micro structural analysis is to examine and describe textural changes and reaction products due to Alkali Silica Reaction (ASR). This in concretes with different filler types accelerated one year according to the concrete prism method CSA CAN A23.2 14A. Micro structural analyses have been carried out on fluorescent impregnated thin sections (TS) and fluorescents impregnated polished section (PS).

The report examines and describes cracks, reaction products, fillers and capillary porosity in the samples.

It is revealed that deleterious ASR and significant cracking of coarse aggregates occur in samples CAN 1 (reference) and CAN 2. (Tau filler). In the CAN 18 sample (glass filler) gel is observed and the reaction classified as minor. No sign of ASR has been observed in sample CAN 5 (rhyolite filler).

Stikkord/key words

Byggteknikk	Betong	Bestandighet	Alkalireaksjon	Strukturanalyse
Building technology	Concrete	Durability	Alkali Silica Reaction	Micro structural analysis

Norsk betong- og tilslagslaboratorium AS (NBTL) er et uavhengig norsk selskap opprettet 11. juli 2002. Et av formålene med selskapet er å tilby kostnadseffektiv prøving og tjenester av høy kvalitet til byggindustrien, byggherrer og betong - og tilslagsbransjen.



Innhold

- 1 Introduction**
- 2 Results**
- 3 Summarizing results**
- 4 Conclusions**
- 5 References**

Appendices 1: Photos, 9 pages



1 Introduction

The aim with this micro structural analyses is to examine and describe textural changes and reaction products in concretes mixed with different filler types. The concrete samples have been exposed 1 year at 38 degree C° in storage condition given by the Canadian concrete test method CSA CAN A23.2 14A. The investigation has been carried out by use of fluorescent impregnated thin sections (TS) and fluorescents impregnated polished section (PS) examined by polarizing microscope, stereo microscope and UV - light. The dimensions of thin sections are 30 mm x 48 mm and polished sections 100 mm x 70 – 75 mm. In the following, an observation of textural changes and reaction product caused by Alkali Silica Reaction (ASR) is described.

2 Results

2.1 Sample Can 1 (reference concrete)

Polished section:

Nearly all the coarse aggregates have cracks. Cracks occur mostly as internal single cracks in aggregates which often runs out into the cement paste, and cracks in the cement paste connecting one or several “reacted” aggregates (reaction type 5 /1/), *see photos 1 and 2*. White coloured reaction product (gel with shrinkage cracks) has been observed in cracks and air voids.

Thin section (polished)

Many of the coarse aggregates are cracked, but no crack runs out in the cement past. Internal cracks up to 0.2 mm occur in coarse aggregates. Some of these cracks have widened up in a way suggesting partial dissolution of mineral crystals, *see photos 3 and 4*. However, reaction product (e.g. gel) has not been observed in aggregates or the cement paste. This even the cracking pattern in aggregates and cement paste suggest cracks to be caused by ASR.

The capillary porosity observed under UV light is homogeneous and suggest water/cement ratio to be 0.45.


2.2 Sample Can 2 (concrete with Tau filler)

Polished section:

Many of the coarse aggregates have cracks. Cracks occur mostly as internal single cracks in aggregates which often runs out into the cement paste, and cracks in the cement paste connecting one or several “reacted” aggregates (reaction type 5 /1/), *see photos 5 and 6*. White coloured reaction product (gel with shrinkage cracks) has been observed in cracks and air voids.

Thin section

Some of the coarse aggregates are cracked. Internal cracks are mostly visible under fluorescence light. Some few cracks in aggregates are widened up to 0.1 mm in a way suggesting partial dissolution of mineral crystals. Reaction product occurs in aggregates and in the cement paste. In aggregates brown coloured crypto crystalline reaction product occur in



internal cracks /1/. In the cement paste some cracks runs out from aggregates and connects reacted aggregates. Opaque gel fills the cracks and occur occasionally laminated. Tau filler is not visible in the cement past, *see photos 7, 8 and 9*.
The capillary porosity observed under UV light is homogeneous and slightly lower than the reference CAN 1 concrete.

2.3 Sample Can 5 (concrete with rhyolite filler)

Polished section:

In UV - light some of the coarse aggregates have fine internal cracks. Only one crack has been observed to run out into the cement paste. No reaction product have been observed, *see photos 10 and 11*.

Thin section

In coarse aggregates cracks (crack width 0.01 mm) are only visible by use of fluorescent light. Reaction products are not observed in aggregates or other places in the cement paste. Rhyolite filler which are added to the concrete is difficult to identify in thin section. This because of the “small” particle size and that rhyolite coincide with the cement paste. However, some rhyolite particles with plagioclase crystals and “glassy” matrix have been identified, *see photos 12 and 13*. The particle size varies from 0.13 mm to 0.03 mm. The amount of rhyolite particles is insignificant.

The capillary porosity observed under UV light is inhomogeneous and significant lower than the reference CAN 1 concrete.

2.4 Sample Can 18 (concrete with glass filler)

Polished section:

In UV - light some of the coarse aggregates appear with fine internal cracks. No crack has been observed to run out into the cement paste. No reaction product has been observed, *see photos 14 and 15*.

Thin section

In coarse aggregates cracks (crack width 0.01 mm) are visible only by use of fluorescent light. Reaction product is observed in one 0.5 mm air void filled with opaque gel and few micro cracks running out from coarse aggregates, *see photos 16 and 18*. Glass filler particles in the cement paste are easily identified by use of polarizing light with added lambda plate (increase the light with one order). Glass particles occur angular and often flaky. The particle size varies from 0.13 mm to 0.002 mm, but some glass particles might be smaller, *see photo 17*.

The capillary porosity observed under UV light is inhomogeneous and significant lower than the reference CAN 1 concrete.

3 Summarizing results

The observations from polished sections and thin sections are summarised in table 1



Table 1 Summarized observations

Sample	Cracks	Gel	ASR	Filler/size	Cap. porosity
CAN 1	many	yes*	Deleterious*	none	w/c- ratio 0.45
CAN 2	many	yes	Deleterious*	not observed	slightly reduced
CAN 5	few	no	none	few/ 0.13 -0.03mm	significant reduced
CAN 18	few	yes	Minor*	many/ 0.13 -0.002 mm	significant reduced

* gel occur only in polished section and not in the thin section

** deleterious when ASR causes cracks in the cement paste. Minor when ASR not causes cracks.

4 Conclusions

ASR:

Deleterious ASR and significant cracking of coarse aggregates occur in samples CAN 1 and CAN 2. In sample CAN 1 gel has been observed in the polished section but not in the thin section even the cracking pattern suggest ASR. Gel is most likely dissolved by water during preparation of the polished thin section. In the CAN 18 sample gel is only observed in an air void and few micro cracks. Therefore reaction is classified as minor. The observation of gel in micro cracks suggest an origin from reacted natural aggregates. No sign of ASR has been observed in sample CAN 5.

Filler:

In the CAN 2 sample Tau filler cannot be identified in thin section probably because Tau filler appear like other types of filler from natural sand. In the CAN 5 sample rhyolite filler occur in the fractions 0.13 mm to 0.03 mm. Only few rhyolite filler particles have been observed and in a much lesser amount than justified by the mix proportion. This could be caused by: 1) rhyolite particles have reacted with the cement paste (puzzolane reaction) and “disappeared” or 2) rhyolite particles occur in the cement paste but are invisible and cannot be identified in the thin section. The last possibility because rhyolite is difficult to distinguish from the cement paste and more or less coincide with the cement paste. In the CAN 18 sample glass filler is easily identified and many particles have been observed. Particle size varies from 0.13 mm to 0.002 mm. Smaller particles might occur but cannot be observed in thin section. Some glass filler particles occur with irregular edges suggesting partial dissolution and reaction with the cement paste.

Capillary porosity

The capillary porosity in CAN 1 sample compared with standards is of the same order as equivalent water/cement- ratio 0.45. The capillary porosity of sample CAN 2 is slightly lesser than sample CAN 1. The samples CAN 5 and CAN 18 have a significant lower capillary porosity. The reduced capillary porosity measured in samples with fillers might be caused by: 1) puzzolane reaction with consequence of lower capillary porosity in the cement paste or 2) higher water demand caused by added filler material with consequence of less free water available for hydratization of cement (lower water/cement – ratio).

5 Referances

/1/ **Viggo Jensen 1993:** “Alkali Aggregate Reaction in Southern Norway”, Doctor Technicae Thesis, Division of geology and mineral resources engineering, The Norwegian Institute of Technology, University of Trondheim

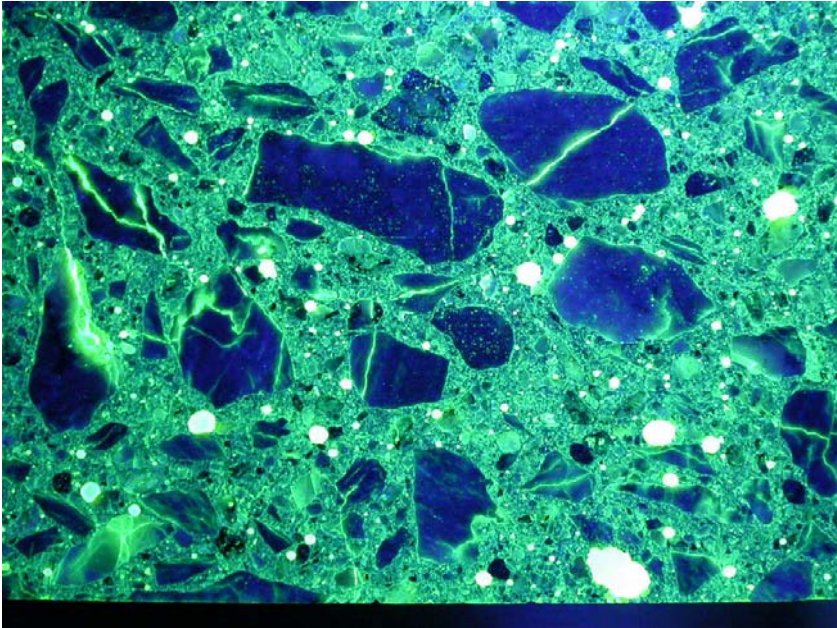


Photo 1 CAN 1 polished section photographed in UV – light. High of photo is 7 cm

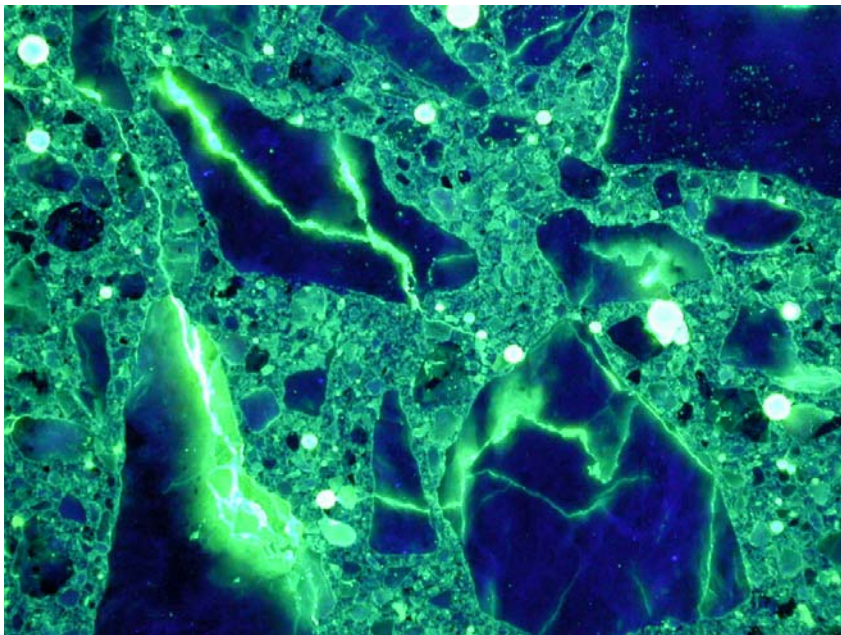


Photo 2 CAN 1 polished section photographed in UV – light. Detail

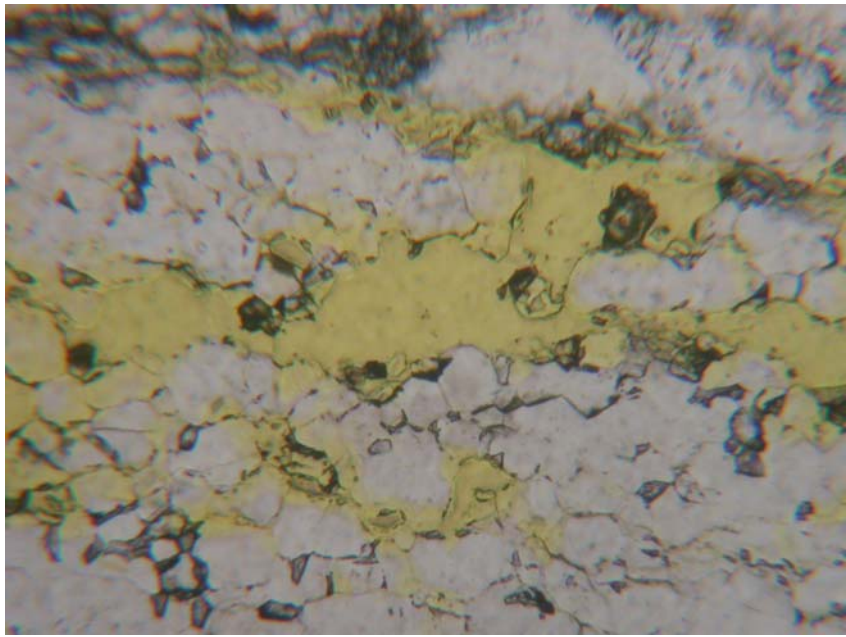


Photo 3 CAN 1 thin section. Possible dissolution of quartz crystals in reacted aggregate. Length of photo is 0.5 mm



Photo 4 CAN 1 thin section. Same as photo 3. Polarized light. Dissolution of quartz crystals in reacted aggregate. Length of photo is 0.5 mm

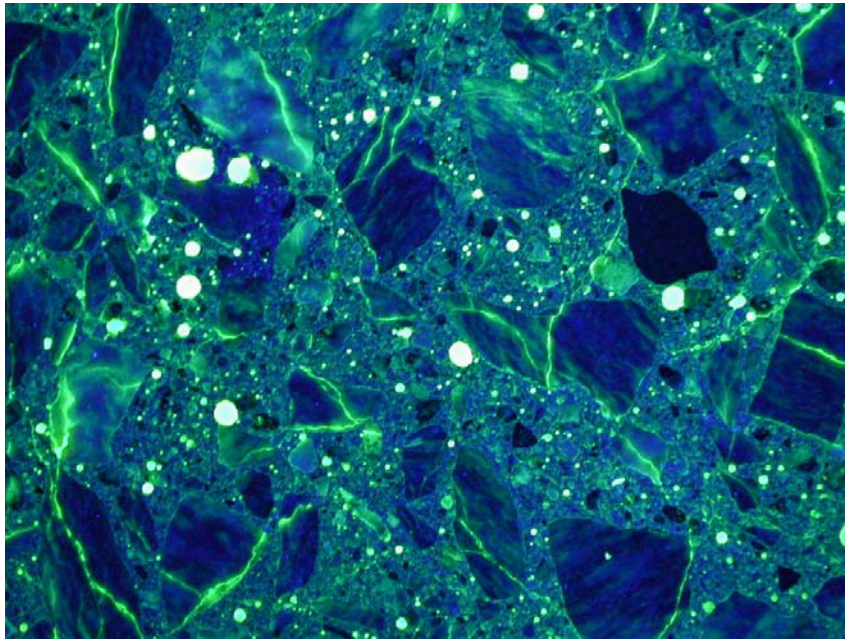


Photo 5 CAN 2 polished section photographed in UV – light. High of photo is 7 cm

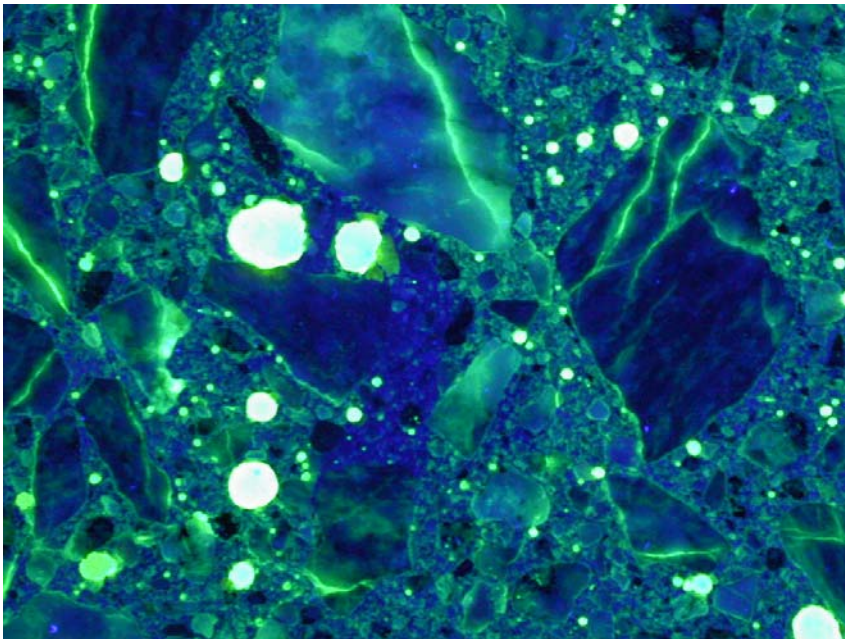


Photo 6 CAN 2 polished section photographed in UV – light. Detail

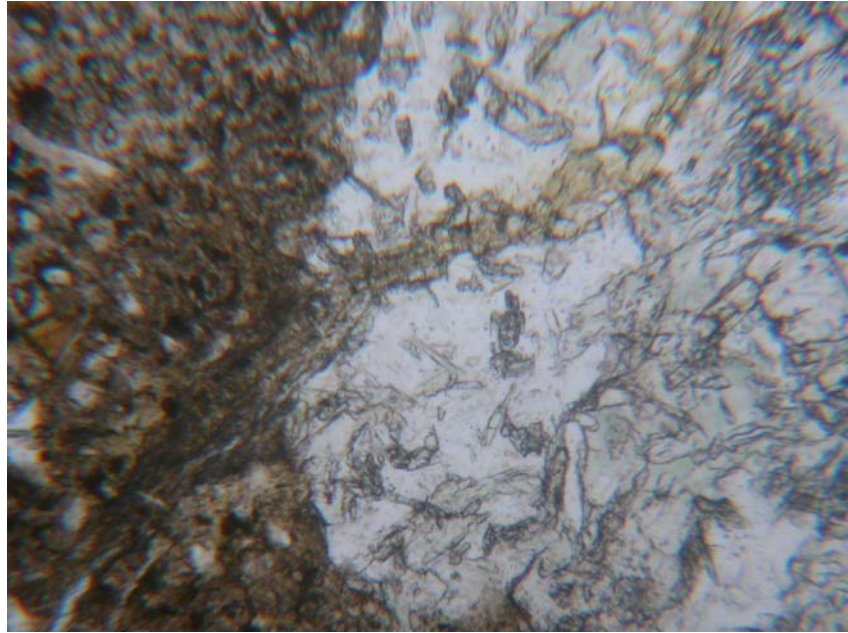


Photo 7 CAN 2 thin section. Reacted aggregate where gel in a crack runs out in to the cement paste. Ordinary light. Length of photo is 0.5 mm

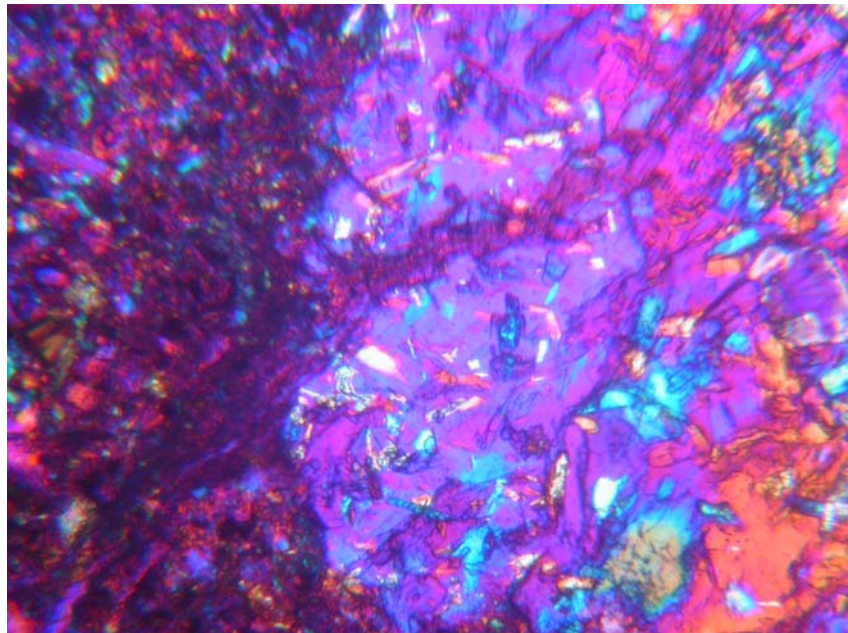


Photo 8 CAN 2 thin section. Same as photo 8. Reacted aggregate where gel in a crack runs out into the cement paste. Gypsum. Length of photo is 0.5 mm

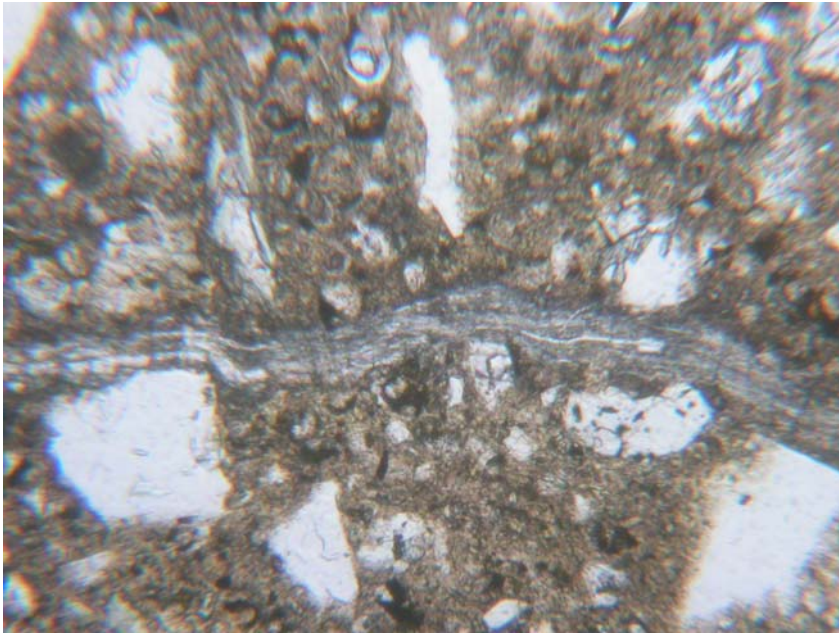


Photo 9 CAN 2 thin section. Gel in a crack in the cement paste. Ordinary light. Length of photo is 0.5 mm

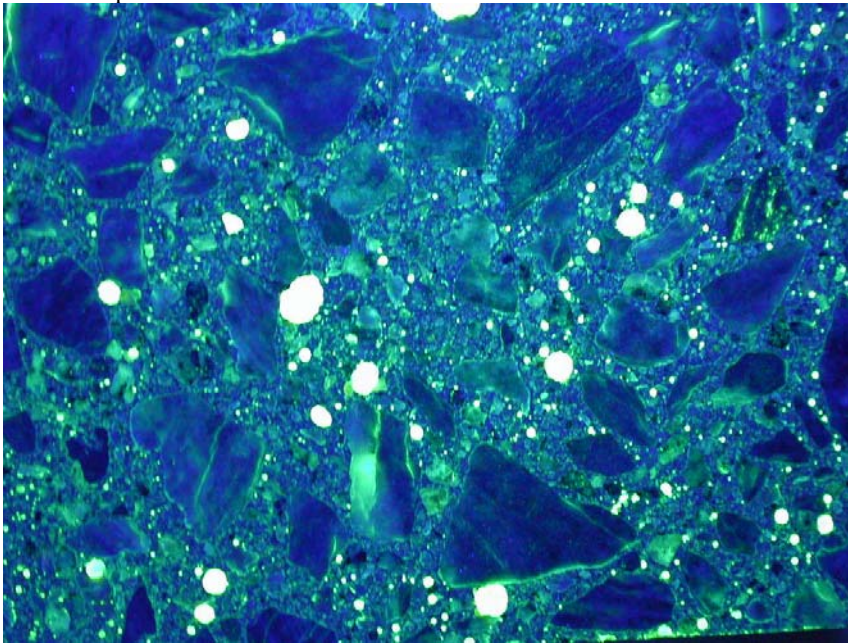


Photo 10 CAN 5 polished section photographed in UV – light. High of photo is 7 cm



Photo 11 CAN 5 polished section photographed in UV – light. Detail

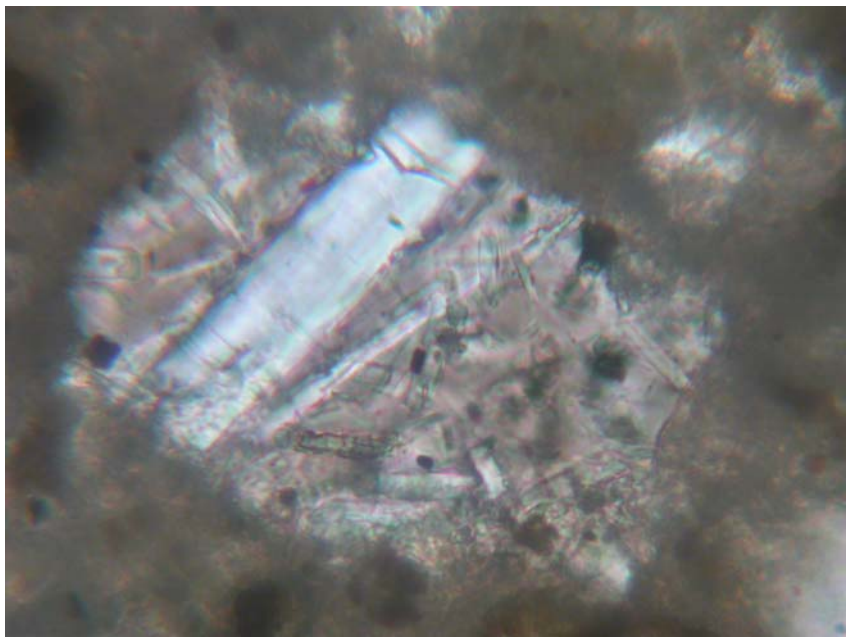


Photo 12 CAN 5 thin section. Rhyolite particle in the cement paste. Ordinary light. Length of photo is 0.125 mm

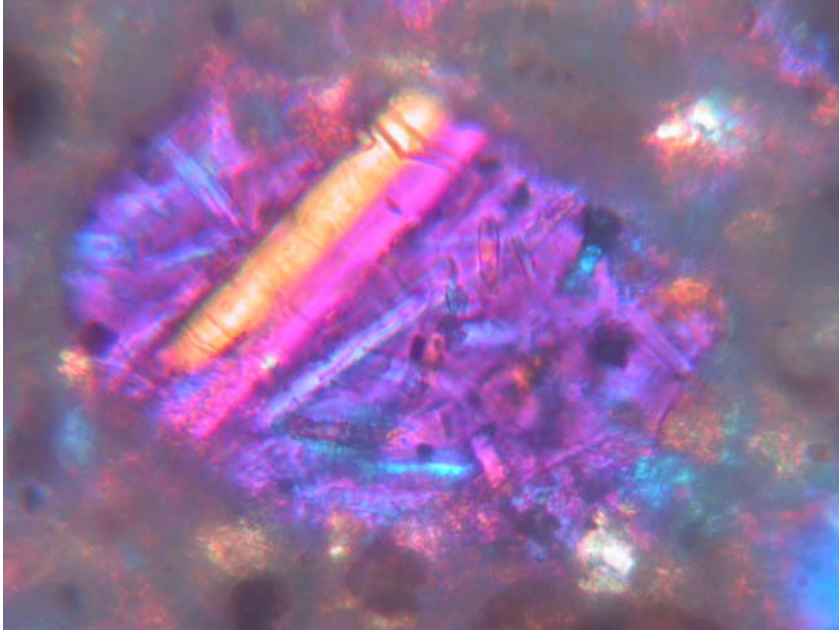


Photo 13 CAN 5 thin section. Same as photo 12. Rhyolite particle in the cement paste. Gypsum.. Length of photo is 0.125 mm

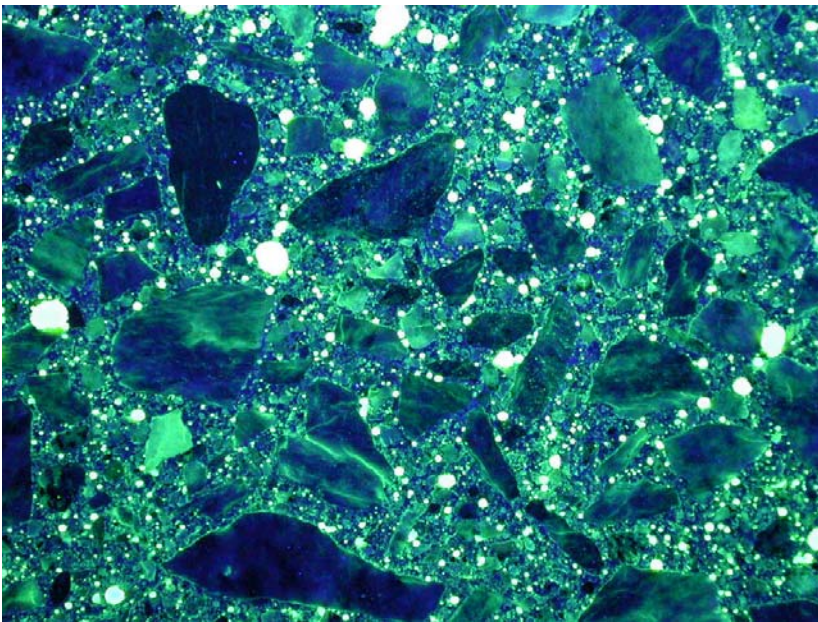


Photo 14 CAN 18 polished section photographed in UV – light. High of photo is 7 cm

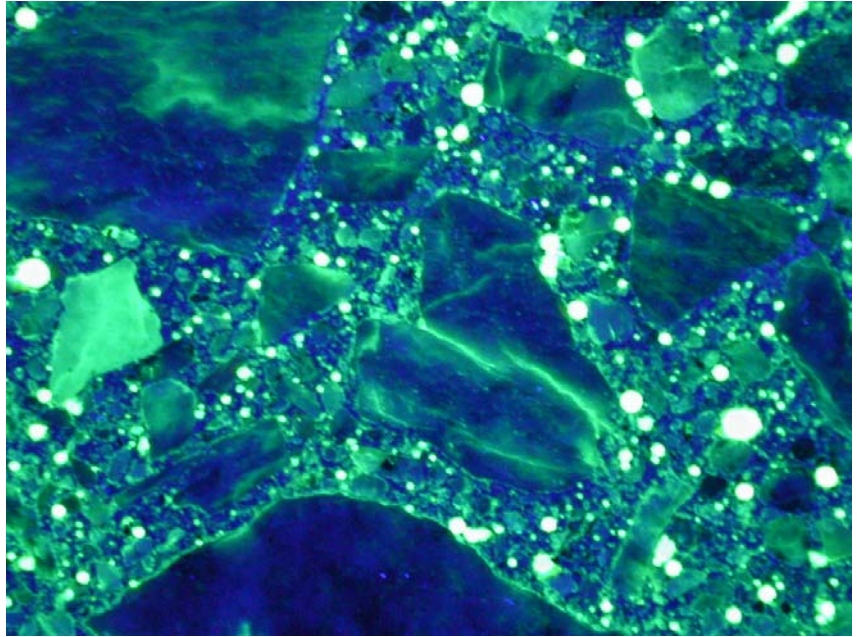


Photo 15 CAN 18 polished section photographed in UV – light. Detail

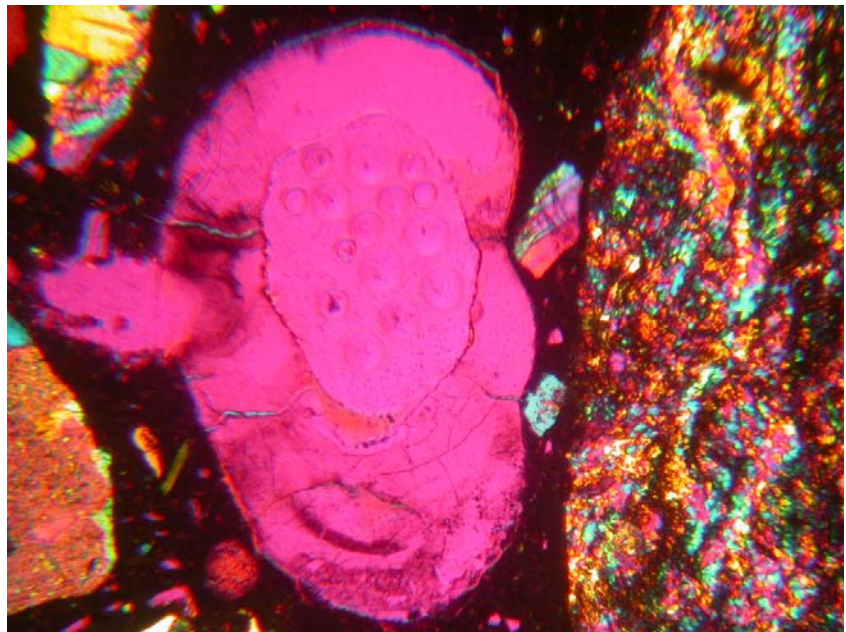


Photo 16 Gel filling in an air void. Gypsum. Length of photo is 0.9 mm

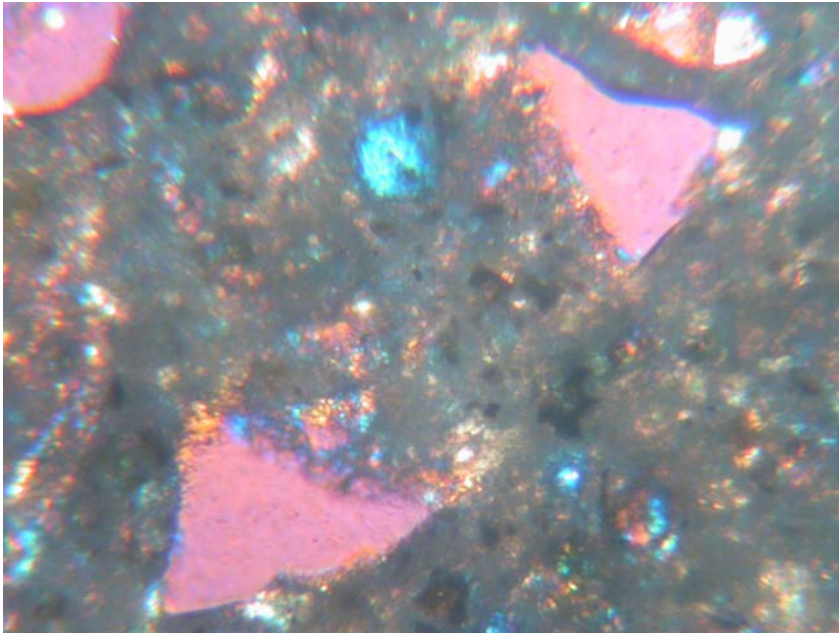


Photo 17 Glass filler particles in cement paste. Note the irregular edges of particles suggesting partial dissolution of glass. Gypsum. Length of photo is 0.4 mm

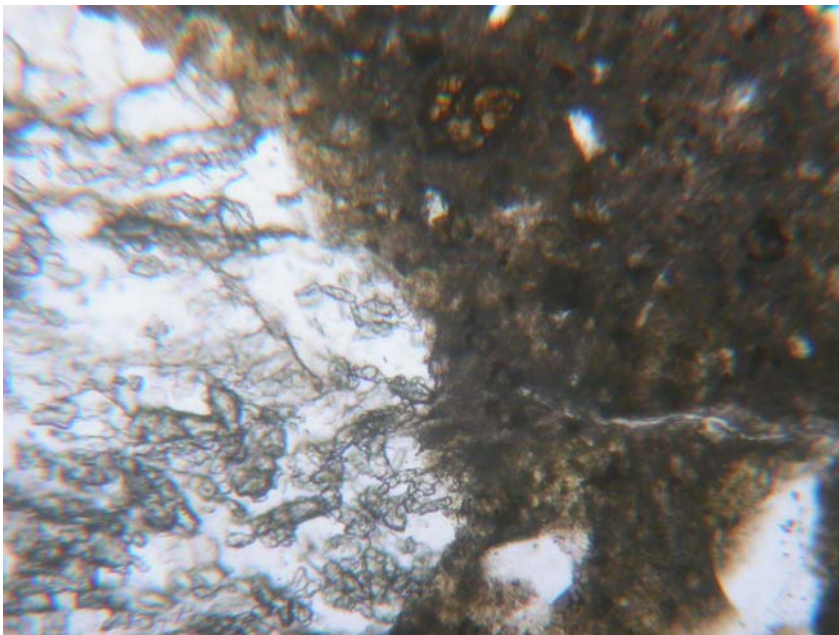


Photo 18 Gel in a crack which runs out from aggregate particle. Ordinare light. Length of photo is 0.5 mm

Appendix E

Optical microscopy report with photos – mortar specimens

**SINTEF****TEST REPORT****SINTEF Civil and Environmental Engineering**
Cement and ConcreteAddress: N-7465 Trondheim
NORWAY
Location: Richard Birkelands vei 3
Telephone: +47 73 59 52 24
Fax: +47 73 59 71 36

Enterprise No.: NO 948 007 029 MVA

Certified Test House No. HU2



CLIENT(S)

Bård Pedersen
NTNU-Department of structural engineering
N-7465 TRONDHEIM

CLIENT'S REF

Agreement of 2003-12-17 / Bård Pedersen

TYPE OF COMMISSION

THIN SECTION ANALYSES OF MORTAR PRISMS

FILE CODE

CLASSIFICATION

Confidential

ELECTRONIC FILE CODE

I:\pro\22M048.10\Report SA-exposed prisms.doc

DISCIPLINARY SIGNATURE

Harald Justnes

REPORT NO.

22M048.10

PROJECT NO.

DATE

22M048.10

2004-06-29

PERSON RESPONSIBLE

Marit Haugen

PAGES/APPENDICES

2/1

1 BACKGROUND

This work has been carried out in order to examine two different mortars exposed to “The accelerated mortar bar test” with the scope of detecting possible differences. The first mortar is composed with mylonite aggregate from Tau (without filler - according to standard method), while the other contains both mylonite aggregate (Tau) and mylonite filler (Tau, 0-20 µm).

2 SAMPLES

2 mortar prisms (40 mm x 40 mm x 160 mm) marked “22M048.10, 4/9-00, 21 with filler from Tau” and “22M224.02, Mix No 5, 11/9-02, Reference 41” were sawn in the middle, perpendicular to the length axis, and inspected visually. A remarkable difference between the two mortar prisms is that the reference prism has a larger amount of big air voids and more white coloured precipitation in the air voids than the prism with filler from Tau.

3 EXAMINATIONS

From a cross section in the middle of both prisms 1 fluorescence impregnated thin section (30 mm x 50 mm) was prepared. Three of the four exposed surfaces of the mortar prisms are therefore represented in the thin section. In the report the thin section from the prism with filler from Tau is named “Filler section”, and the thin section from the reference prism is named “Ref. section”. Microscopy analyses of the thin sections in a polarization microscope were carried out with photographs for documentation.

The test results only relate to the items tested.

This report must neither be translated nor published in extracted or abbreviated form prior to receiving approval from SINTEF
Tested objects and spare specimens can be disposed off 1 month after the Test Report date.

4 RESULTS

The observations in the thin sections from the mortar prisms are as follows:

- The “Ref. section” reveals much more microcracks and fine cracks than the “Filler section”, and the cracks occur through the whole thin section. The cracks in the “Filler section” are mainly observed near the exposed surfaces (in a zone of about 6 mm thickness), while the inner part has only a few cracks
- In the “Ref. section” a strong cracking/partly dissolution of aggregate grains is observed through the whole thin section. In the “Filler section” this can mainly be observed near the exposed surfaces (in a zone of about 6 mm thickness)
- In the “Ref. section” a larger amount of alkali gel is observed in the air voids and cracks than in the “Filler section”, and this occurs through the whole thin section. In the “Filler section” such gel can mainly be observed near the exposed surfaces (in a zone of about 6 mm thickness)
- In the “Ref. section” there is a larger amount of big air voids than in the “Filler section”

5 CONCLUSION

In the reference mortar there are much more microcracks, fine cracks, big air voids, more alkali gel, stronger cracking in aggregate grains and more partly dissolved aggregate grains than in the mortar with Tau filler. Cracking, partly dissolution of aggregate grains and gel are in the mortar with Tau filler mainly observed near the exposed surfaces (in a zone of about 6 mm thickness).

The results indicate that the mortar with filler from Tau is more dense, and that the rate of alkali ingress from the exposure solution is lower. It seems like the Tau filler has densified this mortar since the nominal w/c is equal for both mortars.

APPENDIX 1: Photographs

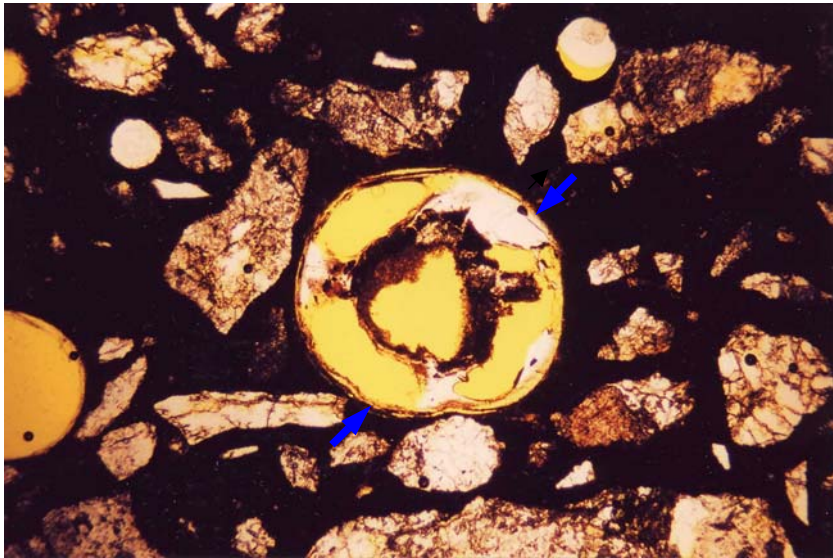


Figure 1 The picture shows alkali gel (bright and brownish, marked with arrows) in air voids in the “Ref. section”. The size of the picture is 4.2 mm x 2.7 mm.

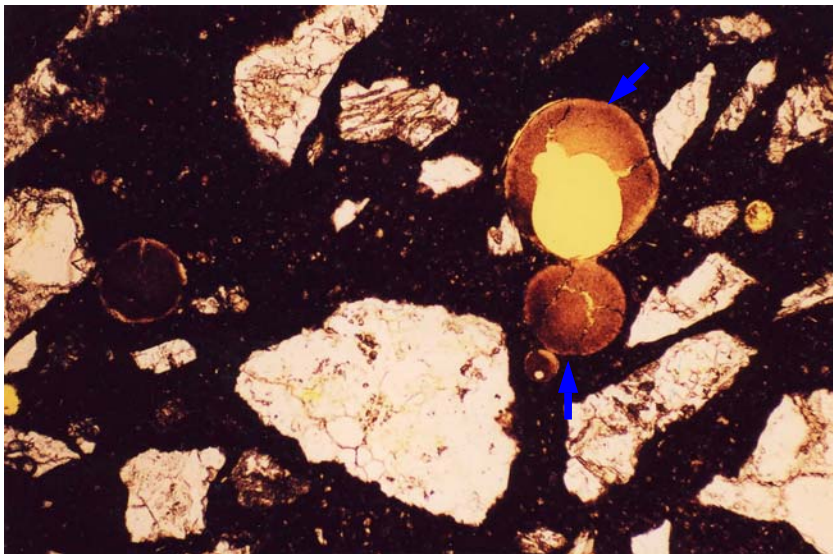


Figure 2 The picture shows alkali gel (brownish, marked with arrows) in air voids in the “Filler section”. The size of the picture is 4.2 mm x 2.7 mm.

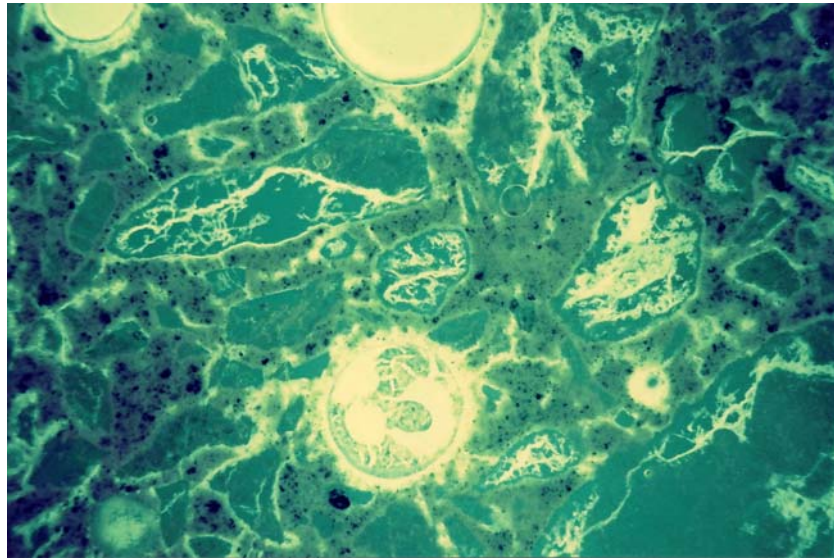


Figure 3 The picture shows cracks and partly dissolution of aggregate grains (yellow areas) in the “Ref. section” (fluorescence light). The size of the picture is 4.2 mm x 2.7 mm.

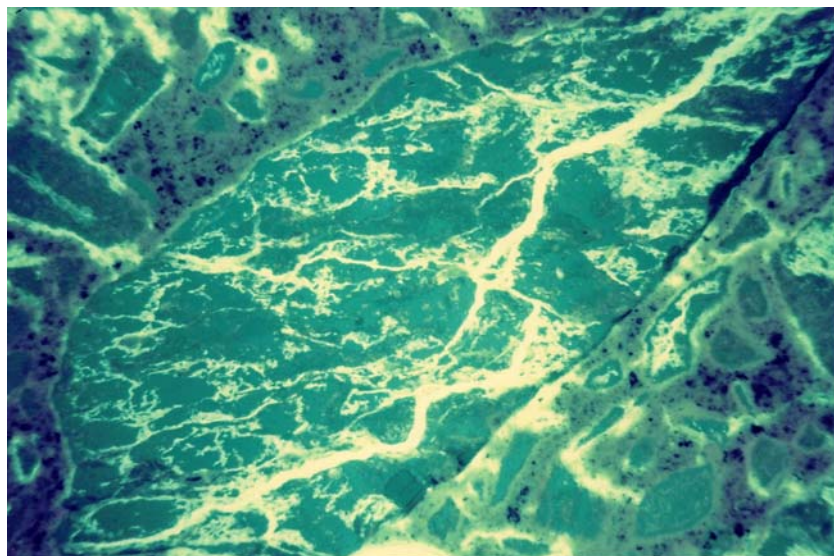


Figure 4 The picture shows partly dissolution of a mylonite (yellow areas) grain in the “Ref. section” (fluorescence light). The size of the picture is 4.2 mm x 2.7 mm.

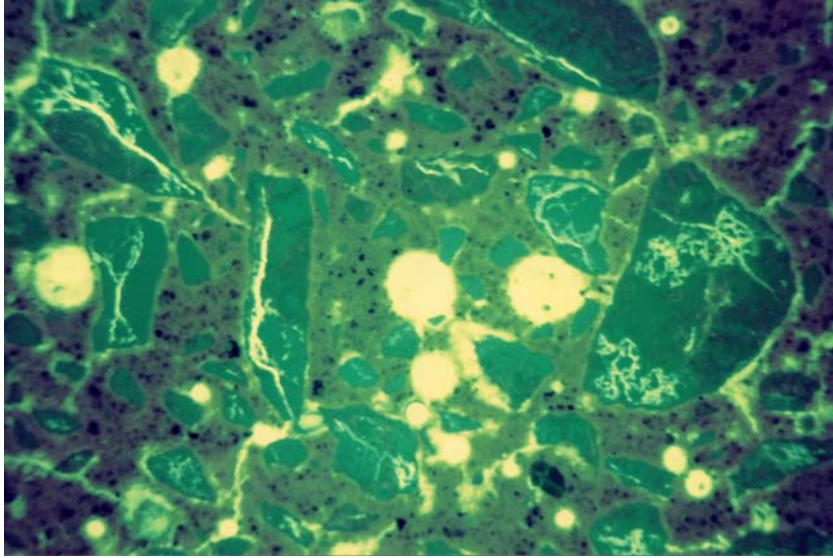


Figure 5 The picture shows cracks and partly dissolution of aggregate grains (yellow areas) in the outer zone of the “Filler section” (fluorescence light). The size of the picture is 4.2 mm x 2.7 mm.

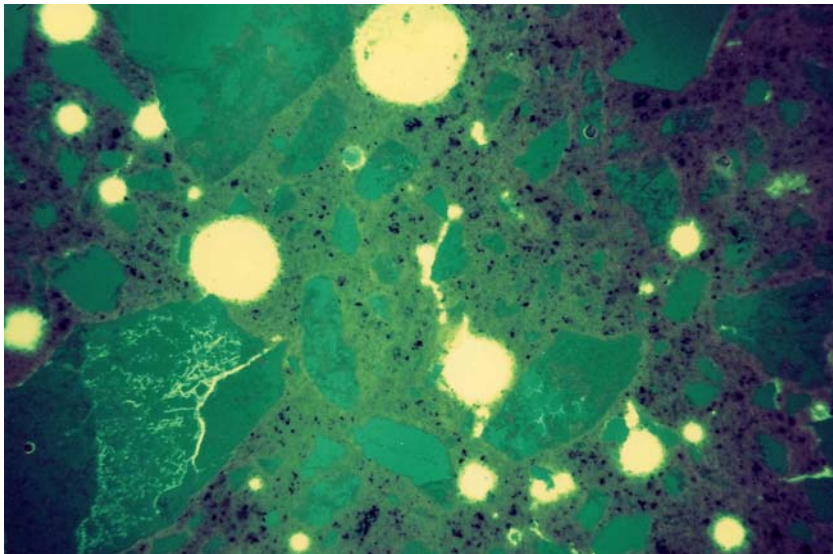


Figure 6 Most of the picture shows the dense mortar inside the outer zone of the “Filler section” (fluorescence light). The size of the picture is 4.2 mm x 2.7 mm.

**DEPARTMENT OF STRUCTURAL ENGINEERING
NORWEGIAN UNIVERSITY OF SCIENCE AND TECHNOLOGY**

N-7491 TRONDHEIM, NORWAY
Telephone: +47 73 59 47 00 Telefax: +47 73 59 47 01

"Reliability Analysis of Structural Systems using Nonlinear Finite Element Methods",
C. A. Holm, 1990:23, ISBN 82-7119-178-0.

"Uniform Stratified Flow Interaction with a Submerged Horizontal Cylinder",
Ø. Arntsen, 1990:32, ISBN 82-7119-188-8.

"Large Displacement Analysis of Flexible and Rigid Systems Considering Displacement-
Dependent Loads and Nonlinear Constraints", K. M. Mathisen, 1990:33,
ISBN 82-7119-189-6.

"Solid Mechanics and Material Models including Large Deformations",
E. Levold, 1990:56, ISBN 82-7119-214-0, ISSN 0802-3271.

"Inelastic Deformation Capacity of Flexurally-Loaded Aluminium Alloy Structures",
T. Welo, 1990:62, ISBN 82-7119-220-5, ISSN 0802-3271.

"Visualization of Results from Mechanical Engineering Analysis",
K. Aarnes, 1990:63, ISBN 82-7119-221-3, ISSN 0802-3271.

"Object-Oriented Product Modeling for Structural Design",
S. I. Dale, 1991:6, ISBN 82-7119-258-2, ISSN 0802-3271.

"Parallel Techniques for Solving Finite Element Problems on Transputer Networks",
T. H. Hansen, 1991:19, ISBN 82-7119-273-6, ISSN 0802-3271.

"Statistical Description and Estimation of Ocean Drift Ice Environments",
R. Korsnes, 1991:24, ISBN 82-7119-278-7, ISSN 0802-3271.

"Properties of concrete related to fatigue damage: with emphasis on high strength
concrete", G. Petkovic, 1991:35, ISBN 82-7119-290-6, ISSN 0802-3271.

"Turbidity Current Modelling", B. Brørs, 1991:38, ISBN 82-7119-293-0, ISSN 0802-3271.

"Zero-Slump Concrete: Rheology, Degree of Compaction and Strength. Effects of Fillers as
Part Cement-Replacement", C. Sørensen, 1992:8, ISBN 82-7119-357-0, ISSN 0802-3271.

"Nonlinear Analysis of Reinforced Concrete Structures Exposed to Transient Loading", K.
V. Høiseth, 1992:15, ISBN 82-7119-364-3, ISSN 0802-3271.

"Finite Element Formulations and Solution Algorithms for Buckling and Collapse Analysis of Thin Shells", R. O. Bjærum, 1992:30, ISBN 82-7119-380-5, ISSN 0802-3271.

"Response Statistics of Nonlinear Dynamic Systems",
J. M. Johnsen, 1992:42, ISBN 82-7119-393-7, ISSN 0802-3271.

"Digital Models in Engineering. A Study on why and how engineers build and operate digital models for decision support", J. Høyte, 1992:75, ISBN 82-7119-429-1, ISSN 0802-3271.

"Sparse Solution of Finite Element Equations",
A. C. Damhaug, 1992:76, ISBN 82-7119-430-5, ISSN 0802-3271.

"Some Aspects of Floating Ice Related to Sea Surface Operations in the Barents Sea",
S. Løset, 1992:95, ISBN 82-7119-452-6, ISSN 0802-3271.

"Modelling of Cyclic Plasticity with Application to Steel and Aluminium Structures",
O. S. Hopperstad, 1993:7, ISBN 82-7119-461-5, ISSN 0802-3271.

"The Free Formulation: Linear Theory and Extensions with Applications to Tetrahedral Elements with Rotational Freedoms", G. Skeie, 1993:17, ISBN 82-7119-472-0, ISSN 0802-3271.

"Høyfast betongs motstand mot piggdekkslitasje. Analyse av resultater fra prøving i Veisliter'n", T. Tveter, 1993:62, ISBN 82-7119-522-0, ISSN 0802-3271.

"A Nonlinear Finite Element Based on Free Formulation Theory for Analysis of Sandwich Structures", O. Aamlid, 1993:72, ISBN 82-7119-534-4, ISSN 0802-3271.

"The Effect of Curing Temperature and Silica Fume on Chloride Migration and Pore Structure of High Strength Concrete", C. J. Hauck, 1993:90, ISBN 82-7119-553-0, ISSN 0802-3271.

"Failure of Concrete under Compressive Strain Gradients",
G. Markeset, 1993:110, ISBN 82-7119-575-1, ISSN 0802-3271.

"An experimental study of internal tidal amphidromes in Vestfjorden",
J. H. Nilsen, 1994:39, ISBN 82-7119-640-5, ISSN 0802-3271.

"Structural analysis of oil wells with emphasis on conductor design",
H. Larsen, 1994:46, ISBN 82-7119-648-0, ISSN 0802-3271.

"Adaptive methods for non-linear finite element analysis of shell structures",
K. M. Okstad, 1994:66, ISBN 82-7119-670-7, ISSN 0802-3271.

"On constitutive modelling in nonlinear analysis of concrete structures",
O. Fyrilev, 1994:115, ISBN 82-7119-725-8, ISSN 0802-3271.

"Fluctuating wind load and response of a line-like engineering structure with emphasis on motion-induced wind forces", J. Bogunovic Jakobsen, 1995:62, ISBN 82-7119-809-2, ISSN 0802-3271.

"An experimental study of beam-columns subjected to combined torsion, bending and axial actions", A. Aalberg, 1995:66, ISBN 82-7119-813-0, ISSN 0802-3271.

"Scaling and cracking in unsealed freeze/thaw testing of Portland cement and silica fume concretes", S. Jacobsen, 1995:101, ISBN 82-7119-851-3, ISSN 0802-3271.

"Damping of water waves by submerged vegetation. A case study of laminaria hyperborea", A. M. Dubi, 1995:108, ISBN 82-7119-859-9, ISSN 0802-3271.

"The dynamics of a slope current in the Barents Sea", Sheng Li, 1995:109, ISBN 82-7119-860-2, ISSN 0802-3271.

"Modellering av delmaterialenes betydning for betongens konsistens", Ernst Mørtzell, 1996:12, ISBN 82-7119-894-7, ISSN 0802-3271.

"Bending of thin-walled aluminium extrusions", Birgit Søvik Opheim, 1996:60, ISBN 82-7119-947-1, ISSN 0802-3271.

"Material modelling of aluminium for crashworthiness analysis", Torodd Berstad, 1996:89, ISBN 82-7119-980-3, ISSN 0802-3271.

"Estimation of structural parameters from response measurements on submerged floating tunnels", Rolf Magne Larssen, 1996:119, ISBN 82-471-0014-2, ISSN 0802-3271.

"Numerical modelling of plain and reinforced concrete by damage mechanics", Mario A. Polanco-Loria, 1997:20, ISBN 82-471-0049-5, ISSN 0802-3271.

"Nonlinear random vibrations - numerical analysis by path integration methods", Vibeke Moe, 1997:26, ISBN 82-471-0056-8, ISSN 0802-3271.

"Numerical prediction of vortex-induced vibration by the finite element method", Joar Martin Dalheim, 1997:63, ISBN 82-471-0096-7, ISSN 0802-3271.

"Time domain calculations of buffeting response for wind sensitive structures", Ketil Aas-Jakobsen, 1997:148, ISBN 82-471-0189-0, ISSN 0802-3271.

"A numerical study of flow about fixed and flexibly mounted circular cylinders", Trond Stokka Meling, 1998:48, ISBN 82-471-0244-7, ISSN 0802-3271.

"Estimation of chloride penetration into concrete bridges in coastal areas", Per Egil Steen, 1998:89, ISBN 82-471-0290-0, ISSN 0802-3271.

"Stress-resultant material models for reinforced concrete plates and shells", Jan Arve Øverli, 1998:95, ISBN 82-471-0297-8, ISSN 0802-3271.

“Chloride binding in concrete. Effect of surrounding environment and concrete composition”, Claus Kenneth Larsen, 1998:101, ISBN 82-471-0337-0, ISSN 0802-3271.

“Rotational capacity of aluminium alloy beams”,
Lars A. Moen, 1999:1, ISBN 82-471-0365-6, ISSN 0802-3271.

“Stretch Bending of Aluminium Extrusions”,
Arild H. Clausen, 1999:29, ISBN 82-471-0396-6, ISSN 0802-3271.

“Aluminium and Steel Beams under Concentrated Loading”,
Tore Tryland, 1999:30, ISBN 82-471-0397-4, ISSN 0802-3271.

"Engineering Models of Elastoplasticity and Fracture for Aluminium Alloys",
Odd-Geir Lademo, 1999:39, ISBN 82-471-0406-7, ISSN 0802-3271.

"Kapasitet og duktilitet av dybelforbindelser i trekonstruksjoner",
Jan Siem, 1999:46, ISBN 82-471-0414-8, ISSN 0802-3271.

“Etablering av distribuert ingeniørarbeid; Teknologiske og organisatoriske erfaringer fra en norsk ingeniørbedrift”, Lars Line, 1999:52, ISBN 82-471-0420-2, ISSN 0802-3271.

“Estimation of Earthquake-Induced Response”,
Símon Ólafsson, 1999:73, ISBN 82-471-0443-1, ISSN 0802-3271.

“Coastal Concrete Bridges: Moisture State, Chloride Permeability and Aging Effects”
Ragnhild Holen Relling, 1999:74, ISBN 82-471-0445-8, ISSN 0802-3271.

”Capacity Assessment of Titanium Pipes Subjected to Bending and External Pressure”,
Arve Bjørset, 1999:100, ISBN 82-471-0473-3, ISSN 0802-3271.

“Validation of Numerical Collapse Behaviour of Thin-Walled Corrugated Panels”,
Håvar Ilstad, 1999:101, ISBN 82-471-0474-1, ISSN 0802-3271.

“Strength and Ductility of Welded Structures in Aluminium Alloys”,
Miroslaw Matusiak, 1999:113, ISBN 82-471-0487-3, ISSN 0802-3271.

“Thermal Dilation and Autogenous Deformation as Driving Forces to Self-Induced Stresses in High Performance Concrete”, Øyvind Bjøntegaard, 1999:121, ISBN 82-7984-002-8, ISSN 0802-3271.

“Some Aspects of Ski Base Sliding Friction and Ski Base Structure”,
Dag Anders Moldestad, 1999:137, ISBN 82-7984-019-2, ISSN 0802-3271.

"Electrode reactions and corrosion resistance for steel in mortar and concrete",
Roy Antonsen, 2000:10, ISBN 82-7984-030-3, ISSN 0802-3271.

"Hydro-Physical Conditions in Kelp Forests and the Effect on Wave Damping and Dune Erosion. A case study on Laminaria Hyperborea", Stig Magnar Løvås, 2000:28, ISBN 82-7984-050-8, ISSN 0802-3271.

"Random Vibration and the Path Integral Method",
Christian Skaug, 2000:39, ISBN 82-7984-061-3, ISSN 0802-3271.

"Buckling and geometrical nonlinear beam-type analyses of timber structures",
Trond Even Eggen, 2000:56, ISBN 82-7984-081-8, ISSN 0802-3271.

"Structural Crashworthiness of Aluminium Foam-Based Components",
Arve Grønsund Hanssen, 2000:76, ISBN 82-7984-102-4, ISSN 0809-103X.

"Measurements and simulations of the consolidation in first-year sea ice ridges, and some aspects of mechanical behaviour",
Knut V. Høyland, 2000:94, ISBN 82-7984-121-0, ISSN 0809-103X.

"Kinematics in Regular and Irregular Waves based on a Lagrangian Formulation",
Svein Helge Gjørund, 2000-86, ISBN 82-7984-112-1, ISSN 0809-103X.

"Self-Induced Cracking Problems in Hardening Concrete Structures",
Daniela Bosnjak, 2000-121, ISBN 82-7984-151-2, ISSN 0809-103X.

"Ballistic Penetration and Perforation of Steel Plates",
Tore Børvik, 2000:124, ISBN 82-7984-154-7, ISSN 0809-103X.

"Freeze-Thaw resistance of Concrete. Effect of: Curing Conditions, Moisture Exchange and Materials",
Terje Finnerup Rønning, 2001:14, ISBN 82-7984-165-2, ISSN 0809-103X

Structural behaviour of post tensioned concrete structures. Flat slab. Slabs on ground",
Steinar Trygstad, 2001:52, ISBN 82-471-5314-9, ISSN 0809-103X.

"Slipforming of Vertical Concrete Structures. Friction between concrete and slipform panel",
Kjell Tore Fosså, 2001:61, ISBN 82-471-5325-4, ISSN 0809-103X.

"Some numerical methods for the simulation of laminar and turbulent incompressible flows",
Jens Holmen, 2002:6, ISBN 82-471-5396-3, ISSN 0809-103X.

"Improved Fatigue Performance of Threaded Drillstring Connections by Cold Rolling",
Steinar Kristoffersen, 2002:11, ISBN: 82-421-5402-1, ISSN 0809-103X.

"Deformations in Concrete Cantilever Bridges: Observations and Theoretical Modelling",
Peter F. Takács, 2002:23, ISBN 82-471-5415-3, ISSN 0809-103X.

"Stiffened aluminium plates subjected to impact loading",
Hilde Giæver Hildrum, 2002:69, ISBN 82-471-5467-6, ISSN 0809-103X.

"Full- and model scale study of wind effects on a medium-rise building in a built up area",
Jónas Thór Snæbjörnsson, 2002:95, ISBN82-471-5495-1, ISSN 0809-103X.

"Evaluation of Concepts for Loading of Hydrocarbons in Ice-infested water",
Arnor Jensen, 2002:114, ISBN 82-417-5506-0, ISSN 0809-103X.

”Numerical and Physical Modelling of Oil Spreading in Broken Ice”,
Janne K. Økland Gjøsteen, 2002:130, ISBN 82-471-5523-0, ISSN 0809-103X.

”Diagnosis and protection of corroding steel in concrete”,
Franz Pruckner, 20002:140, ISBN 82-471-5555-4, ISSN 0809-103X.

“Tensile and Compressive Creep of Young Concrete: Testing and Modelling”,
Dawood Atrushi, 2003:17, ISBN 82-471-5565-6, ISSN 0809-103X.

“Rheology of Particle Suspensions. Fresh Concrete, Mortar and Cement Paste with Various
Types of Lignosulfonates”, Jon Elvar Wallevik, 2003:18, ISBN 82-471-5566-4,
ISSN 0809-103X.

“Oblique Loading of Aluminium Crash Components”, Aase Reyes, 2003:15, ISBN 82-471-
5562-1, ISSN 0809-103X.

“Utilization of Ethiopian Natural Pozzolans”, Surafel Ketema Desta, 2003:26,
ISSN 82-471-5574-5, ISSN:0809-103X.

“Behaviour and strength prediction of reinforced concrete structures with discontinuity
regions”, Helge Brå, 2004:11, ISBN 82-471-6222-9, ISSN 1503-8181.

“High-strength steel plates subjected to projectile impact. An experimental and numerical
study”, Sumita Dey, 2004:38, ISBN 82-471-6281-4 (elektr. Utg.), ISBN 82-471-6282-2
(trykt utg.), ISSN 82-471-6282-2.